Terms and Conditions of Use of Digitised Theses from Trinity College Library Dublin

Copyright statement

All material supplied by Trinity College Library is protected by copyright (under the Copyright and Related Rights Act, 2000 as amended) and other relevant Intellectual Property Rights. By accessing and using a Digitised Thesis from Trinity College Library you acknowledge that all Intellectual Property Rights in any Works supplied are the sole and exclusive property of the copyright and/or other IPR holder. Specific copyright holders may not be explicitly identified. Use of materials from other sources within a thesis should not be construed as a claim over them.

A non-exclusive, non-transferable licence is hereby granted to those using or reproducing, in whole or in part, the material for valid purposes, providing the copyright owners are acknowledged using the normal conventions. Where specific permission to use material is required, this is identified and such permission must be sought from the copyright holder or agency cited.

Liability statement

By using a Digitised Thesis, I accept that Trinity College Dublin bears no legal responsibility for the accuracy, legality or comprehensiveness of materials contained within the thesis, and that Trinity College Dublin accepts no liability for indirect, consequential, or incidental, damages or losses arising from use of the thesis for whatever reason. Information located in a thesis may be subject to specific use constraints, details of which may not be explicitly described. It is the responsibility of potential and actual users to be aware of such constraints and to abide by them. By making use of material from a digitised thesis, you accept these copyright and disclaimer provisions. Where it is brought to the attention of Trinity College Library that there may be a breach of copyright or other restraint, it is the policy to withdraw or take down access to a thesis while the issue is being resolved.

Access Agreement

By using a Digitised Thesis from Trinity College Library you are bound by the following Terms & Conditions. Please read them carefully.

I have read and I understand the following statement: All material supplied via a Digitised Thesis from Trinity College Library is protected by copyright and other intellectual property rights, and duplication or sale of all or part of any of a thesis is not permitted, except that material may be duplicated by you for your research use or for educational purposes in electronic or print form providing the copyright owners are acknowledged using the normal conventions. You must obtain permission for any other use. Electronic or print copies may not be offered, whether for sale or otherwise to anyone. This copy has been supplied on the understanding that it is copyright material and that no quotation from the thesis may be published without proper acknowledgement.

Functional analysis of the *TLO* gene family in *Candida albicans* and *Candida dubliniensis*

A thesis submitted to the University of Dublin in fulfillment of the requirements for the degree of Doctor of Philosophy by

Hannah Boyle

November 2015

Microbiology Research Unit,

Division of Oral Biosciences,

Dublin Dental University Hospital,

University of Dublin,

Trinity College Dublin.

Ph.D.
School of Dental Sciences

Declaration

I declare that this thesis has not been submitted as an exercise for a degree at this or any other university and it is entirely my own work. I agree to deposit this thesis in the University's open access institutional repository or allow the library to do so on my behalf, subject to Irish Copyright Legislation and Trinity College Library conditions of use and acknowledgement.

Table of Contents

Chapter 3. Doxycycline Induced Expression of *C. dubliniensis TLO1* and *TLO2*

Chapter 4. Deletion of *MED3* in *C. dubliniensis* Wild Type and in ΔΔ*Cdtlo* and Comparative Analysis of the *CdMED3* and *CdTLO* mutant strains

Chapter 5. Truncation of CdTlo1 Protein

Chapter 6. Tandem affinity purification of CdTlo1 and analysis by mass spectrophotometry

Chapter 7. Construction of *C. dubliniensis tloΔΔ* mutant expressing *C. albicans TLO* genes

Chapter 8 General Discussion

Bibliography

Index of figures

Page numbers refer to text page preceding the figure(s)

Index of Tables

Page numbers refer to text page preceding the table(s)

Acknowledgements

Firstly, I wish to thank my supervisor Professor Derek Sullivan for his continual support and guidance throughout the duration of my project, as well as a big thank you to Professor Gary Moran for all of his help and insight into various aspects of this project and allowing me to endlessly 'pick his brain'. Thank you very much to the Head of Division, Professor David Coleman and Laboratory Manager Dr. Mary O' Donnell for their provision of great resources, excellent management and running of the Microbiology Lab.

I cannot even begin to express my gratitude to my fellow *Candida* buddies Peter Flanagan, Dr. Peter Hyde and in particular Dr. John Haran, who have helped me out on so many occasions, whether it be by guiding me through protocols, acting as my soundboards for different project ideas and numerous discussions on the yeasty delight that is *Candida.* Thank you to everyone in the Microbiology lab that made every teatime, lunch, after-work drinks and Christmas party so enjoyable. I can only hope that any other colleagues I have in the future will provide me with as many hilariously entertaining, interesting and just plain bizarre conversations as all of you have. Thank you to Dr. Maria Boyle for the endless onslaught of jokes and doodles, long may it continue!

I would like to say a massive thank you to my wonderful boyfriend Karl for constantly encouraging me and supporting me throughout the duration of my PhD, and enduring my project-related mumblings and grumblings over the last 4 years! Thank you to my parents for providing me with the determination to succeed in getting my doctorate, and to my little brother Charlie for his curiosity about my project that allowed me to successfully explain molecular genetics to an eleven year old!

Abbreviations

.tiff	Tagged image file format
°C	Degrees centigrade
Δ	Deletion (of a gene or part of a gene)
~	Approximately
AIDS	Acquired immune deficiency syndrome
bp	Base pair
BSA	Bovine serum albumin
cAMP	Cyclic adenosine monophosphate
cm	Centimetre
C_t	Cycle threshold
DEPC	Diethylpyrocarbonate
dH_2O	Deionised water
DNA	Deoxyribonucleic acid
DNAse	Deoxyribonuclease
dNTPs	di-Nucleotide triphosphate
DOX	Doxycycline
DTT	Dithiothreitol
EDTA	Ethylenediamine tetraacetic acid
et al.	And others
FBS	Fetal bovine serum
g	Gram
h	Hour(s)
HIV	Human immunodeficiency virus
H_2O_2	Hydrogen peroxide
i.e.	That is
kb	Kilobase
LN_2	Liquid nitrogen
LTR	Long terminal repeat
µg	Microgram
µl	Microlitre
µm	Micrometre
M	Molar
min	Minute

ml	Millilitre
mM	Millimolar
NADPH	Nicotinamide adenine dinucleotide phosphate
NAT	Nourseothricin
NAT_{100}	YEPD (agar/broth) with 100 μg/ml
NAT_2	YEPD (agar/broth) with 2 μg/ml
NLS	Nuclear localisation site
nm	Nanometre
O.D.	Optical density
OPC	Oropharyngeal candidiasis
ORF	Open reading frame
PBS	Phosphate buffer solution
PCR	Polymerase chain reaction
PMSF	Phenylmethylsulfonyl fluoride
Pol II	RNA polymerase II
PTFL	Polytetrafluoroethylene
qRT-PCR	Quantative real- time PCR
RHE	Reconstituted human epithelial
RNA	Ribonucleic acid
ROS	Reactive oxygen species
r.p.m	Revolutions per minute
SOC	Super optimal broth with catabolite repression
TAP	Tandem affinity purification
TBE	Tris- borate EDTA
TE	Tris- EDTA
Tet	Tetracycline
TEV	Tobacco etch virus
UV	Ultraviolet
VVC	Vulvovaginal candidiasis
v/v	Volume per volume
w/v	Weight per volume
YEPD	Yeast Extract Peptone Dextrose
YEPM	Yeast Extract Peptone Maltose
YNB	Yeast nitrogen base
YNB+a.a.	Yeast nitrogen base with amino acids

Publication

Haran, J., Boyle, H., Hokamp, K., Yeomans, T., Liu, Z., Church, M., Fleming, A. B., Anderson, M. Z., Berman, J., Myers, L. C., Sullivan, D. J. & Moran, G. P. (2014). Telomeric *ORFs* (*TLOs*) in *Candida* spp. encode Mediator subunits that regulate distinct virulence traits. *PloS Genetics,* **10**, e1004658.

OPEN ACCESS Freely available online

PLOS | GENETICS

Telomeric *ORFs* (*TLOs*) in *Candida* spp. Encode Mediator Subunits That Regulate Distinct Virulence Traits

John Haran[1☯], Hannah Boyle[1☯], Karsten Hokamp[2], Tim Yeomans[1], Zhongle Liu[3], Michael Church[2], Alastair B. Fleming[2], Matthew Z. Anderson[4¤], Judith Berman[4,5], Lawrence C. Myers[3], Derek J. Sullivan[1*], Gary P. Moran[1*]

1 Division of Oral Biosciences, Dublin Dental University Hospital, University of Dublin, Trinity College Dublin, Dublin, Ireland, **2** School of Genetics and Microbiology, University of Dublin, Trinity College Dublin, Dublin, Ireland, **3** Department of Biochemistry, Geisel School of Medicine at Dartmouth, Hanover, New Hampshire, United States of America, **4** Department of Genetics, Cell Biology and Development, University of Minnesota, Minneapolis, Minnesota, United States of America, **5** Department of Microbiology and Biotechnology, George S. Wise Faculty of Life Sciences, Tel Aviv University, Ramat Aviv, Israel

Abstract

The *TLO* genes are a family of telomere-associated ORFs in the fungal pathogens *Candida albicans* and *C. dubliniensis* that encode a subunit of the Mediator complex with homology to Med2. The more virulent pathogen *C. albicans* has 15 copies of the gene whereas the less pathogenic species *C. dubliniensis* has only two (*CdTLO1* and *CdTLO2*). In this study we used *C. dubliniensis* as a model to investigate the role of *TLO* genes in regulating virulence and also to determine whether *TLO* paralogs have evolved to regulate distinct functions. A *C. dubliniensis tlo1Δ/tlo2Δ* mutant is unable to form true hyphae, has longer doubling times in galactose broth, is more susceptible to oxidative stress and forms increased levels of biofilm. Transcript profiling of the *tlo1Δ/tlo2Δ* mutant revealed increased expression of starvation responses in rich medium and retarded expression of hypha-induced transcripts in serum. ChIP studies indicated that Tlo1 binds to many ORFs including genes that exhibit high and low expression levels under the conditions analyzed. The altered expression of these genes in the *tlo1Δ/tlo2Δ* null mutant indicates roles for Tlo proteins in transcriptional activation and repression. Complementation of the *tlo1Δ/tlo2Δ* mutant with *TLO1*, but not *TLO2*, restored wild-type filamentous growth, whereas only *TLO2* fully suppressed biofilm growth. Complementation with *TLO1* also had a greater effect on doubling times in galactose broth. The different abilities of *TLO1* and *TLO2* to restore wild-type functions was supported by transcript profiling studies that showed that only *TLO1* restored expression of hypha-specific genes (*UME6, SOD5*) and galactose utilisation genes (*GAL1* and *GAL10*), whereas *TLO2* restored repression of starvation-induced gene transcription. Thus, Tlo/Med2 paralogs encoding Mediator subunits regulate different virulence properties in *Candida* spp. and their expansion may account for the increased adaptability of *C. albicans* relative to other *Candida* species.

Citation: Haran J, Boyle H, Hokamp K, Yeomans T, Liu Z, et al. (2014) Telomeric *ORFs* (*TLOs*) in *Candida* spp. Encode Mediator Subunits That Regulate Distinct Virulence Traits. PLoS Genet 10(10): e1004658. doi:10.1371/journal.pgen.1004658

Editor: Geraldine Butler, University College Dublin, Ireland

Received July 9, 2014; **Accepted** August 11, 2014; **Published** October 30, 2014

Data Availability: The authors confirm that all data underlying the findings are fully available without restriction. Genomic data files are available from Gene Expression Omnibus at NCBI (accession numbers: GSE59113, GSE60173).

Funding: This project was funded by Science Foundation Ireland, grant numbers RFP.1/GEN/3044, RFP.1/GEN/3042 and O4/IN3/B463 to GPM and DJS (www.SFI.ie). JB was supported by the NIH, grant number R01AI075096. JH was supported by the Faculty of Health Sciences, Trinity College Dublin and by an award from the Society for General Microbiology President's fund to visit the laboratory of JB. The funders had no role in study design, data collection and analysis, decision to publish, or preparation of the manuscript.

Competing Interests: The authors have declared that no competing interests exist.

* Email: Derek.sullivan@dental.tcd.ie (DJS); gpmoran@dental.tcd.ie (GPM)

☯ These authors contributed equally to this work.

¤ Current address: Department of Molecular Microbiology and Immunology, Brown University, Providence, Rhode Island, United States of America

Introduction

Candida albicans is a commensal yeast commonly recovered from mucosal surfaces in humans. *C. albicans* is also a versatile opportunistic pathogen, responsible for a variety of superficial infections as well as more severe, life threatening infections in severely immunocompromised patients. Phenotypic versatility is an important characteristic of *C. albicans* and this flexibility allows *C. albicans* to adapt to this wide range of niches in the human host [1–3]. Over the past decade, transcriptional profiling of *C. albicans* using microarray and RNA-seq technologies has revealed that rapid adaptation to local environmental conditions involves elaborate, programmed shifts in transcription pattern. The biochemistry of transcriptional regulation has been studied intensively in the model yeast *S. cerevisiae*. Most genes transcribed by RNA polymerase II (PolII) require a carefully orchestrated series of events to initiate transcription. The formation of the pre-initiation complex and recruitment of PolII requires the function of Mediator, a large multi-subunit protein complex [4,5]. Mediator is thought to be required to bridge DNA-bound transcription factors with the rest of the transcriptional machinery [6,7]. The complex is generally divided into three modules: a head, middle and tail. The tail region includes Med2, Med3 and Med15/Gal11 and is thought to be the part of Mediator that

Author Summary

Candida albicans and *C. dubliniensis* are fungal pathogens of humans. Both species possess *TLO* genes encoding proteins with homology to the Med2 subunit of Mediator. The more virulent pathogen *C. albicans* has 15 copies of the *TLO* gene whereas the less pathogenic species *C. dubliniensis* has only two (*TLO1* and *TLO2*). In this study we show that a *C. dubliniensis* mutant missing both *TLO1* and *TLO2* is defective in virulence functions, including hyphal growth and stress responses but forms increased levels of biofilm. Analysis of gene expression in the *tlo1Δ/tlo2Δ* mutant revealed extensive differences relative to wild-type cells, including aberrant expression of starvation responses in nutrient-rich medium and retarded expression of hypha-induced transcripts in serum. Tlo1 protein was found to interact with genes and this was associated with both gene activation and repression. *TLO1* was found to be better at restoring hyphal growth compared to *TLO2* and but was less effective than *TLO2* in supressing biofilm formation in the *tlo1Δ/tlo2Δ* strain. Thus, Tlo proteins regulate many virulence properties in *Candida* spp. and the expansion of the *TLO* family in *C. albicans* may account for the increased adaptability of this species relative to other *Candida* species.

interacts directly with transcription factors such as Gal4 and Gcn4 [8].

Most components of Mediator are highly conserved between *S. cerevisiae* and *C. albicans* [9]. However, completion of the *C. albicans* genome sequence [10,11] revealed a family of up to 15 telomeric (*TLO*) genes that were subsequently found to encode a domain with homology to the Mediator tail subunit Med2 of *S. cerevisiae* [9,12,13]. This *TLO* gene expansion is unique to *C. albicans*, as most of the less pathogenic non-*albicans Candida* species such as *C. tropicalis* and *C. parapsilosis* have only one *TLO* gene. *C. dubliniensis*, the closest relative to *C. albicans* has two *TLO* genes, namely *TLO1* and *TLO2*. *TLO1* (*Cd36_72860*) is located internally on chromosome 7 and *TLO2* (*Cd36_35580*) is at a telomere-adjacent locus on the right arm of chromosome R [14]. *C. dubliniensis TLO2* appears to be the ancestral locus, based on synteny with, and homology to, the single *C. tropicalis* orthologue CTRG_05798.3 [14]. All candidal *TLO* genes share the Med2-like domain of the *C. albicans TLOs* and appear to be the *MED2* orthologs in these species. Indeed, biochemical studies have shown that like the *S. cerevisiae* Med2 protein, Tlo proteins co-purify with the *C. albicans* orthologs of mediator tail module components Med3 and Med15 [9].

The 15 *TLO* genes in the *C. albicans* type strain SC5314 can be classified into four distinct clades based on gene structure, including the highly expressed *TLOα* clade (6 members), a single *TLOβ* gene, the poorly expressed *TLOγ* clade (7 members) and a single *TLOψ* gene which is a pseudogene [12]. Biochemical studies have shown that the levels of Tloα and Tloβ proteins is in vast excess to the amount necessary to be a stoichiometric subunit of Mediator (9) and stands in stark contrast to the situation in *S. cerevisiae*, where the Med2 subunit is expressed at roughly equivalent amounts to other subunits of the complex. Due to the large numbers of *TLO* genes in *C. albicans*, functional analysis of Mediator has largely been restricted to other subunits, including Med3 (tail domain), Med31 (middle domain), Med20 (head domain) and Med13/Srb9 (kinase domain). Med31 and Med20 are required for the transition of *C. albicans* yeast cells to filamentous hyphae and for biofilm formation, two important pathogenic traits of the organism [9,15]. Med31 is required for expression of the genes *ALS1* and *ALS3* that encode cell-surface proteins involved in biofilm production, consistent with the poor biofilms produced by *med31Δ* mutants. In addition, Med31 is required for the expression of genes regulated by the transcription factor *Ace2*, which regulates many genes involved in cell wall remodelling during cell separation. Consistent with this, the *med31Δ* mutant exhibits defective cytokinesis. Deletion of *MED3* resulted in a stronger filamentous growth defect, resulting in short pseudohyphae in serum or liquid media supplemented with GlcNac [9]. Deletion of Mediator subunits also has complex effects on the transcriptional circuit governing the white-opaque switch, a phenotypic transition involved in mating [16].

C. albicans is the most prevalent pathogenic fungal species. The closely related species *C. dubliniensis* is responsible for far fewer infections and is a minor component of the human oral flora [14,17]. The yeast-to-hypha transition is an important virulence trait of *C. albicans* and *C. dubliniensis* forms fewer hyphae than *C. albicans* in response to most *in vitro* and *in vivo* hypha-inducing stimuli [17]. *C. dubliniensis* requires much stronger environmental cues, including nutrient depletion, in order to activate a transcriptional response that will induce the yeast-to-hypha transition [18–20]. Less effective transcriptional responses may also account for the increased susceptibility of *C. dubliniensis* to environmental stress relative to *C. albicans* [21]. It has been suggested that the expansion of the *TLO* family in *C. albicans* may account for the greater transcriptional flexibility and adaptability of this species relative to *C. dubliniensis* and the other non-*albicans Candida* species [22]. However, direct analysis of *TLO* null mutants has not been attempted in *C. albicans*, due to the large number of *TLO* genes and the likelihood of redundancy in the *TLO* family.

In this study, we exploited the closely related species *C. dubliniensis* as a model to study *TLO* gene function and to construct the first *tlo* null strains. We found that *C. dubliniensis* mutants lacking both *TLO1* and *TLO2* (*tlo1Δ/tlo2Δ*) exhibit widespread changes in the transcription of virulence-associated genes. ChIP analysis detected Tlo1 within the coding regions of ORFS, as well as subtelomeric regions and the Major Repeat Sequence (MRS). Interestingly, in strains lacking only one of the two *TLO* genes, expression of distinct subsets of genes was altered. We propose that expansion of the *TLO* family, even to only two members, has facilitated the evolution of functional diversity and may be of particular importance in the evolution of an expanded set of *TLO* paralogs together with the increased virulence in *Candida albicans*.

Results

Candida dubliniensis possesses two expressed *TLO* paralogs

The two *Candida dubliniensis TLO* genes, *TLO1* and *TLO2*, encode proteins of 320 and 355 amino acids, respectively, and share 58% identity. Homology to each other and to the *C. albicans* Tlo proteins is concentrated in the N-terminal 120 residues of the proteins. Tlo1 and Tlo2 share 81% identity in this N-terminal region, which also exhibits homology to *S. cerevisiae* Med2 (Figure 1A). The amino acid sequence of Tlo2 is 25 residues longer and contains a central triplet repeat of the motif KAAAKVKEEQ. *C. dubliniensis* is a diploid organism and gene deletion studies (see below) and Southern blot analysis confirmed that *C. dubliniensis* strain Wü284 has two alleles of *TLO1* (Figure S1). However, Southern blot experiments could detect only one allele of *TLO2* at the telomere of chromosome R (ChR) in strain

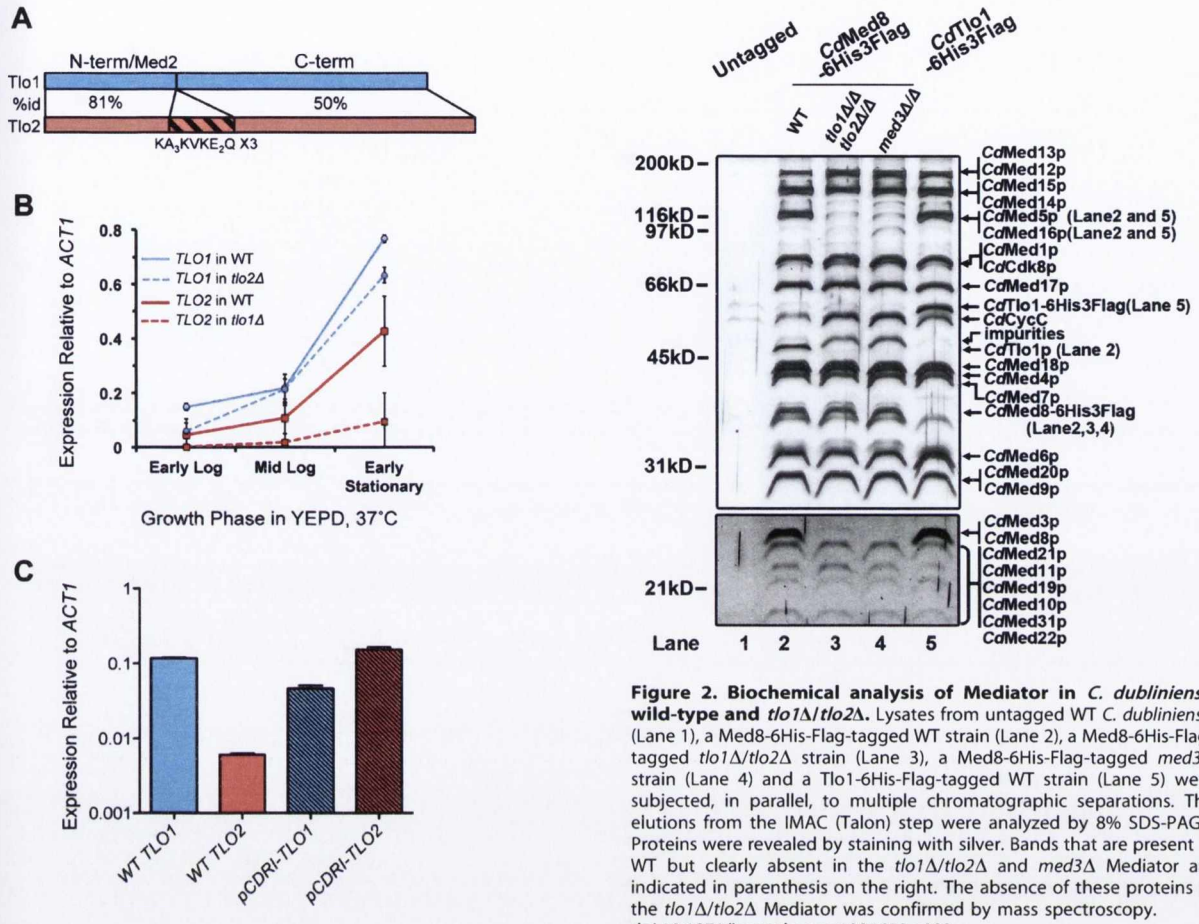

Figure 1. Structure and expression of *C. dubliniensis TLO* genes. (A) *TLO1* and *TLO2* encode proteins of 320 and 355 amino acids respectively that exhibit 81% identity in the N-terminal Med2-like domain, and 50% identity in the C-terminal portion of the protein. In addition, Tlo2 has an internal triplet repeat, indicated. (B) Expression of *TLO1* and *TLO2* was measured by QRT-PCR using gene-specific primers during growth in YEPD broth at 37°C in early exponential (1.5 h-post inoculation), mid-exponential (8 h) and early stationary phase (18 h) in strain Wü284 (WT). The effect of deletion of either *TLO1* or *TLO2* on the expression of the other paralog was also analysed. (C) Expression of reintegrated copies of *TLO1* and *TLO2* in plasmid pCDRI in the *tlo1Δ/tlo2Δ* strain.
doi:10.1371/journal.pgen.1004658.g001

Figure 2. Biochemical analysis of Mediator in *C. dubliniensis* wild-type and *tlo1Δ/tlo2Δ*. Lysates from untagged WT *C. dubliniensis* (Lane 1), a Med8-6His-Flag-tagged WT strain (Lane 2), a Med8-6His-Flag-tagged *tlo1Δ/tlo2Δ* strain (Lane 3), a Med8-6His-Flag-tagged *med3Δ* strain (Lane 4) and a Tlo1-6His-Flag-tagged WT strain (Lane 5) were subjected, in parallel, to multiple chromatographic separations. The elutions from the IMAC (Talon) step were analyzed by 8% SDS-PAGE. Proteins were revealed by staining with silver. Bands that are present in WT but clearly absent in the *tlo1Δ/tlo2Δ* and *med3Δ* Mediator are indicated in parenthesis on the right. The absence of these proteins in the *tlo1Δ/tlo2Δ* Mediator was confirmed by mass spectroscopy.
doi:10.1371/journal.pgen.1004658.g002

Wü284, indicating that one copy of ChR in Wü284 was truncated resulting in loss of one allele of *TLO2* (Figure S1). PCR analysis of the *tlo2Δ* strain confirmed that bases 1 to 918 of the second *TLO2* allele are deleted due to this truncation, with only a small 150 bp remnant of the ORF remaining. Analysis of gene expression by QRT-PCR revealed that *TLO1* mRNA is expressed over 2-fold higher than *TLO2* mRNA in YEPD at 37°C (Figure 1B).

C. dubliniensis Tlo proteins and Med3 are components of the Mediator tail module

We first asked if *C. dubliniensis* Tlo is a component of Mediator. To address this, we purified Mediator from whole cell extracts of *C. dubliniensis* wild-type and *tlo1Δ/tlo2Δ* mutant cells using a dual affinity tag on the *C. dubliniensis* ortholog of the conserved Med8 subunit of Mediator. The resulting Mediator complex was analyzed for purity by SDS-PAGE and for composition by mass spectroscopy with untagged WT *C. dubliniensis* serving as a control. Biochemical analysis showed that the *C. dubliniensis* Mediator, like *C. albicans*, is composed of a complete set of orthologs of the *S. cerevisiae* complex (Figure 2). Mediator purified from the *tlo1Δ/tlo2Δ* mutant lacked tail subunits Med3, Med15, Med16 and Med5 subunits (Figure 2, Lane 3). Importantly, Mediator purified from the *C. dubliniensis tlo1Δ/tlo2Δ* strain or from a *med3Δ* null strain had equivalent composition, lacking tail components Tlo1, Med3, Med5, Med15 and Med16 (Figure 2, Lanes 3 and 4).

To determine the relative abundance of Tlo proteins compared to other Mediator subunits, we constructed strains carrying Tlo1-HA, Med3-HA and Med8-HA tagged derivatives. Immunoblotting of whole cell extracts revealed that *C. dubliniensis* Tlo1 Mediator subunit is expressed in amounts comparable to the Med3 Tail Module and Med8 Head Module subunits (Figure S2). Consistent with this finding, purification of an affinity tagged Tlo1 protein from *C. dubliniensis* yielded only the Mediator associated form (Figure 2, Lane 5) and no free Tlo1 protein. Thus, in *C. dubliniensis* Tlo1 appears to be acting solely as a component of Mediator.

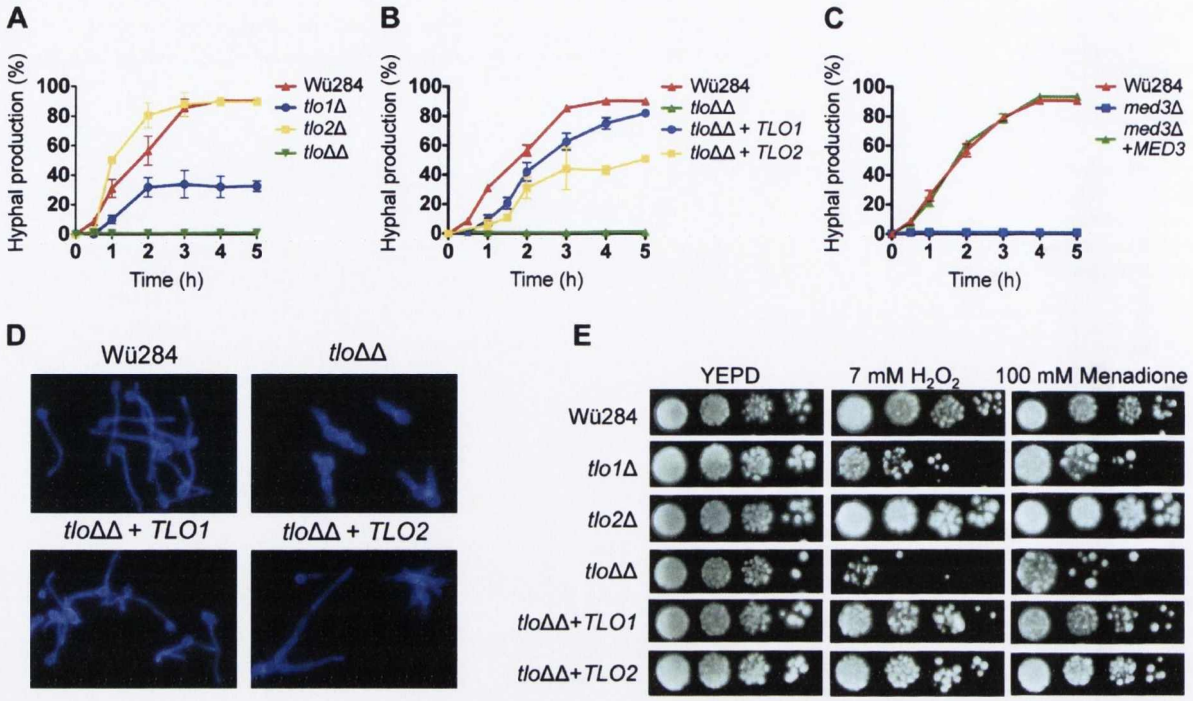

Figure 3. Phenotypic analysis of *C. dubliniensis tlo⊿* and *med3*Δ mutants. The rate of formation of true hyphae in water supplemented with 10% serum was measured in the *tlo1*Δ, *tlo2*Δ and *tlo1*Δ/*tlo2*Δ (*tlo*ΔΔ) mutants relative to Wü284 (A), in the *TLO1* and *TLO2* reintegrants (*tlo*ΔΔ+*TLO1/2*)(B) and in the *med3*Δ mutant (C). Measurements were taken over a period of 5 h by counting the number of cells producing unconstricted germ-tubes and expressing this value as a percentage of the whole population. (D) Cellular morphology of Wü284, the *tlo1*Δ/*tlo2*Δ (*tlo*ΔΔ) mutant and *TLO1* and *TLO2* reintegrated strains in 10% serum following staining with calcofluor white. (E) Oxidative stress susceptibility in *tlo*Δ mutants. Susceptibility to oxidative stress was assessed by spotting 20 μl aliquots of 10-fold serially diluted suspensions (10^6 to 10^3 cells/ml) of the indicated strains on YEPD agar plates containing 7 mM H_2O_2 or 100 mM menadione. Plates were incubated for 48 h at 37°C.
doi:10.1371/journal.pgen.1004658.g003

TLO1 activates hyphal growth to a greater extent than *TLO2*

Deletion of *TLO2* did not reduce filamentous growth significantly (Figure 3A), while deletion of *TLO1* resulted in reduced hyphal production (Figure 3A), as reported previously [14]. However, the double *tlo1*Δ/*tlo2*Δ mutant (*tlo*ΔΔ) had a more severe filamentation defect than the *TLO1* deletion alone, suggesting that *TLO2* partly compensates for the deletion of *TLO1* in the single mutant (Figure 3A, 3D). The cellular morphology of the *tlo1*Δ/*tlo2*Δ mutant in 10% serum was characteristically pseudohyphal (Figure 3D).

In order to investigate if *TLO1* and *TLO2* are functionally different, we reintroduced *TLO1* and *TLO2* individually to the *tlo1*Δ/*tlo2*Δ mutant using a previously described integrating vector pCDRI. This strategy was employed as it allowed us to express both *TLO1* and *TLO2* to similar levels (Figure 1C) thus allowing a direct comparison of their ability to complement the phenotypes of the *tlo1*Δ/*tlo2*Δ mutant. Introduction of *TLO1* could restore true hypha production to almost wild-type levels, whereas *TLO2* restored hypha formation to approximately 50% of wild-type levels (Figure 3B, 3D). These data show that *TLO1* and *TLO2* differ in their ability to activate filamentous growth.

Deletion of *TLO1* and *TLO2* produces multiple phenotypes

The colony morphology of the *tlo1*Δ, *tlo2*Δ and *tlo1*Δ/*tlo2*Δ mutant strains following growth on nutrient-rich solid medium (YEPD agar) at 37°C was indistinguishable from that of wild-type. At the cellular level, the *tlo1*Δ/*tlo2*Δ mutant grew as short chains of 3–4 cells, which is indicative of a defect in cytokinesis (Figure S3A). A similar phenotype was described by Uwamahoro et al. [15] in a *C. albicans med31*Δ mutant. Wild-type cytokinesis was restored in the *tlo1*Δ/*tlo2*Δ mutant following reintroduction of *TLO1* but not *TLO2* (Figure S3A). Growth defects of *tlo* mutants became apparent when grown on non-optimal media. On Spider agar, the wild-type strain formed smooth white colonies, typical of *C. dubliniensis* on this medium. However, the *tlo1*Δ/*tlo2*Δ mutant formed heavily wrinkled colonies on this medium (Figure S3B). Wild-type smooth colonies could be restored by complementation of the *tlo1*Δ/*tlo2*Δ mutant with either *TLO1* or *TLO2* (Figure S3B). Following 5 days incubation on Pal's medium, the double mutant produced extensive levels of pseudohyphae, but unlike wild-type which produced copious amounts of chlamydospores on this medium, no terminal differentiation of these pseudohyphae to chlamydospores was observed (Figure S4A). The *TLO1* mutant and the *tlo1*Δ/*tlo2*Δ double mutant also exhibited longer doubling times in several different liquid media, including YEPD (Table 1). When galactose was substituted for glucose in YEP medium (YEP-GAL), the growth rate of the *tlo1⊿* and the *tlo1*Δ/*tlo2*Δ mutants was reduced with doubling times 1.4 to 1.6 times longer than wild-type doubling times, respectively (Table 1). Growth in synthetic liquid Lee's medium was also retarded, with a doubling time 1.6 fold higher than that of wild-type. The addition of 1% peptone restored growth to WT levels in the *tlo1*Δ/*tlo2*Δ mutant

Table 1. Doubling times (min) of *tloΔ* mutants and complemented strains *in vitro*.*

Growth Media	Wü284	*tlo1Δ*	*tlo2Δ*	*tloΔΔ*	*tloΔΔ+TLO1*	*tloΔΔ+TLO2*
YEPD	94.92	104.6	91.72	102.9	*nd*	*nd*
	0.9865	*0.9502*	*0.9783*	*0.9044*	*nd*	*nd*
YEP-Galactose	95.17	129.2	106.8	149.3	84.29	103.1
	0.9828	*0.9933*	*0.9995*	*0.9821*	*0.9916*	*0.9974*
YEP-Succinate	89.31	110.8	91.88	132	94.46	112
	0.9228	*0.9835*	*0.9826*	*0.9037*	*0.9707*	*0.8614*
Lee's defined medium	100.6	106.6	97.27	157.6	127.3	130.1
	0.978	*0.9598*	*0.9836*	*0.7243*	*0.8682*	*0.9675*
Spider medium	152.4	168.2	145.4	178.7	161.1	175.9
	0.9535	*0.9842*	*0.9528*	*0.966*	*0.9464*	*0.9456*

* The coefficient of determination (r^2) value is shown italicised below each doubling time value as an indicator of confidence in the data when analysed using regression.

doi:10.1371/journal.pgen.1004658.t001

(Figure S4B) while the addition of carbon sources or individual amino acids to solid Lee's medium did not.

Reintroduction of either *TLO1* or *TLO2* in the *tlo1Δ/tlo2Δ* double mutant background restored doubling times to wild-type levels in YEP-GAL. However, reintroduction of *TLO1* had a significantly greater effect on doubling time compared to complementation with *TLO2*. In contrast, either *TLO1* or *TLO2* restored the growth defect on Lee's medium to the same degree (Table 1).

We next investigated if *TLO* genes affect a range of stress responses. Supplementation of YEPD agar with H_2O_2 (7 mM) or menadione (100 mM), which generate reactive oxygen species, inhibited growth of the *tlo1Δ/tlo2Δ* mutant, partly inhibited growth of the *tlo1Δ* mutant, while growth of the *tlo2Δ* single mutant was largely unaffected by these oxidizing agents (Figure 3E). Reintroduction of either *TLO1* or *TLO2* to the *tlo1Δ/tlo2Δ* strain restored wild type growth in the presence of both H_2O_2 and menadione, indicating that both *TLO* genes have a role in the growth of cells under oxidative stress.

med3Δ phenocopies a *tlo1Δ/tlo2Δ* mutant

Tlo proteins are components of the Mediator complex, which is thought to facilitate interactions between Mediator and DNA-bound transcriptional activators [8]. As Tlo protein and Med3 are required for the stability of the Mediator tail in *C. dubliniensis* (Figure 2), we hypothesized that deletion of *MED3* and *TLO* genes should result in similar phenotypic effects. To test this, we compared the phenotypes of *C. dubliniensis tlo1Δ/tlo2Δ* and *med3Δ* mutants. The *C. dubliniensis med3*Δ mutant, similar to the *C. albicans med3*Δ mutant [9] and the *C. dubliniensis tlo1Δ/tlo2Δ* mutant was unable to form true hyphae in 10% serum (Figure 3C) and exhibited extended doubling times in YEP-Gal (Figure S5A) and increased susceptibility to H_2O_2 (Figure S5B). All of these properties could be restored to wild-type levels in the *med3*Δ mutant with the reintroduction of a wild-type copy of *MED3* on pCDRI (Figure 3C, S4A, S4B).

Tlo proteins regulate the transcription of a diverse set of genes

Since Mediator is important for transcription regulation, we analysed RNA expression patterns in the *tlo1*Δ/*tlo2*Δ mutant relative to wild-type cells grown in nutrient-rich growth conditions (YEPD at 37°C) and grown in hyphal inducting conditions (water plus 10% serum, optimal for *C. dubliniensis* hypha formation). During exponential growth in YEPD, a total of 746 genes exhibited a 1.5-fold or greater increase in expression and 635 genes exhibited a 1.5-fold or greater reduction in expression ($Q \leq 0.05$; Figure 4A). This scale of differential gene expression observed in our *tlo1Δ/tlo2Δ* is similar to that seen in *S. cerevisiae* Mediator tail mutants [23,24]. In the nutrient-rich YEPD broth, the *tlo1Δ/tlo2Δ* mutant exhibited a transcriptional profile that resembled a response to nutrient starvation (Figure 4B). The induced set of genes was enriched for processes associated with catabolism of alternative carbon and nitrogen sources such as *N*-acetyl-glucosamine (*NAG1, NAG3, NAG4, NAG6*), amino acids (e.g. *GDH2, CAR1, PUT2, PUT1, LPD1, FDH1* and *FDH3*) and fatty acids. The *tlo1*Δ/*tlo2*Δ mutant cells also up-regulated key genes of gluconeogenesis (*PCK1* and *FBP1*) and the glyoxylate cycle (*ICL1* and *MDH1*) (Figure 4B). In concert with this, the *tlo1*Δ/*tlo2*Δ mutant also caused down-regulation of genes encoding glycolytic enzymes (*PFK1*, *PFK2*, *FBA1*, *GPM1* and *ENO1*) and the glycolytic regulator *TYE7*. The *tlo1*Δ/*tlo2*Δ mutant also exhibited a greater than 2-fold decrease in expression of genes encoding proteins important for sulphur amino acid biosynthesis (e.g. *SAM2, MET1, MET6, MET10, MET14, MET16*) and ergosterol biosynthesis (*ERG1, ERG9, ERG25*). In addition, some hypha-specific genes were induced in the *tlo1*Δ/*tlo2*Δ mutant grown in YEPD. This included *IHD1*, *RBT5* and *SAP7* (induced in *C. dubliniensis* hyphae) as well as several regulators of biofilm and hyphal growth (*BCR1*, *NRG1*, *SFL1*, *TEC1* and *EED1*).

Gene Set Enrichment Analysis (GSEA) was used to compare the *tlo1*Δ/*tlo2*Δ regulated genes with published microarray datasets. GSEA indicated that the set of genes differentially expressed in the *tlo1*Δ/*tlo2*Δ mutant was enriched for genes induced during infection of RHE [25] and genes both induced and repressed during infection of bone-marrow derived macrophages [26] (Figure S6).

We also examined the transcript profile of the *tlo1Δ/tlo2Δ* mutant in 10% serum relative to wild-type (Figure 4A). After 1 h, 868 genes were significantly up-regulated 1.5-fold or greater and 816 ORFs downregulated ($Q \leq 0.05$) relative to wild-type expression at the same time point. In this medium the *tlo1Δ/tlo2Δ* mutant exhibited reduced expression of several key regulators of filamentous growth including *RAS1*, *RIM101*, *EFG1* and *UME6*. In addition, the hyphal growth regulating cyclins *CLN3* and

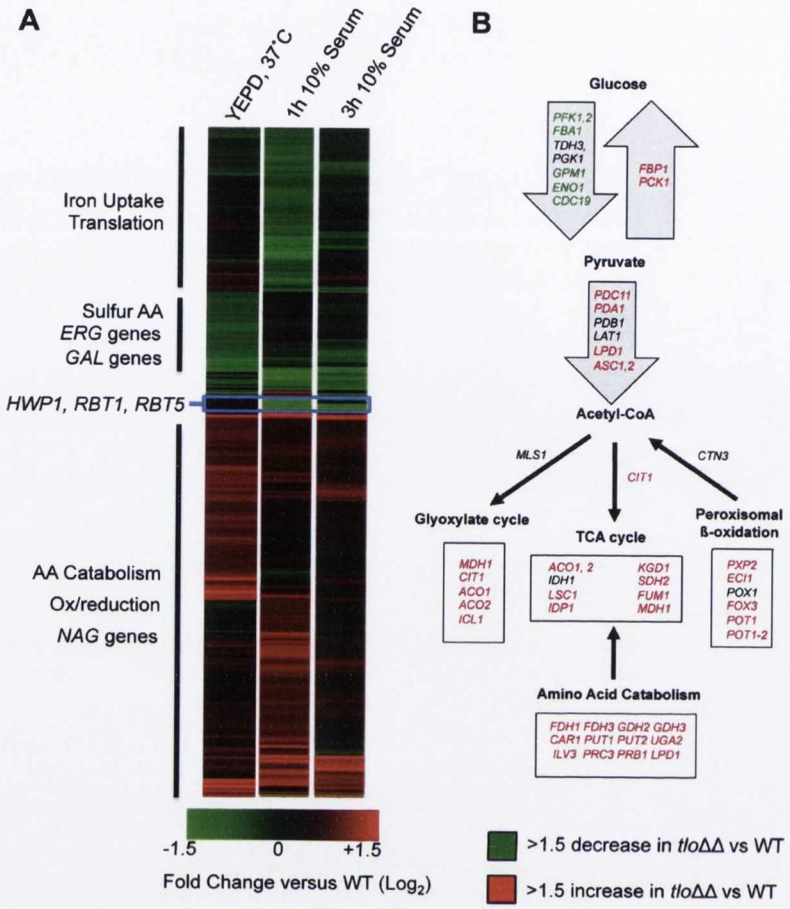

Figure 4. Microarray gene expression profiling of the *tlo1Δ/tlo2Δ* (*tloΔΔ*) mutant in YEPD and 10% serum. (A) A heat map generated in GeneSpring GX12 showing all 1.5 fold regulated genes in the *tlo1Δ/tlo2Δ* (*tloΔΔ*) mutant relative to wild type strain Wü284 during exponential growth in YEPD broth and following inoculation in 10% (v/v) serum (1 h and 3 h). The fold change (Log_2) relative to wild-type is color coded as indicated in the lower panel. GO terms associated with up and down regulated clusters are indicated on the left. (B) A cartoon metabolic map of the *tlo1Δ/tlo2Δ* (*tloΔΔ*) mutant showing the changes in expression of genes involved in energy metabolism during growth in YEPD. Genes in green exhibit a 1.5-fold or greater reduction in expression relative to wild-type whereas those in red exhibited a 1.5-fold increase in expression. Genes in black were not significantly changed.
doi:10.1371/journal.pgen.1004658.g004

HGC1 were also down regulated in the *tlo1Δ/tlo2Δ* mutant. The *tlo1Δ/tlo2Δ* mutant also exhibited reduced expression of many cell wall proteins whose induction is chracteristic of the yeast-to-hypha transition in *C. dubliniensis*, including *HWP1*, *RBT1*, *RBT5* and *SOD5* [20]. Paradoxically the *tlo1Δ/tlo2Δ* mutant exhibited a more rapid induction of the hypha-specific gene *ECE1* following 1 h incubation in serum, and expression remained elevated relative to wild-type at 3 h. In addition to hyphal genes, the *tlo1Δ/tlo2Δ* mutant exhibited reduced expression of galactose metabolic genes *GAL1*, *GAL7* and *GAL10*.

After 3 hours in 10% serum, a similar number of genes were differentially expressed 1.5-fold or greater (n = 1726). However, the level of differential expression at many genes had decreased by 3 h (Figure 4A).

TLO1 and *TLO2* restore expression of different subsets of genes

In order to investigate whether *TLO1* and *TLO2* regulate similar or different sets of genes, we analysed the transcript profiles of the *TLO1* and *TLO2* complemented mutants rather than the *tlo1Δ* and *tlo2Δ* single mutants, as the complemented strains exhibited equivalent expression of *TLO1* or *TLO2* (Figure 1B, 1C). Both *TLO1* and *TLO2* largely restored the transcript profile of the *tlo1Δ/tlo2Δ* mutant back to wild-type levels in both YEPD and 10% serum (Figure 5A, 5B). However, some *TLO*-specific transcript patterns were also detectable. Sixty-one genes were regulated in a *TLO*-specific manner in YEPD (Table S1). In comparison to the *TLO1*-complemented strain, the *TLO2*-complemented strain showed a greater reduction in expression of many *tlo1Δ/tlo2Δ* induced genes, including many hyphal genes (*IHD1*, *SAP7* and *EED1*), negative regulators of hyphal growth (*NRG1* and *SFL1*) and some starvation-induced genes such as *CAR1*, *GDH3*, *NAG3* and *NAG4* (Figure 5C). The *TLO2* complemented strain was also better at restoring wild-type levels of *SOD6* expression relative to the *TLO1* complemented strain (Figure 5C).

In 10% serum, *TLO1* was more effective at restoring expression of several genes required for induction of, and induced during,

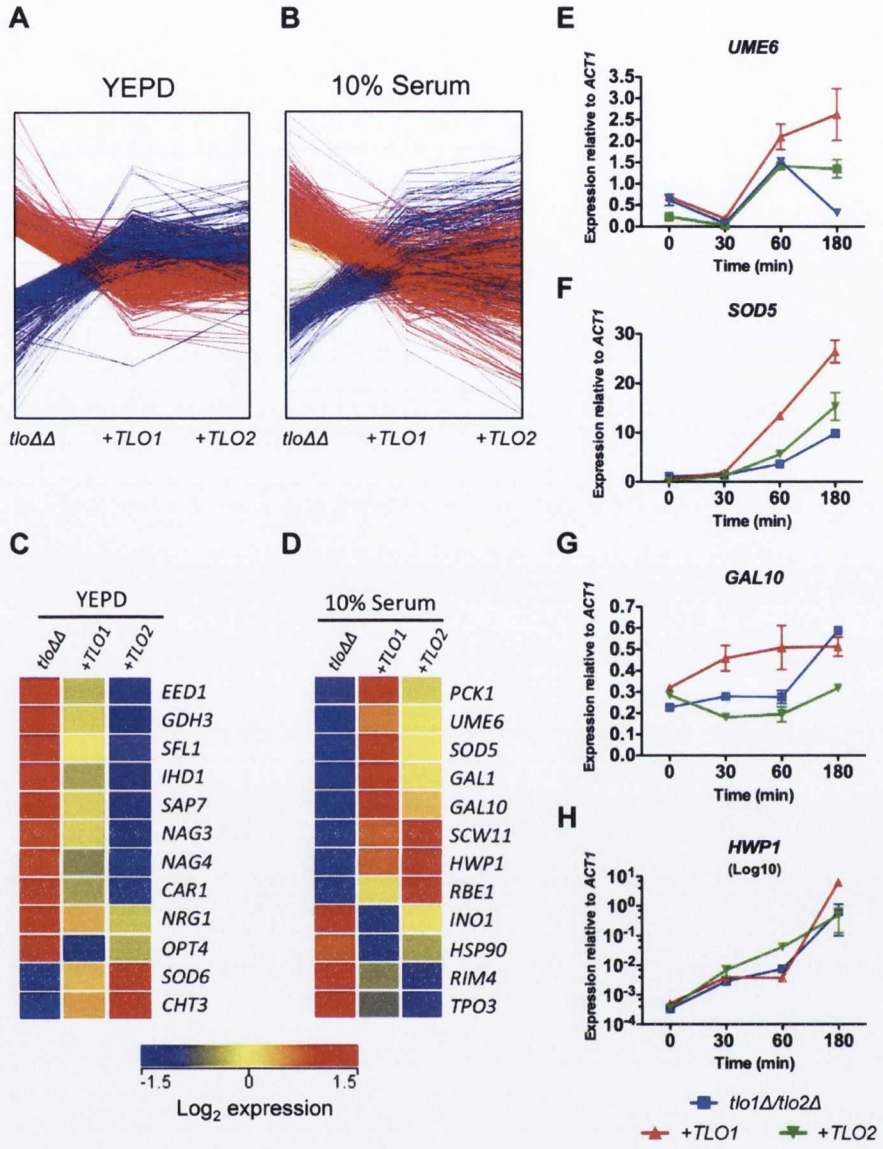

Figure 5. Reintroduction of *TLO1* or *TLO2* in the *tlo1*Δ/*tlo2*Δ (*tlo*ΔΔ) mutant restores wild-type levels of expression of overlapping and distinct sets of genes. (A) A graph plotting the change in expression of genes up regulated (red lines) or down regulated (blue lines) in the *tlo1*Δ/*tlo2*Δ (*tlo*ΔΔ) mutant following complementation with either *TLO1* (+*TLO1*) or *TLO2* (+*TLO2*) in YEPD or (B) 10% (v/v) serum. (C) Heat map of selected genes that were differentially expressed in the *tlo1*Δ/*tlo2*Δ (*tlo*ΔΔ) mutant during growth in YEPD broth (C) or 10% (v/v) serum (D) that exhibited a *TLO1* or *TLO2* specific restoration to wild-type in expression. Colors in the first column (*tlo1*Δ/*tlo2*Δ) represent the fold change in expression of the indicated genes in *tlo*ΔΔ vs wild-type; colors in columns 2 and 3 (+*TLO1* and +*TLO2*) represent the fold change in expression of the indicated genes following reintegration of *TLO1* or *TLO2* versus *tlo*ΔΔ. (E to H) QRT-PCR of the indicated genes was carried out following 30, 60 and 180 min incubation in 10% (v/v) serum at 37°C. Gene expression was determined using Sybr green technology and gene-specific levels are expressed relative to *ACT1*. Primer sequences are listed in Table S5.
doi:10.1371/journal.pgen.1004658.g005

filamentous growth including *UME6* and *SOD5* (Table S2, Figure 5D). *TLO1* was also a more effective inducer of *GAL1* and *GAL10* expression, which may explain why restoration of growth in galactose medium was more effective in the *TLO1* reintegrant relative to the *TLO2* complemented strain (Figure 5D). In contrast, *TLO2* was more effective at inducing *HWP1* expression (Figure 5D). More detailed analysis of hyphal-induced gene expression by QRT-PCR corroborated these microarray findings and supported the existence of a temporal defect in the induction of hypha specific genes in the *tlo1*Δ/*tlo2*Δ mutant. QRT-PCR showed that *UME6* and *SOD5* exhibited weak levels of induction in the *tlo1*Δ/*tlo2*Δ mutant relative to the *TLO1* reintegrant (Figure 5E, 5F). Although addition of *TLO2* led to a minor increase in *SOD5* expresssion, complementation with *TLO1* restored high-level induction of *SOD5*. Similarly, induction of *GAL10* also occurred more rapidly in the *TLO1*-reintegrated

strain relative to both the *tlo1Δ/tlo2Δ* mutant and the *TLO2*-reintegrated strain (Figure 5G) Conversely, QRT-PCR confirmed that *TLO2* restored more rapid induction (~10-fold) of the *HWP1* transcript following 1 h incubation in serum relative to the *TLO1* reintegrant (Figure 5H). However *HWP1* expression in the *tlo1Δ/tlo2Δ* mutant and *TLO1* reintegrant reached similar levels following three hours incubation in serum (Figure 5H).

This transcriptional analysis of the *TLO1* and *TLO2* complemented strains for the first time demonstrate functional diversification of Tlo proteins and show that different Tlos can regulate distinct subsets of genes.

Deletion of *MED3* disrupts transcription of a similar set of genes

This study has shown that deletion of *MED3* in *C. dubliniensis* results in similar phenotypes to those observed in the *tlo1Δ/tlo2Δ* mutant. In order to determine whether these gene deletions resulted in similar changes in transcript profile, we compared gene expression in the *tlo1Δ/tlo2Δ* and the *med3Δ* mutant in YEPD broth and in 10% serum. Hierarchical clustering was used to compare all 1.5-fold regulated genes in strains *tlo1Δ/tlo2Δ* and *med3Δ* during exponential growth. This comparison demonstrated the similarity of the transcriptional changes in both mutants relative to wild-type cells (Figure 6A). A large number (n = 47) of these commonly down-regulated genes were associated with the GO term "ribosome biogenesis" ($P = 3.89 \times 10^{-19}$; FDR = 0.0). In YEPD, both mutants exhibited aberrantly increased expression of the hypha-specific genes *IDH1*, *RBT5* and *SAP7* as well as the regulators *TEC1* and *EED1*. Activation of starvation responses was also evident in the *med3Δ* strain, which like the *tlo1Δ/tlo2Δ* strain exhibited increased expression of genes involved in gluconeogenesis (*PCK1, FBP1*) and the glyoxylate cycle (*ICL1, MDH1*). Decreased expression of glycolytic genes was less pronounced in *med3Δ*, however we could detect decreased expression (>1.5-fold) of *PFK1*, *PFK2*, *CDC19* the glycolytic regulator *TYE7* (Figure S7). Similar to *tlo1Δ/tlo2Δ*, *med3Δ* also exhibited increased expression of genes involved in oxidation/reduction processes, including amino acid catabolism (Figure 6B) in addition to reduced expression of genes involved in sulphur amino acid metabolism (*CYS3, MET1, 2, 4, 10*) and ergosterol metabolism (*ERG1, ERG251*).

Following 1 h growth in water plus 10% serum the *med3Δ* and *tlo1Δ/tlo2Δ* mutants again exhibited a common set of co-regulated genes, however in serum many *med3Δ* mutant-specific responses could also be identified (Figure 6B, 6C). The common gene set included regulators of filamentous growth, cell wall proteins and galactose metabolic genes (Figure 6B). Importantly, the *med3Δ* mutant specifically exhibited an increase in expression of glycolytic genes (n = 11; Figure 6C, S6) and genes encoding histones and proteins involved in chromatin assembly (n = 18). The *med3Δ* mutant also exhibited reduced transcription of genes associated with the GO terms "DNA replication" (n = 43) and "telomere maintenance" (n = 18) (Figure 6C).

These data indicate that in exponentially growing cells, Tlo proteins and Med3 are involved in regulating very similar processes. However, in response to specific environmental cues, these proteins may be required for regulation of specific sets of genes.

Deletion of *TLOs* has different effects on virulence traits compared to a *C. albicans med31Δ* mutant

Uwamahoro *et al.* [15] showed that in *C. albicans* deletion of *MED31*, encoding a middle subunit of Mediator affected cytokinesis, filamentous growth and biofilm formation. Similarly, the *C. dubliniensis tlo1Δ/tlo2Δ* mutant described here also grew as chains of cells, typical of mutants with defects in cytokinesis (Figure S3A). However, the *C. albicans med31Δ* mutant was capable of filamentous growth in response to serum, whereas the *C. dubliniensis tlo1Δ/tlo2Δ* mutant is incapable of forming true hyphae in serum. GSEA analysis of our *C. dubliniensis tlo1Δ/tlo2Δ* mutant transcript data identified a significant enrichment for genes that are also affected in a *C. albicans med31Δ* mutant [15]. Interestingly, while the *tlo1Δ/tlo2Δ* and the *med31Δ* deletions affected similar genes, the *C. dubliniensis tlo1Δ/tlo2Δ* mutant showed increased expression of genes that were both Med31-activated and -repressed in *C. albicans* (Figure 7A). Inspection of these differentially expressed genes identified several genes required for biofilm formation that were downregulated in the *C. albicans med31Δ* mutant and induced in the *C. dubliniensis tlo1Δ/tlo2Δ* mutant, including *ALS1*, *TEC1* and *SUC1*. Uwamahoro *et al.* [15] showed that reduced *ALS1* expression in the *C. albicans med31Δ* mutant was largely responsible for the defect in biofilm formation. As the *C. dubliniensis tlo1Δ/tlo2Δ* mutant exhibited increased expression of *ALS1*, we examined whether this mutant was affected in biofilm formation. In contrast to the *med31Δ* mutant phenotype, deletion of *TLO1* and *TLO2* in *C. dubliniensis* enhanced biofilm growth on plastic surfaces (Figure 7B). In this case, complementation with *TLO2* reduced the amount of biofilm formation more than complementation with *TLO1* (ANOVA $P<0.05$) (Figure 7B). Thus the mediator middle domain has a different effect on biofilm formation than does the mediator tail domain.

Tlo proteins regulate a core set of Med2 regulated genes

The genetic and biochemical data presented here and by Zhang *et al.* [9] support a hypothesis that Tlo proteins are the candidal orthologs of *S. cerevisiae* Med2. In order to support this, we decided to compare the transcript profile of the *C. dubliniensis tlo1Δ/tlo2Δ* mutant and the *S. cerevisiae med2Δ* mutant to identify if there is an evolutionarily conserved core regulon controlled by these proteins [27]. Although the experimental details of the two studies vary, a comparison of all genes regulated 1.5-fold or greater in both mutants could identify a small but significant overlap in regulated genes (Figure S8). Carbohydrate metabolism genes that were downregulated in both mutants included the carbohydrate metabolism master regulator *TYE7* and genes regulating carbohydrate catabolism and glycerol biosynthesis (*PFK1, FBA1, GPH1, GDB1*). One of the signatures of the *tlo1Δ/tlo2Δ* mutant profile was the downregulation of sulphur amino acid metabolism and in *S. cerevisiae*, we could also detect down regulation of *MET6* and *MET13* as well as several other conserved genes regulating amino acid catabolism (*GCV1, GCV2, SHM2*). Both mutants exhibited a general increase in the expression of genes encoding enzymes involved in oxidation-reduction processes (Figure S8).

ChIP supports a role for Tlo1 in transcriptional activation and repression

In order to characterise Tlo1-DNA interactions, we carried out chromatin immunoprecipitation and high-density *C. dubliniensis* microarray (ChIP-chip) of HA-tagged Tlo1 from cells grown in YEPD broth at 30°C. On a genome wide level, we found extensive binding of Tlo1 to all chromosomes. The regions exhibiting the greatest enrichment included subtelomeric and telomeric regions and the Major Repeat Sequence (MRS) (Figure 8A). Outside of these regions, the interaction of Tlo1 was closely associated with the coding regions of genes (Figure 8A). Excluding subtelomeric

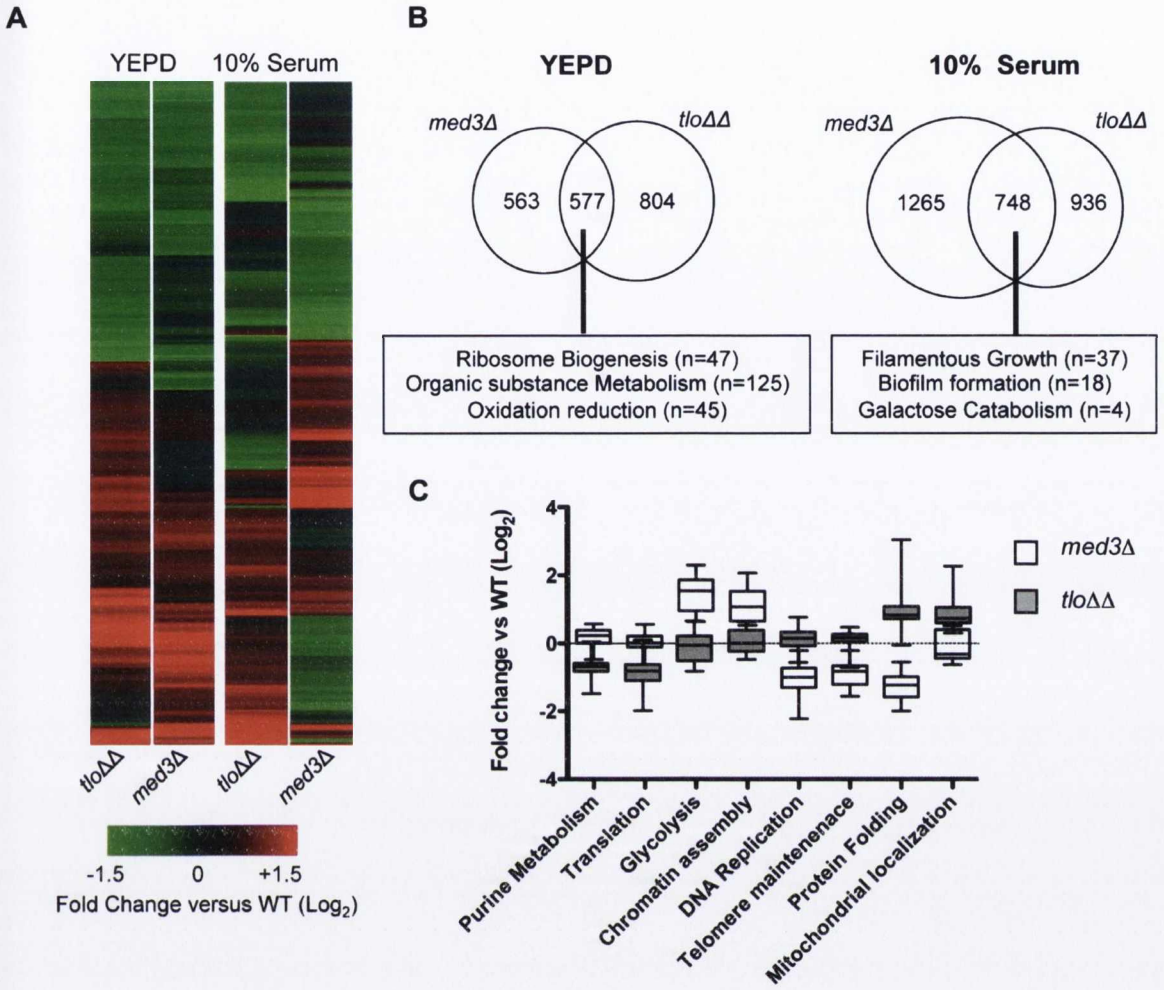

Figure 6. Microarray gene expression profiling of the *med3Δ* mutant in YEPD and 10% (v/v) serum. (A) A heat map generated in GeneSpring GX12 showing all 1.5 fold regulated genes in the *tlo1Δ/tlo2Δ* (*tloΔΔ*) and *med3Δ* mutants relative to wild type strain Wü284 during exponential growth in YEPD broth and following inoculation in 10% serum (1 h). The fold change (Log_2) relative to wild-type is color coded as indicated in the lower panel. (B) Venn diagrams illustrating the numbers of genes commonly regulated greater than 1.5-fold in the *tlo1Δ/tlo2Δ* (*tloΔΔ*) and *med3Δ* mutants following growth in YEPD broth or 10% serum. The box below indicates major functional classes of commonly regulated genes identified by GO term analysis using the GO Term finder at CGD (http://www.candidagenome.org/). (C) Graph plotting the expression levels (Log_2 fold change versus wild-type) of genes associated with selected GO terms in the *tlo1Δ/tlo2Δ* (*tloΔΔ*) and *med3Δ* mutants during growth in 10% (v/v) serum.

doi:10.1371/journal.pgen.1004658.g006

regions, only 45 intergenic regions exhibited a significant enrichment peak not associated with a coding region. In addition, we did not observe any association between Tlo1 and 57 putative Pol III transcribed tRNAs and snRNAs. Tlo1 was enriched at 1,617 ORFs in the *C. dubliniensis* genome (27% of all nuclear genes; Ringo Peak Score 0.8).

Due to recent discussions in the literature regarding artefacts in ChIP data [28–30], we restricted detailed analysis to a group of 367 genes that exhibited highly significant Tlo1-enrichment (Ringo peak score 0.9; Table S3). The region of Tlo-enrichment was centred on the coding region with extension into 5′ and 3′ flanking non-coding regions (Figure S9A). The level of Tlo-enrichment at the 5′ region was variable and was generally <100 bp in length, however extensions up to 1000 bp in length were observed (Figure S9B). QRT-PCR analysis of DNA generated in replicate ChIP experiments confirmed the high levels of enrichment observed at *PUT1* and *ACT1* and low enrichment levels observed at non-enriched genes such as *CLN1* and Cd36_51290 and an intergenic region on chromosome 5 (bp 521680–521729) (Figure 8B, 8C). Due to the repetitive nature of the repeat sequences in the MRS, it was not possible to accurately determine the level of enrichment in this region by QRT-PCR.

Using fluorescence intensity data extracted from our gene expression microarrays, we compared the expression levels of the Tlo1-associated ORFs relative to non-Tlo1 associated ORFs. Tlo1-associated ORFs were found to exhibit higher expression levels (average 1.8-fold) in YEPD compared to those genes that are not occupied (Figure S9C). However, a plot of enrichment score versus expression level did not identify a direct correlation between Tlo1 enrichment and expression. Importantly, the most highly

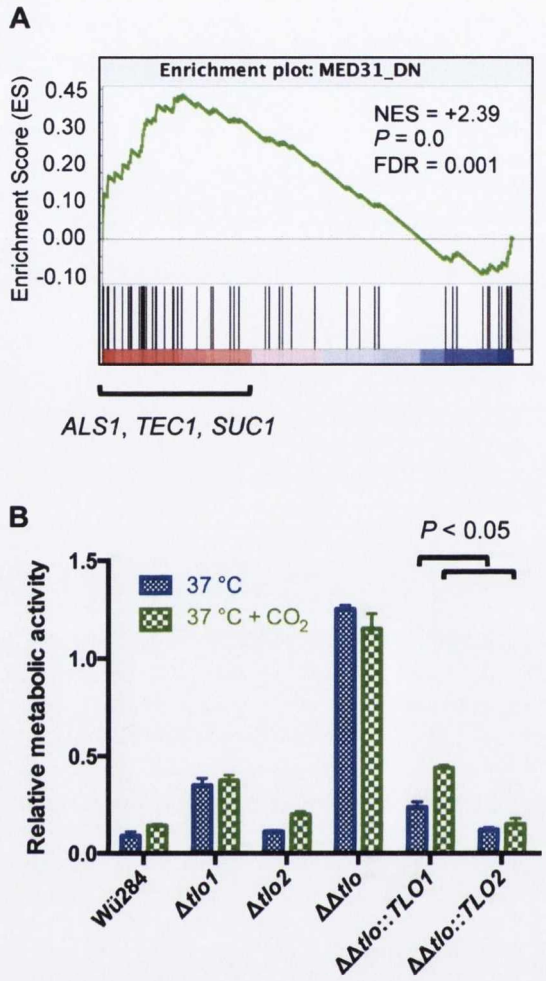

Figure 7. Deletion of *TLOs* has different effects on biofilm formation compared to a *med31*Δ mutant. (A) Gene Set Enrichment Analysis (GSEA) plot showing differential expression of genes down-regulated in a *C. albicans med31*Δ mutant in the *tlo1*Δ/*tlo2*Δ mutant (i.e. they are upregulated in the *tlo1*Δ/*tlo2*Δ mutant) (B) Biofilm formation was assessed in the indicated strains on plastic surfaces at 37°C in the presence or absence of 5% CO_2 as indicated. Adherent biomass determined by an XTT reduction assay. The experiment was carried out in triplicate on three separate occasions (n = 9) and error bars represent the standard deviation from the mean. *P* values above figure are the result of one-way ANOVA with Tukey's post hoc test.
doi:10.1371/journal.pgen.1004658.g007

enriched genes (n = 367; Ringo peak score 0.9) covered a broad spectrum of expression levels, including genes expressed at high and low levels in YEPD (Figure 9A). We analysed the GO terms associated with these Tlo1-enriched genes and identified significant numbers of highly expressed genes associated with the GO categories glycolysis (n = 7; $P = 0.003$) and the TCA cycle (n = 7; $P = 0.048$)(Figure 9A). Manual inspection of the gene list also identified highly expressed genes involved in translation (n = 5) and sulphur amino acid metabolism (n = 4). Tlo1-enriched genes that are poorly expressed in YEPD were associated with the GO categories glyoxylate cycle (n = 3; $P = 0.09$), GlcNac catabolic process (n = 6, $P = 0.094$), amino acid catabolic process (n = 10; $P = 0.018$) and hexose transport (n = 9; $P = 0.057$). Manual inspection also identified poorly expressed genes encoding nitrogen scavenging transporters (e.g. *FRP6, MEP21, MEP22, DAL1, UGA6*) and genes involved in gluconeogenesis (*PCK1* and *FBP1*). Many YEPD repressed, hypha-specific genes were also enriched including *EED1*, *RBT1*, *HWP1*, *HWP2* and *IHD1*.

These data show that Tlo1 is present at many highly expressed metabolic genes in addition to genes normally repressed in YEPD (starvation, hyphal genes) indicating a dual role in transcriptional activation and repression. In order to support this hypothesis, we analysed the transcription of these categories of Tlo1-enriched genes in our *tlo1*Δ/*tlo2*Δ mutant. This analysis found that the highly expressed genes involved in glycolysis and sulfur amino acid metabolism exhibited significantly reduced expression (ANOVA; $P<0.05$) in the *tlo1*Δ/*tlo2*Δ mutant relative to wild type cells, indicating that Tlo1 occupancy is required for maintaining the high level of expression of these genes (Figure 9B). The exceptions to this finding were the genes encoding enzymes of the TCA cycle, which although highly expressed in wild-type cells, exhibited increased expression in the *tlo1*Δ/*tlo2*Δ mutant. In addition, highly Tlo1-occupied, low expression genes exhibited increased expression in the *tlo1*Δ/*tlo2*Δ mutant, including genes involved in starvation responses, nitrogen scavenging mechanisms, *N*-acetyl glucosamine catabolism and the hyphal GPI-anchored proteins (Figure 9B). These data indicate that Tlo1 and the Mediator complex are involved in both transcriptional activation and repression of different classes of genes. The fact that Tlo1-enriched genes exhibit regulation in the *tlo1*Δ/*tlo2*Δ mutant also provides support for hypothesis that Tlo proteins interact with these ORFs.

Discussion

Despite the importance of Mediator in transcriptional regulation, few studies have investigated the role of Mediator in regulating virulence-associated characteristics in pathogenic eukaryotic microrganisms. The discovery of a widely dispersed telomeric gene family with homology to Med2 in the pathogenic yeast *C. albicans* has accelerated the level of interest in Mediator in this fungus. Published data suggest important roles for Mediator in regulating important biological processes in *C. albicans*, including filamentous growth (Med3), biofilm formation (Med31, Med20) and white-opaque switching (multiple subunits) [9,15,16]. Because functional analysis of the 15 *TLO* paralogs in *C. albicans* remains technically challenging, we turned to *C. dubliniensis*, which shares many characteristics with *C. albicans* but contains only two *TLO* orthologs, thereby providing an ideal genetic background in which to investigate the degree to which *TLO* gene function(s) have diverged between the two *TLO* paralogs. It has been hypothesized that in *C. albicans*, Mediator could form variant complexes that contain different Tlo/Med2 subunits that could be differentially recruited to activate or repress different subsets of genes in response to specific stimuli [9,12]. *C. dubliniensis*, which has only two Tlo proteins that appear to associate primarily with Mediator, provides an invaluable tool to understand first, how different *TLO* genes may affect Mediator function and second how the presence of multiple variant *TLO* genes contributes to virulence.

In *C. dubliniensis*, *tlo1*Δ deletion mutants are defective in hyphal growth [14]. Here, we constructed a null *tlo1*Δ/*tlo2*Δ double mutant strain of *C. dubliniensis*. The *tlo1*Δ/*tlo2*Δ strain exhibits a wide range of phenotypic defects, indicating that they play a central role in global transcriptional control. Consistent with a role in regulating hyphal growth, deletion of both *TLO* genes reduced expression of many of the key regulators of

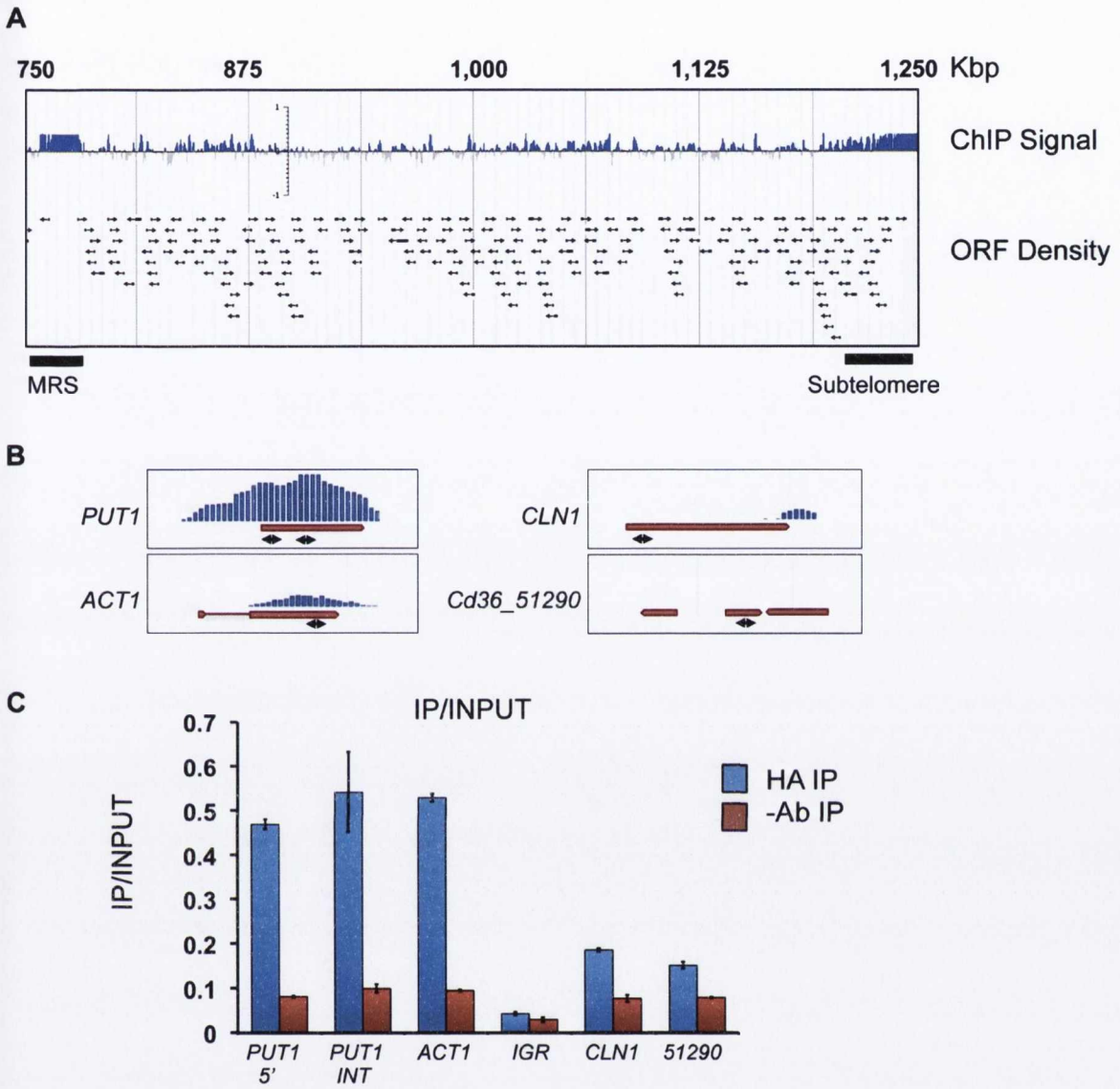

Figure 8. Localization of Tlo1-DNA interaction by ChIp-Chip analysis. (A) A map of the right arm of *C. dubliniensis* chromosome 5 showing Tlo1-HA enriched areas, including the subtelomeric and Major Repeat Sequence (MRS) regions. Arrows indicate the position of individual ORFs. All chromosomes can be visualised here: http://bioinf.gen.tcd.ie/jbrowse/?data=cdub. (B) ChIP-chip Enrichment profiles for *PUT1, ACT1, CLN1* and CD36_51290. Double headed arrows show approximate positions of amplimers used in QRTPCR confirmation experiments. (C) QRT-PCR confirmation of the enrichment levels shown in panel B using gene-specific primers and an intergenic region (IGR)-specific primer set (Chr5 521680–521729 bp)(Table S5). Amplification was carried out on immunoprecipitated chromatin in anti-HA antibody samples (HA-IP) and no antibody (-AB IP) negative control samples. Relative enrichment values refer to the quantity of DNA amplified from anti-HA immunoprecipitated samples ('enriched') relative to total input chromatin ('non-enriched').
doi:10.1371/journal.pgen.1004658.g008

morphogenesis including signal transducers (*RAS1, RIM101*) transcriptional regulators (*EFG1, UME6*) and kinases (*HGC1*), resulting in largely pseudohyphal growth phenotypes with reduced expression of key hyphal genes (*SOD5, RBT5, HWP1*). The *tlo1*Δ/*tlo2*Δ mutant also exhibited increased susceptibility to oxidative stress and reduced growth in the presence of alternative carbon sources. These data demonstrate that the *TLO*s of *Candida* spp. have evolved to regulate many key processes, including those important for virulence and growth in the host. In addition, the importance of Tlo in mediating transcriptional responses important for pathogenicity is shown in the similarity of our transcript profiles to those observed during infection of RHE and bone marrow-derived macrophages (Figure S6) [25,26]. Indeed, a *tlo1*Δ/*tlo2*Δ mutant grown in YEPD mounts a transcriptional response akin to that observed following phagocytosis by macrophages [1]. Recent studies have also shown that Mediator is an important regulator of the *Candida*-macrophage interaction [31]. One key observation regarding the transcriptional changes

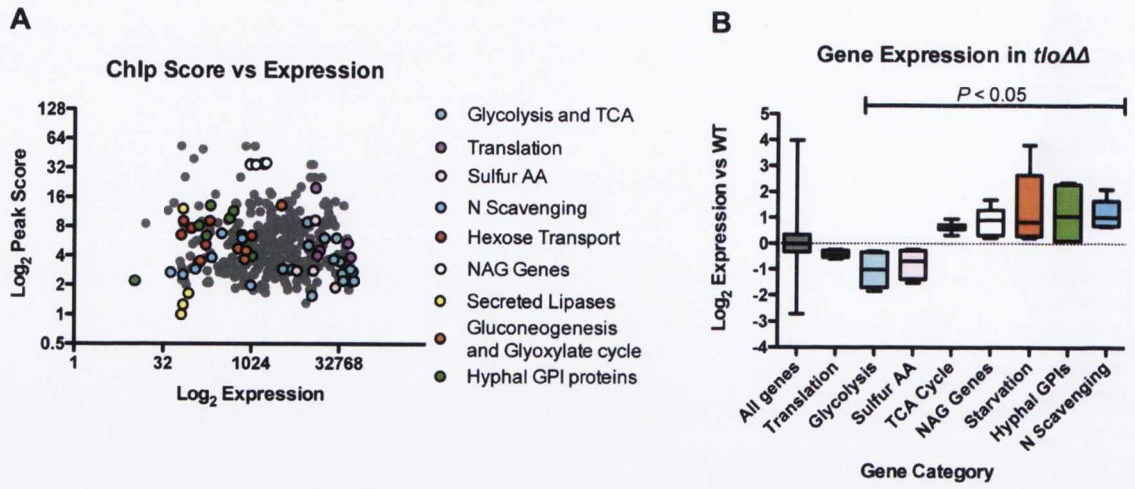

Figure 9. The relationship between Tlo1 binding and gene expression. (A) A plot of Tlo1 enrichment scores for the 367 most highly enriched genes versus the expression levels of those genes in YEPD broth (extracted from microarray data). The categories of highly expressed and repressed genes are color-coded; TCA = Tricarboxylic acid cycle; Sulfur AA = sulphur amino acid biosynthesis; N scavenging = Nitrogen scavenging; NAG = GlcNac metabolism; GPI = glycophosphatidylinositol anchor). (B) Analysis of the expression of Tlo1-enriched groups of genes in the wild type in the *tlo1*Δ/*tlo2*Δ (*tlo*ΔΔ) mutant indicated that the highly expressed, highly enriched genes exhibited reduced expression whereas the poorly expressed and repressed genes exhibited increased expression in the *tlo1*Δ/*tlo2*Δ (*tlo*ΔΔ) mutant. The change in expression in these groups, with the exception of the genes involved on translation, was significant (ANOVA, $P<0.05$).
doi:10.1371/journal.pgen.1004658.g009

observed in the *tlo1*Δ/*tlo2*Δ mutant was the alteration in the kinetics of induction of hypha-specific transcripts. Complementation of the *tlo1*Δ/*tlo2*Δ mutant with Tlo1 resulted in more rapid and higher levels of transcriptional induction of *SOD5*, *UME6* and *GAL10*. Some induction of these transcripts could be observed in the *tlo1*Δ/*tlo2*Δ mutant, however the amplitude of the response was greatly retarded relative to the complemented strains. These data suggest that Tlo proteins play an important role in maximizing the speed and magnitude of transcriptional changes in response to environmental cues. This characteristic is likely to be of great importance in the host where rapid responses could be important for survival, e.g. following phagocytosis or translocation to a different part of the gastrointestinal tract.

In *S. cerevisiae*, the Mediator tail regulates stress responses and the metabolism of carbohydrates and amino acids [23,24,27]. A direct comparison of the genes regulated in our *tlo1*Δ/*tlo2*Δ mutant and an *S. cerevisiae med2*Δ mutant supports this evolutionarily conserved role for Mediator tail in eliciting transcriptional responses to deal with changing environments [27]. In *S. cerevisiae* this effect has been shown to be centred on SAGA-regulated genes [24].

In this study, we also explored the relationship of Tlo proteins with other subunits of Mediator. A defect in filamentous growth was described by Zhang *et al.* in *C. albicans* following deletion of *Med3*, encoding another Mediator tail subunit that interacts with Tlo proteins [9]. Biochemical analysis of the Mediator complex in the *tlo1*Δ/*tlo2*Δ null mutant and the *C. dubliniensis med3*Δ mutant revealed the absence of Med5 and Med16 in Mediator purified from both mutants, suggesting that the entire tail complex is destablilized by loss of Tlo or Med3 proteins. Consistent with this idea, the *C. dubliniensis med3*Δ and *tlo1*Δ/*tlo2*Δ null mutants exhibited remarkably similar phenotypes and transcriptional profiles when cultured in YEPD. However, in response to hyphal stimulating conditions, many differences in transcriptional responses could be observed in the *tlo1*Δ/*tlo2*Δ strain and the *med3*Δ mutant strain (Figure 6), suggesting that Mediator complexes with different tail substituents may exist *in vivo* in response to specific environmental conditions. Alternatively, the deletion of either Med3 or Tlo protein may release the remaining Tail module Mediator subunits to form a sub-complex that can interact with cellular components independently of the remainder of the complex.

We next examined the relationship of Tlo with the Mediator middle subunit, Med31, described by Uwamahoro *et al.* [15]. The *C. dubliniensis tlo1*Δ/*tlo2*Δ null mutant exhibited a defect in cell separation and *CHT3* expression, which is consistent with the defect in cytokinesis described in the *C. albicans med31* mutant by Uwamahoro *et al.* [15]. These data support previous studies that suggest that regulation of cytokinesis and possibly Ace2-regulated genes is a conserved function of mediator in yeast [15,32]. However, a *med31*Δ mutant was still capable of true hyphal growth in liquid medium whereas the *tlo1*Δ/*tlo2*Δ null mutant was completely unable to form true hyphae under the same conditions. The most striking difference in phenotype was the increased ability of the *C. dubliniensis tlo1*Δ/*tlo2*Δ mutant to form biofilm. The *C. albicans med31*Δ mutant exhibits reduced biofilm growth relative to wild-type and decreased expression of the biofilm regulator *TEC1* and the adhesin *ALS1* (Figure 7A). The *C. dubliniensis tlo1*Δ/*tlo2*Δ null mutant exhibited increased expression of many *med31*Δ downregulated genes, including *TEC1* and *ALS1*, although the roles of these genes in biofilm formation in *C. dubliniensis* have yet to be confirmed. These data illustrate the very different and possibly opposing roles that mediator tail and middle subunits may have in transcriptional regulation in *Candida* spp.

Our ChIP analysis of Tlo1 for the first time indicates the level of Tlo and Mediator occupancy across the *Candida* genome. Although Mediator tail subunits are unlikely to interact directly with DNA, they associate closely with DNA-bound transcription factors and histones and have been successfully isolated in association with DNA in other yeasts [8,33]. We identified extensive Tlo1 binding across all *C. dubliniensis* chromosomes.

Tlo1 was closely associated with Pol II transcribed ORFs as well as the telomeres and the MRS. Binding of Mediator to telomeres and sub-telomeric genes has been described in *S. cerevisiae* and Mediator has been shown to have an additional role in heterochromatin maintenance [33,34]. Our data suggests that Mediator could play a similar role in *Candida* spp. The significance of Tlo1-enrichment at the MRS is more difficult to explain as the function of this repeat element is unknown. Further studies will be required to verify this interaction.

In order to limit the numbers of possible ChIP artefacts, often associated with highly expressed genes, we have used a very stringent cut off to define highly enriched genes. This Tlo1-enriched gene set includes repressed and moderately expressed genes, supporting the assumption that our data set is not biased for highly expressed ORFs. In addition, the highly expressed genes identified in our ChIP analysis are regulated following deletion of Tlo, supporting a direct, functional interaction with these ORFs.

The association of Mediator subunits with the coding regions of Pol II transcribed ORFs has been observed in Mediator ChIP localization experiments in other yeasts and suggests that Tlo1 may be involved in transcript elongation or in chromatin interactions at coding regions [35,36]. We observed that although Tlo1-occupied genes on average were expressed higher than non-occupied genes (average 1.8-fold), Tlo1 was associated with ORFs having a range of expression levels. To further investigate the significance of Tlo1 ORF occupancy and Tlo1-dependent gene expression, we compared the regulation of specific classes of Tlo1 occupied genes in our *tlo1*Δ/*tlo2*Δ mutant. Highly expressed genes encoding enzymes involved in amino acid synthesis, glycolysis and translation required Tlo1 to maintain high levels of expression. In contrast, genes that exhibited low levels of expression under the conditions analysed were repressed by Tlo1. These data suggest a dual role for Tlo1 in mediating transcriptional activation and repression. Specifically, Tlo1 was required to maintain transcription of genes involved in glycolysis and translation and to repress starvation responses (glyoxylate cycle, gluconeogenesis) and several hypha-specific genes. Localisation of Mediator to both expressed and repressed genes has been observed in *S. cerevisiae* and the ability of the complex to carry out opposing regulatory functions is likely due to its ability to adopt different modular conformations [36]. Specifically, the kinase module in *S. cerevisiae*, consisting of Cdk8, Cyclin C, Srb8 and Srb9 has been shown to associate with Mediator to repress transcription [36]. A specific role for the kinase module in transcriptional repression has yet to be determined in *Candida* spp.

The *C. dubliniensis* genome harbors two *TLO* orthologs, two alleles of *TLO1* and one allele of *TLO2*. One of the central goals of our study was to determine whether different *TLO* genes could regulate different processes. To compare the effects of single copies of *TLO1* and *TLO2*, we complemented the *tlo1*Δ/*tlo2*Δ mutant independently with either *TLO1* or *TLO2*. Each of the *TLO* genes complemented *tlo1*Δ/*tlo2*Δ mutant phenotypes, albeit to different degrees; *TLO1* was better at restoring true hyphal growth and growth in galactose. *TLO2* supressed biofilm growth to a greater extent than *TLO1*. With regard to *TLO2*, it should be noted that the level of expression of the reintegrated allele was significantly higher than the wild-type allele, which may have resulted in higher levels of Tlo2 activity. However, despite this, the reintegrated *TLO2* allele did not restore filamentous growth to the same extent as wild-type *TLO1*.

Support for these functional differences was obtained when the transcript profiles of the *TLO1* and *TLO2* complemented strains were compared. It was observed that *TLO1* could restore *GAL* gene induction to a greater extent than *TLO2*. During hyphal growth, *TLO1* also restored expression of *UME6* and *SOD5* to a greater degree than *TLO2*. In contrast, during growth in YEPD *TLO2* was required for repressing transcription of aberrantly expressed hyphal genes such as *IHD1*, *SAP7* and *EED1* and the negative regulators of hyphal growth *SFL1* and *NRG1*. *TLO2* was also required for suppression of many starvation induced genes involved GlcNac metabolism (*NAG3, NAG4*) and amino acid metabolism (*CHA1, GDH3*). The data suggest that the two *TLO* paralogs in *C. dubliniensis* have evolved to regulate overlapping as well as distinct subsets of genes. Under standard growth conditions, both *TLO1* and *TLO2* are expressed in *C. dubliniensis*, suggesting that two distinct pools of Mediator exist at any one time, with the ability to regulate different subsets of genes. The implications of our study for *C. albicans* biology, where there are potentially 15 different Tlo-Mediator complex varieties with differing transcriptional activating activities, are immense. It is tempting to speculate that this variety in Mediator activity, or a varying pool of non-Mediator associated Tlo protein, could contribute to the phenotypic plasticity and adaptability of this fungus and may go towards explaining why its incidence as a commensal and opportunist is far greater compared to its close relatives *C. tropicalis* and *C. dubliniensis* which do not have this expanded repertoire of Med2 paralogs.

Over the last decade, a wealth of studies have described the global transcriptional responses of *C. albicans* to environmental stress, pH changes and nutrient availability amongst others. It is clear from these studies that one of the characteristics of *C. albicans* is its ability to rapidly respond to environmental change by mediating rapid transcriptional responses. The current study suggests a vital role for the Tlos in mediating the speed and scale of these responses, which are associated with characteristics required for commensalism (nutrient acquisition, metabolism) and pathogenicity (starvation responses, filamentation) indicating a key role for Tlo-regulated responses in the lifestyle of *C. albicans*. This, coupled with the potential diversity in the activity of the different Tlo paralogs may have contributed to the ability of *C. albicans* to colonise many diverse niches and thus to evolve to be a highly successful commensal and pathogen.

Materials and Methods

Candida strains and culture conditions

All *Candida* strains were routinely cultured on yeast extract-peptone-dextrose (YEPD) agar, at 37°C. Solid Lee's medium and Spider medium were used as described previously [37,38]. Pal's agar medium was also used for chlamydospore induction as described previously [39]. For liquid culture, cells were grown shaking (200 rpm) in YEPD broth at 30°C or 37°C. In order to determine the doubling time of each strain, the optical densities (600_{nm}) of cultures in the exponential phase of growth were plotted and analysed using the exponential growth equation function in Graphpad Prism (GraphPad, CA, USA). Doubling times and r^2 values in Table 1 were calculated from three replicate growth curves. Glucose (2% w/v) was substituted with galactose (2% w/v) where indicated. Hyphal induction was carried out in sterile Milli-Q H_2O supplemented with 10% (v/v) fetal calf serum at 37°C. Samples were randomized and the proportion of germ-tubes or true-hyphae in 300 cells was assessed at intervals by microscopic examination of an aliquot of culture with a Nikon Eclipse 600 microscope (Nikon U.K., Surrey, U.K.). Experiments were performed on at least three separate occasions.

Genotypes of strains used in this study are listed in Table S4. Gene disruption of *TLO1* (Cd36_72860) and *TLO2* (Cd36_35580)

was achieved through use of the *SAT1* flipper cassette system [40]. Deletion constructs were created by PCR amplifying the 5′ flanking regions of *TLO1* or *TLO2* with the primer pairs CTA21KF/CTA1X and CTA22KF/CTA2X respectively and the 3′ flanking regions with the primer pairs CTA1S/CTA21SIR and CTA2S/CTA22SIR, respectively (Table S4). Ligation of these products in the corresponding restriction sites in plasmid pSFS2A resulted in the construction of plasmids pTY101 (*TLO1*) and TY102 (*TLO2*) as described [19]. The deletion construct was used to transform *C. dubliniensis* Wü284 as described previously [19] and deletion of genes was confirmed by Southern blotting (Figure S1). A single transformation with TY102 was sufficient to delete *TLO2* in strain Wü284 which was found to have a truncation in one copy of ChrR, resulting in the presence of only one copy of *TLO2*. Deletion of *MED3* was carried out using a primer tailing method with the primers MED3M13F/MED3M13R as described [41]. Reintroduction of wild-type *TLO* genes or *MED3* was achieved by PCR amplification of the entire ORF plus their upstream and downstream regulatory sequences using primer pairs CdTLO1FP/CdTLO1RP for *CdTLO1*, CdTLO2FP/CdTLO2RP for *CdTLO2* and MED 3FP/MED3RP for *MED3* (Table S5) and ligation of these into the *C. dubliniensis* integrating vector pCDRI to yield plasmids pCdTLO1, pCdTLO2, and pCdMED3 respectively. These plasmids were transformed as described previously [19].

Biochemical analysis of mediator

Mediator was purified from *C. dubliniensis* strains containing Mediator subunits tagged at their C-terminus with either HA or 6His-FLAG. *CdMED8*- and *CdTLO1*-tagging cassettes were amplified from pFA-3HA-SAT1 or pFA-6His3Flag-SAT1 using the primer pairs pZL420/pZL421 and pZL422/pZL423, respectively, as described previously [9]. Whole-cell extracts were made from strains that were untagged or had a single copy of Tlo1 or other Mediator subunit tagged with a HA or 6His-FLAG and subjected to multiple chromataographic separations as described previously [9]. The elutions from the immobilized metal affinity chromatography (IMAC; Talon Kit, Clontech Laboratories, CA, USA) step were analyzed by SDS-PAGE as indicated and proteins were revealed by staining with silver as described previously [9].

Induction of biofilm formation

Biofilm mass was determined using an XTT reduction assay to assess metabolic activity. Prior experiments with planktonic cells indicated that wild-type and *tlo*Δ mutant strains exhibited similar rates of XTT reduction. To induce biofilm growth, a suspension of 1×10^6 cells of each strain was prepared in 10% (v/v) foetal calf serum from 18 h cultures grown in YEPD broth at 30°C with shaking at 200 rpm A 100 µl volume of each suspension was added to triplicate wells of a 96-well, flat-bottomed polystyrene plate (Greiner BioOne) with lid. Plates were then incubated for 24 h or 48 h in a static incubator (Gallenkamp) set to 37°C. Growth in the presence of 5% (v/v) CO_2 was carried out in a static tissue culture incubator with 5% (v/v) relative humidity (Gallenkamp). All wells were then washed 5 times with 200 µl sterile PBS to remove non-adherent cells. After the final wash, 200 µl of 200 µg/ml XTT supplemented with 50 µg/ml CoEnzyme Q (Sigma-Aldrich) was added to each well and incubated at 37°C in the dark for 50 min. A 100 µl aliquot of this suspension was transferred to a fresh plate and the absorbance measured at 480 nm using a Tecan Plate Reader system (Tecan). Results were analysed and graphed using Microsoft Excel (Microsoft).

Transcriptional profiling with oligonucleotide microarrays

The *C. dubliniensis* whole genome oligonucleotide microarray used in this study was previously described [20]. RNA was extracted from cells grown to an OD 600 nm of 0.8 in YEPD broth at 37°C or from cells (1×10^6) inoculated in 10% (v/v) fetal calf serum at 37°C. Cell pellets were snap frozen in liquid N_2 and disrupted using the Mikro-Dismembrator S system (Sartorius Stedim Biotech, Göttingen, Germany). RNA was prepared using the Qiagen RNeasy mini-kit. A 200 ng aliquot of total RNA was labelled with Cy5 or Cy3 using the Two-Color Low Input Quick Amp labeling Kit (Agilent Technologies) according to the manufacturer's instructions. Array hybridization, washing, scanning and data extraction was carried out in GenePix Pro 6.1 (Axon) as described [20]. For each condition, four biological replicate experiments were performed, including two dye swap experiments. Raw data were exported to GeneSpring GX12 and signals for each replicate spot were background corrected and normalized using Lowess transformation. Log_2 fluorescence ratios were generated for each replicate spot and averaged. Genes differentially expressed (1.5-fold) relative to wild-type were identified from those that passed a *t*-test ($P\leq0.05$) and satisfied a post-hoc test (Storey with Bootstrapping) with a corrected Q value ≤0.05. Hierarchical clustering was used to compare gene expression in each condition using the default settings in Genespring GX12. The Gene Set Enrichment Analysis (GSEA) PreRanked tool (available to download at www.broadinstitute.org/gsea/index.jsp) was used to investigate whether our data sets were enriched for particular genes present in published data sets [42]. This analysis required the use of a database of publicly available genome-wide data sets, constructed by Andre Nantel (National Research Council of Canada, Montreal), that can be downloaded from the Candida Genome Database (CGD). This database included 171 lists of up- and down-regulated genes from microarray experiments, *in vivo* promoter targets derived from ChIP-chip experiments performed on 36 transcription factors, members of 3,601 Gene Ontology (GO) term categories, and 152 pathways, as curated by CGD, amongst others, and is fully described by Sellam *et al.* [43]. Genes in our expression data sets were first 'ranked' based on Log2 values from highest to lowest. The GSEA PreRanked tool was then used to determine if particular gene sets in the database were enriched towards the top or bottom of this ranked list. Enrichment plots show the level of enrichment towards the top (red) or bottom (blue) of the ranked list. The normalized enrichment score (NES) indicates the level of enrichment at the top (positive NES) or bottom (negative NES) of the ranked list and is supported by a p value and a False Discovery Rate (FDR) value to indicate the likelihood of false positive results.

Microarray data have been submitted to Gene Expression Omnibus (GEO), accession number: GSE59113.

Real-time PCR analysis of gene expression

RNA for QRT-PCR was isolated using the RNeasy Mini-kit (Qiagen). Cells were disrupted using a FastPrep bead beater (Bio101). RNA samples were rendered DNA free by incubation with Turbo-DNA free reagent (Ambion, Austin, TX). cDNA synthesis was carried out using the Superscript III First strand synthesis sytem for RT-PCR (Life technologies) as described by Moran et al. [19] Reactions were carried on an ABI7500 Sequence Detector (Applied Biosystems, Foster City, CA) using MicroAmp Fast Optical 96-well Reaction plates (Applied Biosystems) in 20 µl reactions using 1X Fast SYBR Green PCR Master Mix (Applied Biosystems), 150 nM of each oligonucleotide (Table S4) and 2 µl of diluted template (10 ng). Cycling conditions used

were 95°C for 20 sec, followed by 40 cycles of 95°C for 3 sec and 60°C for 30 sec, the latter of which was the point of detection of fluorescence. This was followed by a melt curve stage as a quality control point. Gene expression levels were normalized against the expression levels of the constitutively expressed *ACT1* gene in the same cDNA sample. Gene specific primers are shown in Table S5. Each gene-specific set was shown to amplify at a similar efficiency (within 10%) to the control *ACT1* primer set in primer optimization experiments.

Chromatin immunoprecipitation and microarray hybridisation (ChIP-chip)

C. dubliniensis strain Tlo1-HA, derived from strain Wü284, was grown at 30°C degrees and harvested at an OD 600 nm of 2.0. A secondary cross-linking strategy was employed to fix chromatin that involved initial treatment of cells with dimethyl adipimidate (10 mM) for 45 min with agitation at room temperature followed by cross-linking with 1% formaldehyde. Cells were washed twice in PBS prior to spheroplasting in 5 ml of spheroplasting buffer (1.2 M sorbitol, 20 mM 4-(2-hydroxyethyl)-1-piperazineethanesulfonic acid [HEPES] pH 7.4) containing 0.4 mg/ml Zymolyase 100T (Seikagaku Corp., Japan) and incubated for 2.5 h 30°C with rotation. DNA isolation and fragmentation was carried out as described in Ketel *et al* [44] using a Branson sonifier to yield DNA fragments of 500–600 bp. Chromatin immunoprecipitation (ChIP) was carried out as described by Ketel et al. [44] using an anti-HA mouse monoclonal antibody (clone 12CA5) which was incubated overnight at 4°C on a rotating wheel. The following day, 70 µl of Protein A agarose beads (Santa Cruz Biotech, California, USA) were added and mixed at 4°C for 4 h. DNA was recovered as described by Ketel et al [44] and resuspended in 80 µl TE buffer for downstream applications.

Microarray chip analysis (CGH Microarray) was carried out as described in the Agilent Yeast ChIP-on-chip analysis protocol handbook (Version 9.2, 2007). Competitive hybridization was carried out on a whole genome *C. dubliniensis* oligonucleotide microarray consisting of 175,758 unique 60mer probes, spaced at 20 bp intervals (Agilent Technologies). Experiments were performed with triplicate biological replicate samples. The IP samples were labelled with Cy3 and input samples (total lysate control) were labelled with Cy5. One sample was dye swapped. Array hybridisation and washing were carried out using standard Agilent Technologies CGH hybridisation buffers and washes. Scanning of the array was carried out on an Agilent G2565B rotating multi-slide hyb-scanner (Agilent Technologies) using a 5 µm resolution and PMT settings at 100% for both channels (Green/Red). The scan area was set to 61×21.6 mm. The raw images were processed using Agilent Feature Extraction software suite v 10.5.1.1. and feature extraction was automatically carried out using the 'CGH automatic' programme to align and normalise fluorescent probe spots on the array.

Data were read into the Bioconductor [45] package Ringo [46] and pre-processed with the "nimblegen" method. This was followed by merging of replicates and smoothing with a window half size of 500 bp. ChIP-enriched regions were calculated with an enrichment threshold based firstly on a 0.8 percentile, followed by a more stringent 0.9 percentile which was used for the analysis presented here. Genes were assigned to an enrichment region if they overlapped up to 500 bp away from the gene boundaries. For visualisation of the data a JBrowse [47] instance was set up on http://bioinf.gen.tcd.ie/jbrowse/?data=cdub. The ChIP data have been submitted to GEO, accession number GSE60173.

Supporting Information

Figure S1 Southern immunoblots of *Nde*I digested genomic DNA from *C. dubliniensis*. Hybridizing fragments were detected using a digoxigenin-labeled probe homologous to bases +51–250 of *TLO1* (100% homology) and bases +51–248 of *TLO2* (87% homology). *TLO1* and *TLO2* hybridizing Fragments were predicted to be 14.07 Kb and 5.96 Kb in size. Only one copy of *TLO2* was detected in Wü284, hence the absence of a second hybridizing allele in lane 3 (*tlo2*Δ).
(TIFF)

Figure S2 Immunoblotting of whole cell extracts of *C. dubliniensis* using an anti-HA antibody for detection Tlo1-HA, Med8-HA and Med3-HA. Whole-cell extracts were made from strains that were untagged or had a single copy of a Tlo or other Mediator subunit tagged with the HA epitope. The strain used for each extract is listed above the lanes. Multiple volumes were loaded for each strain to allow normalization with an anti-tubulin antibody.
(TIFF)

Figure S3 (**A**) Microscopic appearance of *tlo1*Δ/*tlo2*Δ (*tlo*ΔΔ) mutant cells and reintegrant strains (+*TLO1* or +*TLO2*) stained with calcofluor white. (B) Colony morphology of *tlo1*Δ/*tlo2*Δ (*tlo*ΔΔ) mutants and reintegrant strains (+*TLO1* or +*TLO2*) on Spider agar medium.
(TIFF)

Figure S4 Additional phenotypes in the *tlo1*Δ/*tlo2*Δ mutant. (A) Production of pseudohyphae and chlamydospores (indicated by arrow) following growth on solid Pal's medium (B) Comparative growth on solid Lee's medium. Lee's medium was supplemented with 1% (w/v) peptone in the lower panel, as indicated.
(TIFF)

Figure S5 Phenotypes in the *C. dubliniensis med3*Δ mutant. (A) Growth of the *med3*Δ mutant in YEP-Gal. (B) Susceptibility of the *med3*Δ mutant to hydrogen peroxide.
(TIFF)

Figure S6 Enrichment plots from Gene Set Enrichment Analysis (GSEA) of the transcript profile of the *tlo1*Δ/*tlo2*Δ mutant showing enrichment for genes regulated during infection of reconstituted human epithelium (RHE, [25]) and bone marrow derived macrophages (BMDM, [26]).
(TIFF)

Figure S7 Heat map showing the expression of glycolytic and gluconeogenic (highlighted) pathway encoding genes in the *tlo1*Δ/*tlo2*Δ mutant and the *med3*Δ mutant during growth in YEPD broth and 10% serum. Each gene is represented by data from duplicate microarray spots.
(TIFF)

Figure S8 Tlo proteins regulate similar processes to Med2 in *S. cerevisiae*. Venn diagrams illustrating the numbers of orthologous genes commonly regulated in an *S. cerevisiae Scmed2* mutant and the *C. dubliniensis tlo1*Δ/*tlo2*Δ (*tlo*ΔΔ) mutants following growth in YEPD broth. *P* values were generated by hypergeometric probability testing (http://www.geneprof.org/GeneProf/tools/hypergeometric.jsp).
(TIFF)

Figure S9 (A) Composite, smoothed Tlo1-enrichment plot generated with a sliding window of 100 bp from the plots of the 367 highly-enriched genes (Ringo peak score 0.9) (B) Box-plot graph showing the distribution and length of Tlo1 enrichment at the 5′ and 3′ ends of 367 highly-enriched genes (Ringo peak score

0.9) (C) Graph showing average expression levels of Tlo1 occupied genes (n = 1613, mean 4783) and non-occupied genes (n = 3744, mean 2620) in wild-type *C. dubliniensis*. Expression data are raw, background corrected fluorescence intensity signals extracted from microarray data sets. *P* value generated with unpaired, two-tailed t-test.
(TIFF)

Table S1 List of genes exhibiting *TLO1*- or *TLO2*-specific regulation following complementation of the *tlo1Δ/tlo2Δ* (*tloΔΔ*) mutant with either *TLO1* (+*TLO1*) or *TLO2* (+*TLO2*). Transcript profiles were generated on cells grown to OD 600_{nm} 0.8 in YEPD at 37°C. Expression values are to Log_2 ratios.
(XLSX)

Table S2 List of genes exhibiting *TLO1*- or *TLO2*-specific regulation following complementation of the *tlo1Δ/tlo2Δ* (*tloΔΔ*) mutant with either *TLO1* (+TLO1) or *TLO2* (+TLO2). Transcript profiles were generated on cells grown for 1 h in 10% serum at 37°C. Expression values are to Log_2 ratios.
(XLSX)

Table S3 List of genes considered highly enriched for Tlo1-HA (Ringo peak score 0.9) in ChIP-chip experiments in YEPD broth. Column '*tloΔΔ* vs WT YEPD' indicated Log_2 gene expression ratios in the *tlo1Δ/tlo2Δ* (*tloΔΔ*) mutant relative to wild-type generated in gene expression microarrays. 'YEPD Expression level' refers to the raw, background corrected, Loess normalised fluorescent intensity level for that gene in gene expression microarray experiments.
(XLSX)

Table S4 Strains of *Candida* spp. used in this study.
(DOCX)

Table S5 Oligonucleotide primers used in this study.
(DOCX)

Acknowledgments

Mass spectroscopy was carried out by Scott Gerber (Geisel School of Medicine at Dartmouth). Files for running Gene Set Enrichment Analysis (GSEA) on microarray data were kindly supplied by Andre Nantel (Biotechnology Research Institute, National Research Council of Canada, Montreal, Quebec) *via* the Candida Genome Database (CGD).

Author Contributions

Conceived and designed the experiments: JH HB TY ZL LCM MC ABF MZA JB DJS GPM. Performed the experiments: JH HB TY ZL. Analyzed the data: JH HB ZL LCM KH ABF MZA JB DJS GPM. Contributed reagents/materials/analysis tools: LCM JB ABF DJS GPM. Wrote the paper: GPM.

References

1. Lorenz MC, Bender JA, Fink GR (2004) Transcriptional response of Candida albicans upon internalization by macrophages. Eukaryotic Cell 3: 1076–1087.
2. Pérez JC, Johnson AD (2013) Regulatory Circuits That Enable Proliferation of the FungusCandida albicans in a Mammalian Host. PLoS Pathog 9: e1003780.
3. Kadosh D, Johnson AD (2005) Induction of the Candida albicans filamentous growth program by relief of transcriptional repression: a genome-wide analysis. Mol Biol Cell 16: 2903–2912.
4. Conaway RC, Conaway JW (2011) Origins and activity of the Mediator complex. Seminars in Cell and Developmental Biology 22: 729–734.
5. Malik S, Roeder RG (2010) The metazoan Mediator co-activator complex as an integrative hub for transcriptional regulation. Nature Reviews Genetics 11: 761–772.
6. Björklund S, Gustafsson CM (2005) The yeast Mediator complex and its regulation. Trends in Biochemical Sciences 30: 240–244.
7. Thompson CM, Young RA (1995) General requirement for RNA polymerase II holoenzymes in vivo. Proc Natl Acad Sci USA 92: 4587–4590.
8. Ansari SA, Morse RH (2013) Mechanisms of Mediator complex action in transcriptional activation. Cell Mol Life Sci 70: 2743–2756.
9. Zhang A, Petrov KO, Hyun ER, Liu Z, Gerber SA, et al. (2012) The Tlo Proteins Are Stoichiometric Components of Candida albicans Mediator Anchored via the Med3 Subunit. Eukaryotic Cell 11: 874–884.
10. Braun BR, van Het Hoog M, d'Enfert C, Martchenko M, Dungan J, et al. (2005) A human-curated annotation of the Candida albicans genome. PLoS Genet 1: 36–57.
11. van Het Hoog M, Rast TJ, Martchenko M, Grindle S, Dignard D, et al. (2007) Assembly of the Candida albicans genome into sixteen supercontigs aligned on the eight chromosomes. Genome Biol 8: R52.
12. Anderson MZ, Baller JA, Dulmage K, Wigen L, Berman J (2012) The Three Clades of the Telomere-Associated TLO Gene Family of Candida albicans Have Different Splicing, Localization, and Expression Features. Eukaryotic Cell 11: 1268–1275.
13. Bourbon H-M (2008) Comparative genomics supports a deep evolutionary origin for the large, four-module transcriptional mediator complex. Nucleic Acids Res 36: 3993–4008.
14. Jackson AP, Gamble JA, Yeomans T, Moran GP, Saunders D, et al. (2009) Comparative genomics of the fungal pathogens Candida dubliniensis and Candida albicans. Genome Res 19: 2231–2244.
15. Uwamahoro N, Qu Y, Jelicic B, Lo TL, Beaurepaire C, et al. (2012) The Functions of Mediator in Candida albicans Support a Role in Shaping Species-Specific Gene Expression. PLoS Genet 8: e1002613.
16. Zhang A, Liu Z, Myers LC (2013) Differential Regulation of White-Opaque Switching by Individual Subunits of Candida albicans Mediator. Eukaryotic Cell 12: 1293–1304.
17. Moran GP, Coleman DC, Sullivan DJ (2012) Candida albicans versus Candida dubliniensis: Why Is C. albicans More Pathogenic? Int J Microbiol 2012: 205921.
18. Stokes C, Moran GP, Spiering MJ, Cole GT, Coleman DC, et al. (2007) Lower filamentation rates of Candida dubliniensis contribute to its lower virulence in comparison with Candida albicans. Fungal Genet Biol 44: 920–931.
19. Moran GP, MacCallum DM, Spiering MJ, Coleman DC, Sullivan DJ (2007) Differential regulation of the transcriptional repressor NRG1 accounts for altered host-cell interactions in Candida albicans and Candida dubliniensis. Mol Microbiol 66: 915–929.
20. O'Connor L, Caplice N, Coleman DC, Sullivan DJ, Moran GP (2010) Differential filamentation of Candida albicans and C. dubliniensis is governed by nutrient regulation of UME6 expression. Eukaryotic Cell: doi:10.1128/EC.00042-10.
21. Enjalbert B, Moran GP, Vaughan C, Yeomans T, MacCallum DM, et al. (2009) Genome-wide gene expression profiling and a forward genetic screen show that differential expression of the sodium ion transporter Ena21 contributes to the differential tolerance of Candida albicans and Candida dubliniensis to osmotic stress. Mol Microbiol 72: 216–228.
22. Moran GP, Coleman DC, Sullivan DJ (2011) Comparative genomics and the evolution of pathogenicity in human pathogenic fungi. Eukaryotic Cell 10: 34–42.
23. Miller C, Matic I, Maier KC, Schwalb B, Roether S, et al. (2012) Mediator Phosphorylation Prevents Stress Response Transcription During Non-stress Conditions. Journal of Biological Chemistry 287: 44017–44026.
24. Ansari SA, Ganapathi M, Benschop JJ, Holstege FCP, Wade JT, et al. (2011) Distinct role of Mediator tail module in regulation of SAGA-dependent, TATA-containing genes in yeast. EMBO J 31: 44–57.
25. Zakikhany K, Naglik JR, Schmidt Westhausen A, Holland G, Schaller M, et al. (2007) In vivo transcript profiling of Candida albicans identifies a gene essential for interepithelial dissemination. Cell Microbiol 9: 2938–2954.
26. Marcil A, Gadoury C, Ash J, Zhang J, Nantel A, et al. (2008) Analysis of PRA1 and its relationship to Candida albicans- macrophage interactions. Infect Immun 76: 4345–4358.
27. van de Peppel J, Kettelarij N, van Bakel H, Kockelkorn TTJP, van Leenen D, et al. (2005) Mediator Expression Profiling Epistasis Reveals a Signal Transduction Pathway with Antagonistic Submodules and Highly Specific Downstream Targets. Molecular Cell 19: 511–522.
28. Park D, Lee Y, Bhupindersingh G, Iyer VR (2013) Widespread misinterpretable ChIP-seq bias in yeast. PLoS ONE 8: e83506. doi:10.1371/journal.-pone.0083506.
29. Teytelman L, Thurtle DM, Rine J, van Oudenaarden A (2013) Highly expressed loci are vulnerable to misleading ChIP localization of multiple unrelated proteins. Proceedings of the National Academy of Sciences 110: 18602–18607.
30. Fan X, Struhl K (2009) Where Does Mediator Bind In Vivo? PLoS ONE 4: e5029. doi:10.1371/journal.pone.0005029.t002.
31. Uwamahoro N, Verma-Gaur J, Shen HH, Qu Y, Lewis R, et al. (2014) The Pathogen Candida albicans Hijacks Pyroptosis for Escape from Macrophages. mBio 5: e00003–14–e00003–14. doi:10.1128/mBio.00003-14.
32. Mehta S, Miklos I, Sipiczki M, Sengupta S, Sharma N (2009) The Med8 mediator subunit interacts with the Rpb4 subunit of RNA polymerase II and Ace2 transcriptional activator in Schizosaccharomyces pombe. FEBS Lett 583: 3115–3120.
33. Liu Z, Myers LC (2012) Med5(Nut1) and Med17(Srb4) are direct targets of mediator histone H4 tail interactions. PLoS ONE 7: e38416.

34. Peng J, Zhou JQ (2012) The tail-module of yeast Mediator complex is required for telomere heterochromatin maintenance. Nucleic Acids Res 40: 581–593.
35. Zhu X, Wirén M, Sinha I, Rasmussen NN, Linder T, et al. (2006) Genome-Wide Occupancy Profile of Mediator and the Srb8-11 Module Reveals Interactions with Coding Regions. Molecular Cell 22: 169–178.
36. Andrau J-C, van de Pasch L, Lijnzaad P, Bijma T, Koerkamp MG, et al. (2006) Genome-Wide Location of the Coactivator Mediator: Binding without Activation and Transient Cdk8 Interaction on DNA. Molecular Cell 22: 179–192.
37. Liu H, Köhler J, Fink GR (1994) Suppression of hyphal formation in Candida albicans by mutation of a STE12 homolog. Science 266: 1723–1726.
38. Lee KL, Buckley HR, Campbell CC (1975) An amino acid liquid synthetic medium for the development of mycellal and yeast forms of Candida albicans. Med Mycol 13: 148–153.
39. Al-Mosaid A, Sullivan DJ, Coleman DC (2003) Differentiation of Candida dubliniensis from Candida albicans on Pal's agar. J Clin Microbiol 41: 4787–4789.
40. Reuss O, Vik A, Kolter R, Morschhäuser J (2004) The SAT1 flipper, an optimized tool for gene disruption in Candida albicans. Gene 341: 119–127.
41. Spiering MJ, Moran GP, Chauvel M, MacCallum DM, Higgins J, et al. (2010) Comparative transcript profiling of Candida albicans and Candida dubliniensis identifies SFL2, a C. albicans gene required for virulence in a reconstituted epithelial infection model. Eukaryotic Cell 9: 251–265.
42. Subramanian A, Tamayo P, Mootha VK, Mukherjee S, Ebert BL, et al. (2005) Gene set enrichment analysis: a knowledge-based approach for interpreting genome-wide expression profiles. Proc Natl Acad Sci USA 102: 15545–15550.
43. Sellam A, van het Hoog M, Tebbji F, Beaurepaire C, Whiteway M, et al. (2014) Modeling the Transcriptional Regulatory Network That Controls the Early Hypoxic Response in Candida albicans. Eukaryotic Cell 13: 675–690.
44. Ketel C, Wang HSW, McClellan M, Bouchonville K, Selmecki A, et al. (2009) Neocentromeres form efficiently at multiple possible loci in Candida albicans. PLoS Genet 5: e1000400.
45. Gentleman RC, Carey VJ, Bates DM, Bolstad B, Dettling M, et al. (2004) Bioconductor: open software development for computational biology and bioinformatics. Genome Biol 5: R80.
46. Toedling J, Skylar O, Sklyar O, Krueger T, Fischer JJ, et al. (2007) Ringo–an R/Bioconductor package for analyzing ChIP-chip readouts. BMC Bioinformatics 8: 221.
47. Westesson O, Skinner M, Holmes I (2013) Visualizing next-generation sequencing data with JBrowse. Brief Bioinformatics 14: 172–177.

Chapter 1

General Introduction

1.1. Pathogenic Fungi

Among the approximate 611,000 species of fungi known only a small number of these are pathogenic to humans (Mayer *et al.* 2013). The most common fungal diseases that manifest in humans are superficial nail and skin infections. Superficial infections affect approximately 25% of the world's population and are primarily attributed to dermatophytes, which cause well characterised infections such as *Tinea pedis* "athlete's foot", ringworm and fungal nail infections (Havlickova *et al.,* 2008). Dermatophytes are acquired environmentally through passage from mammalian reservoirs to humans (Achterman & White, 2012). Although described as superficial infections, athlete's foot occurs in a fifth of adults, ringworm affects 200 million people worldwide and nail infections affect ~ 10% of the general population, indicating a significant impact on humans (Thomas *et al.,* 2010).

Over the last forty years, opportunistic fungal pathogens have been identified as significant causes of life-threatening infections in immunocompromised and immunosuppressed individuals. Fungi have the ability to occupy highly divergent niches, such as highly osmotic environments, plants and mammalian hosts. *Aspergillus fumigatus* and *Cryptococcus neoformans* are ubiquitous in nature and grow in environmental niches such as soil (Pérez-Martín & Di Pietro, 2012). Humans frequently encounter the spores, yeasts and mycelial fragments of these fungi, and these interactions can normally be controlled by the innate immune system, particularly by alveolar macrophages (Woods, 2003; Hohl & Feldmesser, 2007; Ma & May, 2009). However, evidence suggests that the inhaled fungal fragments can persist within macrophages and provide a reservoir for secondary infections when the host immune system is weakened (d'Enfert, 2009). Invasive fungal infections are associated with a high mortality rate, often exceeding 50% (Brown *et al.,* 2012).

Opportunistic fungal diseases are an increasingly significant cause of morbidity and mortality in immunocompromised patients, and are associated with increased costs to healthcare globally (Menzin *et al.*, 2009). These opportunistic fungal pathogens that have emerged over the last few decades have thrived and their frequency has increased due to the expanding number of immunologically impaired individuals in the population, new antifungal selective pressures and shifting environmental conditions. A study carried out by Drgona *et al.* (2014) outlined the clinical and economic burden associated with invasive fungal infection. This study found that the incremental cost of treating invasive fungal infections ranges between €10,530 and €51,033 depending on the certainty of infection and the degree to which the infection was followed up (Drgona *et al.*, 2014). Specifically, the average treatment costs for antifungal treatment, namely voriconazole and amphotericin B ranges between €25,353 to €26,974 in a 12-week treatment course and €30,026 to €33,616 for life-long treatment (Jansen *et al.*, 2006).

The most important opportunistic fungal pathogens are *Candida* species, which pose a major threat to immunocompromised and immunosuppressed patients. *Candida albicans* and other *Candida* species are common commensals of the healthy human body, in particular the gastrointestinal tract, the oral cavity, the genital tract and the skin (Calderone, 2002).

1.2. The Genus *Candida*

1.2.1. Epidemiology of *Candida* spp.

Candida spp. are the 4th most common causative agents of hospital-acquired bloodstream infections in the US and the 6th most common in Europe with a mortality rate of up to 38% (Omrum and Anaissie, 1996; Rees *et al.*, 1998; Pfaller *et al.*, 2001; Marchetti *et al.*, 2004). Although the genus *Candida* contains over 200 species, approximately twelve of these species have been associated with human infection. Pathogenic species include *Candida albicans,*

Candida dubliniensis, Candida parapsilosis, Candida glabrata, Candida tropicalis and *Candida krusei.* These are members of the *Saccharomycetacea* family, which contains the non-pathogenic model yeast *Saccharomyces cerevisiae,* a benign distant relative of *C. albicans,* which is the most common and pathogenic yeast (Jackson *et al.,* 2009).

Candida species are among the most pathogenic fungi known. They are one of the most prevalent causes of opportunistic mycoses in humans, and have been reported to be the cause of up to a third of nosocomial blood infections (Walsh & Groll, 1998; Miceli *et al.,* 2011). *Candida* species are commonly found as commensals of the orogastrointestinal tract and the vaginal cavity of most healthy individuals (Kim and Sudbery, 2011). However in the immunosuppressed and immunocompromised, *Candida* species can cause infections ranging from superficial; such as oropharyngeal candidiasis (OPC) to systemic bloodstream infections that can disseminate to the organs, resulting in death in approximately 50% of bloodstream infections (Berman and Sudbery, 2002; Eggimann *et al.,* 2003).

There are a wide range of predisposing factors for superficial candidiasis, including immune deficiency, pregnancy, poor oral hygiene, old age and infancy (Hay, 1999). Superficial vaginal infections are particularly common; vulvovaginal candidiasis (VVC) is thought to affect up to 75% of women at least once in their lifetime (Sobel, 1997). The symptoms of vaginal candidiasis are irritation and discomfort, with a creamy discharge present in some cases (Sobel, 1984). Despite the high incidence of VVC, the underlying risk factors for the disease are not apparent; although it has been suggested that increased risk of occurrence can be attributed to the use of antibiotics, oral contraceptives and reproductive hormones (Sullivan *et al.,* 2004). Particular population groups are more predisposed to superficial oral infections than others. Patients infected with human immuno-deficiency virus (HIV) and individuals with acquired immune deficiency syndrome (AIDS) are commonly diagnosed with OPC. Oropharyngeal candidiasis infections usually manifest as the commonly known "thrush"

which causes plaques on the tongue and mucous membranes, and can result in painful lesions in the oral mucosa. The most common forms of oral candidiasis are acute pseudomembranous candidiasis, chronic erythematous candidiasis, acute erythematous candidiasis, and chronic hyperplastic candidiasis (Williams & Lewis, 2011). Pseudomembranous infection results in solitary or confluent white plaques, erythematous candidiasis causes loss of the tongue papillae and is the only form of candidiasis that is consistently painful, while chronic hyperplastic candidiasis can present on any oral mucosal surface and appears either as smooth or nodular white lesions usually in the corners of the mouth as seen in Figure 1.1 (Holmstrup & Besserman, 1983; Samaranayake *et al.* 1990; Park, *et al.* 2011; Williams & Lewis, 2011).

There are many risk factors for systemic *Candida* infections, including neutropenia resulting from immunosuppressants used for organ transplants, chemotherapy and catheterisation, and can lead to problematic infections such as meningitis and endocarditis (Sullivan *et al.*, 2004; De Rosa *et al.*, 2009). Following tissue damage, pathogenic *Candida* species can directly enter the bloodstream by penetrating the epithelium or by disseminating from biofilms that can form on medical devices inserted into patients such as catheters, central nervous system shunts, endoprostheses and artificial joints (Chandra *et al.*, 2001, Mavor *et al.*, 2005).

The most prevalent *Candida* spp. in human infections is *C. albicans,* which is present in 40-60% of invasive candidiasis cases (Odds *et al.*, 2007). *Candida glabrata* and *C. tropicalis* are present in 20-30%, *C. parapsilosis* is present in 10-20%, *C. krusei* is present in 5-10% while *C. dubliniensis* and *C. luitaniae* are present in less than 5% of bloodstream infections (De Rosa *et al.*, 2009). Although *C. albicans* is responsible for most infections, specific clinical features have been described in association with other *Candida* spp. The most common forms of infection caused by non-*albicans* species of *Candida* described here are summarised in Table 1.1 (Eggiman *et al.*, 2003).

(A)

(B)

(C)

(D)

Figure 1.1. Images of the primary forms of oral candidiasis. **(A)** acute pseudomembranous candidiasis; **(B)** chronic erythematous candidiasis; **(C)** acute erythematous candidiasis; and **(D)** chronic hyperplastic candidiasis.

This figure has been adapted from Williams & Lewis, (2011).

Species	Common clinical features
C. glabrata	Systemic candidiasis, candidaemia, urinary tract infections
C. tropicalis	Candidaemia, systemic candidiasis
C. parapsilosis	Candidaemia, deep infections associated with implanted devices. Responsible for most candidaemia among neonates
C. krusei	Candidaemia, endophthalmitis, diarrhoea in newborns
	Rare clinical features
C. dubliniensis	Oropharyngeal infections in HIV-positive patients

Table 1.1. Summary of non-*albicans Candida* infections in humans: species-related clinical features. Adapted from Eggiman *et al.* (2003).

1.2.2. Treatment of *Candida* infections and antifungal resistance

There are currently four groups of antifungal drugs used in the treatment of candidiasis. Although the antifungals used in clinical treatment appear to be diverse and numerous, there are only a few currently available to treat mucosal or systemic infections (Mathew and Nath, 2009). Antifungals are primarily characterised based on their mechanism of action. The polyenes are represented by amphotericin B and nystatin and target ergosterol, a fungal cell membrane sterol. Polyenes cause the fungal cell to become porous, resulting in cell death (White *et al.,* 1998; Perlin, 2015). The main disadvantage of polyenes is that they are nephrotoxic at high concentrations and must be intravenously injected due to their poor solubility (Heitman *et al.,* 2006). Azoles are the largest family of antifungal drugs and are commonly used to treat candidiasis by acting as inhibitors of lanosterol 14-α-demethylase, an enzyme involved in the biosynthesis of ergosterol (Hof, 2006). Examples of azoles include miconazole, ketoconazole, fluconazole, voriconazole and itraconazole. The third group are nucleoside analogues, inhibitors of DNA/RNA synthesis, such as 5-flucytosine. The most recently discovered group of antifungal drugs are the echinocandins, of which caspofungin, micafungin and anidulafungin are the most commonly used examples. Echinocandins are lipopeptidic antifungal agents that inhibit the (1,3)-β-D-glucan synthase, resulting in the formation of cell walls with impaired structural integrity (Grover, 2010; Spampinato and Leonardi, 2013).

Superficial infections can be treated with topical amphotericin B, nystatin, or miconazole. However immunocompromised and AIDS patients with superficial candidiasis may not respond well to these therapies and therefore oral systemic therapies with fluconazole, itraconazole, or ketoconazole are used to treat these infections (Hay, 1999; Patel *et al.* 2012). The incidence of species of *Candida* with reduced susceptibility and innate resistance to azoles such as fluconazole means that polyenes and echinocandins are currently the preferred treatment options for critically ill patients (De Rosa *et al.,* 2009).

An increasingly serious concern in the treatment of fungal infections is resistance to antifungals- in particular azoles and 5-flucytosine. The most common resistance mechanisms are based on alterations in the target enzyme and the activity of drug efflux pumps. Antifungal resistance describes the inability of a fungal infection to respond to treatment (Alexander and Perfect, 1997). Resistance to antifungals can be classified into three groups; intrinsic, acquired (i.e. develops following exposure to the antifungal), and "clinical resistance" which refers to a fungal isolate that appears to be susceptible to the antifungal during laboratory testing, but results in relapse of infection when administered to a patient (Kontoyiannis and Lewis, 2002). Clinical resistance of fungi is most commonly observed in AIDS and neutropenic patients, or patients with infected prosthetics (Alexander and Perfect, 1997). Multidrug combination therapy and limiting the frequency of the usage of the newer categories of antifungal therapies are methods employed to combat the development of drug resistance (Karkowska-Kuleta *et al.*, 2009).

1.2.3. Virulence factors of *Candida* spp.

Since opportunistic *Candida* species are usually innocuous members of the human microbiome it has been difficult to identify the role of specific virulence factors and the pathogenesis of candidal infections has been shown to involve the complex interaction of numerous fungal and host factors. However, over the last two decades *Candida* biologists have identified a number of particular traits that have been proposed to contribute to candidal virulence.

1.2.3.1. Candida morphology

The majority of *Candida* species grow as blastospores. However, the ability to switch between different forms of growth is an important virulence trait associated with *Candida* spp. and is referred to as polymorphism. *Candida* species typically grow as oval-shaped budding yeast cells that bud from daughter cells that detach from the mother cell as is outlined in Figure 1.2,

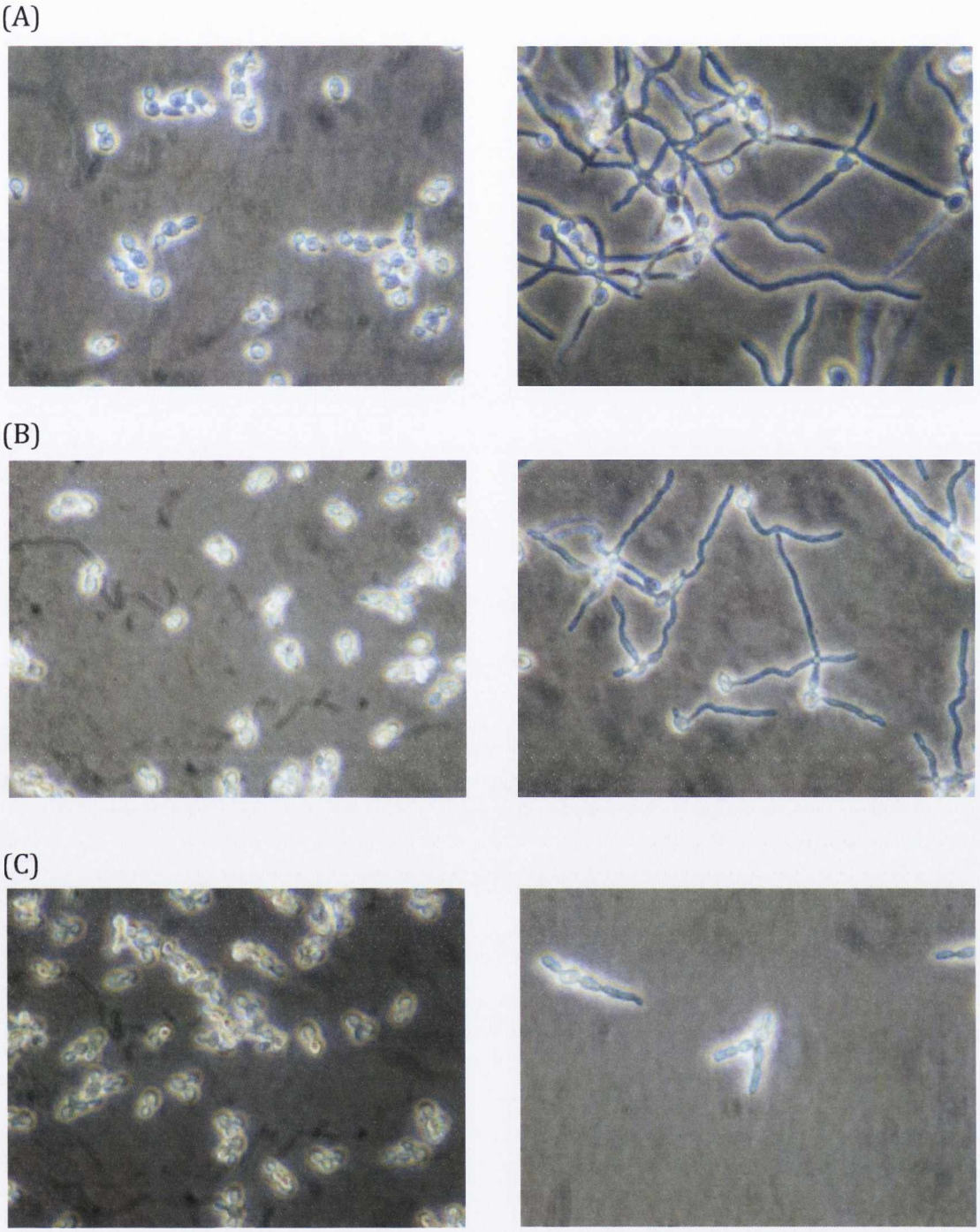

Figure 1.2. Morphological forms of *Candida albicans* and *Candida dubliniensis*. **(A)** *C. albicans* wild-type SC5314 as budding yeast (left) and true hyphae (right). **(B)** *C. dubliniensis* wild-type Wü284 as budding yeast (left) and true hyphae (right). **(C)** *C. dubliniensis tlo*ΔΔ mutant with hyphal formation defect growing as budding yeast (left) and pseudohyphae (right).

or in the filamentous hyphal growth form (in *C. albicans* and *C. dubliniensis* only) which is described as an elongated tube, formed as a result of continuous growth at the tip of a cell, where cells are separated by septa. Other growth forms include pseudohyphae and chlamydospores, however the role of pseudohyphae remains unclear and chlamydospores have yet to be isolated from patient samples (Staib and Morschhäuser, 2007; Soll, 2009). Hyphae have the ability to exert mechanical force and aid in the penetration of epithelial surfaces. They are reportedly vital for adhesion and invasion, and contribute to biofilm formation. Hyphae are able to damage endothelial cells, aiding escape from the bloodstream of the host into host tissue (Kumamoto and Vinces, 2005). Yeast cells are important for initial colonisation of host surfaces and dissemination throughout the body (Finkel and Mitchell, 2010).

A number of environmental cues have been shown to induce hyphal growth. *Candida albicans* is well adapted to growth in humans and can form true hyphae under a range of environmental conditions such as the presence of serum, neutral pH, 5% (v/v) CO_2, and in the presence of *N*-acteyl-D-glucosamine (GlcNac) (Eckert *et al.,* 2007). Furthermore, hyphal growth can be induced in synthetic growth media such as Lee's medium (which contains a mix of amino acids), Spider medium (which contains mannitol as a carbon source), and mammalian tissue culture medium such as M199 (Lee *et al.*, 1975; Liu *et al.,* 1994). Hypha-specific gene expression is negatively regulated by a complex of transcriptional regulators; Tup1 in association with Nrg1 and Rfg1 (Braun and Johnson, 1997; Kadosh and Johnson, 2005). Positive regulation is governed by a number of transcription factors, namely Efg1, Cph1, Cph2, Tec1, Flo8, Czf1, Rim101 and Ndt80 (Sudbery, 2011). In liquid media Efg1 is necessary for hyphal formation in response to serum, CO_2, neutral pH and GlcNac, and on solid media such as Spider medium, while Cph1 and its activating pathway are only required for hyphal formation on solid Spider medium (Liu *et al.,* 1994; Stoldt *et al.,* 1997). Efg1 is proposed to be the major regulator of hyphal formation under most conditions. Separate

upstream signaling pathways activate Efg1 and Cph1. The Efg1 pathway is based on cyclic AMP, whereas the Cph1 the pathway depends on a mitogen-activated protein kinase (MAPK) signaling pathway (Braun and Johnson, 2000; Leberer *et al.,* 2001). Ras1 stimulates both pathways (Feng *et al.,* 1999). These signal transduction pathways result in the transcription of hypha-specific genes necessary for polarised growth and inhibition of cell separation; *UME6, EED1* and *HGC1,* as outlined in Figure 1.3 (Sudbery, 2011). It has been shown that yeast and filamentous forms of growth are both important for virulence. It may be worth noting that *C. glabrata,* which is the second most causative species of systemic infections does not form hyphae (Finkel and Mitchell, 2010; Sudbery, 2011).

1.2.3.2. Phenotypic switching

Several *Candida* species have been observed to undergo a form of phenotypic switching which results in an interchange between different cell and colonial morphologies. It has been suggested that this epigenetic switch could contribute to the capacity of *Candida* species to adapt to the changing environment during human host invasion (Karkowska-Kuleta *et al.,* 2009). The best studied example of this phenomenon is white-opaque switching in *C. albicans* (Ramírez-Zavala *et al.,* 2008) which results in a reversible switch between white colonies, which are composed of smooth round cells, and opaque colonies, which are composed of elongated dimpled cells (Slutsky *et al.,* 1987). Opaque cells are the mating-competent form of *Candida* spp (Miller & Johnson, 2002). Following intravenous infection, white cells have been shown to be more virulent than opaque cells, however, opaque cells are more virulent in models of cutaneous infection (Kvaal *et al.,* 1999). Switching between the white and opaque forms spontaneously occurs at a relatively low frequency; white or opaque cell populations usually contain about 0.1% of cells of the opposite phase (Ramírez-Zavala *et al.,* 2008). The low frequency of switching allows a semi-stable maintenance of the white and opaque growth forms once they are established and also ensures that some cells in the population are pre-adapted to altered environmental conditions upon encountering new host

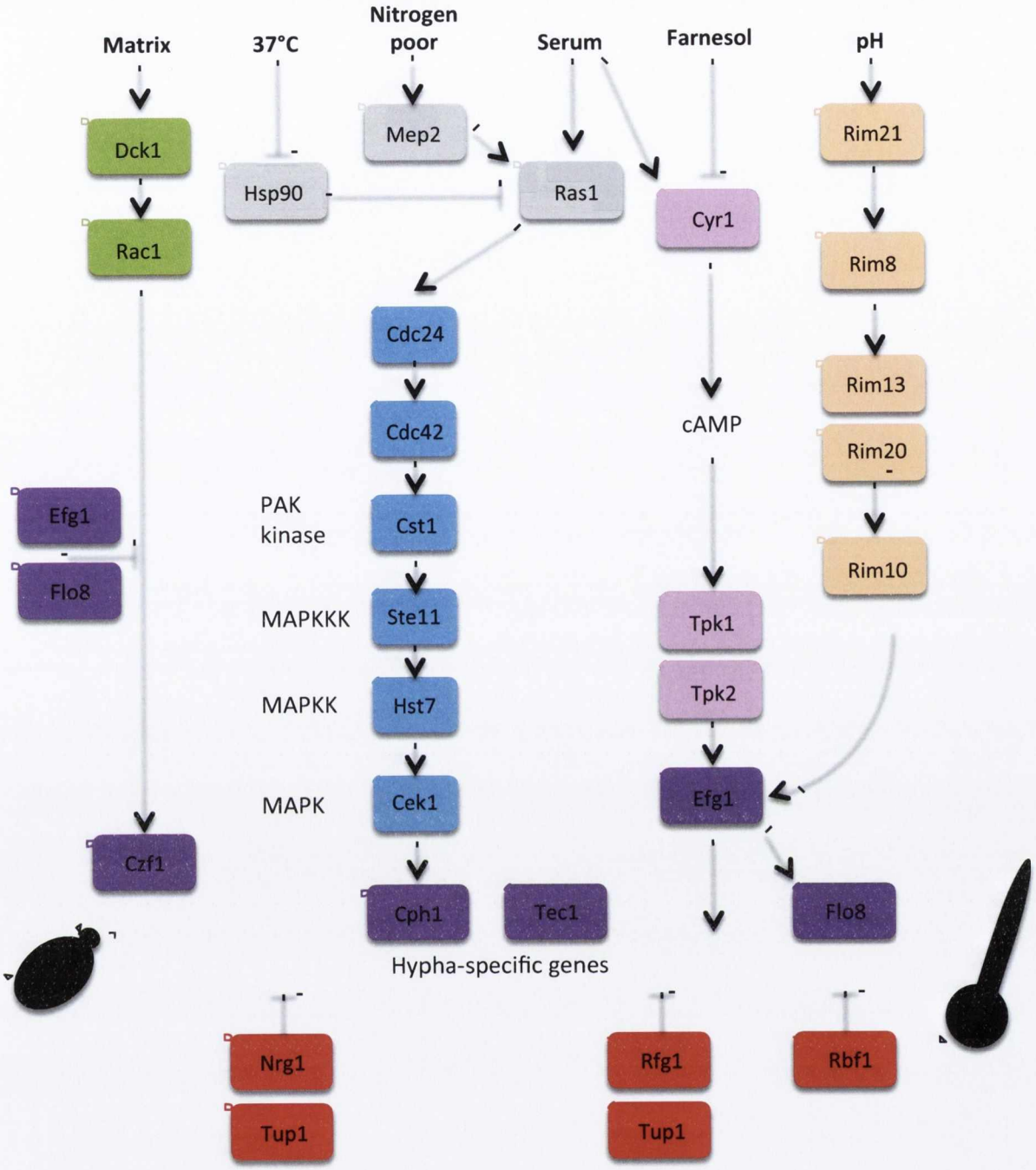

Figure 1.3. Signal transduction pathways leading to morphogenesis. Environmental cues feed through upstream pathways to activate transcription factors. The cyclic AMP-dependent pathway that targets the transcription factor Efg1 is thought to have a major role. Protein factors are colour coded as follows: MAPK pathway is blue, cAMP pathway is pink, transcription factors are purple, negative regulators are red, matrix-sensing pathway is green, pH sensing pathway is orange and other proteins involved in signal transduction are grey.

This figure has been adapted from Sudbery, 2011.

niches (Soll, 2009). Given that opaque cells are unstable at 37 °C, it has been proposed that switching from the white to opaque forms may be relevant in host niches with lower temperatures, like the skin, which also facilitates mating (Lachke *et al.,* 2003). In 2002, Miller and Johnson discovered the role of white-opaque switching in mating. This research demonstrated that a/α cells had to undergo homozygosis at the mating type locus (MTL) in order to switch between white and opaque, which was observed to be necessary for mating (Miller & Johnson, 2002). Lockhart *et al.* (2003) found this to be true for most natural strains of *C. albicans.* In order to mate, diploid cells must undergo homozygosis at the mating type locus to a/a or α/α, either by the loss of one copy of chromosome 5, crossing over or gene conversion (Wu *et al.,* 2005; Wu *et al.,* 2007). The retained copy is then duplicated. The resulting MTL-homozygous cell then switches from a white a/a or α/α cell phenotype, architecturally similar to the a/α yeast cell phenotype, to the opaque cell phenotype, with a large vacuole and a cell wall-containing pimple-like structures (Anderson & Sol, 1987; Slutsky *et al.,* 1987). Alternative mating types secrete pheromones that result in protrusions from stimulated cells of opposite mating type (Bennett *et al.,* 2003; Lockhart *et al.,* 2003; Wong *et al.,* 2003). The protrusions elongate, fuse and the nuclei shift into the conjugation tube where they also fuse, resulting in the formation of a daughter cell (Lockhart *et al.,* 2003; Bennett *et al.,* 2005).

1.2.3.3. Biofilm formation

A major virulence trait associated with *Candida* spp. is their ability to form biofilms. Biofilms are structured, complex communities of microbes that adhere to both organic and synthetic surfaces (Douglas, 2003; Finkel & Mitchell, 2010; Lindsay *et al.,* 2014). Infections caused by biofilms can be the result of single species or a mix of bacterial or fungal species (Douglas, 2003). *Candida albicans* biofilms contain *Candida* cells in yeast and hyphal growth forms that are bound to an extracellular matrix made of polysaccharides, in particular the cell wall polymer β 1,3 glucan (Bonhomme *et al.,* 2011; Kim & Sudbery *et al.,* 2011).

Molecular mechanisms that control the various events involved in biofilm formation have been investigated through specific gene deletions in *C. albicans* (Ramage *et al.*, 2002; Nobile & Mitchell, 2006; ten Cate *et al.*, 2009). Previous biofilm studies revealed that null mutant strains lacking the Efg1 and Cph1 regulators of the yeast-to-hypha switch were less able to produce biofilm, thereby confirming the role of morphogenesis in the formation of *C. albicans* biofilms (Bonhomme *et al.*, 2011). Following on from this discovery, a number of additional mutants with morphogenic defects have been shown to decrease biofilm formation. The zinc finger transcription factor Bcr1 was shown to be vital in the regulation of the production of adhesins and the expression of cell wall associated proteins; Als1, Als3 and Hwp1 (Nobile and Mitchell, 2005). Another zinc finger transcription factor Zap1 is thought to regulate the production of the components of the extracellular matrix (Kim & Sudbery, 2011). Adhesins Eap1 and Ywp1 appear to contribute to early stage and late stage biofilm formation respectively (Granger *et al.*, 2005; Li & Palecek, 2008). Late stage biofilm formation involves a vital dispersal step, where yeast cells that have not adhered to the biofilm disseminate into the surrounding area, aiding the spread of infection (Finkel & Mitchell, 2010). It has been suggested that this dispersion stage may be responsible for device-associated candidaemia and subsequent disseminated invasive disease (Uppuluri *et al.*, 2010). Biofilm formation is a key pathogenic trait of *Candida* species given that biofilms promote resistance of *Candida* species to antifungal therapies (Douglas, 2003; Lindsay *et al.*, 2014). Bacteria that grow in biofilms can be up to a thousand times more resistant to antibiotics than cells that grow independently of biofilms (Donlan & Costerton, 2002). *Candida* species have demonstrated similar levels of resistance (Douglas, 2003). Although the mechanisms of antifungal resistance of biofilms have not been completely elucidated, it has been proposed that resistance is due to the restricted diffusion of drugs through the extracellular matrix (Cuéllar-Cruz *et al.*, 2012).

Due to its clinical significance, biofilm formation in *C. albicans* has been well characterised. However limited information is available on biofilm formation in non-*albicans* species, which are becoming increasingly prevalent in health care associated infections (Silva *et al.,* 2012; Silva-Dias, *et al.,* 2015). Silva-Dias *et al.* (2015) carried out a study in order to characterise virulence factors such as adhesion ability and biofilm formation in a range of *Candida* spp. The study comprised of 184 clinical isolates of different *Candida* species, namely *C. albicans, C. glabrata, C. parapsilosis, C. tropicalis, C. krusei,* and *C. guilliermondii.* Despite their lower isolation frequency *C. guilliermondii* is an important cause of mucocutaneous infection and high mortality rates are associated with *C. krusei* infections (Estevill *et al.,* 2011). According to the study, *C. tropicalis, C. guilliermondii,* and *C. krusei* were the species with the highest biomass production, followed by *C. parapsilosis, C. glabrata,* and *C. albicans.* This study also indicated that *C. albicans* and *C. glabrata* are the fastest at forming biofilms, which may account for their increased prevalence in nosocomial infections (Silva-Dias *et al.,* 2015). It should be noted that *C. parapsilosis* has the ability to form biofilms quite successfully; on indwelling devices in particular, and that *C. parapsilosis* isolates with increased biofilm have been associated with candidiasis (Kuhn *et al.,* 2004). A study carried out by Tumbarello *et al.* (2007) investigating the effects of biofilm-forming *Candida* strains on mortality revealed that with regards to *C. parapsilosis,* the mortality rate for isolates forming biofilm *in vitro* was 71.4%, as opposed to 28% for biofilm deficient isolates.

1.2.3.4. Adhesins

Adhesins are proteins required for the adhesion of a pathogen to host cells and synthetic surfaces, which are key initial processes in establishing infection. Adhesins aid adherence to host surfaces and to medical devices such as stents and catheters (Chandra *et al.,* 2001). A number of genes are associated with adherence such as the agglutinin-like sequence (Als) family of proteins (Hoyer, 2001). There are seven Als glycosylated proteins that aid cell-cell recognition in *Saccharomyces cerevisiae,* however, in *C. albicans,* only Als1, Als3 and Als5

function as adhesins (Fu *et al.,* 1998; Gaur *et al.,* 1999; Calderone & Fonzi, 2001; Hoyer, 2001). A study carried out by Nobile *et al.* (2008) demonstrated that Als1 and Als3 have a major role in biofilm formation in vivo, given that reductions in *ALS1* and *ALS3* gene dosage resulted in severe biofilm defect. Hwp1 and Int1 are also important proteins in adhesion (Nobile *et al.* 2008). Hwp1 contains an amino-terminal sequence with similarities to transglutaminase, promoting stabilised adherence of Hwp1 to human cells. Int1 is an integrin-like protein, vital for cell-to-cell interactions and cell to extracellular matrix interactions (Gale *et al,* 1996; Calderone & Fonzi, 2001).

1.2.3.5. Secreted hydrolases and lipases

Secreted hydrolases are proteins secreted by *Candida* species following adhesion that enable the pathogen to penetrate host cells. One class of secreted hydrolases are the secreted aspartyl proteinases (Saps), which mediate hydrolytic degradation of host tissues. Saps are believed to contribute to the adhesion and invasion of host tissues through the degradation of cell surface structures or the destruction of cells and molecules of the immune system to resist microbiocidal attack (Hamal *et al.,* 2004; Hornbach *et al.,* 2009). *SAP2* in particular has been proposed to be important for invasion and the spread of infection into the bloodstream (De Bernardis *et al.,* 1999; Naglik *et al.,* 2004). Saps have broad substrate specificity and are able to degrade a variety of human proteins such as albumin, haemoglobin, keratin, collagen and almost all immunoglobulins (Ray & Payne, 1990). Lipases are another group of hydrolytic enzymes produced by *Candida* species that have been shown to exhibit cytotoxic effects on host cells (Paraje *et al.,* 2009).

1.2.3.6. Fitness attributes

Other pathogenic traits of *Candida* spp. are the ability to rapidly adapt to fluctuations in pH within their environment, metal acquisition systems, stress response systems and metabolic adaptability (Biswas *et al.,* 2007). Iron, zinc, copper and manganese are all vital metals

necessary in trace amounts for the survival and growth of all living organisms. Pathogenesis depends on a pathogens' ability to assimilate vital nutrients from the environment and their host. Iron acquisition by *Candida* spp. is carried out using three systems: a reductive system that mediates iron acquisition from the environment, a siderophore uptake system, whereby *Candida* spp. acquire iron from siderophores produced by other microbes, and a heme-iron uptake system, which acquires iron from haemoglobin and heme-proteins. Members of the heme-receptor family, Rbt5, Rbt51, Csa1, Csa2 and Pga7, mediate this process (Almeida *et al.*, 2009). Zinc is presumptively acquired by *Candida* spp. using a newly discovered mechanism by which the zinc-binding protein Pra1 binds extracellular zinc and re-associates with the cell (Citiulo *et al.*, 2012). Fungal growth also depends on the ability to assimilate copper and manganese, though these mechanisms are currently unknown (Mayer *et al.*, 2013).

1.2.3.7. Stress response

Many pathogens have the ability to tolerate the environmental stresses that may be experienced in the human body and they achieve this by mounting specific stress responses. Phagocytes of the host immune system generate reactive oxygen species (ROS) such as superoxide and nitric oxide radicals as part of the host defence system. *Candida* spp. mount a stress response after exposure to the host defence system in the form of detoxifying proteins such as the superoxide dismutase (SOD) family of proteins, namely Sod1 and Sod5, and the catalase Cat1 (Martchenko *et al.*, 2004). These proteins have proven essential for pathogenesis in murine models of systemic candidiasis (Mayer *et al.*, 2013). In fungi, the mitogen-activated protein (MAP) kinase pathways sense and transmit environmental signals (including stresses) through phosphorylation. There are three MAP kinase signalling pathways in *Candida* species: Mkc1, Hog1 and Cek1 (Monge *et al.*, 2006). The Mkc pathway is predominantly responsible for cell integrity maintenance, cell wall biogenesis and formation of biofilms (Monge *et al.*, 2006). The Hog1 pathway mediates oxidative, thermal and osmotic stress response, morphogenesis and formation of the cell wall (Monge *et al.*, 2006). The Cek1

pathway regulates mating, filamentation and thermal stress adaptation (Monge *et al.*, 2006; Mayer *et al.*, 2013).

1.3. *Candida dubliniensis*

1.3.1. The emergence of *Candida dubliniensis*

Epidemiological analysis of the *Candida* species associated with OPC in HIV and AIDS patients in Ireland led to the discovery and characterisation of *Candida dubliniensis* by Sullivan *et al.* in 1995. Phenotypic analysis originally suggested that the isolates were *C. albicans*, and consequently they were initially referred to as "Atypical *C. albicans* isolates" because they formed true hyphae and chlamydospores; traits which had previously been exclusively attributed to *C. albicans* (Sullivan *et al.*, 1995). However comparison of rDNA sequences of the two species suggested that the isolates constituted a novel distinct species. A number of phenotypic and genetic characteristics can be used to differentiate *C. albicans* and *C. dubliniensis*. Namely, the chlamydospores produced by *C. dubliniensis* under specific conditions are more abundant than in *C. albicans* (Coleman *et al.*, 1997). *Candida dubliniensis* grows poorly or not at all at 42 °C and produce dark green colonies when primarily isolated from clinical specimens on the chromogenic medium CHROMagar (Sullivan *et al.*, 1997; Sullivan & Coleman, 1998). Polymerase chain reaction (PCR) was used by Donnelly *et al.* (1999) to rapidly differentiate *C. albicans* and *C. dubliniensis* from primary isolates using *C. dubliniensis*-specific PCR primers for the *ACT1* intron. The primers were used in a blind test with 122 *C. dubliniensis* isolates, 53 *C. albicans* isolates, 10 isolates of *C. stellatoidea* and representative isolates of other clinically relevant *Candida* and other yeast species. Only the *C. dubliniensis* isolates yielded the *C. dubliniensis*-specific 288 bp amplimer (Donnelly *et al.*, 1999).

1.3.2. Comparative phenotypes of *Candida dubliniensis* and *Candida albicans*

Comparative phenotypic studies have shown that although *C. dubliniensis* may undergo phenotypic switching more readily than *C. albicans,* it is less capable of efficiently forming true hyphae (Sullivan *et al.,* 2005; Stokes *et al.,* 2007). One of the most common conditions used to induce hyphal growth is nutrient-rich YEPD supplemented with 10% (v/v) fetal bovine serum (FBS) at 37 °C. Over 80% of *C. albicans* cells can filament within 2 h when introduced to this condition. *Candida dubliniensis* is the only *Candida* spp. other than *C. albicans* that can form true hyphae (Sullivan *et al.,* 1997; Sullivan & Coleman, 1998). However, *C. dubliniensis* struggles to form true hyphae in YEPD serum and requires nutrient poor media (e.g. water with 10% FBS) to generate levels of hyphae comparable with *C. albicans.* Under these conditions, *C. dubliniensis* cells appear 90% hyphal after ~ 3 h. This suggests that nutrient starvation is necessary for hyphal induction by *C. dubliniensis* (O'Connor *et al.,* 2010). Furthermore, *C. dubliniensis* also appears to form hyphae less efficiently than *C. albicans* in Lee's medium, in the presence of CO_2 and defined media such as RPM1 1640 (Moran *et al.,* 2007; Stokes *et al.,* 2007).

It was shown in a study carried out by Staib and Morschhäuser (2005) that the *NRG1* gene, which codes for a transcriptional repressor, is differentially regulated between *C. albicans* and *C. dubliniensis* on Staib medium (a nutrient poor medium originally developed for the culture of *Cryptococcus neoformans*). In *C. albicans,* the constitutive expression of *NRG1* on Staib medium causes the cells to remain as budding yeast. In contrast, in *C. dubliniensis,* cells grow as hyphae or chlamydospores, as a result of the down-regulation of *CdNRG1.* As a result of this study, Moran *et al.,* (2007) examined the role of Nrg1p in filamentation regulation and virulence in *C. dubliniensis.* They found that the homozygous deletion of *CdNRG1* resulted in increased levels of hyphae that enhanced the survival and invasion of *C. dubliniensis* in macrophage and reconstituted human epithelial (RHE) models. Therefore, differential expression of *CdNRG1* in response to nutrient availability may be responsible for the lack of

filamentation of *C. dubliniensis* under a variety of conditions and may be a contributing factor to the differences in virulence exhibited by the two species (Moran *et al.*, 2007).

1.3.3. Comparative virulence of *Candida dubliniensis* and *Candida albicans*

Although *C. dubliniensis* shares a range of phenotypes with and is genetically very closely related to *C. albicans,* there is a major disparity in the prevalence and ability of the two species to cause disease. In a study of the epidemiology of candidemia carried out by Kibbler *et al.* in 2003 it was found that although *C. albicans* was present in over 60% of bloodstream infections, *C. dubliniensis* was present in just 2% of cases. A recent study of OPC in HIV/AIDS patients carried out by Patel *et al.* (2012) reported that while *C. albicans* was the most frequently isolated species (found in 62% of cases), of the non-*albicans* species identified in the study, *C. dubliniensis* was the third most frequently isolated after *C. glabrata,* with 12% of isolates identified as *C. dubliniensis* and 17% of isolates identified as *C. glabrata.* A number of studies have been carried out in recent years to identify the frequency of *Candida* spp. in infection, and the distribution of *C. dubliniensis* is varied (Hamza *et al.*, 2008; Agwu *et al.*, 2011; Patel *et al.*, 2012). In 2011, Agwu *et al.* carried out a study to investigate the distribution of *Candida* spp. associated with oral lesions in HIV-positive patients in Southwest Uganda. They observed a complete absence of *C. dubliniensis* within the patient group of 306 individuals with mixed species infections. However a study carried out in Tanzania recovered a single *C. dubliniensis* isolate in a survey of 292 patients, while in a study of institutionalised pediatric HIV/AIDS patients in South Africa, 26% harboured *C. dubliniensis* (Blignaut, 2007; Hamza *et al.*, 2008).

Reconstituted human epithelial tissue invasion model studies carried out by Stokes *et al.* (2007) were used to compare the ability of *C. albicans* and *C. dubliniensis* to invade human tissue. Stokes *et al.* (2007) observed in RHE samples infected with *C. albicans* extensive growth of both yeast and hyphal cells were apparent 12 h post-inoculation. Between 12 and

24 h the RHE displayed signs of tissue damage, while invasion of deeper parts of the epithelium by *C. albicans* were observed after 24 h. After 48 h, in the RHE model colonised by *C. albicans* very few epithelial cells remained attached to the membrane. In contrast, the *C. dubliniensis* RHE model contained only yeast cells at all time points, with a very small minority of hyphal and pseudohyphal cells present in certain sections. By 12 h very few *C. dubliniensis* yeast cells had attached to the epithelium and only after 24 h was slight tissue damage apparent. At 48 h the level of tissue damage had increased, but was far lower than that seen with *C. albicans.* This disparity in virulence was also confirmed using the oral-intragastric murine infection model, in which *C. albicans* colonised mice far more efficiently and was able to establish infection more successfully than *C. dubliniensis.* In order to compare the ability of *C. albicans* and *C. dubliniensis* to colonise and infect the gastrointestinal tissue Stokes *et al.* (2007) employed an oral-intragastric infant mouse infection model and inoculated the two species together in co-culture and alone. Up until day 6, Stokes *et al.* observed similar levels for both species. However, at days 8 and 10 the levels of *C. albicans* remained high while no *C. dubliniensis* was detectable. This study provides significant evidence for the disparity in virulence between *C. albicans* and *C. dubliniensis* (Stokes *et al.*, 2007).

A study undertaken by Spiering *et al.* in 2010 observed similar RHE results to those observed by Moran *et al.* (2004). Spiering *et al.* (2010) used *C. albicans* DNA microarrays to compare global gene expression of *C. albicans* and *C. dubliniensis* in an RHE model. In addition to observing the growth patterns of *C. albicans* and *C. dubliniensis,* they observed differences in gene expression patterns between the two species. When *C. albicans* caused major tissue damage, up-regulated expression of a number of known hyphally regulated genes was observed, while this was not seen in *C. dubliniensis.* Furthermore, several genes of unknown function in *C. albicans* that are absent or significantly divergent in *C. dubliniensis* were up-regulated during infection. One such gene was *SFL2,* which showed an increase in expression

in *C. albicans* within 30 min in the RHE model. Homozygous deletion of *SFL2* in *C. albicans* resulted in the loss of ability to form true hyphae under a variety of hyphal-inducing conditions. Overexpression of *SFL2* resulted in increased filamentation in *C. albicans* and the formation of pseudohyphae in *C. dubliniensis.* The deletion in *C. albicans* had no effect in a murine model but led to decreased RHE colonisation, suggesting a possible role for *SFL2* in an oral mucosal infection model (Spiering *et al.,* 2010). Interestingly, Spiering *et al.* (2010) observed similarly up-regulated patterns between *C. albicans* and *C. dubliniensis* in genes involved in primary metabolism and carbon utilisation genes. The up-regulation of primary metabolism genes in mammalian tissues has previously been solely attributed to *C. albicans,* and the up-regulation of carbon utilisation genes in *C. dubliniensis* suggests common pathways between the two species for physiological adaptation to the RHE environment (Thewes *et al.,* 2007; Zakikhany *et al.,* 2007; Spiering *et al.,* 2010).

1.3.4. Genomic comparison of *Candida dubliniensis* and *Candida albicans*

In order to elucidate the disparity in virulence between *C. albicans* and *C. dubliniensis* Moran *et al.* (2004) carried out a comparative genomic hybridisation study. Genomic DNA from *C. albicans* and *C. dubliniensis* was co-hybridised to a *C. albicans* DNA microarray and the relative hybridisation efficiency of *C. albicans* and *C. dubliniensis* DNA to each gene-specific spot was compared. Genomic DNA of *C. dubliniensis* was reported to hybridise to 95.6% of *C. albicans* gene sequences, indicating a nucleotide homology of greater than 60% between the two species. The residual 4.4% of sequences, which represent 247 genes, indicated divergence of less than 60% between *C. albicans* and *C. dubliniensis,* or absence in *C. dubliniensis.* Given that the vast majority of *C. albicans* genes are conserved in *C. dubliniensis,* this indicates that the two species are likely to have diverged recently and thus most likely inhabit similar environments in the body (Moran *et al.,* 2004).

The most definitive attempt to understand why *C. albicans* and *C. dubliniensis* differ so greatly in their capacity to cause disease in humans involved the sequencing of the *C. dubliniensis* genome to permit comparison with that of *C. albicans* (Jackson *et al.*, 2009). Although this comparison identified a very high level of synteny and sequence similarity between the two species, a number of disparities were also observed. One of these disparities occurs with genes of the SAP family, which are virulence factors that mediate hydrolytic responses to host tissues. *SAP1, SAP4, SAP5* and *SAP6* are found in in *C. albicans*, while *C. dubliniensis* lacks *SAP4* and *SAP5*. Furthermore, *C. dubliniensis* lacks the hyphal-associated *HYR1*, which encodes highly decorated, repetitive cell-wall proteins that are induced during hyphal differentiation in *C. albicans* (Bailey et al. 1996). While the absence of two *SAP* genes and *HYR1* are due to deletions in *C. dubliniensis, C. albicans* was also found to have a number of novel insertions i.e. the invasin-like *ALS3* (Hoyer *et al.* 1998; Phan *et al.* 2007; Almeida *et al.* 2008). *ALS* genes encode a family of repetitive cell-surface proteins that are involved in host cell adhesion and are important for the initiation and continuation of infection (Fu *et al.* 2002; Sheppard *et al.* 2004; Zhao *et al.* 2007). *ALS3* is found on chromosome R in *C. albicans*, but is absent from the same position in *C. dubliniensis* (Jackson *et al.*, 2009). The filamentous growth regulator (FGR) genes are an example of the reductive evolution that *C. dubliniensis* is suggested to be undergoing. There are sixteen of these genes present in *C. albicans*, however in *C. dubliniensis* six have been deleted and eight are pseudogenes. Furthermore, a disparity lies in the *IFA* gene family that encode putative transmembrane proteins. There are thirty-one present in *C. albicans* while *C. dubliniensis* has twenty-one (Jackson *et al.* 2009).

The most significant difference in gene families between the two species is the TeLOmere-associated (*TLO*) gene family. In *C. albicans*, fifteen of these genes are present in the genome, as opposed to two in *C. dubliniensis* (i.e. *CdTLO1* and *CdTLO2*) (Jackson *et al.*, 2009). As this gene family stands out as the family with the largest copy number disparity between the two

species, through gene expansion in *C. albicans* rather than through gene deletion in *C. dubliniensis,* they have recently been subjected to further scrutiny.

1.3.5. The *TLO* gene family

Alteration in gene copy number is a genetic response to new or stressful environments, which allows organisms to adapt to altered conditions. Most variation of the genome is exhibited in telomeric regions (Dujon *et al.,* 2004; Carreto *et al.,* 2009). The *TLO* gene family of *C. albicans* is an example of gene family expansion near the telomeres (Butler *et al.,* 2009). The fifteen *TLO* genes that are present in *C. albicans* have an average similarity of 96.5% and are primarily located sub-telomerically on each chromosome. In contrast in *C. dubliniensis* the two *TLO* orthologues *CdTLO1* and *CdTLO2* are more divergent, being 74.9% similar, with *CdTLO2* located sub-telomerically on chromosome R, and *CdTLO1* located internally on chromosome 7 (Figure 1.4) (Jackson *et al.,* 2009). Synteny suggest that *C. albicans TLO2* is the ancestral locus, as a *TLO2* orthologue is present in the same sub-telomeric locus in *C. albicans, C. dubliniensis, C. tropicalis* and *C. parapsilosis* (Sullivan *et al.,* 2015). Sub-telomeric recombination is thought to have led to the expansion of the *C. albicans TLO* gene copy number (Anderson *et al.,* 2012).

When first identified, the Tlo proteins' functions were unknown. Originally, yeast one-hybrid data and the presence of a conserved domain with high similarity to Med2, a component of the RNA polymerase II Mediator complex, suggested that the Tlo proteins code for a family of putative transcriptional regulators (Kaiser *et al.,* 1999; Björklund and Gustafsson, 2005). A study carried out by Anderson *et al.* (2012) in an attempt to characterise the structure and expression patterns of the *C. albicans TLO* gene family found that there are three clades of *TLO* genes based on sequence similarity; α, β and γ (Figure 1.4). All three clades contain the predicted Med2 binding domain. They also identified a 15th *TLO* pseudogene that lacks the Med2 binding domain. The main distinguishing factor between the three clades is the

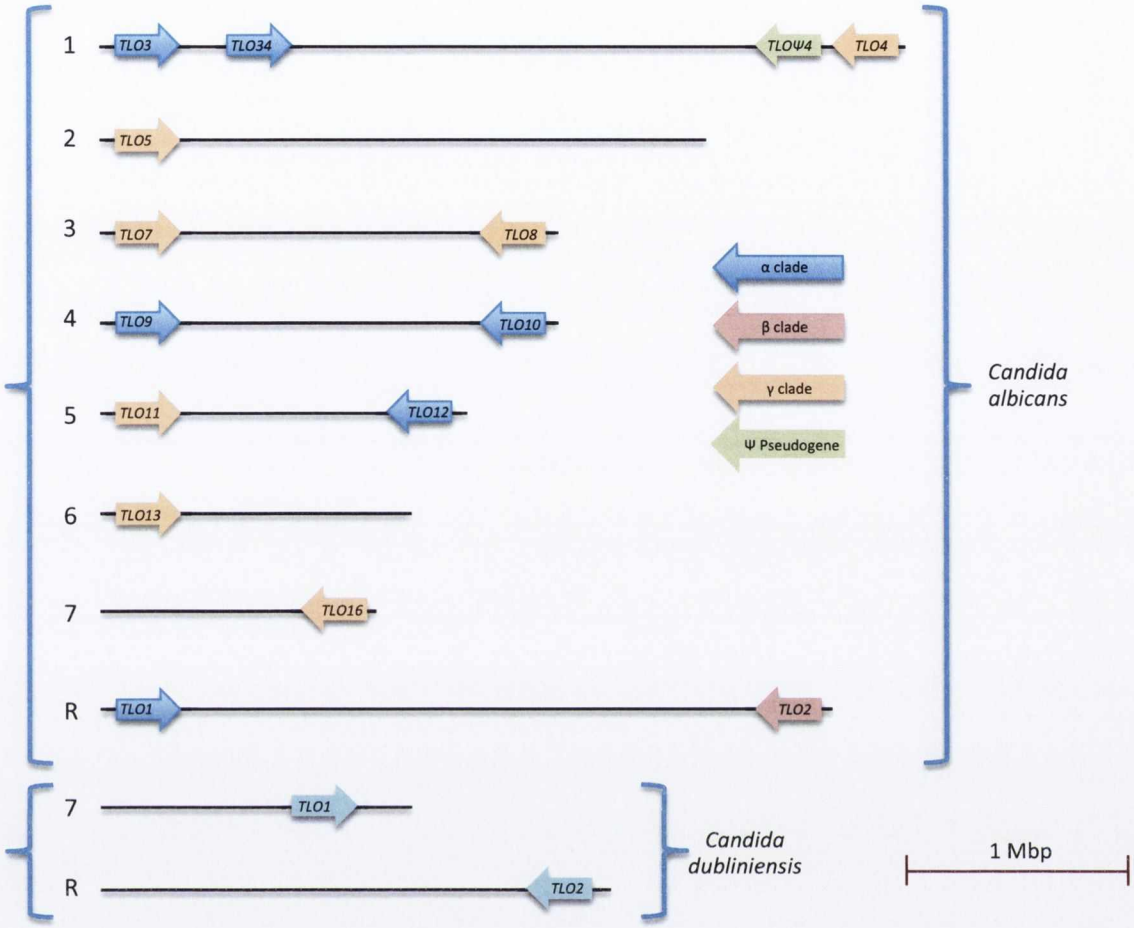

Figure 1.4. *TLO* genes of *Candida albicans* and *Candida dubliniensis.*
Chromosomal gene locations and orientations of *TLO* genes in *C. albicans* and *C. dubliniensis.* Direction of transcription indicated by directional arrows. Chromosomes are labeled to the left of the illustration. While karyotypes are not accurate, a scale of 1 Mbp is shown. Anderson *et al.* (2012) proposed the re-assignment of the *TLO* genes into clades as shown using the indicated colour scheme. *C. dubliniensis TLOs* have not been assigned to clades.

presence of long terminal repeat (LTR) insertions that alter coding sequences, driven by retrotransposon activity (Sullivan *et al.*, 2015). Anderson *et al.* (2012) found the Tlo proteins encoded by all three clades are located in the nucleus, while the Tloγ proteins are also found in the mitochondria. The highest expression levels were found for the *TLOα* genes, with *TLOγ* expressed at lowest levels. These authors also suggested that the broad range of expression levels and localisation arrangements may result in an equally wide range of compositions of the subunits of the Mediator complex, which may help *C. albicans* adapt to the extensive array of host niches it occupies. Since the two species differ so much in their repertoire of *TLO* genes it is also tempting to hypothesise that this may at least partly explain why, despite their great genomic similarity, *C. albicans* is a far more accomplished pathogen than *C. dubliniensis.*

In order to investigate the functions carried out by the *TLO*s and their encoded proteins with regards to processes involved in virulence, it was necessary to genetically manipulate the *TLO* genes. Given that *C. dubliniensis* shares many characteristics with *C. albicans* and codes for only two *TLO* genes as opposed to 15, genetic analysis could be achieved more readily in *C. dubliniensis* than in *C. albicans.* Previous work has shown that the homozygous deletion of *CdTLO1* and *CdTLO2* affects morphogenesis, environmental stress response and growth/metabolism (Jackson *et al.*, 2009; Haran *et al.*, 2014). The deletion of *CdTLO1* appears to affect the phenotype to a greater extent than the deletion of *CdTLO2.* Furthermore, DNA microarray studies carried out in our lab to investigate the effect of deletion of the *CdTLO*s on the *C. dubliniensis* genome have shown that genes involved in morphogenesis/cell wall, environmental stress response and growth/metabolism are both up-regulated and down-regulated in the absence of the *TLO*s, suggesting that the Tlos are both positive and negative regulators of gene expression (Haran *et al.*, 2014).

1.4. The Tlos and the Yeast Mediator Complex

1.4.1. The Yeast Mediator Complex

The yeast Mediator complex is conserved among eukaryotes. The yeast Mediator is composed of 25 subunits, which are structurally and functionally organised into modules (Dotson *et al.*, 2002). The core complex is comprised of 21 subunits divided into the Head, Middle and Tail domains (Davis *et al.*, 2002; Guglielmi *et al.*, 2004) (Figure 1.5). A fourth domain, termed the Cdk (cyclin dependent kinase) module contains four proteins and is generally involved in repression (Holstege *et al.*, 1998; Myers and Kornberg, 2000; Borggrefe *et al.*, 2002; Guglielmi *et al.*, 2004; Elmlund *et al.*, 2006). The Mediator complex directly binds to pol II and functions at every stage of transcription, from recruiting pol II to genes during signal transduction to modulating the activity of pol II during transcription initiation and elongation (Conaway and Conaway, 2011). It is thought that the Mediator plays the role of an interface between the proteins involved in regulation and the basal pol II transcription machinery (Björklund and Gustafsson, 2005). The yeast Mediator transcription factor complex is associated with RNA polymerase II, with essential roles in transcription in *S. cerevisiae* (Kim *et al.*, 1994). The head and middle regions are proposed to interact with pol II, while the tail region is responsible for recognition and binding of activators. The Med3 protein subunit of the mediator interacts with Med2 within the tail module (Bhoite *et al.*, 2001).

1.4.2. Tlo proteins are orthologues of Med2

The presence of a Med2 domain in the Tlos originally suggested that the Tlos are homologues of Med2 in the tail region of the Mediator. Zhang *et al.* (2012) confirmed using biochemical analysis that the Tlo proteins are subunits of the Mediator complex. Through biochemical studies they found that at least five of the fifteen *C. albicans TLO*s could be incorporated into the CaMediator complex, with the expectation that all expressed Tlo proteins can associate with the Mediator. Unpublished data from L.C. Myers (personal communication) has shown

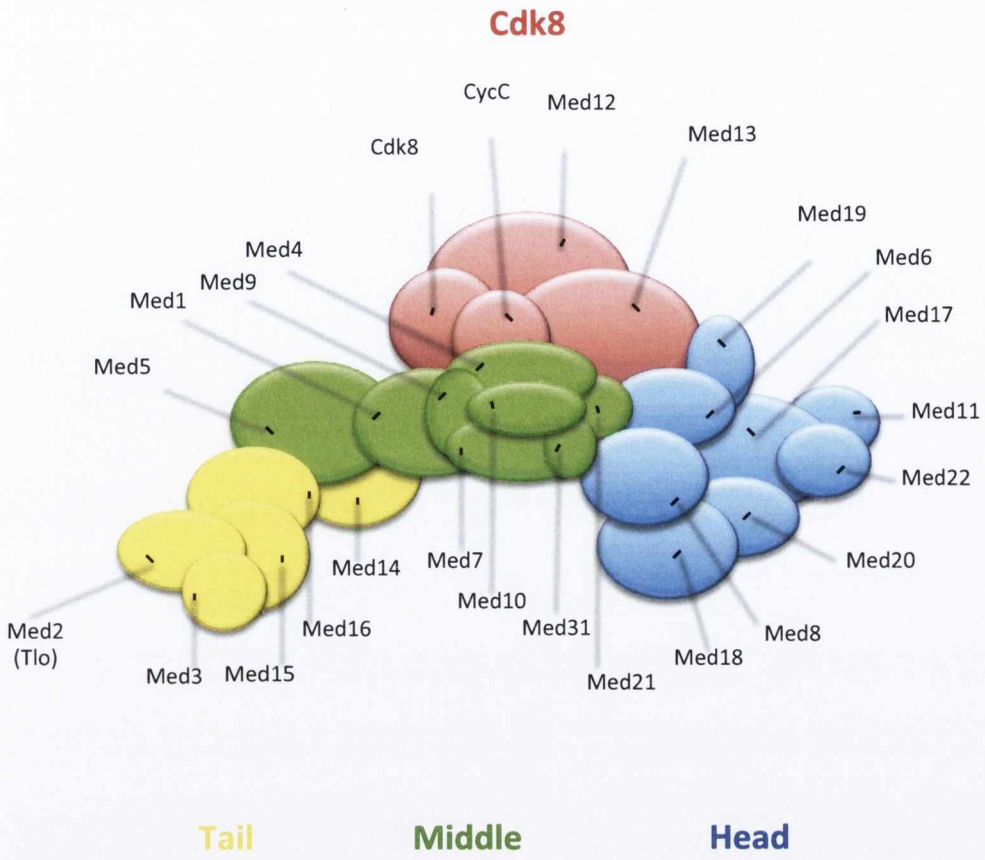

Figure 1.5. Model of the organisation of the yeast Mediator complex. Tlo proteins assigned to Med2 in the tail region as described by Zhang *et al.,* (2012).

that although *C. dubliniensis* has two paralogues of the *TLOs*, only one of them is detectable within the Mediator. In the case of *C. albicans*, Zhang *et al.* (2012) observed that after what is required for Mediator, there is still an excess of free Tlo protein. They have also hypothesised that the excess Tlo protein observed in *C. albicans* may perform additional functions independently of its functions associated with Mediator.

1.5. The aims of this study

- Confirm the function of the Tlos in *C. dubliniensis* by re-introducing *CdTLO1* and *CdTLO2* to the *Cdtlo*ΔΔ mutant background and investigating the effect on phenotype and the effect on the transcript profile.
- Confirm the Tlos are orthologues of Med2 by generating a homozygous *MED3* mutant strain and comparing the phenotype and transcript profile to that of the *Cdtlo*ΔΔ mutant.
- Confirm the Tlos are subunits of the yeast Mediator complex by carrying out Tandem Affinity Purification (TAP) on CdTlo1.
- To identify if Tlo orthologues encode proteins with distinct function in *C. dubliniensis* and *C. albicans* by introducing *CaTLO1, CaTLO3* and *CaTLO4* into the *Cdtlo*ΔΔ mutant background and investigating the effect on phenotype and the effect on the transcript profile.

Chapter 2

General Materials & Methods

2.1. General Microbiological Methods

2.1.1. Strains and growth conditions

The strains of *Candida* spp. used in this study and their genotypes are listed in Table 2.1. Unless indicated otherwise, all strains were obtained from the laboratory collection of the Microbiology Research Unit, Division of Oral Biosciences, Dublin Dental University Hospital, Trinity College, Dublin 2. *Escherichia coli* strain XL10-Gold (Stratagene endA1, glnV44, recA1, thi-1, gytrA96, relA1, lac, Hte Δ(mcrA) 183, Δ(mcrCB-hsdSMR-mrr)173 tet^R F`[proAB $lacI^qZ$ ΔM15, Tn10(Tet^R Amy Cm^R)] (Stratagene, La Jolla, California, USA) was used as the host strain for all plasmids.

All *Candida* strains were routinely maintained on Yeast Extract Peptone Dextrose (YEPD) medium (10 g/L yeast extract [Sigma-Aldrich, Tallaght, Dublin, Ireland], 20 g/L Bactopeptone [Difco], 20 g/L dextrose [Sigma], pH 5.5). Cells were grown at 30 °C or 37 °C unless stated otherwise, statically (Gallenkamp, Leicester, UK) or in an orbital incubator (New Brunswick Scientific Company Inc., Edison, New Jersey, USA) rotating at 200 r.p.m. Strains were grown aerobically unless stated otherwise. Nourseothricin-resistant strains were cultured on YEPD agar containing nourseothricin [100 μg/ml (NAT_{100})/ 2 μg/ml (NAT_2) to select for sensitive revertants] (cloNAT, Werner Bioagents, Germany). To recover nourseothricin sensitive revertants the dextrose component of the YEPD was replaced with 20 g/L and 40 g/L maltose (Sigma-Aldrich). Uridine auxotrophic (*ura3*Δ/*ura3*Δ) *C. dubliniensis* strains were grown on YEPD supplemented with 50 μg/ml uridine.

E. coli strains were maintained on Luria-Bertani (LB) pH 7.4 agar and LB agar containing 100 μg/ml ampicillin (Penbritin, GlaxoSmithKline, Stonemasons Way, Rathfarnham, Dublin, Ireland) (L_{amp}) or 50 μg/ml chloramphenicol (L_{chloro}) at 37 °C.

Lee's Medium (Lee *et al.*, 1975) was prepared by adding 12.7 g of salts mix (5 g $(NH_4)_2SO_4$, 0.2 g $MgSO_4.7H_2O$, 2.5 g K_2HPO_4, 5.0 g NaCl), 4.714 g of L-amino acid mix (0.5g L-alanine, 1.3 g L-leucine, 1.0 g L-lysine, 0.1 g L-methionine, 0.0714 g L-ornithine, 0.5 g L-phenylalanine, 0.5 g L-proline, 0.5 g L-threonine) and 12.5 g of glucose. The pH was adjusted to either pH 4.5 or pH 6.5 and sterilised by filtration. Prior to use, the stock solution was supplemented with 1ml/L 0.001% (w/v) biotin (0.01 g/L), 1 ml/L 400 mM arginine (84.2 g/L L-arginine monohydrochloride), 1 ml/L 1 M Trace Metals Stock I (203 g/L magnesium chloride hexahydrate, 147 g/L calcium chloride dehydrate) 1 ml/L 1M Trace Metals Stock II (0.6 g/L zinc sulphate heptahydrate, 2.7 g/L iron (III) chloride hexahydrate, 0.6 g/L copper sulphate pentahydrate). Rice agar Tween (RAT) medium was used for chlamydospore formation (Kirkpatrick *et al.*, 1998). It was prepared by dissolving 15 g rice extract agar (Sigma) in 1 L distilled water. Following sterilisation by autoclaving, 1% (v/v) Tween 80 was added (Sigma).

2.1.2. Chemicals and enzymes

Chemicals and reagents used in this study were all of molecular biology-grade or analytical-grade sourced from Sigma-Aldrich, Roche (Roche Products [Ireland] Limited, 3004 Lake Drive, Citywest, Dublin 24, Ireland). Promega (Promega Corporation, Madison, Wisconson, USA), Bioline (London, United Kingdom), Ambion (Bio-Sciences, Crofton Road, Dun Laoghaire, Dublin, Ireland), Agilent (Agilent Technologies, Cork), GE Healthcare Life Sciences (Filial Sverige, Uppsala, Sweden), Life Technologies (Crofton Road, Dun Laoghaire, Co. Dublin). DNA molecular markers, DNA loading dyes, enzymes and dNTPs were all obtained from Sigma Aldrich, Promega and New England Biolabs (Ipswich, MA, USA), stored at -20 °C and subsequently used according to manufacturers' instructions. Doxycycline hyclate was purchased from Sigma-Aldrich and stock solutions were stored in the dark at 4 °C.

Strain	Origin*	Parent	Genotype	Reference(s)
C. albicans SC5314	USA		Wild-type	Gillum *et al.* (1984)
C. dubliniensis Wü284	Germany		Wild-type. Genotype I	Morschhauser *et al.* (1999)
CdUM1A**	N/A	Wü284	Wü284 (ura3Δ1::*MPA^R-FLIP/URA3*)	Staib *et al.* (2001)
*Cdtlo*ΔΔ	DDUH	ΔCd*tlo1*	*tlo1*ΔΔ::FRT/ *tlo2*ΔΔ::FRT	Jackson *et al.* (2009)
*Cdtlo*ΔΔ-*CdTLO1*	DDUH		*tlo1*ΔΔ::FRT/ *tlo2*ΔΔ::FRT, *CDRI/cdrI*Δ::pCDRI-*CdTLO1*	Jackson *et al.* (2009)
*Cdtlo*ΔΔ-*CdTLO2*	DDUH		*tlo1*ΔΔ::FRT/ *tlo2*ΔΔ::FRT, *CDRI/cdrI*Δ::pCDRI-*CdTLO2*	Jackson *et al.* (2009)
*Cdtlo*ΔΔ-*CdTLO1*	DDUH		*tlo1*ΔΔ::FRT/ *tlo2*ΔΔ::FRT, *ADH1*/adh1::ptet-*CdTLO1*	This study (2015)
*Cdtlo*ΔΔ-*CdTLO2*	DDUH		*tlo1*ΔΔ::FRT/ *tlo2*ΔΔ::FRT, *ADH1*/adh1::ptet-*CdTLO2*	This study (2015)
*Cdmed3*Δ	DDUH	Wü284	*MED3-1/med3-2*Δ::FRT	Haran *et al.* (2014)
*Cdmed3*Δ- *CdMED3*	DDUH		*MED3-1/med3-2*Δ::FRT, *CDRI/cdrI*Δ::pCDRI-*CdMED3*	This study (2015)
CdUM1A-*CdTLO1*	DDUH		Wü284 (ura3Δ1::*MPA^R-FLIP/URA3*)::*CdTLO1*	This study (2015)
CdUM1A-*CdTLO2*	DDUH		Wü284 (ura3Δ1::*MPA^R-FLIP/URA3*)::*CdTLO2*	This study (2015)
*Cdtlo*ΔΔ-*CaTLO1*	DDUH		*tlo1*ΔΔ::FRT/ *tlo2*ΔΔ::FRT,*CDRI/cdrI*Δ::pCDRI-*CaTLO1*	This study (2015)
*Cdtlo*ΔΔ-*CaTLO3*	DDUH		*tlo1*ΔΔ::FRT/ *tlo2*ΔΔ::FRT,*CDRI/cdrI*Δ::pCDRI-*CaTLO3*	This study (2015)
*Cdtlo*ΔΔ-*CaTLO4*	DDUH		*tlo1*ΔΔ::FRT/ *tlo2*ΔΔ::FRT,*CDRI/cdrI*Δ::pCDRI-*CaTLO4*	This study (2015)
*Cdtlo*ΔΔ-N-*TLO1*3xHA	DDUH		*tlo1*ΔΔ::FRT/ *tlo2*ΔΔ::FRT,*CDRI/cdrI*Δ::pCDRI-*N-TLO1* 3xHA	This study (2015)
*Cdtlo*ΔΔ-N-*TLO1*	DDUH		*tlo1*ΔΔ::FRT/ *tlo2*ΔΔ::FRT,*CDRI/cdrI*Δ::pCDRI-*N-TLO1*	This study (2015)

Table 2.1. *Candida* strains used in this study

*DDUH refers to the Dublin Dental University Hospital strain collection

** Derivative of Wü284

Plasmid	Description	Reference
pNIM	*E. coli* plasmid for tetracycline-regulatable gene expression by the pTET promoter containing the dominant *SAT1* selection marker.	Park and Morschhauser, (2005)
pCDRI	*E. coli* plasmid for gene integration in *Candida* species containing the *SAT1* resistance marker. Ampicillin resistant.	Moran *et al.*, (2007)
pSFS2	*E. coli* plasmid with cassette for gene deletions in *C. albicans*; flipase under pSAP2 inducible promoter and tACT1 terminator, *SAT1* dominant marker under pACT1 promoter. Chloramphenicol resistant.	Reuss *et al.*, (2004)
pFA-TAP-CaURA3	*E. coli* plasmid derived from the pFA-vector for tandem affinity purification of proteins. Contains the *URA3* resistance marker and a Protein A analogue.	Gola *et al.*, (2003), Lavoie *et al.*, (2008).

Table 2.2. Plasmids used in this study

2.1.3. Buffers and solutions

Ultrapure Milli-Q Biocel-purified water (resistivity 18.2 MΩcm) (Millipore, Carrigtohill, Cork, Ireland) was used for all buffers and solutions. Molecular biology grade water (Sigma-Aldrich) was used for resuspension of nucleic acids, oligonucleotides and PCR. Phosphate Buffered Saline (PBS) solution was prepared from PBS tablets (Difco, Magna Business Park, Citywest, Dublin 24) in accordance with manufacturers' instructions and sterilised by autoclaving. Tris-EDTA (TE) containing 10 mM Tris-HCl, 1mM EDTA pH 8.0 was used as a buffer for storage of DNA. Tris-Borate EDTA (TBE) at a concentration of 20 X containing 0.45 M Trizma base, 0.45 M boric acid and 0.01 M EDTA was diluted in ultrapure water to a final concentration of 0.5 X and used as a buffer for agarose gel electrophoresis. All solutions were stored at room temperature unless otherwise stated.

2.2. Morphology and growth experiment methods

2.2.1. Hyphal induction in liquid media

Each strain to be studied was grown at 37 °C for 48 h on YEPD agar. From each plate a single colony was inoculated into 2 ml YEPD broth and grown overnight at 30 °C with shaking at 200 r.p.m in an orbital incubator. Overnight cultures were centrifuged for 3 min at 14,000 r.p.m and washed twice with sterile phosphate buffer solution (PBS). Cells were re-suspended in 1 ml of PBS and counted using a Neubauer haemocytometer (Merienfield glassware) at 10^{-2} dilution. A volume of 2.5 x 10^5 cells per ml of this cell suspension was added to 2 ml volumes of sterile ultrapure H_2O, supplemented with 10% w/v fetal bovine serum (FBS) (and doxycycline [10-50 μg/ml] for experiments including DOX-inducible strains) in each well of a six-well tissue culture plate (Greiner Bio-One, Germany). Plates were incubated at 37 °C in a static incubator. Plates were removed from incubation at specific time-points and the numbers of true hyphal cells were quantified, visualised and illustrated as a percentage of 100 cells using a Nikon E600 microscope and a Nikon TMS-F inverted light

microscope. Replicate plates were set up for each time-point measured so as to not interrupt incubation periods between time-points. Each experiment was carried out on three separate occasions.

2.2.2. Hyphal induction on solid media

Spider agar was prepared using 1% (w/v) nutrient broth, 1% (w/v) mannitol, 0.2% (w/v) K_2HPO_4 and 1.35% (w/v) Bactoagar (Liu *et al.*, 1994). Following standard growth on YEPD plates, cells were inoculated onto Spider plates and incubated at 30 °C or 37 °C in a static incubator for 5 days. Plates were visualised using a Nikon E600 microscope and a Flash n' Go plate visualiser (IUL Instruments, Barcelona, Spain). Each experiment was carried out on three separate occasions.

2.2.3. Spot plate assay

Overnight cultures were centrifuged for 3 min at 14,000 r.p.m. and washed twice with sterile phosphate buffer solution (PBS). Cells were re-suspended in 1 ml of PBS and counted using a Neubauer haemocytometer (Merienfield glassware) at 10^{-2} dilution and standardised to 2 x 10^6 cells/ml. Volumes of 5-15 µl from serial dilutions (10^0 to 10^{-4}) were spotted onto YEPD agar plates containing hydrogen peroxide (H_2O_2) (Sigma-Aldrich) (2.5 mM–6 mM). The plates were incubated at 37 °C (or at 30 °C and 42 °C if heat was the experimental factor) for 48 h in a static incubator. Plates were observed for levels of growth and photographed using a Flash n' Go plate visualiser (IUL Instruments). Each experiment was carried out on three separate occasions.

2.2.4. Growth rate determination

Strains were grown in YEPD at 30 °C overnight (18h), with shaking at 200 r.p.m in an orbital incubator. The cells were centrifuged for 3 min at 14,000 r.p.m and washed twice with sterile PBS and counted as previously described. Cells were inoculated into 50 ml of the appropriate

medium to obtain a final concentration of 2 x 10^6 cells/ml. Cultures were incubated at 37 °C with shaking at 200 r.p.m for up to 10 h, with O.D. 600 nm measurements recorded hourly using a spectrophotometer (Thermo Scientific, Ireland). Each experiment was carried out on three separate occasions. Measurements were graphed using Microsoft Excel. Data from exponential growth was imported to Prism Graph pad and the data for each strain was fit to a curve using non-linear regression/exponential curve. Doubling time was calculated for each strain, using the formula ln(2)/k where k is the rate constant expressed as inverse of time. Doubling times from each replicate were pooled and standard deviations calculated using Microsoft Excel.

2.3. Isolation and analysis of nucleic acids from *Candida* cells

2.3.1. Extraction of genomic DNA from *Candida* cells

Candida cells were cultured by streaking onto YEPD agar followed by incubation at 37 °C for 48 h. Cells were inoculated in YEPD broth and incubated at 30 °C at 200 r.p.m. over night. Following incubation, cells were harvested from 1.5 ml of culture in microcentrifuge tubes (Eppendorf, Germany). The supernatant was removed and the pellet re-suspended in 200 µl of 2% (v/v) Breaking Buffer (2% Triton X-100, 1% (w/v) SDS, 10 mM Tris HCL (pH 8.0), 1 mM EDTA and 100mM NaCl). The cell suspension was added to a 2 ml screw cap tube (Sarstedt, Germany) containing 0.3 g acid washed sterile glass beads (Sigma-Aldrich) and 200 µl of phenol-chloroform-isoamyl alcohol in the ratio of 24:24:1. The cells were disrupted for 1 minute in a Fastprep FP120 Cell Dismembranator (Thermo-Scientific). The lysate was centrifuged at 14,000 r.p.m. for 10 min. The upper aqueous phase was removed and extracted with an equal volume of chloroform-isoamyl alcohol in a ratio of 24:1. The extraction was centrifuged for 2 min at 13,000 r.p.m. and the upper aqueous phase was again removed to a fresh 1.5 ml tube (Eppendorf, Germany). Nucleic acids were precipitated with the addition of 20 µl of 3 M sodium acetate (pH 5.0) and 400 µl of 70% (w/v) ethanol at -20 °C. Nucleic acids

were centrifuged at 14,000 r.p.m. for 10 min and the pellet washed with 500 µl of 70% (w/v) ethanol. The pellet was re-suspended in 50 µl ultrapure H_2O. Concentration and integrity of the DNA was determined using a Nanodrop (Thermo Scientific, UK) and stored at -20 °C.

2.3.2. Genotype confirmation

Oligonucleotide primers were synthesised by Sigma-Aldrich using standard synthesis conditions, dissolved to 100 µM in molecular biology grade water (Sigma-Aldrich) and stored at -20 °C. All oligonucleotides used in this study are listed in Table 2.2. Polymerase chain reaction (PCR) was carried out using either the GoTaq® system (Promega) or the Expand High Fidelity PCR system (Roche Diagnostics Ltd.) according to manufacturers' instructions.

PCR products were visualised by agarose gel electrophoresis using 0.8% (w/v) agarose gels containing 1% (v/v) GelRed™ (Biotium, Hayward, California, USA) for expected products over 1 kb, and 2% (w/v) agarose gels for expected products under 1 kb. TBE was used as the running buffer for electrophoresis. GelRed™ bound nucleic acid was visualised using a UV transilluminator (Ultra Violet Products Ltd., Cambridge, United Kingdom) at 345 nm. PCR products were routinely purified using the Genelute™ PCR Clean-Up kit (Sigma-Aldrich) or the Wizard® SV Gel and PCR Clean-Up System (Promega). Sequencing of DNA was carried out commercially by Source Bioscience DNA Sequencing (Dublin 8, Ireland).

2.3.3. RNA extraction and cDNA synthesis

Given the sensitivity of experiments being carried out, it proved that the most suitable method of extraction was to flash-freeze the cells using liquid nitrogen (LN_2), mechanical disruption and column extraction of RNA. This method produced higher yields than column-only methods.

Amplification	Name	Restriction site	Primer sequence 5' ➔3'
ACT1 **primers**	ACT1FW		AGCTCCAGAAGCTTTGTTCAGACCAG
	ACT1RV		TGCATACGTTCAGCAATACCTGGG
qRT-PCR primers	TLO1 qPCR F		GTGTGTCGCCGTTATGATTG
	TLO1 qPCR R		CTAGCTTCTGCCTCCCGTTT
	TLO2 qPCR F		AGCTGGACCCAACAATGAAC
	TLO2 qPCR R		GCAACACACCACTTTGCATC
	GAL10Fw		GTGCAGGCTATTGAAACTGTG
	GAL10Rv		TCACCAGGGCCAATATCTC
	SOD5Fw		GTCCATTCCCATATCATGTCC
	SOD5Rv		AGGGGTTGAAATGGTTCTCG
	RBT5Fw		TTGGCTSSSGCTGGTGAAGC
	RBT5Rv		TCAGCAGCAGTGGTTTCTTG
	HWP1Fw		CAGCTGGTATTAAAACTAACCCAGC
	HWP1Rv		ATTCTAATGTGGTTGGAATAGCACC
	ECE1Fw		ATTGCTGATATGCCATTTGTTGTTAG
	ECE1Rv		CAATCTGACGATGGCATTAGTAACAT
	UME6Fw		TACCACCACCACCACCAT
	UME6Rv		TATCCCATTTCCAAGTCCA
	PCK1_qPCR_Fw		AGGTCACCCAACTATCAAATCC
	PCK1_qPCR_Rv		GTGGACGAAATGGTAGTGCCTT
	EAP1_qPCR_Fw		TCCTACCCAGGCCAATACAA
	EAP1_qPCR_Rv		TGTGTACCTGGTGGTGCTCC
	ENO1_qPCR_F		AGGTGTTTTGAAAGCCGTTG
	ENO1_qPCR_R		CCTTGACTAAAGCTGGGGCA
	HSP90_qPCR_F		CCCCAAAAGGACCAAAAAGT
	HSP90_qPCR_R		ACCGGCATTAGATTCCCAGA
	CAT1_qPCR_F		ACGCTAAAGGTTCAGGTGCTT
	CAT1_qPCR_R		CCTCTTGGGTCTCTAGCGGT
	TEC1_qPCR_F		TGAGAAATGCCAATGGACAA
	TEC1_qPCR_R		ACCACAAGATCTACCGGCAATCT
	EED1_qPCR_F		CTGGTCAAAACTCAACGAACTCCGA

Table 2.3. Oligonucleotides used in this study

	EED1_qPCR_R		TGAGACGGGCGTAGTTGGT
PCR primers	CdTLO1F1	*Sal*I	GACCTGTCGACAGCCATGTCAGCTAACT
	CdTLO1R1	*Bgl*II	TGAAGATCTAACACATCAATTACCAAATTGG
	CdTLO2F1	*Sal*I	GACCTGTCGACCAGCCATGTCAGCCAATTTAC
	CdTLO2R1	*Bgl*II	TGAAGATCTACTACCCTATCAATTACCAAACT
	pNIM1 Insert F1		TGCCTTGGGTGGCTATTTTA
	pNIM1 Insert R1		TCGTTTCTGATGGGCTTTTC
	CdADH1_5_F		GCACATTAAAACTGTCCAACCAA
	CdADH1_5_R		TGTCTATCAAATAATTCGATAG
	CdADH1_3_F		GAAAAGCCCATCAGAAACGA
	CdADH1_3_R		CCATGAAGTTTGAGGTATTGA
	cartTA_F		CTGCATCTTTTACAGCAACA
	cartTA_R		AATACTTTATAAAAGCTAAGCTA
	M13_MED3F		AAAGGTCAGGGAGTCCAATCGCCTACAAAAAACAAA
			TATAAAGGGTAACCAAATGTGATACTGAGCAACCAT
			AGTTAGAT-GTAAAACGACGGCCAGT
	M13_MED3R		AAACTGTGTTATATATAATACATACATCTATATATG
			CTTCGAAATAAATGTTAGTGATACTACTCTGAAGAA
			CGAGCTACTGTTACAC-GGAAACAGCTATGACCATG
	MED3_F		GAAGTCCAATCGCCTACAAA
	MED3_DKO_F		TAGTAAAGCAAGTCATAATATACA
	MED3_DKO_R		CTTGTGAAGTGAGATATTTCAT
	FLP_R		GTATATGTGCCTACTAACGC
	MED3_INT_F		CCTTGGCCACTATACCTACAAATC
	MED3_INT_R		GCTCACAGACGCCTTCTTTG
	MED3_notI_F	*Not*I	ATAAGAATGCGGCCGCGTAAAGCAAGTCATAATATACAA
	MED3_sacII_R	*Sac*II	GGACCGCGGCTTGTGAAGTGAGATATTTCAT
	P_tlo1_F	*Xho*I	GCGCTCGAGTTTCTGACAACCGCTTCACG
	N_tlo1_3XHA_R	*Hind*III	GCGAAGCTTCTAAGCGTAATCTGGAACGTCATATGGATATCC
			TGCATAGTCCGGGACGTCATAGGGATAGCCCGCATAGTCAGG
			AACATCGTATGGGTACCCGGGGATCCGTCGACCCTTTGGGGC

		CTGGTTCTCTC
ACT1_F		TCACCAGATTTATTGCCAACG
Ntlo1_R_screen		TATATCGTTGAGTGAGTTCT
ACT1_terminator_R		GAATGAATGGGATGAATCATC
Internal_seq_Ntlo1_F		CATTCAAGGGTTTAATGATATCTTAGAGA
Internal_seq_Ntlo1_R		GGTCGCTTAGTTGTTGTATGATCGAT
Ntlo1_F_xhoI	*Xho*I	GCGCTCGAGTTTCTGACAACCGCTTCACG
Ntlo1_R_hindIII	*Hind*III	GCGAAGCTTCTTTGGGGCCTGGTTCTCTC
Tlo1_TAP_F		GACCTTGCTTGATGGAGGCTTGGATGGGGACAATAGCAACAA
		CGACAATCAAGTCAATGAAGAGTTTGATGTAGATAGCTTCTT
		GAACCAATTTGGTAATAGGTCGACGGATCCCCGGGGTT
Tlo1_TAP_R		AAATCTGGTGGGATATATTCTCTGTAGTAGTCTCAAATACGA
		TCGGAATAACAAACAAGGTAAATGTACATGTTACATGGAGTT
		GTACTAAATTGATATTCGATGAATTCGAGCTCGTT
Tlo2_TAP_F		GATATTAGCCGGCTTGAATATGAACTTGCTTGATGACGCCAA
		CACCTTCAACGATAATGAAGAGTTTGATGTGGATAGTTTCTT
		AAACCAGTTTGGTAATGGTCGACGGATCCCCGGGTT
Tlo2_TAP_R2		CCATTGACAGAAGGTAAGTTTACTTGTTGGACCTCGGAATCG
		TTGTATAATGTTTGGGTGAGGTAAGGCCAAGGATAACTTCAA
		CTTCAAGGCGTCTGAAGACACAGTCGATGAATTCGAGCTCGTT
Tlo1_TAP_integr_F		CCACACTGCTTCTCCAAGG
Tlo1amp_TAP_integrR		ATGGAGTAGCTGGCGTTGA
Tlo1amp_TAP_integrF		ACACTGGTAATGATGCGCGA
Tlo_inTAPintegr_R		ACTTATAATGGCGCGCCTCA
Tlo2_TAPscr_F		CACCTGGCCATCTACAGTAA
Tlo2_amp_Rev		CGTCACTTGATTCAGCTCTC
Tlo2_ampF		GGAACTGGACCCTGAAGTTGTT
TAP_cassette_F		AATCCATGGAAGAGAAGATG
TAP_cassette_R		CTAGAAGGACCACCTTTGATT
CIp10_Fwd		TACAATCAAAGGTGGTCCT
CIp10_Rev		CAATTAACCCTCACTAAAGG
Tlo1TAPFgene		TTGTGATCACCCAATTCTT
Tlo1TAPRgene		TGGTTGATGGTAAAGAAACG
Tlo2TAPFgene		CCATTCCAACAAGCTATAGGT

Tlo2TAPRgene		CCTATTTGAGCTAGACACACTACC
CaTLO1xhoI_F	*Xho*I	CCGCTGAGTGATCATACATATCTTAACTTAG
CaTLO1hindIII_R	*Hind*III	GGGAAGCTTCTGTATATGTCTTGTAGAAC
CaTLO3 xhoI_F	*Xho*I	CCGCTCGAGTATAGCTAGATACGTGTA
CaTLO3 hindIII_R	*Hind*III	GGGAAGCTTCGTATTCCTGTACCA
CaTLO4 xhoI_F	*Xho*I	CCGCTCGAGTGCATCTGTGACAATATT
CaTLO4 hindIII_R	*Hind*III	GGGAAGCTTAGAAAGCAGAGACCGC

All oligonucleotides were synthesised by Sigma Aldrich (Co. Wicklow, Ireland)

A single colony from a fresh YEPD agar plate was inoculated into 2 ml of YEPD broth and grown overnight at 30 °C with shaking at 200 r.p.m. in an orbital incubator. Overnight cultures were centrifuged in a 1.5 ml microcentrifuge tube (Eppendorf) for 3 min at 12,000 r.p.m. and washed three times using sterile PBS and re-suspended in 1 ml sterile PBS. Cells were counted using a Neubauer haemocytometer at 10^{-2} dilution. Cells were standardised to a concentration of 2 x 10^6 cells/ml and added to 50 ml of desired growth medium, in a Pyrex conical flask fitted with an air-permeable rubber bung, mixed and incubated at 37 °C in an orbital incubator with shaking at 200 r.p.m. At pre-determined time-points (for water and serum experiments) or at an O.D. value of 0.8 at 600 nm (for YEPD experiments) flasks were removed from incubation and cultures were centrifuged using a bench-top centrifuge (Eppendorf 5417C, Eppendorf, Germany) for 10 min at 2,000 r.p.m. All of the supernatant except 1 ml was discarded; with the 1 ml used to re-suspend the pellet. The cells were added drop-wise to 30 ml of LN_2 in 50 ml polystyrene Falcon tubes with gentle mixing. Upon evaporation of the remaining LN_2, the tubes were stored at -80 °C until use (for up to 72 h).

In order to extract the RNA, the frozen pellets of cells were transferred to polytetrafluoroethylene (PTFL) vessels (Sartorius Mechatronics, Goettingen, Germany), containing a tungsten-carbide grinding ball (Sartorius Mechatronics). All apparatus were soaked in RNAse Away® (Sigma-Aldrich), followed by rinsing in 0.1% (w/v) Diethylpyrocarbonate (DEPC) water and then pre-cooled with LN_2. PTFL vessels were sealed and processed on a micro-dismembranator S (Sartorius Mechatronics) at 1,500 r.p.m. twice for 1 min. The grinding ball was carefully removed and 600 µl Buffer RLT (Qiagen, West Sussex, UK) was added with gentle mixing until the fine powder was fully melted. The solution was added to 2 ml tubes (Eppendorf, Hamburg, Germany) and equilibrated with an equal volume of 70% w/v ice cold ethanol. The protocol was then continued as outlined for 'Purification of total RNA' in the Qiagen RNeasy kit manual (Qiagen, 2010). RNA samples were treated with Turbo DNase Free (Ambion, Austin, TX, USA) to digest and remove any

double-stranded DNA and were stored at -80 °C. Concentration and integrity of the RNA was determined using a Nanodrop (Thermo Scientific, UK).

A concentration of 1 µg of DNase-treated RNA was used to reverse transcribe cDNA using the Superscript II First Strand Synthesis system (Invitrogen). Initially, 1 µg of RNA, 1 µl of dNTPs (10 mM) (Promega) and 1 µl of Oligo (dT) 18 (500 µg/ml) (Promega) were heated to 65 °C for 5 min in a thermocycler and chilled on ice for 5 min. After 5 min, 4 µl of First Strand Buffer, 1 µl of 0.1 M DTT, 1 µl of RNAse OUT and 1 µl of Superscript III RT were added to each reaction tube. The reaction was reverse transcribed by holding the reaction tube at 50 °C for 1 h. The reaction was inactivated at 70 °C for 15 min as per manufacturers' instructions and stored at -20 °C.

2.3.4. Quantative Real-Time Polymerase Chain Reaction (qRT-PCR) validation and gene expression analysis

qRT-PCR was carried out using Fast SYBR Green Master Mix (Applied Biosystems) in a 15 µl reaction volume in conjunction with an AB7500 Real Time PCR system (Applied Biosystems) to measure gene expression levels from cDNA. Output was analysed by the comparative C_t ($2^{\Delta\Delta C_t}$) method to calculate up- and down- fold regulation of expression of specific genes (Schmittgen & Livak, 2008). All primers used for qRT-PCR are listed in Table 2.2 and were intially verified for comparative amplification efficiency against the endogenous control *ACT1* to ensure the primers for each gene to be measured were within the recommended 10% of each other, as described by Schmittgen & Livak (2008). Reactions were carried out in 96-well reaction plates in triplicate on each run on three separate occasions. Integrated software (Applied Biosystems) was used to analyse the results.

2.4. Recombinant DNA techniques

2.4.1. Isolation of plasmid DNA from *Escherichia coli*

Escherichia coli cells containing a plasmid of interest were grown on L_{amp} or L_{chloro} at 37 °C for 18 h. A single colony was inoculated in L_{amp} or L_{chloro} broth and grown at 37 °C overnight in an orbital incubator. Plasmid extraction was carried out using either the PureYield™ Plasmid Miniprep System (Promega) or the Plasmid Miniprep Kit (Sigma) in accordance with the manufacturers' instructions.

2.4.2. Restriction enzyme digest and ligation of DNA fragments

DNA fragments containing restriction enzyme cut sites were digested with the appropriate restriction endonuclease sourced from Promega or New England Biosystems as recommended. Digests were carried out in 100 µl reaction volumes which contained 80 µl of H_2O, 5 µl of DNA template, 10 X of the Buffer (Promega) corresponding to the restriction enzyme, 1 X Bovine Serum Albumin (BSA) (Promega) and 2 µl of each restriction enzyme. Reactions were set up in 1.5 ml microcentrifuge tubes (Eppendorf, Germany) and incubated for either 2 h or overnight at 37 °C -depending on manufacturers' specifications- in a shaking water bath (Focus Scientific Solutions). Digested DNA fragments were loaded on 0.8% agarose (Sigma Aldrich) gels in 0.5 X TBE. DNA products were visualised using a UV transilluminator and, where necessary, desired bands were excised from the gel using a sterile scalpel. Purification was carried out using the Wizard® SV Gel and PCR Clean up System (Promega). Ligation reactions were set up containing sterile H_2O, 10 X Ligase Buffer (Promega), the vector and insert to be ligated and T4 DNA ligase (Promega) in a final volume of 30 µl. Molar ratios of vector to insert of 1:1, 1:3 and 1:10 were used, where the vector was constant. Reactions were ligated at 16 °C for 2 h, followed by overnight refrigeration at 4 °C.

2.4.3. Transformation of competent *E. coli* by heat shock

For the transformation of the ligation reactions *E. coli* XL10 High Efficiency Electrocompetent cells were used. Competent cells were thawed on ice and 200 µl was added to each ligation reaction. Samples were chilled on ice for 5 min. DNA/ *E. coli* mixes were heat-shocked at 42 °C for exactly 2 min then transferred to ice for exactly 2 min. Following the addition of 1 ml of pre-warmed S.O.C. medium (2 % tryptone, 0.5 % yeast extract, 10 mM sodium chloride, 2.5 mM potassium chloride, 10 mM magnesium chloride, 10 mM magnesium sulphate, 20 mM glucose [Sigma-Aldrich]), the reaction tubes were incubated at 37 °C for 1.5 h with shaking. Following recovery, 100 µl of cells were plated onto pre-warmed L_{amp} plates and incubated overnight at 37 °C.

2.4.4. Transformation of *Candida* species by electroporation and selection with nourseothricin

A single colony of the strain to be transformed was inoculated into 50 ml of YEPD broth and grown overnight at 30 °C with shaking at 200 r.p.m in an orbital incubator to an $O.D._{600}$ of 1.6 to 2.0 (approximately 0.5 to 1.0 x 10^7 cells/ml). Cultures were centrifuged in a Falcon tube at 2,500 x g for 5 min. Cells were re-suspended in 8 ml dH_2O. To the re-suspended cells 1 ml 10X TE buffer pH 7.5 and 1 ml 1 M Lithium Acetate pH 7.5 (Sigma Aldrich) were added. Cells were incubated at 30 °C with shaking for 1 h. Following incubation, 250 µl of 1 M DTT (Sigma Aldrich) was added to the cells and incubated for a further 30 min with shaking and 40 ml dH_2O was then added to the cells and centrifuged as described above. Cells were washed in 50 ml ice cold dH_2O and centrifuged as described above. Cells were washed in 10 ml ice cold 1 M Sorbitol (Sigma Aldrich) and centrifuged at 2,500 x g for 5 min. All trace of supernatant was removed and the pellet was re-suspended in 50 µl 1 M Sorbitol and left on ice. DNA (0.2 to 10.0 µg) in a volume of 5-10 µl of water was added to 40 µl of cell suspension for each transformation as well as 40 µl of cell suspension for a no DNA control transformation. DNA and cell suspensions were mixed gently with a pipette tip and transferred to a chilled (4 °C)

0.2 cm electroporation cuvette (Sigma Aldrich). The samples were electroporated in a Minipulser (Bio-Rad, CA, USA) on the SC2 setting. After pulsing, 1 ml pre-warmed YEPD was added to the cuvette. The transformed cells were transferred to sterile 1.5 ml microcentrifuge tubes (Eppendorf, Germany) and incubated with shaking for 2-3 h at 37 °C. Following recovery 100 µl aliquots of transformed cells and controls were plated onto NAT_{100} plates and incubated at 37 °C for 2-3 days.

2.5. Two Colour DNA Microarray-based gene expression and analysis

2.5.1. Preparation of RNA to be analysed by DNA Microarray

Samples to be analysed were prepared based on the protocol outlined in the Two-Color Microarray-Based Gene Expression Analysis Low Input Quick Amp Labeling protocol (Agilent Technologies, 2012). All reactions and dilutions were performed in 1.5 ml microcentrifuge tubes (Eppendorf) unless otherwise stated. Each experiment consisted of 8 samples: four control and four experimental, each prepared as biological replicates, including two dye swap experiments.

RNA 'Spike-In' mixes were prepared. Spike A and B mixes (Agilent Technologies) were thawed, mixed thoroughly and heated to 37 °C for 5 min and mixed again. Dilutions of each Spike-In mix were carried out using Milli-Q water (Millipore) resulting in final dilutions for a 100 ng template of 1:20, 1:800, 1:12,800 and 1:25,600. DNAse-treated RNA samples were prepared as described in Section 2.3.3. In four separate tubes, using two of the control samples and two of the experimental samples, 100 ng of RNA was added to 2 µl of the 1:25,600 dilution Spike-In Mix A to a final volume of 3.5 µl using Milli-Q water (Millipore). In four additional tubes the same process above was carried out using the remaining biological replicates, resulting in 8 tubes in total, four with Spike-In Mix A and four with Spike-In Mix B.

2.5.2. Labelling and amplification

Labelling and amplification reactions were carried out using the Low Input Quick Amp Labeling Kit, Two-Color (Agilent Technologies). To prepare the T7 primer mix 0.8 µl of T7 primer was combined with 1 µl of nuclease-free water (Agilent Technologies) and the 1.8 µl mix was added to each RNA Spike-In mix, resulting in a total volume of 5.3 µl in each tube. The reactions were incubated at 65 °C for 10 min in a circulating water bath (Thermo Fisher Scientific) followed by immediate incubation on ice for 5 min. To prepare the cDNA master mix to a volume of 4.7 µl, the 5 X First Strand Buffer was pre-warmed at 80 °C for 3-4 mins. Following brief mixing, 2 µl of the pre-warmed 5 X First Strand Buffer was combined with 1 µl of 0.1 M DTT, 0.5 µl of 10 mM dNTP Mix and 1.2 µl Affinity Script Rnase Block Mix (Agilent Technologies). The mix was added to each of the 8 sample tubes for a final volume of 10 µl. Mixes were incubated at 40 °C in a circulating water bath (Thermo Fisher Scientific) for 2 h , followed by a 15 min incubation in a circulating water bath (Thermo Fisher Scientific) at 70 °C. Samples were then incubated on ice for 5 min.

Two Transcription Master Mixes were prepared to a volume of 6 µl containing 0.75 µl of Nuclease-free water, 3.2 µl 5 X Transcription Buffer, 0.6 µl of 0.1 M DTT, 1 µl NTP Mix, 0.21 µl T7 RNA Polymerase Blend and 0.24 µl of either Cyanine 3-CTP or Cyanine 5-CTP (Agilent Technologies). Sample tubes containing Spike-In Mix A were combined with 6 µl of master mix containing Cyanine 3-CTP and sample tubes containing Spike-In Mix B were combined with 6 µl of master mix containing Cyanine 5-CTP. Samples were incubated in a circulating water bath (Thermo Fisher Scientific) for 2 h at 40 °C.

2.5.3. Clean up and purification

Each of the amplified cRNA samples were purified using the RNeasy Mini Kit (Qiagen), with 84 µl of nuclease-free water added to each of the 8 samples to provide a total volume of 100 µl. To each sample, 350 µl of Buffer RLT (containing 10% v/v β-Mercaptoethanol (Sigma-

Aldrich) was added and mixed thoroughly, followed by 250 µl of 100% v/v ethanol (Sigma-Aldrich) and mixed thoroughly by pipetting. The 700 µl mix was transferred to a RNeasy Mini Spin Column and the protocol was followed as per manufacturers' instructions. Purified samples were eluted in a final volume of 30 µl of RNase-Free Water (Qiagen). All samples were maintained on ice at this point to prevent degradation.

In order to quantify and assess the quality of the cRNA 1 µl of each sample was measured on a NanoDrop Spectrophotometer (Thermo Fisher Scientific) using the RNA quantification settings. The yield and specific activity of each reaction was determined by calculating the concentration of cRNA (µg) using the formula:

$$\text{Total cRNA (µg)} = \frac{\text{(Concentration of cRNA (ng)) x 30 µl (elution volume)}}{1000}$$

The success of each labelling reaction was determined using the concentration of cRNA and Cy dye as follows:

$$\frac{\text{(Concentration of Cy3 or Cy5)}}{\text{Concentration of cRNA}} \text{ X 1000 = pmol Cy3 or Cy5 per µg cRNA}$$

The results of the equation above should yield a result higher than the recommended yield of 0.825 µg and a specific activity of 6 pmol Cy3 or Cy5 per µg cRNA. If these thresholds were not met the samples were discarded and the protocol was repeated.

2.5.4. Hybridisation

Following confirmation of the quality of the labelled cRNA samples, the fragmentation mix was prepared in new microcentrifuge tubes (Eppendorf). The mix consisted of 825 ng of a Cy3 labelled cRNA and 825 ng of a Cy5 cRNA combined with 1 X Gene Expression Blocking Agent, 1X Fragmentation Buffer and nuclease-free water (Agilent Technologies) to a final volume of 55 µl. This resulted in four differentially labelled sample mixes, such that the first

mix contained a Cy3-labelled control sample and a Cy5-labelled experimental sample, while the second mix contained a Cy5-labelled control sample and a Cy3-labelled experimental sample etc. This method of 'dye swap' was carried out in order to eliminate dye bias with regards to the hybridisation intensity.

The four mixes were incubated at 60 °C for 30 min and immediately cooled on ice for 1 min. At a ratio of 1:1, 2 X Hi-RPM Hybridisation Buffer was added to each sample. The mixes were very carefully pipetted up and down so as not to introduce bubbles and centrifuged at 13,000 x g for 1 min. The samples were placed on ice and the 4 X 44K DNA microarray slide (Agilent Technologies) was loaded into a hybridisation chamber (Agilent Technologies). Once the microarray slide was in place, 100 µl of each sample was loaded onto one of the four microarray tiles. A gasket slide was loaded into the chamber base with the label facing up and aligned with the chamber base. The chamber was sealed and incubated in a hybridisation oven (Thermo Fisher Scientific) at 65 °C for 17 h with a rotation of 10 x g.

2.5.5. Washing

Prior to use all dishes, racks and stir bars were rinsed with Milli-Q (Millipore) water. A slide-staining dish was filled with Gene Expression Wash Buffer 1 (Agilent Technologies) and the microarray slide apparatus was disassembled in the dish at room temperature and incubated for 1 min. A second slide-staining dish was also filled with Gene Expression Wash Buffer 1 and the slide was transferred to the second dish and incubated for 1 min. The slide was then transferred to a third slide-staining dish was filled with Gene Expression Wash Buffer 2 that was pre-warmed to 37 °C and incubated for 1 min.

2.5.6. Scanning and image processing

The slide was removed from the buffer and immediately placed into the scanning chamber of a Genepix 4100A scanner (Molecular Devices, Sunnyvale, CA, USA). The microarray slides

were scanned at 5 μm resolution at wavelengths 635 nm and 532 nm. Image files were saved as .tiff (Tagged Image File Format) images. Array slides were aligned with a *C. dubliniensis* template .GAL file using Genepix Pro software version 6.1.0.4 (Molecular Devices). Individual dots were characterised based on signal to noise ratio (SNR) flags and background using Genepix Pro software (Molecular Devices). Array spots were flagged as absent if the signal was less than background of 1 standard deviation in both fluorescent channels. Resulting images were saved as GenePix Results (GPR) files.

2.5.7. Microarray analysis

Results fom GPR files were analysed using Genespring GX software version 11.0 (Agilent Technologies) and signals for each replicate spot were background corrected and normalised using Lowess normalisation. For display purposes, Log2 fluorescence ratios were generated for each replicate spot and averaged. Data were filtered on flags; Present (P), Marginal (M) and Absent (A) based on SNR values and base fluorescence as described previously. Data flagged as Absent were excluded from the analysis. Genes differentially expressed (1.5-fold) relative to wild-type were identified from those that passed a t-test ($P \leq 0.05$) and satisfied a post-hoc test (Storey with Bootstrapping) with a corrected Q value ≤ 0.05. Hierarchical clustering was used to compare gene expression in each condition using the default settings.

Chapter 3

Doxycycline Induced Expression of *C. dubliniensis TLO1* and *TLO2*

3.1. Introduction

3.1.1. Hypha-specific genes

The formation of hyphae is an important aspect of the virulence of *Candida albicans.* Hyphae permit *C. albicans* to invade epithelial tissues and access the bloodstream (Filler & Sheppard, 2006; Zhu *et al.,* 2010). As previously outlined in Section 1.2.3, hyphal growth is induced by a number of environmental cues such as the presence of serum, neutral pH, 5% v/v CO_2, GlcNac and growth on synthetic growth media such as Lee's medium and Spider medium (Sudbery, 2011). An outline showing many of the genes associated with the pathways involved in the transcriptional regulation of hypha-specific genes was provided in Figure 1.3. A complex that consists of the transcriptional core-repressor Tup1 in association with Nrg1 or Rfg1 negatively regulates hypha-specific gene expression (Kadosh & Johnson, 2001; 2005; Murad *et al.* 2001). Positive regulation is governed by a number of transcription factors such as Efg1, Cph1, Cph2, Tec1, Flo8, Czf1, Rim101 and Ndt80 (Sudbery, 2011). Efg1 is thought be a major regulator of hypha-formation under most conditions, given that it is required for filamentation in response to serum, CO_2, GlcNac, neutral pH and solid Spider medium (Braun & Johnson, 2000). Cph1 and its upstream activating pathway are only required for hyphal induction on solid Spider medium (Liu *et al.,* 1994; Leberer *et al.,* 1996). The adenylyl cyclase Cyr1 integrates environmental signals from a range of sources and is essential for the formation of hyphae (Rocha *et al.,* 2001). Temperature shift sensing is carried out by the inhibitor heat shock protein 90 (Hsp90) (Shapiro *et al.,* 2009). There are three additional genes that play vital roles in hyphal formation: *UME6, HGC1* and *EED1.* Null mutants for *EED1* and *UME6* are unable to form true hyphae (Banerjee *et al.,* 2008; Martin *et al.,* 2011). *HGC1* null mutants can form very short germ tubes before reverting to non-polarised growth (Zheng *et al.,* 2004). Previous studies carried out in our laboratory have revealed that the homozygous deletion of *CdTLO1* and *CdTLO2* in the *Candida dubliniensis* wild type strain results in the loss of the ability to form true hyphae in hyphal inducing conditions (10% w/v

FBS). Interestingly, the deletion of only *CdTLO1* resulted in a significant depletion of hyphal formation from 90% to 40%, while the deletion of *CdTLO2* had no effect, suggesting that the *TLO*s, in particular *CdTLO1* play an important role in the formation of hyphae in *C. dubliniensis* (Haran *et al.*, 2014).

3.1.2. Genes involved in oxidative stress response

During phagocytosis *Candida* cells are engulfed and exposed to oxidative fungicidal molecules such as hydrogen peroxide. Fungal dissemination is reportedly reduced in the presence of reactive oxygen species (ROS) (Lopes da Rosa *et al.*, 2010). *Candida albicans* is more resistant to oxidative stress than the non-pathogenic model yeasts *Saccharomyces cerevisiae* and *Schizosaccharomyces pombe* (Enjalbert *et al.*, 2003; Nikolaou *et al.*, 2009). However, despite this all three species induce a similar set of antioxidant genes following H_2O_2 exposure (Enjalbert *et al.*, 2006). This core set of genes includes catalase (*CAT1*), the glutathione peroxidases (*GPX*) and the superoxide dismutases (*SOD*). These oxidative stress response genes are also induced in *C. albicans* following exposure to macrophages and neutrophils, suggesting that *C. albicans* induces respiratory burst in these phagocytes. Studies carried out by Miramon *et al.* (2012) and Walker *et al.* (2009) have revealed that *C. albicans* is also exposed to high levels of ROS before phagocytosis, however oxidative stress responses do not appear to be induced once systemic kidney infections have been established by *C. albicans* cells. Based on these studies, it would appear that oxidative stress responses are key for phagocytosis survival, but less important for systemic infection development (Da Silva Dantas *et al.*, 2015). Stress response experiments previously carried out in our laboratory revealed that the deletion of *CdTLO1* resulted in a significant decrease in the ability to grow under oxidative stress conditions induced by 6 mM H_2O_2, similar to that which was observed in the *Cdtlo*ΔΔ mutant, while the deletion of *CdTLO2* resulted in no change in oxidative stress susceptibility. This suggests that the *CdTLO*s are important for oxidative stress response, in particular *CdTLO1* (Haran *et al.* 2014).

3.1.3. Carbohydrate metabolism

A pathogens' ability to grow in a wide range of hosts depends not only on specific virulence factors, but also metabolic flexibility, therefore they must be able to assimilate a variety carbon sources. Carbohydrates are used for generating energy and producing biomolecules. Glycolysis is responsible for converting glucose to pyruvate, enabling fermentation and respiration (Askew *et al.,* 2009). As glycolysis is a central metabolic pathway it is strictly regulated. In *S. cerevisiae,* Gcr1, Gcr2 and Tye7 activate glycolytic gene expression (Uemura & Fraenkel, 1990). Most organisms, including *C. albicans* do not have *GCR1* or *GCR2* homologues, and therefore glycolytic gene transcription must be controlled differently. A study carried out by Askew *et al.* (2009) identified Tye7 and Gal4 as activators of the glycolytic pathway in *C. albicans,* and found that they are also required for pathogenicity. In the absence of glucose, galactose can be converted to glucose in a reaction catalysed by the enzymes of the Leloir pathway (outlined in the Discussion section of this chapter). As in *S. cerevisiae,* galactose induces the transcription of the genes for the Leloir pathway, *GAL1, GAL7* and *GAL10,* in *C. albicans* (Martchenko *et al.,* 2007). It was previously observed in our laboratory that in the absence of *CdTLO1* and *CdTLO2, C. dubliniensis* cells grew poorly in YEP-Gal, with a 30% increase in doubling time observed compared with growth in YEPD. In the absence of *CdTLO1,* the doubling time in YEP-Gal was also increased, but not as highly as in the *Cdtlo*ΔΔ mutant, while the absence of *CdTLO2* resulted in a slight increase in doubling time, suggesting that the *CdTLOs* play a role in the utilisation of galactose as an alternative carbon source (Haran *et al.,* 2014).

3.1.4. Genetic analysis of *Candida* spp.

Over the last few years, genetic manipulation has become a cornerstone in enhancing our knowledge of the biology and pathogenicity mechanisms of *Candida* spp., with new techniques emerging regularly. The analysis of *Candida* spp. at the molecular level is impeded by their diploid nature, the lack of a normal sexual cycle and abnormal codon usage (Berman

and Sudbery, 2002). Although gene disruption remains one of the most important tools to investigate the function of a gene, expression systems that allow researchers to control the expression of particular genes are vital for gene function analysis and behavioural manipulation of an organism (Park and Morschhäuser, 2005). There are a number of regulatable promoters used by researchers that have the ability to induce or repress gene expression in *C. albicans*, such as the *PCK1* promoter, which is repressed by glucose, the *MAL2* promoter, which is repressed by maltose, and the *MET3* promoter, which is repressed by methionine or cysteine (Leuker *et al.*, 1997; Care *et al.*, 1999; Backen *et al.*, 2000). Expression of a gene of interest can be induced or repressed under control of one of the above promoters when cells are grown in the appropriate induction or repression media. However for experimental purposes, it is preferable to alter expression without having to alter the growth medium. Therefore the addition of a substance that results in gene induction or repression without affecting metabolism is far more desirable (Park and Morschhäuser, 2005). One such system is the tetracycline (Tet) system.

3.1.5. The tetracycline-inducible pTET promoter

The Tet system allows control of gene expression independent of growth medium, by the diffusion of a small molecule into cells. The system is based on the tetracycline repressor protein (TetR) from *Escherichia coli*, which binds to the *tet* operator in the promoter region of the tetracycline resistance genes to repress their expression when tetracycline is absent. In the absence of tetracycline or one of its derivatives, such as doxycycline (DOX), the promoter is active and gene transcription occurs at high levels. This is referred to as the "tet-off" system. The "tet-off" system is generally used to turn down gene expression, particularly essential genes that cannot be deleted. The complementary system, "tet-on" requires Tet or DOX to activate transcription (Baron and Bujard, 2000). Park and Morschhäuser (2005) developed a Tet inducible gene expression system for *C. albicans* using DOX. An advantage of this system is that all of the components are contained in one cassette. It contains *SAT1*, the

positive selection marker that confers resistance to nourseothricin, which enables introduction into a *Candida spp.* in a single transformation (Reuss *et al.,* 2004). The DOX-inducible system has been successfully used in previous studies to help identify the function of a number of genes. Martin *et al.* (2009) generated pTET-*UME6* and pTET-*EED1* strains and observed that following the addition of 50 μg/ml of DOX, hyphal formation was restored in *ume6*Δ and *eed1*Δ mutant strains respectively in *C. albicans.* Furthermore, in 2014, Cabral *et al.* used the pTET promoter to overexpress a number of *C. albicans* genes involved in cell wall functions and biofilm formation in order to observe if overexpression altered planktonic growth fitness or strain abundance in a multistrain biofilm. This study yielded mixed results: the overexpression of some genes (*PGA59* and *IHD1*) resulted in increased adherence and an increased or unchanged biofilm biomass. In contrast, overexpression of other genes had a negative impact on adherence and no impact on biofilm formation (*PGA19, PGA32* and *PGA37*), a positive effect on adherence and a negative impact on biofilm formation (*PGA15, PGA22*) or no apparent impact (*PGA42, PHR2* and *TOS1*). These results suggested that the ability of *C. albicans* strains to adhere to biofilms is not the only defining component of biofilm development. The DOX-inducible system was used in this study to express *CdTLO1* and *CdTLO2* in a *Cdtlo*ΔΔ background.

3.1.6. pCDRI plasmid

In addition to the plasmid used to express *CdTLO1* and *CdTLO2* under the control of the DOX-regulatable promoter in the *Cdtlo*ΔΔ background, the pCDRI plasmid was also used to construct *CdTLO1* and *CdTLO2* reintegrants under the control of their native promoter. As described by Moran *et al.* (2007) the *C. dubliniensis* integrating vector pCDRI consists of the plasmid pBluescript II containing the *SAT1* resistance marker from pSFS2A (Reuss *et al.,* 2004) contained on an *Xba*I/*Spe*I fragment and regions +1800 to +2488 of the *CdCDR1* pseudogene. pCDRI was used by Moran *et al.* (2007) to complement a *CdNRG1* null mutant strain to investigate the function of *CdNRG1.*

3.1.7. DNA Microarrays

DNA microarrays are one of the most successful technologies developed with regards to high-throughput and large-scale genomic analyses. They were developed originally to measure the levels of transcription of RNA transcripts obtained from thousands of genes within a genome in one experiment (Trevino *et al.,* 2007). Over the last 20 years, high quality arrays, standardised hybridisation protocols, improved scanning technologies and improved computational analysis methods have been established for DNA microarray experiments, rendering them an essential genomic tool (Trevino *et al.,* 2007). Microarrays allow the simultaneous monitoring of expression levels of thousands of genes in cells (Yang *et al.,* 2001). In a typical microarray experiment using 'spotted arrays', the two mRNA samples to be compared are reverse transcribed into cDNA, labelled using two different fluorescent dyes; Cy5, a red dye and Cy3, a green dye and then simultaneously hybridised to a glass slide. Four biological replicates of each strain are generally used to generate a good estimate of variance and promote statistical confidence (Trevino *et al.*, 2007).

Gene expression levels are indicated by the intensity values generated from hybridisation to single DNA spots, and comparisons of gene expression levels between the two samples are derived from the resulting intensity ratios (Taniguchi *et al.,* 2001). To detect differentially expressed genes, the most common approach is to determine the fold change in fluorescence intensity expressed as the logarithm ($\log_2$) of the sample divided by the reference (Mutch *et al.,* 2001; Yue *et al.,* 2001). Using this method, a fold-change of one means that expression has increased two-fold, resulting in up-regulation of the gene. A fold-change equal to minus one means the expression level has decreased two-fold, where the gene is down-regulated. Zero means the level of expression remains unchanged (Trevino *et al.,* 2007). Experimental and systematic variation in microarray experiments must be considered in order to accurately and precisely measure changes in gene expression. A known contributor of systematic variation is the dye bias associated with Cy3 and Cy5. Dye biases occur as a result of heat and

light sensitivity, efficiency of dye incorporation, experimental variability in hybridisation, and scanner settings when collecting the data (Yang *et al.,* 2001). These factors make it difficult to distinguish between differentially and constantly expressed genes. In order to correct these variations, normalisation is applied to the microarray data.

Given that microarrays contain thousands of probes, these experiments amass large volumes of data. A common practice is to filter out genes that have not shown significant changes in expression across samples or those whose average expression is very low. Following the application of filtering, the next step is to apply statistical analyses to the data. Commonly used statistical tests include the common t-test for analysing two groups of samples in two-dye microarrays whose $\log_2$ ratios generate normal-like distributions following normalisation. Analysis of variance (ANOVA) test can be applied for more than two groups of samples. If the data have not been standardised, Wilcox or Mann-Whitney tests may be applied (Trevino *et al.,* 2007). Following the analysis of microarray data, it is necessary to confirm the microarray findings. Generally, gene expression profiles observed in microarray experiments are confirmed using quantitative real-time PCR (qRT-PCR).

There are a vast number of studies published where DNA microarrays have proved invaluable in the elucidation gene functions. Spiering *et al.,* (2010) used DNA microarrays to identify novel virulence-associated genes in *C. albicans* and to characterise similarities and differences between the closely related *C. albicans* and *C. dubliniensis* by comparing global gene expression in an RHE model of the oral mucosa. This study allowed Spiering *et al.* to identify a number of genes of unknown function in *C. albicans* that were absent or divergent in *C. dubliniensis.* One of the genes identified as having a role in filamentation and virulence in *C. albicans* was *SFL2,* which was significantly up-regulated in *C. albicans* in the RHE model and 50% divergent from its probable orthologue in *C. dubliniensis.* Furthermore, a study carried out by Zakikhany *et al.* (2007) used an oral candidiasis RHE model to dissect the stages of

fungus-host cell interactions from invasion to tissue destruction. Samples from HIV-positive patients suffering from pseudomembranous OPC were used to compare the transcript profile obtained from each *in vivo* stage of infection and identify genes associated with OPC. Zakikhany *et al.* identified *EED1* as an essential gene for epithelial dissemination *in vitro* and *in vivo.*

3.1.8. Recently developed transcriptomics tools

Although DNA microarrays are still effectively used to measure transcriptional changes within the transcriptome, this method has a number of limitations, including the reliance upon existing knowledge of genome sequence, high background noise levels due to cross-hybridisation and the requirement of complex data normalisation methods. RNA-Seq is a relatively new method that provides a more precise measurement of transcript levels using sequence-based approaches to directly determine the cDNA sequence (Wang *et al.,* 2009). In general, a total or fractionated population of RNA is converted to a library of cDNA fragments with adaptors attached to one or both ends. Each molecule, with or without amplification, is then sequenced in a high-throughput manner to obtain short sequences from one end (single-end sequencing) or both ends (pair-end sequencing). Following sequencing, the reads are either aligned to a reference genome or reference transcripts, or assembled *de novo* without the genomic sequence to produce a genome-scale transcription map that consists of both the transcriptional structure and/or level of expression for each gene (Wang *et al.,* 2009). A study carried out by Bruno *et al.* (2010) using RNA-Seq identified 602 *C. albicans* transcripts that did not correspond to known annotated features in the *Candida* Genome Database (CGD). Furthermore, the development of next generation sequencing (NGS) has resulted in a cheaper and higher throughput DNA sequencing method than Sanger sequencing. Next generation sequencing platforms perform massively parallel sequencing, during which millions of fragments of DNA from a single sample are sequenced in unison, thus facilitating high-

throughput sequencing, which allows an entire genome to be sequenced in less than one day (Grada & Weinbrecht, 2013).

3.1.9. qRT-PCR

Real-time reverse transcription PCR is a sensitive method for the detection of low-abundance mRNAs. The extent of gene expression can be determined by measuring the amount of cellular RNA present. For most genes, expression levels vary dramatically between genes, cells or during various experimental conditions (Schmittgen & Livak, 2008). In quantitative PCR, the real-time data is presented relative to another gene, usually referred to as an internal control. These internal control genes are primarily housekeeping genes that are expressed constitutively at high levels, such as *ACT1,* the control gene used in this study. There are two commonly used quantitative methods: the standard curve method and the comparative C_T method (Livak, 1997). In the standard curve method, the input amount for unknown samples is calculated from the standard curve of a specific gene, and normalised to the input amount of a reference gene, which is also calculated from its standard curve (Liu & Saint, 2002). The comparative C_T method detects the relative gene expression with the formula $2^{-\Delta\Delta C_T}$. This formula is based on the assumption that the efficiency of the target gene is similar to the internal control gene (Schmittgen and Livak, 2001).

3.1.10. Aims of this section of the study

The aims of this section of the study were to investigate the role of the *TLO* genes in *C. albicans* and *C. dubliniensis*. We aimed to determine whether the re-introduction of *CdTLO1* and *CdTLO2* to the *Cdtlo*ΔΔ mutant under the control of the DOX-regulatable promoter could restore true hyphal formation, increase growth rate in an alternative carbon source and restore tolerance to oxidative stress. We also characterised the effect of the re-introduction of *CdTLO1* and *CdTLO2* to *Cdtlo*ΔΔ on the transcriptome of *C. dubliniensis.*

3.2. Specific materials and methods

3.2.1. Restriction endonuclease-mediated cloning

3.2.1.1. Preparation of template DNA

Candida cells were streaked onto YEPD agar plates initially and sub-cultured in YEPD broth and incubated as described in Chapter 2. Cells were washed in 1 X PBS and the cell walls were disrupted using the bead beater method. DNA was extracted using phenol-chloroform and re-suspended in 50 µl Ultrapure water. For PCR experiments, the DNA was diluted to provide a 100 ng template.

3.2.1.2. PCR amplification and purification of CdTLO1 and CdTLO2

DNA sequences for *CdTLO1* and *CdTLO2* were downloaded from the Candida Genome Database (CGD). *CdTLO1* and *CdTLO2* were amplified from Wü284 genomic DNA using Expand High Fidelity Polymerase (Roche). The primers used are listed in Table 2.2. Primers CdTLO1SalF1 and CdTLO1BglIIR1 were used to amplify *CdTLO1* and primers CdTLO2SalF1 and CdTLO2BglIIR1 were used to amplify *CdTLO2* in the following PCR reaction; 94 °C for 2 min, 10 cycles of 94 °C for 15 s, 60 °C for 30 s, 68 °C for 2 min 30 s, 20 cycles of 94 °C for 15 s, 60 °C for 30 s, 68 °C for 2 min 30 s with an increase of 5 s per cycle. Final elongation was performed at 68 °C for 2 min. Gel electrophoresis was carried out on 0.8% (w/v) agarose to visualise the 965 bp *CdTLO1* product and the 1.1 kb *CdTLO2* product. Target PCR products were purified using the Genelute PCR Cleanup Kit (Sigma) and stored at -20 °C.

3.2.1.3. Plasmid isolation

Escherichia coli cells containing plasmids were grown as previously described in Chapter 2. Following washing the cells in 1 X PBS, the cells were lysed and the plasmids extracted using the PureYield Plasmid Extraction kit (Promega) or the Genelute Plasmid Miniprep kit (Sigma). Plasmid DNA was stored at -20 °C.

3.2.1.4. Digestion and ligation of DNA fragments

Purified *CdTLO1* and *CdTLO2* alleles and plasmid DNA were digested with *Sal*I and *Bgl*II restriction endonuclease enzymes in a 37 °C water bath for 2-24 h. Digested DNA was purified using the Wizard Gel and PCR Cleanup kit (Promega). With regards to digested pNIM plasmid DNA, the excised *GFP* fragment and the plasmid DNA backbone were separated by gel electrophoresis on 0.8% (w/v) agarose and each DNA fragment gel purified using the Wizard Gel and PCR Cleanup kit (Promega). Ligation reactions were carried out using T4 DNA ligase (Promega) in accordance with the manufacturer's guidelines, as described in Chapter 2. The digested *CdTLO1* and *CdTLO2* DNA fragments were ligated to the digested CdpNIM DNA backbone. Digested *GFP* was also re-ligated to the digested CdpNIM DNA backbone as a control experiment. Ligation reactions were used directly in *E. coli* transformations.

3.2.1.5. Transformation of E. coli competent cells

Each 30 µl ligation mixture was added to 200 µl of competent *E. coli* XL10 Gold cells, heat-shocked, chilled and allowed to recover in S.O.C. medium for 2 h at 37 °C, 200 r.p.m. The recovered cells were plated onto L amp_{100} agar plates and incubated in a static incubator at 37 °C overnight.

3.2.1.6. Screening of transformants by PCR amplification

Antibiotic selection was used to identify the uptake of plasmid containing the ampicillin resistance gene. Transformants were sub-cultured onto fresh L_{amp} agar plates. Plasmid DNA was extracted from each putative transformant and digested with *Sal*I and *Bgl*II to investigate if the enzymatic digestion pattern was correct. Undigested plasmid DNA was used as a template in a PCR reaction to screen for the presence of *CdTLO1* and *CdTLO2,* using primers CdTLO1SalF1 and CdTLO1BglIIR1 for *CdTLO1* and CdTLO2SalF1 and CdTLO2BglIIR1 for *CdTLO2.*

3.2.2. Transformation by electroporation of DOX-inducible *CdTLO1* and *CdTLO2* into *CdtloΔΔ*

A single colony of *CdtloΔΔ* was inoculated into 50 ml of YEPD broth and grown overnight at 30 °C with shaking at 200 r.p.m in an orbital incubator to an $O.D._{600}$ of 1.6 to 2.0 (approximately 0.5 to 1.0 x 10^7 cells/ml). Transformation protocol was carried out as described in Chapter 2.

3.2.3. Screening of putative transformants by PCR amplification

Nourseothricin-resistant transformant colonies were sub-inoculated onto fresh NAT_{100} plates and incubated for 48 h at 37 °C. Genomic DNA was isolated from transformant colonies by overnight growth in YEPD broth, cell disruption using a bead beater and DNA extraction by the phenol-chloroform method. In order to be used as PCR template, the DNA concentration was adjusted to 100 ng/µl in molecular biology grade water (Sigma). Screening for correct transformants was carried out by attempting to PCR amplify specific DNA sequences. Screening was performed for the presence of the *CdTLO1* and *CdTLO2* genes, the *ADH* junctions at which recombination was determined to occur, and the presence of the transactivator *cartTA*. The *CdTLO1* and *CdTLO2* genes were amplified using primers CdTLO1SalF1 and CdTLO1BglIIR1 for *CdTLO1* and CdTLO2SalF1 and CdTLO2BglIIR1 for *CdTLO2.* The recombination junction site was amplified using primers CdADH1_5_F and CdADH1_5_R for the 5' end of the junction and CdADH1_3_F and CdADH1_3_R for the 3' end of the junction and the *cartTA* transactivator was amplified using the cartTA_F and cartTA_R primer pair (Table 2.2).

3.2.4. qRT-PCR gene expression analysis of DOX inducible *CdTLO1* and *CdTLO2*

Verified doxycycline-inducible *CdTLO1* and *CdTLO2* in a *CdtloΔΔ* background were incubated on YEPD plates at 37 °C for 48 h. Single colonies were inoculated into YEPD broths containing 20 µg/ml of doxycycline hyclate (DOX). DOX broths were incubated overnight at 37 °C, 200

r.p.m. DOX broths were centrifuged at 16,000 x g for 3 min and washed in 1X PBS. The supernatant was removed and the cells were either directly used for RNA extraction or flash-frozen in liquid nitrogen and stored at -80 °C. RNA was isolated from cells using a combination of mechanical disruption with a micro-dismembranator S (Sartorius Mechatronics) and extraction with the Qiagen RNeasy kit (Qiagen) as outlined in Chapter 2. cDNA was generated from 1 µg of DNase-treated RNA with Superscript Reverse Transcriptase II according to the manufacturer's instructions. cDNA was stored at -20 °C.

DOX-induced gene expression was analysed by qRT-PCR carried out on 1:100 diluted cDNA. All qRT-PCR experiments were run on an Applied Biosystems 7500 Real-Time PCR system. Fast SYBR Green (Applied Biosystems) was used in 15 µl reaction volumes with 1 µl of cDNA template and 0.75 µl of each primer. Primers used for qRT-PCR in this study can be found in Table 2.2. *ACT1*, the housekeeping gene, was used as an internal endogenous control for each reaction. The output was measured using the C_t method as described in Chapter 2 according to the method described by Schmittgen & Livak (2008).

3.2.5. Hyphal induction in liquid media

3.2.5.1. Growth and maintenance conditions

Candida strains used in this study are listed in Table 2.1. Each strain to be studied was grown at 37 °C for 48 h on YEPD agar. From each plate a single colony was inoculated into 2 ml YEPD broth and grown overnight at 30 °C with shaking at 200 r.p.m in an orbital incubator.

3.2.5.2. Induction and visualisation of hyphae

Induction of hyphae in 10% (v/v) FBS and water was carried out as described in Chapter 2. *Candida* cells were visualised and the numbers of true hyphal cells were counted using an inverted light microscope (Nikon Eclipse 600) and illustrated as a percentage of 100 cells.

Replicate plates were set up for each time-point measured so as to not interrupt incubation periods between time-points.

3.2.6. Hyphal induction and visualisation on solid media

Single *Candida* colonies were inoculated on solid hyphal inducing media (Spider agar) and incubated at 30 °C or 37 °C. Colonies were visually examined in a number of ways. A Flash & Go Automatic Colony Counter (IUL, Barcelona, Spain) was used to obtain images of entire agar plates. Colony fringe morphology was visualised with a Nikon TMS-F inverted microscope (Nikon) and images recorded with a Nikon Coolpix 4500 (Nikon).

3.2.7. Growth rate analysis

Strains were grown in YEPD at 30 °C overnight (18h), with shaking at 200 r.p.m in an orbital incubator. Strains were centrifuged for 3 min at 14,000 r.p.m and washed twice with sterile phosphate buffer solution (PBS) and counted as previously described. Cells were inoculated into 50 ml of the appropriate medium to obtain a final concentration of 2 x 10^6 cells/ml. Cultures were incubated at 37 °C with shaking at 200 r.p.m for up to 10 h, with O.D 600 nm measurements recorded every hour using a spectrophotometer (Thermo Scientific, Ireland). Each experiment was carried out on three separate occasions. Measurements were graphed using Microsoft Excel. Data from exponential growth was imported to Prism Graph pad and the data for each strain was fit to a curve using non-linear regression/ exponential curve. Doubling time was calculated for each strain, using the formula ln(2)/k where k is the rate constant expressed as inverse of time. Doubling times from each replicate were pooled and standard deviations calculated using Microsoft Excel.

3.2.8. Spot plate assay

In order to qualitatively assess the susceptibility of *Candida* isolates and mutant derivatives to various inhibitors overnight cultures grown at 30 °C were spun down, washed and cells

counted and standardised to 2 x 10^6 cells/ml. Volumes ranging from 5 µl -10 µl from serial dilutions (10^{0} to 10^{-5}) were spotted onto inhibitor containing agar plates. The plates were incubated at 37 °C for 48 h in a static incubator. Plates were observed for levels of growth and photographed with a Nikon Coolpix 4500 (Nikon).

3.2.9. Two Colour DNA Microarray-based gene expression and analysis

DNA microarray experiments for this study were carried out as described in Chapter 2. In this study, the conditions used were 1 h growth in sterile ultrapure H_2O supplemented with 10% v/v fetal bovine serum (FBS) and YEPD cultures grown to an $O.D._{600}$ nm of 0.8.

3.3. Results

The results of this study have been published in part in the Haran *et al.* (2014) publication.

3.3.1. Construction of *CdTLO1* and *CdTLO2* DOX-inducible gene expression cassettes

In order to express the *CdTLO1* and *CdTLO2* genes in the *Cdtlo*ΔΔ double mutant background, the pNIM1 plasmid (Park and Morschhäuser, 2005) was utilised to attempt to regulate expression of *CdTLO1* and *CdTLO2* in *Candida dubliniensis.* The pNIM1 plasmid contains an *amp* marker that confers resistance to ampicillin and the positive selection marker *caSAT1,* which confers resistance to nourseothricin (Figure 3.1). In pNIM1 the *caGFP* ORF is fused to the Tet-inducible promoter and flanked by *Sal*I and *Bgl*II restriction sites. The *CdTLO1 and CdTLO2* genes were amplified using the primer pairs CdTLO1F1/CdTLO1R1 and CdTLO2F1/CdTLO2R1, which contained *Sal*I and *Bgl*II restriction sites on the 5′ and 3′ termini, respectively (Table 2.2). In order to replace the *GFP* gene, purified PCR fragments were ligated to pNIM1 (digested with *Sal*I and *Bgl*II and gel purified from *GFP*) and the ligation mixes were then transformed into *E. coli* XL10 Gold electrocompetent cells, which were plated onto L_{amp} agar. Positive transformants were identified by digesting plasmid DNA with the restriction enzymes *Sal*I and *Bgl*II and identifying inserts of the correct size by agarose gel electrophoresis. Following identification of positive transformants, the pNIM1 plasmid containing the *CdTLO1/CdTLO2* insert was digested with the restriction enzymes *Sac*II and *Apa*I and cleaned up, resulting in a linear DNA fragment for transformation.

3.3.2. Transformation of *CdTLO1* and *CdTLO2* into the *Cdtlo*ΔΔ mutant background

DOX-inducible positive *CdTLO1* and *CdTLO2* linear DNA constructs were transformed into *C. dubliniensis tlo*ΔΔ by electroporation. Transformations were carried out multiple times, with varying ranges of DNA concentrations. Transformation efficiency was relatively high at lower DNA concentrations of between 0.2 μg–0.5 μg, such that 0.3 μg of DNA could yield ~ 17

(A)

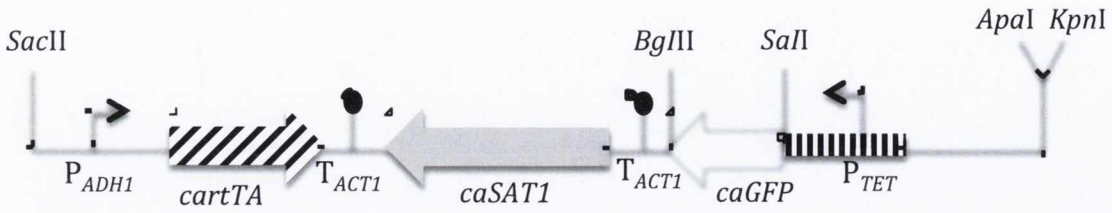

(B)

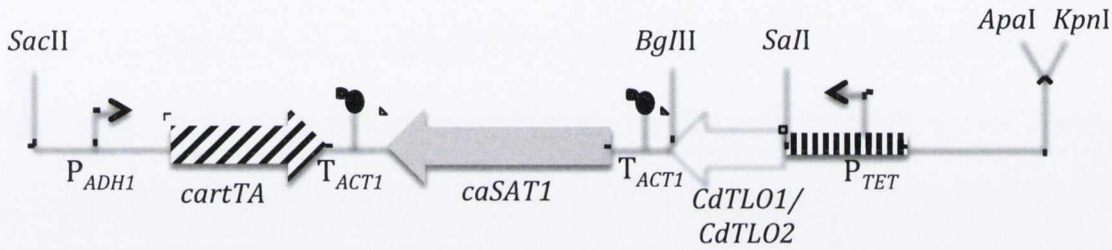

Figure 3.1. (A) Structure of the Tet-inducible gene cassette contained in the pNIM1 plasmid. Unique restriction sites *Bgl*II and *Sal*I can be used to substitute other ORFs for *caGFP*. To excise the cassette from the vector it can be cut with *Sac*II and *Apa*I/ *Kpn*I. **(B)** Shows the cassette containing the *CdTLO1* and *CdTLO2* genes, indicating where the genes integrate into the plasmid when *caGFP* is excised. Adapted from Park and Morschhäuser, (2005).

colonies when grown on NAT_{100} agar plates. Transformants with the cassette inserted into the correct position in the *ADH* locus were identified by PCR screening of isolated genomic DNA for the *CdTLO1/CdTLO2* gene, the *cartTA* transactivator and amplifying either end of the CdpNIM *ADH* recombination junction using the primer pair CdADH1_5_F/ CdADH1_5_R to confirm correct integration of the plasmid into the *ADH* locus at the 5′ end and the primer pair CdADH1_3_F/ CdADH1_3_R to confirm correct integration at the 3′ end.

The pCDRI-*TLO* constructs were linearised using restriction enzyme *Nco*I, cleaned up and transformed into *Cdtlo*ΔΔ by electroporation. Positive transformants inserted into the *CDR* locus were identified using PCR screening of isolated genomic DNA for the *CdTLO1/CdTLO2* gene and correct integration was confirmed by PCR using the primer pair M13R/TAGR (Table 2.2) (Figure 3.2).

3.3.3. qRT-PCR expression analysis of DOX-inducible *CdTLO1* and *CdTLO2*

qRT-PCR was used to measure the expression levels of the *CdTLO* genes in the wild type Wü284 and in the *Cdtlo*ΔΔ mutant with the re-integrated DOX-inducible *CdTLO1* and *CdTLO2* genes. Cells were treated with 20 μg/ml of DOX in hyphal-inducing conditions i.e. water supplemented with 10% w/v FBS and in nutrient-rich YEPD. Given that two sets of re-integrated *CdTLO*s (the DOX-inducible *CdTLO*s and the *CdTLO*s under the control of their native promoter in the *CDR1* locus) were generated in our laboratory, expression levels of both sets were analysed. In this study, the analysis was carried out using the comparative C_T method, which assumes that the transcriptional efficiency of the target gene is similar to the internal control gene (Schmittgen and Livak, 2001). In the hyphal-inducing conditions the wild type strain, in which both *CdTLO* genes are intact, both *CdTLO1* and *CdTLO2* were expressed at low levels relative to *ACT1*, with *CdTLO1* expression 10-fold higher than that of *CdTLO1* expression (Figure 3.3). In both *CdTLO1* re-integrated strains, *CdTLO1* was expressed at levels 2- fold lower than that of wild type. However, with regards to *CdTLO2* expression, a

significant difference was observed. In the DOX-inducible *CdTLO2* strain, *CdTLO2* expression was 1-fold higher than that of wild type, whereas expression in the *CDR1-TLO2* was 10-fold higher than wild type. In YEPD, the expression of *CdTLO1* and *CdTLO2* in Wü284 was very low, with *CdTLO2* more highly expressed. The expression of pTET-*TLO1* was similar to that of wild type, while pTET-*TLO2* was very highly expressed, with expression one hundred-fold higher than in wild type. The expression of *CdTLO1* under the control of the native promoter was almost one hundred-fold higher than that of wild type, while *TLO2* expression in the pCDRI reintegrant was ten-fold higher than that of wild type.

3.3.4. Effect of DOX-inducible *CdTLO1* and *CdTLO2* on hyphal induction in liquid media

Previous studies carried out in our laboratory found that the deletion of the *CdTLO* genes in *C. dubliniensis* affects the ability of *C. dubliniensis* to form true hyphae. This experiment was therefore carried out to examine the effect the DOX-inducible *CdTLO1* and *CdTLO2* genes had on the restoration of the hyphal formation phenotype. All strains were pre-incubated with varying concentrations of DOX (20-50 μg/ml) in 2 ml YEPD overnight. With the wild-type strain, Wü284, levels of about 80%-90% of cells were observed to be in true hyphal form by 3–4 hours of growth at 37 °C in water with 10% FBS (Figure 3.4). Filamentation was induced due to the nutrient, pH and temperature shifts needed for the formation of true hyphae in *C. dubliniensis*. As expected, the deletion of both *CdTLO1* and *CdTLO2* resulted in the inability of true hyphal formation at any time point, with pseudohyphal growth present at all stages (Figure 3.5). In the pTet-*CdTLO1* strain, in which *CdTLO1* had been reintegrated to the *Cdtlo*ΔΔ background, wild type phenotype was observed (Figure 3.5). This was true for all concentrations of DOX used. In the pTet-*CdTLO2* strain, in which *CdTLO2* had been reintegrated in the *Cdtlo*ΔΔ background, hypha formation was also observed, however to a lower degree than was found with *CdTLO1*. At 3 h, cells were a mix of true hyphae (40%-50%) and pseudohyphae (Figure 3.5). This was also true for all concentrations of DOX used. Similar hyphal restoration was observed with the re-integration of the pCDRI::*CdTLO1* and

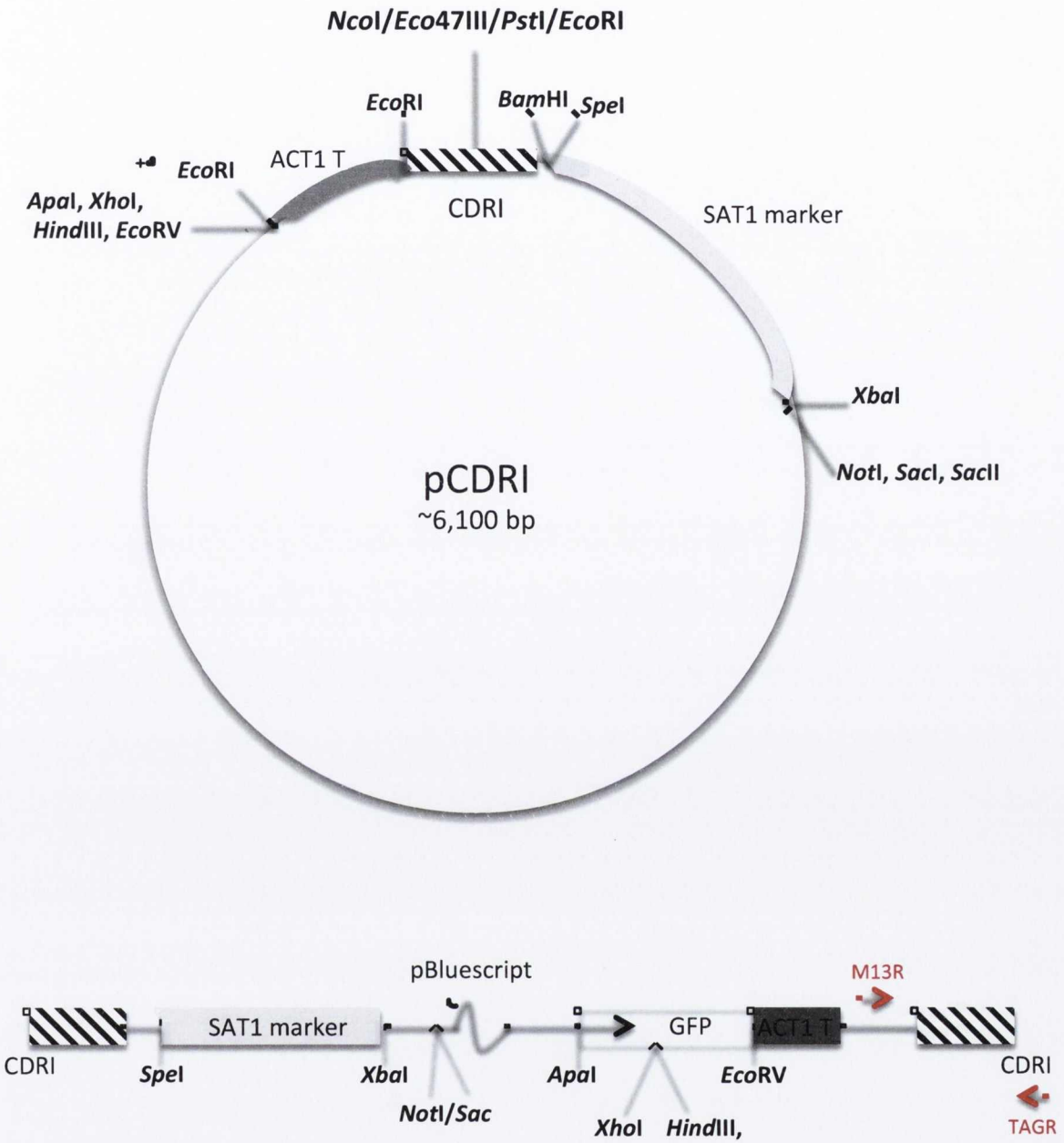

Figure 3.2 Plasmid map of pCDRI. *Not*I and *Sac*I/II or *Xho*I and *Hind*III can be used to insert ORFs. Plasmid can be linearised by cutting with *Nco*I/*Eco*47III/*Pst*I/*Eco*RI. Red arrows indicate primer pair used to PCR screen for correct integration into the CDR locus.

(A)

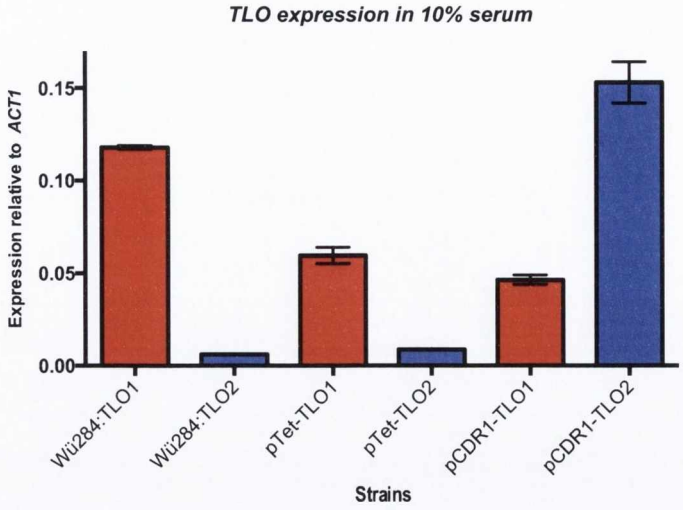

(B)

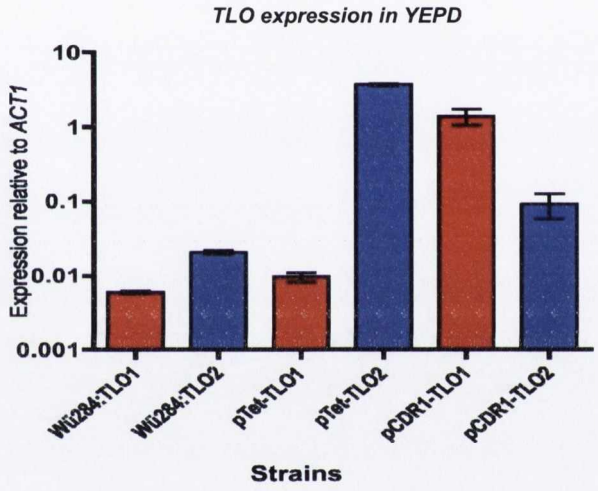

Figure 3.3. Expression of *CdTLO1* and *CdTLO2* in wild type and in the *CdTLO* reintegrants under the control of a DOX-inducible promoter (pTET), treated with 20 µg/ml DOX and under the control of their native promoter (pCDR1) in (A) 10% v/v FBS and water and (B) YEPD $0.8_{O.D.}$. Results are interpreted and displayed relative to *ACT1* expression. Values displayed represent $2^{-\Delta\Delta C}{}_{T}$ values. Error bars represent the standard error of the mean (SEM) of three replicates.

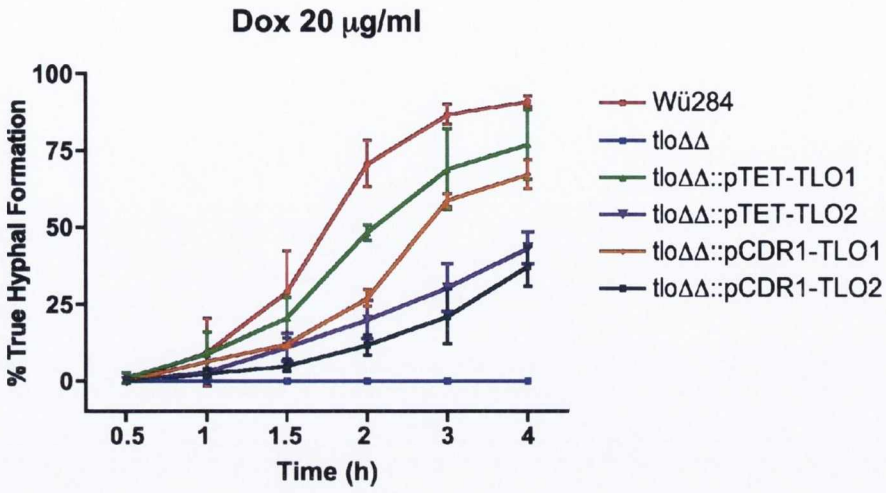

Figure 3.4. Hyphal formation of Wü284, *Cdtlo*ΔΔ, *Cdtlo*ΔΔ::pTET TLO1, *Cdtlo*ΔΔ::pTET TLO2, *Cdtlo*ΔΔ::pCDR1 TLO1 and *Cdtlo*ΔΔ::pCDR1 TLO2 following growth in YEPD followed by inoculation into 10% v/v FBS and a concentration 20 μg/ml of DOX. Similar levels of hyphal formation was observed for all concentrations of DOX (30-50 μg/ml-not shown). Error bars represent the standard error of the mean (SEM) of three replicates.

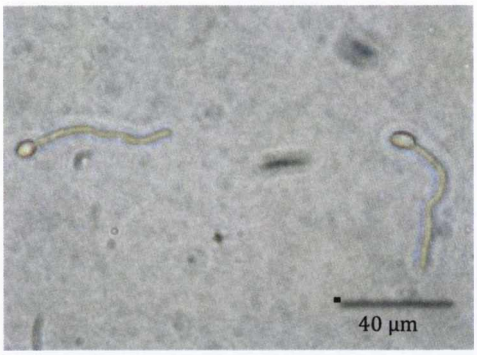

Wü284

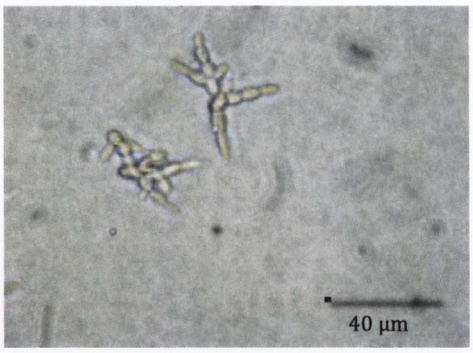

*Cdtlo*ΔΔ

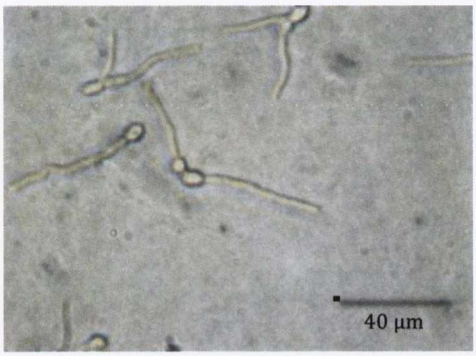

*Cdtlo*ΔΔ::pTET-*TLO1*

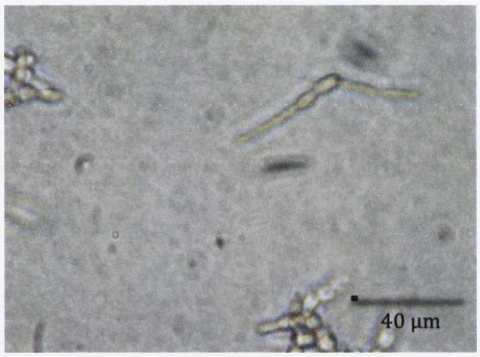

*Cdtlo*ΔΔ::pTET-*TLO2*

Figure 3.5. Photomicrograph showing Wü284, *Cdtlo*ΔΔ, *Cdtlo*ΔΔ::pTET-*TLO1* and *Cdtlo*ΔΔ::pTET-*TLO2* following inoculation into water containing 10% v/v FBS and 20 µg/ml DOX and 3 h of incubation at 37 °C. Scale bar is equal to 40 µm.

pCDRI::*CdTLO2* in the *Cdtlo*ΔΔ background. pCDRI::*CdTLO1* was also ~80% truly hyphal by 3 h of growth, and pCDRI::*CdTLO2* cells were a mix of true hyphae (40%-50%) and pseudohyphae at 3 h (data not shown, provided by J. Haran). Hyphal formation assays were also carried out in the absence of DOX to investigate the affect on the DOX-inducible *CdTLO*s and to ensure the presence of DOX wasn't affecting the wild type, *Cdtlo*ΔΔ, pCDRI::*CdTLO1* and pCDRI::*CdTLO2* strains. As shown in Figure 3.6 wild type was unaffected by DOX, as it grew identically in the presence and absence of DOX, which was also observed for *Cdtlo*ΔΔ, pCDRI::*CdTLO1* and pCDRI::*CdTLO2* strains. However, in the absence of DOX the pTet-*CdTLO1* and pTet-*CdTLO2* strains reverted to the double mutant phenotype and could not form true hyphae.

3.3.5. Effect of DOX-inducible *TLO1* and *TLO2* on growth rate

It was previously demonstrated in our laboratory that the deletion of the *CdTLO*s affected the ability of *C. dubliniensis* to grow in the presence of alternative carbon sources, such as galactose. Growth rates of wild type and the *CdTLO* mutants were measured and differences in the doubling times were observed. To examine the effect of the DOX-inducible *CdTLO1* and *CdTLO2* genes on the growth rate in YEPD, the strains were pre-cultured in YEPD in the presence of DOX (20 μg/ml). Growth in YEPD supplemented with DOX (20 μg/ml) at 37 °C was analysed over a 10 h incubation period. To examine the effect of growth in an alternative carbon source experiments were also performed in which the dextrose/glucose in YEPD was replaced by galactose, an epimer of glucose and again growth at 37 °C was analysed over a 10 h incubation period. Data were fitted to a regression curve, as described in Section 2.2.4 and the doubling times were calculated (Figure 3.7). The presence of DOX appeared to have no effect on wild type or the *Cdtlo*ΔΔ in YEPD, as they both have similar doubling times of 114 min and 106 min respectively. The pTet-*TLO1* and pTet-*TLO2* strains also had similar doubling times of 109 min in YEPD. In YEP-Gal, the wild type Wü284 had a doubling time of 115.8 min. as previously observed in *Cdtlo*ΔΔ disruption studies, the growth rate of the

*Cdtlo*ΔΔ mutant was significantly increased at 156.6 min. It was found that when the pTet-*TLO1* strain was grown in YEP-Gal, the doubling time was similar to that of wild type at 117.8 min. In the case of the pTet-*TLO2* strain, a slightly lower increase in growth rate of 149.0 min was observed. Similar growth patterns were observed upon the introduction of pCDRI-*CdTLO1* and pCDRI-*CdTLO2* to the *Cdtlo*ΔΔ mutant; pCDRI-*CdTLO1* showed increased doubling times, similar to that of wild type, while pCDRI-*CdTLO2* growth was faster than that of the double mutant, but not as fast as pCDRI-*CdTLO1* (Haran *et al.*, 2014).

3.3.6. Effect of DOX-inducible *TLO1* and *TLO2* on oxidative stress response

Work previously carried out in our lab showed that the *Cdtlo*ΔΔ struggled to grow under oxidative stress conditions induced by millimolar concentrations of H_2O_2. Spot plate experiments were performed to investigate if the re-integration of *CdTLO1* and *CdTLO2* restored growth in the presence of oxidative stress conditions induced by 6mM H_2O_2 in combination with a nutrient-rich medium (YEPD). Strains were pre-incubated with varying concentrations of DOX (10-50 μg/ml) in 2 ml YEPD overnight. It was observed that the wild type strains SC5314 (*C. albicans*) and Wü284 (*C. dubliniensis*) grew efficiently in the presence of 6 mM H_2O_2, while, as expected, the ability of the *Cdtlo*ΔΔ mutant was greatly diminished. The growth of pTet-*TLO1* strain was similar to that of wild type, whereas the growth of pTet-*TLO2*, although slightly better than the growth of the double mutant, was still significantly diminished in comparison to wild type (Figure 3.8), despite presence of the DOX-regulatable promoter. This was found to be true for all concentrations of DOX used.

3.3.7. Two colour DNA Microarray-based gene expression and analysis

The phenotypic data above suggest that both the *CdTLO1* and *CdTLO2* genes have the capacity to complement the *Cdtlo*ΔΔ double mutation, suggesting that the two genes have a similar function. Interestingly, *CdTLO1* appears to have a stronger effect than *CdTLO2.* In order to further compare the functions of *CdTLO1* and *CdTLO2* we investigated the effect of expressing

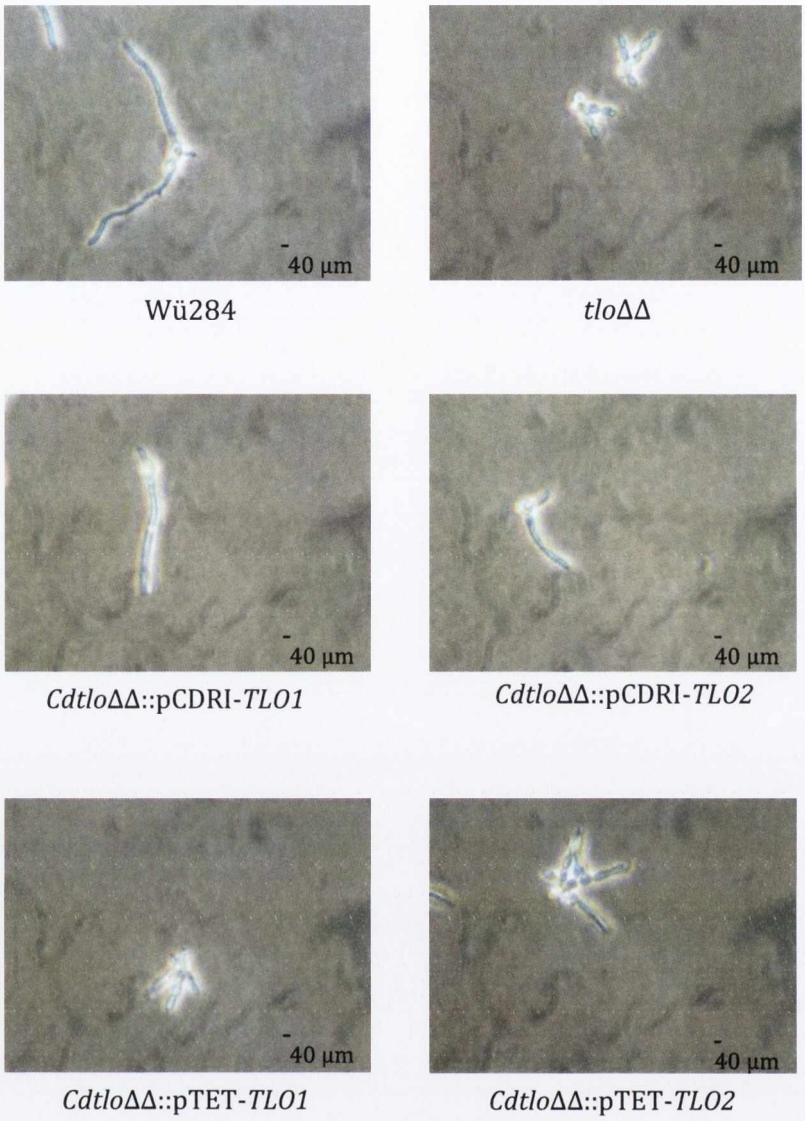

Wü284 *tlo*ΔΔ

*Cdtlo*ΔΔ::pCDRI-*TLO1* *Cdtlo*ΔΔ::pCDRI-*TLO2*

*Cdtlo*ΔΔ::pTET-*TLO1* *Cdtlo*ΔΔ::pTET-*TLO2*

Figure 3.6. Photomicrograph showing Wü284, *Cdtlo*ΔΔ, *Cdtlo*ΔΔ::pCDRI-*TLO1*, *Cdtlo*ΔΔ::pCDRI-*TLO2*, *Cdtlo*ΔΔ::pTET-*TLO1* and *Cdtlo*ΔΔ::pTET-*TLO2* following inoculation into water containing 10% v/v FBS in the absence of DOX and 3 h of incubation at 37 °C. Scale bar is equal to 40 µm.

(A)

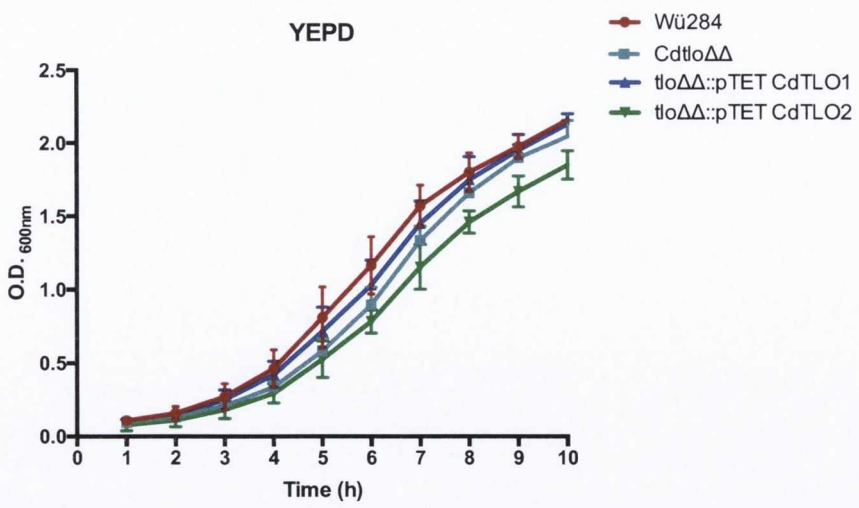

Strain	Wü284	*tloΔΔ*	*tloΔΔ*::pTET TLO1	*tloΔΔ*::pTET TLO2
Doubling time (min)	114.0 *+/- 7.76*	106.0 *+/- 24.64*	109.8 *+/- 6.22*	109.2 *+/- 13.59*

(B)

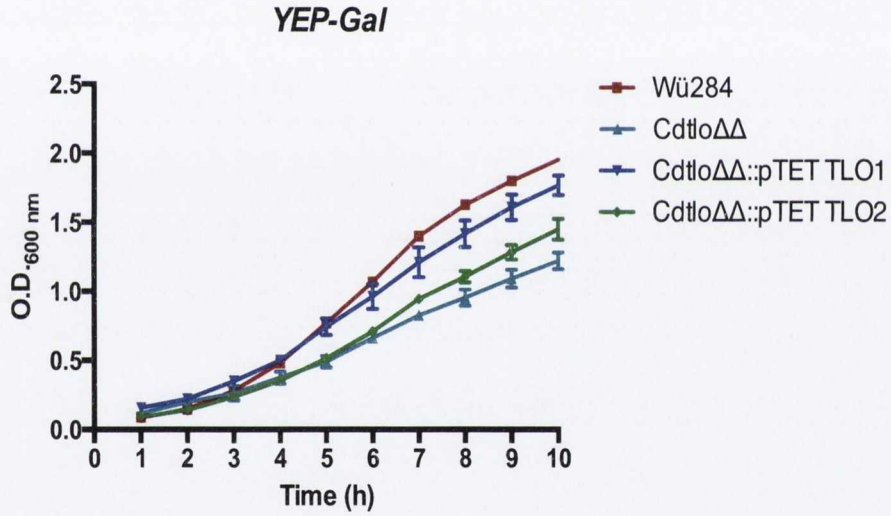

Strain	Wü284	*tloΔΔ*	*tloΔΔ*::pTET TLO1	*tloΔΔ*::pTET TLO2
Doubling time (min)	115.8 *+/- 5.34*	156.6 *+/- 30.15*	117.8 *+/- 9.88*	149.0 *+/-7.35*

Figure 3.7. (A) Graph depicting growth rates of wild type, *C. dubliniensis tloΔΔ* mutant and re-integrated *CdTLO1* and *CdTLO2* in nutrient-rich YEPD media and **(B)** in YEPD with the dextrose/glucose substituted with galactose. Doubling times in minutes. Standard deviations are italicised below each value and represent an average of 3 replicates. Error bars represent the standard error of the mean (SEM) of three replicates.

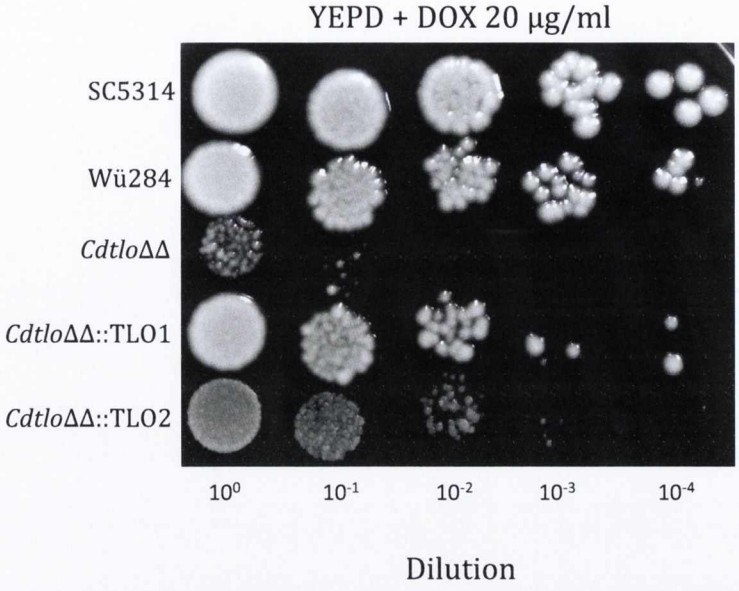

Figure 3.8. Growth of strains in the presence 20 μg/ml of DOX and 6 mM H_2O_2 on nutrient rich YEPD medium following serial dilutions. Similar levels of growth were observed for all concentrations of DOX (30-50 μg/ml not shown). Experiments carried out on three separate occasions.

each gene on global gene expression in the *Cdtlo*ΔΔ double mutant by using DNA microarrays. As described in Section 2.5 two-colour DNA microarrays were used to compare the expression profiles of *Cdtlo*ΔΔ with *Cdtlo*ΔΔ expressing *CdTLO1* or *CdTLO2* during early stages of hyphal growth (i.e. 1 h sH_2O). This condition was chosen to observe the effect of the reintroduction of *CdTLO1* and *CdTLO2* in the early stages of morphogenesis, given that both reintegrated strains begin to form true hyphae in sH_2O after 1 h of incubation at 37 °C. The DOX-inducible *CdTLO1* and *CdTLO2* strains did not yield phenotypic results that were significantly different to those obtained when *CdTLO1* and *CdTLO2* were re-introduced under control of their native promoter in the CDR1 locus. Furthermore, qRT-PCR analysis of both sets of reintegrants revealed that *CdTLO2* was expressed 15-fold higher in the pCDRI-*CdTLO2* strain than in wild type and the pTet-*CdTLO2* strain as observed in Figure 3.3. Based on these observations, the pCDRI *CdTLO* strains were used in DNA microarray studies to ensure no interference from exposure to DOX.

For this study, fluorescence data for each oligonucleotide probe representing a single orf were averaged across four microarray slides and classed as individual entities. Local fluorescent background of the control sample was subtracted from the test sample and $\log_2$ transformed and Lowess normalisation was applied to the data, resulting in 12,034 entities available for analysis, corresponding to 5,987 putative open reading frames in *C. dubliniensis* found in the *Candida* Genome Database (Yang *et al.*, 2001; Inglis, *et al.*, 2012). Statistical tests were applied to the ORFs using the Student's *t* test against zero on four averaged biological samples with a p *value* cut off of ≤0.05. The data sets selected were then compared to the expression profiles of the *Cdtlo*ΔΔ mutant compared to the wild type in order to observe changes in gene expression due to the presence of *TLO1* and *TLO2*.

In an attempt to identify the most significant effects, statistically significant results were filtered using a 1.5-fold-change cut-off in expression. Whole genome clustering (Figure 3.9)

shows the expression profiles of all genes in the *Cdtlo*ΔΔ mutant, *Cdtlo*ΔΔ::*TLO1* and *Cdtlo*ΔΔ::*TLO2.* In order to determine if there were differences in genes expressed between *Cdtlo*ΔΔ::*TLO1* and *Cdtlo*ΔΔ::*TLO2,* the filtered results were separated into genes up-regulated in the presence of *TLO1* compared to those up-regulated in the presence of *TLO2,* and the same for down-regulated genes, with Venn diagrams created for both (Figure 3.10). In the YEPD data set of 759 genes, 385 overlapping genes were up-regulated in the presence of both *TLO1* and *TLO2,* with 93 genes and 281 genes up-regulated exclusively by *TLO1* and *TLO2* respectively [Figure 3.10 (A)]. Of the 835 down-regulated genes, there was an overlap of 495 genes between the two datasets, with 126 genes down-regulated in the presence of *TLO1* only and 214 genes down-regulated in the presence of *TLO2* only [Figure 3.10 (B)]. In the serum data set it was found that 656 genes were up-regulated in both *TLO1* and *TLO2,* with 338 genes up-regulated by *TLO1* only and 260 genes up-regulated by *TLO2* only, with an overlap of 58 genes between *TLO1* and *TLO2* [Figure 3.10 (C)]. When down-regulated genes were compared between *TLO1* and *TLO2,* 718 were shown to be down-regulated, with 414 genes down-regulated in the presence of *TLO1* only, 260 genes down-regulated in the presence of *TLO2* only, and an overlap of 95 genes between *TLO1* and *TLO2* [Figure 3.10 (D)]. Described below are the expression profiles of the genes affected by the absence of the *TLO*s and the effect of restoring the *TLO*s in relation to the phenotypes mentioned previously in this study.

3.3.7.1. Hyphal and cell wall-associated genes

Assays to observe the formation of true hyphae carried out in this study have shown that the deletion of *CdTLO1* and *CdTLO2* in *C. dubliniensis* significantly reduces its ability to form true hyphae, and the re-introduction of either pTet-*CdTLO1* or pCDRI-*CdTLO1,* and to a lesser extent pTet-*CdTLO2* or pCDRI-*CdTLO2* restores this phenotype. Interestingly, *CdTLO2* only partially restores true hyphal formation to the same degree under the control of either the pTet or pCDRI promoter. Microarray analyses have previously shown that many genes

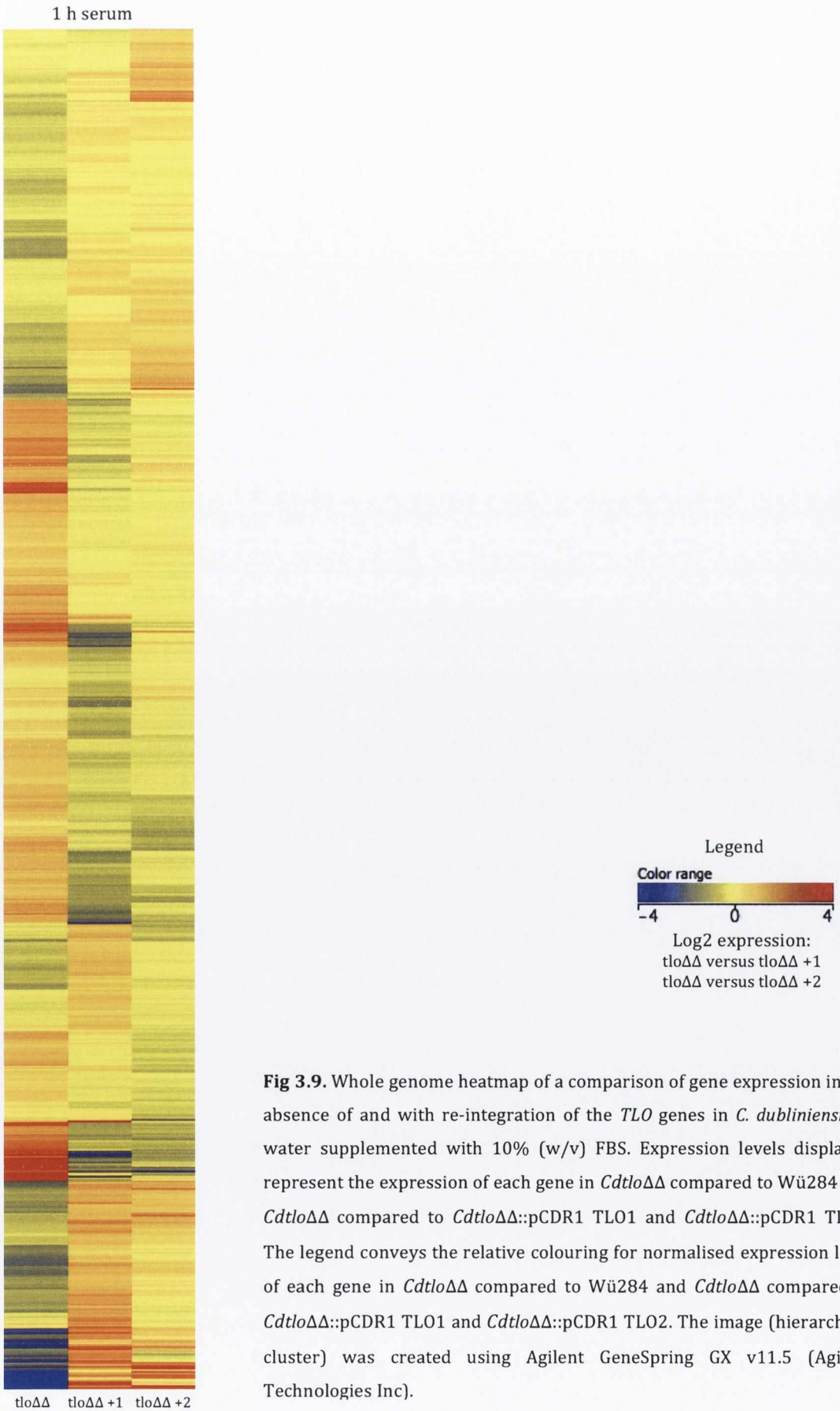

Fig 3.9. Whole genome heatmap of a comparison of gene expression in the absence of and with re-integration of the *TLO* genes in *C. dubliniensis* in water supplemented with 10% (w/v) FBS. Expression levels displayed represent the expression of each gene in *Cdtlo*ΔΔ compared to Wü284 and *Cdtlo*ΔΔ compared to *Cdtlo*ΔΔ::pCDR1 TLO1 and *Cdtlo*ΔΔ::pCDR1 TLO2. The legend conveys the relative colouring for normalised expression level of each gene in *Cdtlo*ΔΔ compared to Wü284 and *Cdtlo*ΔΔ compared to *Cdtlo*ΔΔ::pCDR1 TLO1 and *Cdtlo*ΔΔ::pCDR1 TLO2. The image (hierarchical cluster) was created using Agilent GeneSpring GX v11.5 (Agilent Technologies Inc).

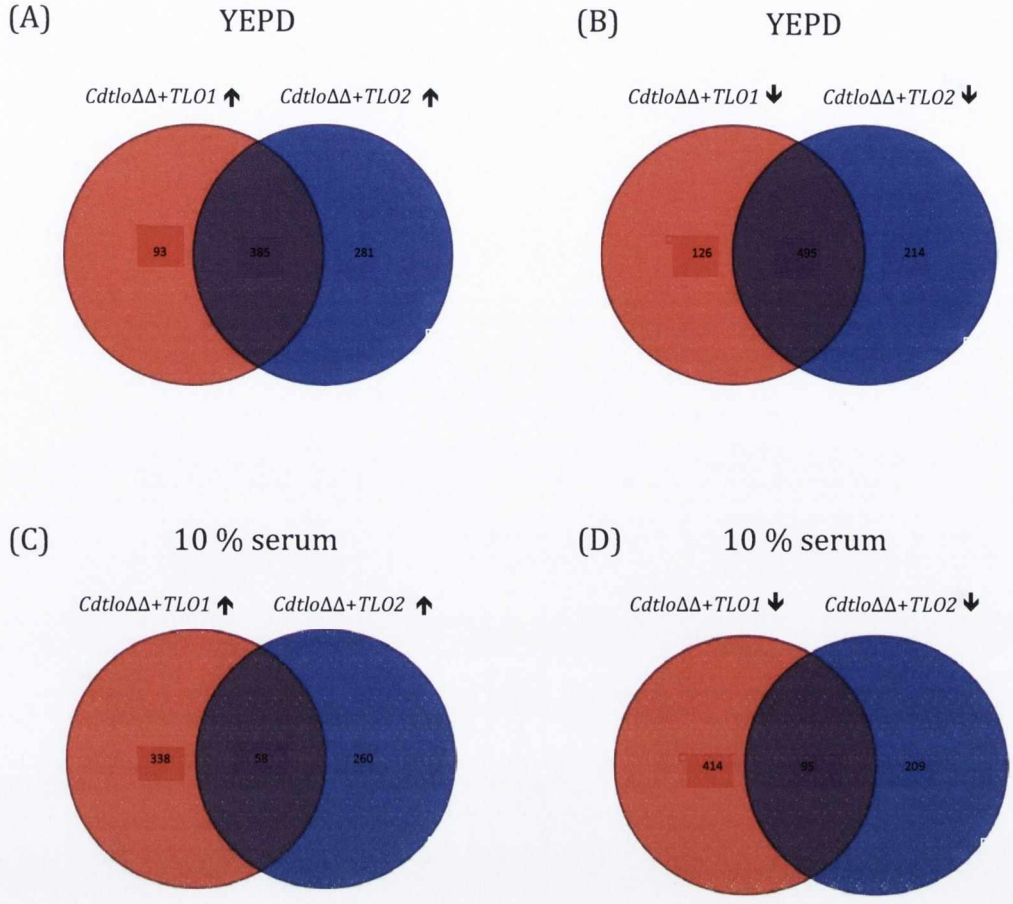

Figure 3.10. Venn Diagrams of *CdTLO1* versus *CdTLO2* representing overlapping and distinct gene numbers from the two mutant microarray datasets. Data is filtered based on a 1.5-fold change in expression. **(A)** and **(B)** represent genes up-regulated and down-regulated in the YEPD microarray dataset. **(C)** and **(D)** represent genes up-regulated and down-regulated in the 1 h serum microarray dataset. Graphs were created using Agilent GeneSpring GX v11.5 (Agilent Technologies Inc).

associated with filamentation and cell wall processes are differentially expressed in *Cdtlo*ΔΔ and Wü284. Microarray experiments carried out in this part of the study aimed to observe the effect of re-introduction of either *CdTLO1* or *CdTLO2* could on global gene expression patterns. Expression patterns were grouped into similar functions and organised using hierarchical clustering (Figure 3.11). Genes encoding cell wall proteins such as *RBT5, DSE1, HWP1, PGA31, CRH11, SMI1* and *ECM21* were all down-regulated in the absence of the *CdTLO* genes. *RBT5* was found to be down-regulated 31-fold, *HWP1* was down regulated 20-fold, while *DSE1* expression was reduced 10-fold. However re-introduction of the *CdTLO*s altered these expression patterns. The expression levels of *HWP1* and *DSE1* were increased 1.95-fold and 1.7-fold in the presence of *CdTLO1,* but were more highly expressed by *CdTLO2,* displaying fold increases of 4.4-fold and 2.1-fold respectively. *RBT5, CRH11, SMI1* and *ECM21* were up-regulated to similar levels in the presence of *CdTLO1* and *CdTLO2,* whereas *PGA31* was up-regulated in the presence of *CdTLO1* but not *CdTLO2.* A dramatic decrease in expression in the absence of the *CdTLO*s was observed for the adhesion-encoding gene *EAP1,* which was down-regulated 13-fold. Unsurprisingly, the re-introduction of *CdTLO1* and *CdTLO2* resulted in a massive increase of *EAP1* expression in comparison with the *CdTLO* double mutant with increases of 10-fold and 3.3-fold respectively observed. Surprisingly, genes known to be involved in filamentation, morphogenesis and cell wall functions such as *SFL1, RNY11, YWP1, DEF1* (*EED1*) and *ECE1* were found to have higher expression levels in the non-hyphal *CdTLO* double mutant in comparison to wild type, while in this study, were found to have decreased expression levels in the presence of *CdTLO1* and *CdTLO2* when compared to the *CdTLO* double mutant, suggesting that the *CdTLO*s have a repressive effect on some hyphal-associated genes.

A study previously carried out in this laboratory identified a group of eight regulatory genes (i.e. *RAS1, TEC1, EFH1, UME6, RIM101, EFG1, NRG1* and *SFL2*), whose expression levels were significantly increased or decreased in response to hyphal-inducing conditions (O'Connor *et*

al., 2010). All of these genes were down-regulated in the absence of the *CdTLO*s in hyphal inducing conditions. While *EFH1* and *SFL2* were not present in the re-integrant data sets, which suggests they were filtered out during significance tests, *RAS1, TEC1, UME6, RIM101* and *EFG1* were observed to be up-regulated in the presence of the re-integrated *CdTLO* genes. *NRG1* was further down-regulated in the presence of the *CdTLO*s; expression was found to be reduced 1-fold in the *Cdtlo*ΔΔ mutant and upon reintroduction of *CdTLO1* and *CdTLO2* expression levels were further decreased by 1.6-fold and 1.1-fold respectively. *HSP90* was up-regulated in the absence of the *CdTLO*s (2-fold), and down-regulated massively in the presence of *CdTLO1* (3.6-fold), with only a slight decrease in expression in the presence of *CdTLO2* (1.4-fold). *UME6* and *EED1* are among the genes stated to have a vital role in hyphal formation. However, both exhibited divergent expression patterns in *Cdtlo*ΔΔ compared to Wü284, and in the *CdTLO1* and *CdTLO2* reintegrants. *UME6* was down-regulated 4-fold in *Cdtlo*ΔΔ compared to Wü284, while re-introduction of *CdTLO1* increased expression 2.9-fold. Expression of *UME6* remained down-regulated 1-fold in the presence of *CdTLO2*, suggesting a primary role for *CdTLO1* in the regulation of *UME6. EED1,* a regulator of RNA polymerase II required for filamentous growth, epithelial cell escape and dissemination was up-regulated 4-fold in the absence of the *CdTLO*s. Re-introduction of *CdTLO1* and *CdTLO2* resulted in a 1.5-fold and 3-fold decrease in expression respectively.

3.3.7.2. Response to oxidative stress

As previously outlined, phenotypic analysis of the *CdTLO* mutant in the presence of oxidative stress resulted in poor growth, while the re-introduction of *CdTLO1* and to a lesser extent *CdTLO2* restored tolerance to H_2O_2. Microarray results correlate with these observations (Figure 3.12 (A)). The superoxide (SOD) genes, associated with the conversion of superoxide radicals to hydrogen peroxide, showed differential expression in the *CdTLO* mutant relative to Wü284. *SOD5* and *SOD6* displayed a significant decrease in expression under hyphal-inducing conditions with 4.3-fold and 7-fold decreases respectively. The re-introduction of

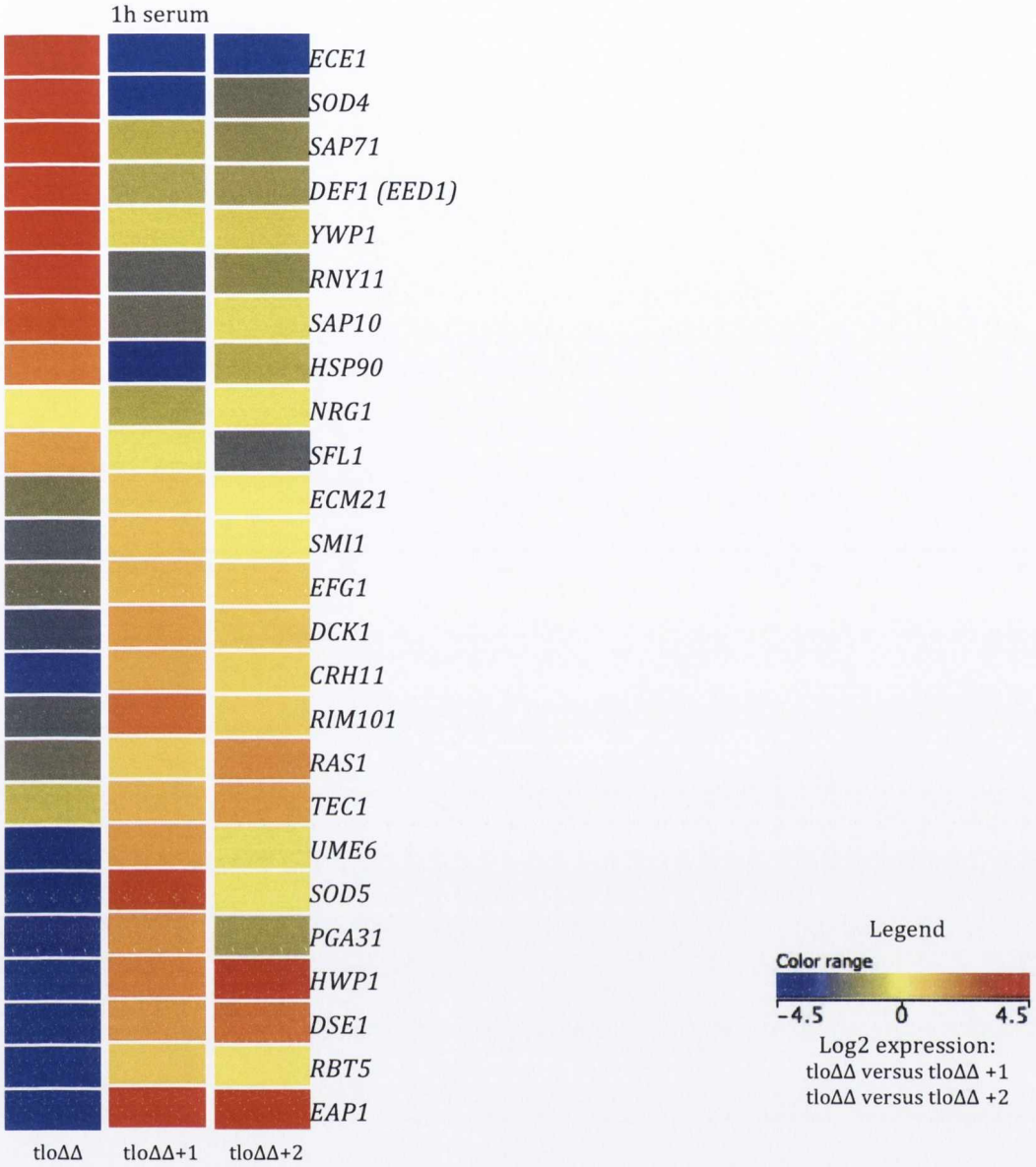

Figure 3.11. Visual heatmap of a comparison of gene expression in the absence and re-integration of the *TLO* genes in *C. dubliniensis* in water supplemented with 10% (v/v) FBS. Expression levels displayed represent the expression of each gene in *Cdtlo*ΔΔ compared to Wü284 and *Cdtlo*ΔΔ compared to *Cdtlo*ΔΔ::pCDR1 TLO1 and *Cdtlo*ΔΔ::pCDR1 TLO2. Each gene is labelled on the right side of the heatmap, using the common gene alias in *C. dubliniensis*, usually named in *C. albicans.* Genes present in this heatmap are involved in hyphal morphogenesis, filamentation or are associated with the cell wall. The legend conveys the relative colouring for normalised expression level of each gene in *Cdtlo*ΔΔ compared to Wü284 and *Cdtlo*ΔΔ compared to *Cdtlo*ΔΔ::pCDR1 TLO1 and *Cdtlo*ΔΔ::pCDR1 TLO2. The image (hierarchical clustering) was created using Agilent GeneSpring GX v11.5 (Agilent Technologies Inc).

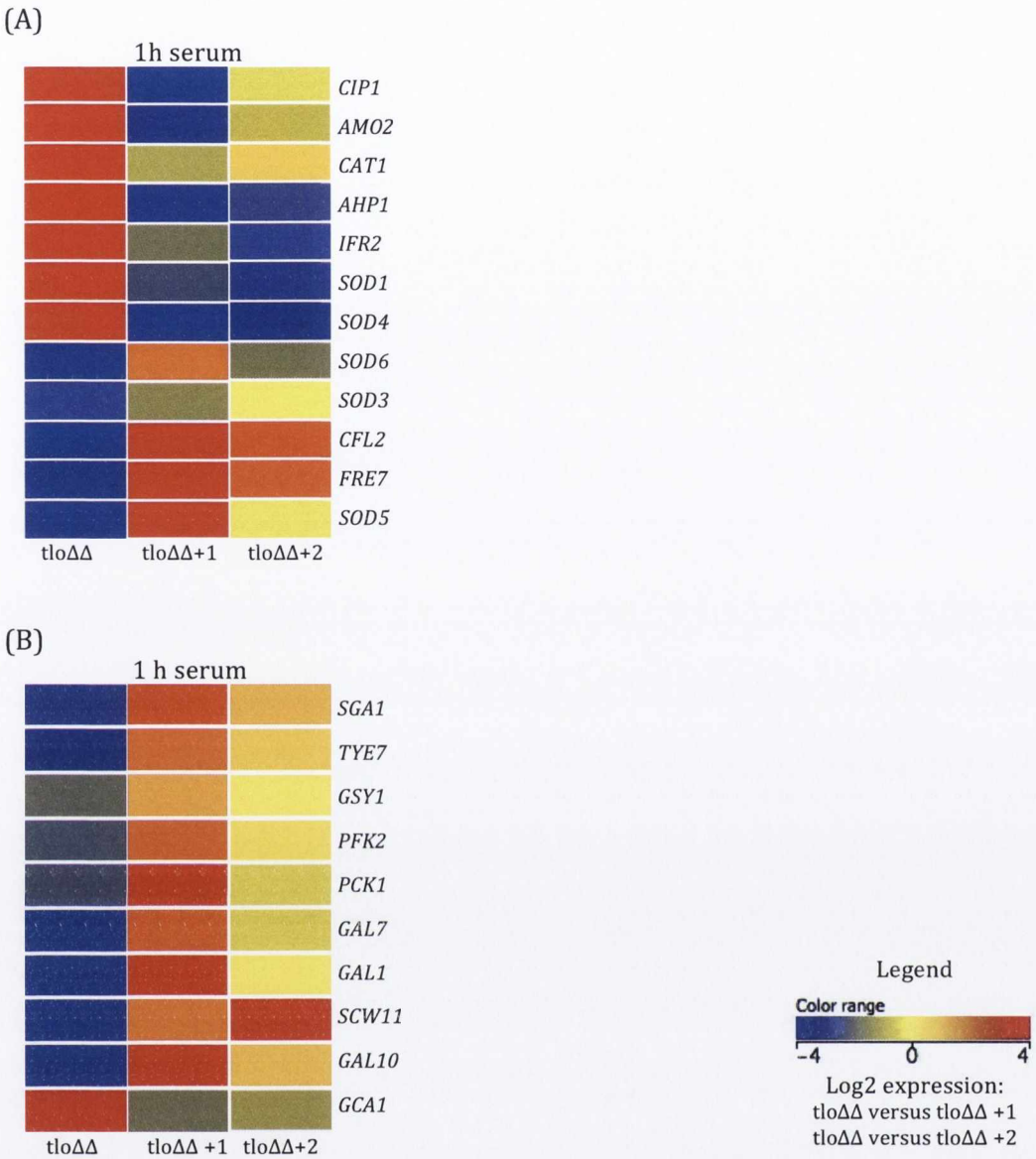

Figure 3.12. Visual heatmap of a comparison of gene expression in the absence and re-integration of the *TLO* genes in *C. dubliniensis* in water supplemented with 10 % (v/v) FBS. Expression levels displayed represent the expression of each gene in *Cdtlo*ΔΔ compared to Wü284 and *Cdtlo*ΔΔ compared to *Cdtlo*ΔΔ::pCDR1 TLO1 and *Cdtlo*ΔΔ::pCDR1 TLO2. Each gene is labelled on the right side of the heatmap, using the common gene alias in *C. dubliniensis*, usually named in *C. albicans*. Genes are grouped by associated process: **(A)** genes involved in oxidative stress response, **(B)** genes involved in carbohydrate utilisation. The legend conveys the relative colouring for normalised expression level of each gene in *Cdtlo*ΔΔ compared to Wü284 and *Cdtlo*ΔΔ compared to *Cdtlo*ΔΔ::pCDR1 TLO1 and *Cdtlo*ΔΔ::pCDR1 TLO2. The image (hierarchical clustering) was created using Agilent GeneSpring GX v11.5 (Agilent Technologies Inc).

CdTLO1 resulted in a marked increase in expression of both *SOD5* which was up-regulated 3-fold and *SOD6* which was up-regulated 1.5-fold. The re-introduction of *CdTLO2* resulted in a slight increase in expression of *SOD5* in comparison to the *CdTLO* mutant and less of an increase in *SOD6* expression. *CFL2,* an oxidoreductase involved in iron utilisation and *FRE7,* a ferric reductase with a role in oxidation-reduction processes are two genes that were also down-regulated in the absence of the *CdTLO*s and up-regulated (6-fold and 3.5-fold respectively in the presence of *CdTLO1* and 2.6-fold and 1.7-fold respectively upon re-introduction of *CdTLO2)* when the *CdTLO*s were re-introduced. Interestingly, in addition to the positive effect of the *CdTLO*s on the expression of genes involved in oxidative stress response, genes that appear to be negatively regulated by the *CdTLO*s were identified. In the absence of the *CdTLO*s *SOD1* and *SOD4* were up-regulated in comparison to wild type and upon re-introduction of the *CdTLO*s, expression of these genes decreased significantly. This observation was true for a number of genes, namely *CIP1;* an oxidoreductase, *AMO2;* a copper amino oxidase involved in oxidation-reduction reactions, *AHP1;* an alkyl hydroperoxide reductase with a role in oxidative stress response and *IFR2;* a zinc-binding dehydrogenase involved in oxidation-reduction. In the absence of the *CdTLOs* an up-regulation was observed in expression. Upon re-introduction of the *CdTLO* genes, expression was decreased in *CdTLO2* and even further decreased in *CdTLO1* in comparison to *Cdtlo*ΔΔ. *CAT1,* a gene encoding a catalase which provides vital intracellular antioxidant activity in response to oxidative stress (Wysong *et al.,* 1998) was also up-regulated in the absence of the *CdTLO*s, with a 3-fold increase in expression observed, with a 1.5-fold decrease upon re-introduction of *CdTLO1* and a 1-fold decrease upon re-introduction of *CdTLO2.* Since it has been shown phenotypically that the absence of the *CdTLO*s affects oxidative stress response, and the re-introduction of *CdTLO1* and *CdTLO2* restores this phenotype, it suggests that the up-regulation of genes such as *SOD1, SOD4, CAT1* and *AMO2* is not sufficient to reverse the phenotypic effect of reducing expression of genes such as *SOD5* and *SOD6.*

3.3.7.3. Galactose utilisation

Work previously carried out in our lab by Haran *et al.* (2014) identified that in the absence of both *CdTLO* genes a number of genes involved in the metabolism of galactose were found to be differentially expressed compared to Wü284 in the early stages of hyphal growth (Figure 3.12 (B)). These include the *GAL* genes; *GAL1* encoding a galactokinase, involved in galactose transport and catabolism; *GAL7* which codes for a galactose-1-phosphate uridylyl transferase and functions in the catabolism of galactose and *GAL10*; which codes for a UDP-glucose 4-epimerase required for the utilisation of galactose (Marthchenko *et al.*, 2007; Slot and Rokas, 2010). All three *GAL* genes were expressed at significantly lower levels in *Cdtlo*ΔΔ compared to Wü284 in 1 h serum, and it was also previously observed that the *Cdtlo*ΔΔ mutant exhibited a slower growth rate in galactose-based growth medium in comparison to Wü284. This study found that the re-introduction of *CdTLO1* resulted in a dramatic increase in the expression of *GAL1, 7* and *10* with fold changes of 6.1, 5.7 and 12.7 respectively observed. The re-introduction of *CdTLO2* also resulted in the up-regulation of the *GAL* genes, albeit to a lesser extent than the levels of *CdTLO1.*

Other genes involved in carbohydrate metabolism were also affected by the deletion of both *CdTLO* genes. *SGA1,* a glucoamylase involved in glycogen metabolism, *TYE7,* a transcription factor involved in glycolysis control, *GSY1,* a UDP glucose/starch glycosyltransferase involved in glycogen biosynthesis and *PFK2,* a phosphofructokinase were all found to be down-regulated in the absence of the *CdTLO*s. Expression increased considerably in the presence of *CdTLO1* and increased to a lesser extent in the presence of *CdTLO2. SGA* expression was up-regulated 4.5-fold and 2-fold in the presence of *CdTLO1* and *CdTLO2* respectively. *TYE7* expression was increased 6-fold in the presence of *CdTLO1* and increased 2.7-fold in the presence of *CdTLO2. GSY1* and *PFK2* were up-regulated 2.3-fold and 3-fold in the presence of *CdTLO1* respectively, and both were up-regulated 1-fold in the presence of *CdTLO2. PCK1,* a phosphoenolpyruvate carboxykinase involved in gluconeogenesis was down-regulated in

*Cdtlo*ΔΔ. In the presence of *CdTLO1* expression increased 3-fold, but in the presence of *CdTLO2, PCK1* remained down-regulated, suggesting *CdTLO1* regulates *PCK1. SCW11,* encoding a cell wall protein with a role in carbohydrate metabolism showed decreased expression in the absence of the *CdTLOs.* Expression increased in the presence of *CdTLO1* was increased even more in the presence of *CdTLO2. GCA1,* which encodes an extracellular glucoamylase involved in starch degradation and is regulated by galactose concentration, was expressed at very high levels in the absence of the *CdTLOs* versus the wild type strain, with a 9-fold increase in expression observed. The re-introduction of *CdTLO1* and *CdTLO2* resulted in a respective 2-fold and 1.6-fold decrease in expression of *GCA1.*

3.3.8. Quantitative Real Time-PCR of selected genes

In order to confirm the findings of the re-integrated *CdTLO1* and *CdTLO2* DNA microarray studies, quantitative real time PCR (qRT-PCR) was carried out as described in Section 2.3.4. A selection of genes that represent key data sets within the microarray results were analysed by qRT-PCR. *ACT1* was the endogenous control used in this study. The genes quantified by qRT-PCR in this study were *GAL10, SOD5, RBT5, UME6, HWP1* and *EED1.* In conjunction with confirming DNA microarray results, the levels of expression for each gene were measured over a time course of 0 min, 30 min, 60 min and 180 min in order to observe whether an increase in time impacted the expression levels of these genes in each strain. In the case of the t0 samples, the cells used were from overnight 30 °C cultures without incubation in water supplemented with 10% (w/v) fetal bovine serum (FBS). For the remaining three time points the RNA samples were prepared as described in Section 2.3.3 with incubation times of 30 min, 60 min and 180 min in water supplemented with 10% (w/v) FBS. Although much of the array data were confirmed, some discrepancies were identified.

3.3.9. qRT-PCR to confirm DNA microarray findings

3.3.9.1. GAL10

The expression patterns of *GAL10* at 60 min in the *Cdtlo*ΔΔ mutant and *CdTLO1* the *Cdtlo*ΔΔ mutant background correlate with the expression profiles found in the microarray. However, the qRT-PCR data suggest *GAL10* expression is lower in *CdTLO2* than in *Cdtlo*ΔΔ, as was observed in the microarray data [Figure 3.13 (A)]. With regards to the time-course experiment the expression of *GAL10* in the *Cdtlo*ΔΔ mutant and reintegrated *CdTLO1* appeared to increase with cell density [Figure 3.13 (A)]. The levels of *GAL10* expression in reintegrated *CdTLO2* however, were more varied. At time zero, the expression of *GAL10* in *CdTLO2* was higher than that of the *Cdtlo*ΔΔ mutant, with a decrease in expression observed at 30 min and 60 min. Expression increased at 180 min but was still lower than the levels of *Cdtlo*ΔΔ and reintegrated *CdTLO1*.

3.3.9.2. SOD5

The expression patterns of *SOD5* at 60 min in the three strains correlated with what was found in the microarray expression profiles of *SOD5* [Figure 3.13 (B)]. In the qRT-PCR time-course experiment the expression levels of *SOD5* in the *Cdtlo*ΔΔ mutant, reintegrated *CdTLO1* and *CdTLO2* were observed to increase with increasing cell density [Figure 3.13 (B)].

3.3.9.3. RBT5

The expression levels of *RBT5* at 60 min correlated somewhat with the microarray data, as *RBT5* expression in reintegrated *CdTLO1* was higher than in the *Cdtlo*ΔΔ mutant. However, according to the microarray data, *RBT5* expression in the *CdTLO1* reintegrant was higher than in reintegrated *CdTLO2*, which was not observed in the qRT-PCR data [Figure 3.13 (C)]. No significant pattern was observed in the expression of *RBT5* in each strain throughout the qRT-PCR time-course experiment [Figure 3.13 (C)]. In the *Cdtlo*ΔΔ mutant, expression drops at 60 min and then increases significantly at 180 min. In the reintegrated *CdTLO1* strain the

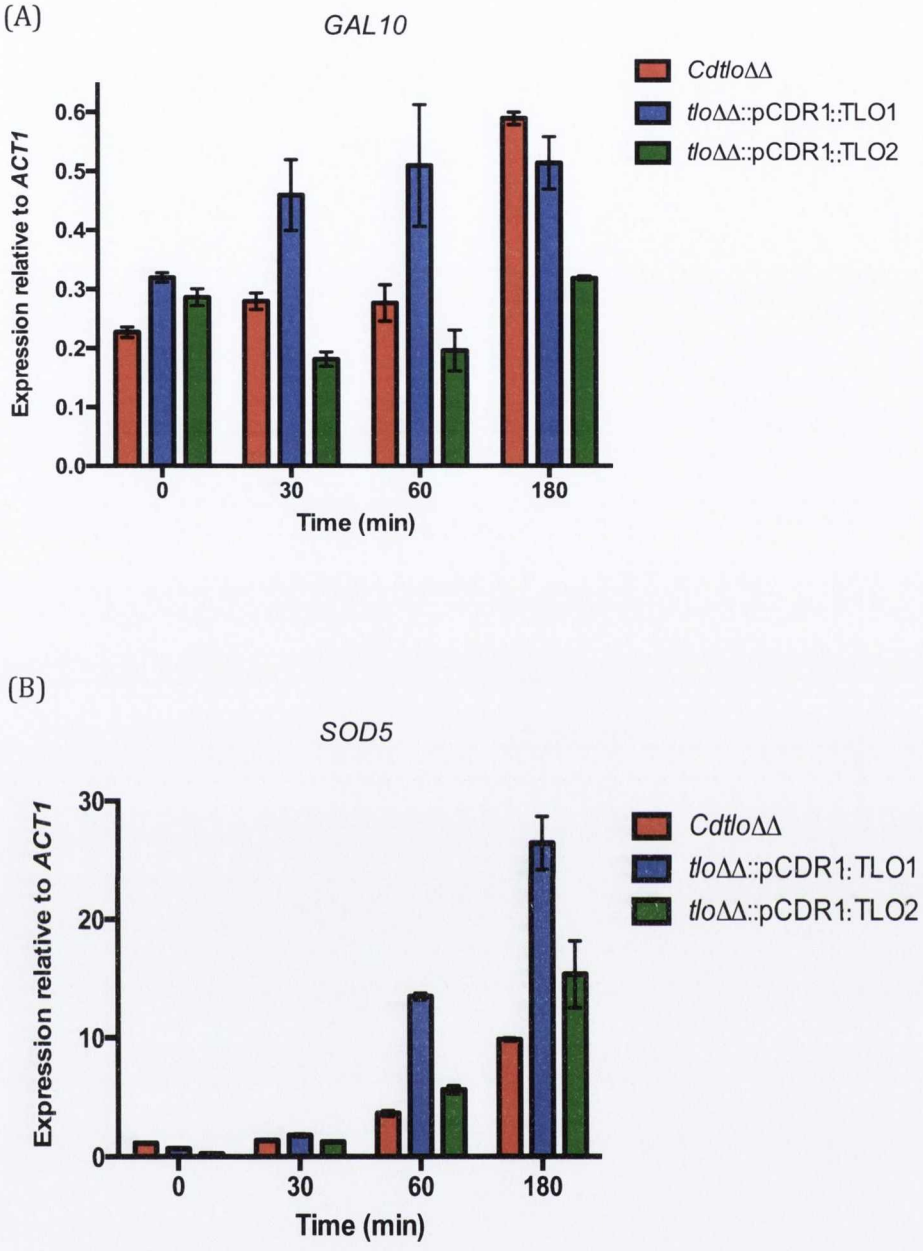

Figure 3.13. qRT-PCR experiments of gene expression in *CdtloΔΔ* and re-integrated *CdTLO1* and *CdTLO2*. Results are interpreted and displayed relative to *ACT1* expression. Values displayed represent $2^{-\Delta CT}$ values. Graphs show expression of **(A)** *GAL10*, **(B)** *SOD5*, **(C)** *RBT5*, **(D)** *UME6*, **(E)** *HWP1* and **(F)** *ECE1* in the absence and re-introduction of the *TLOs*. Error bars represent the standard error of the mean (SEM) of three replicates.

(C)

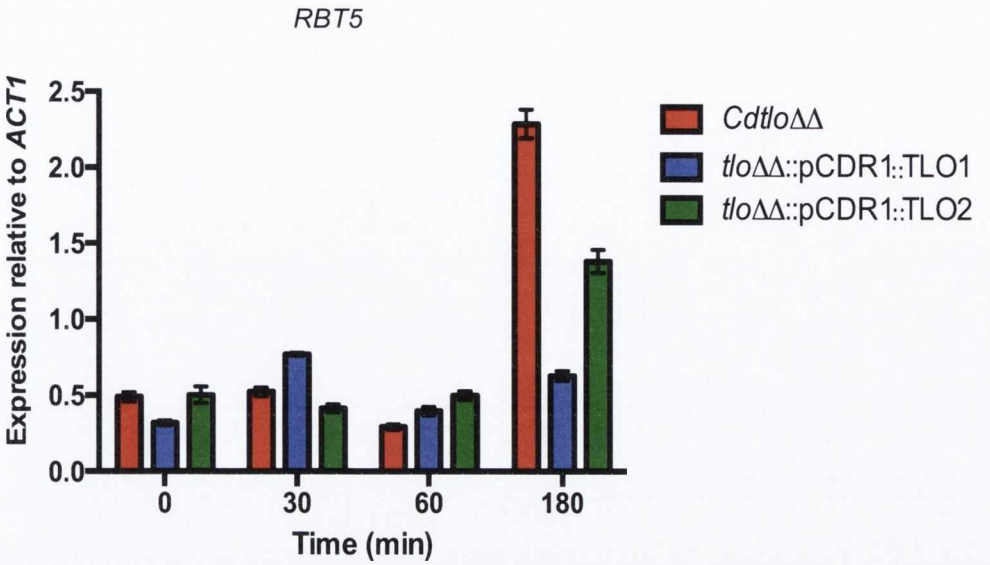

(D)

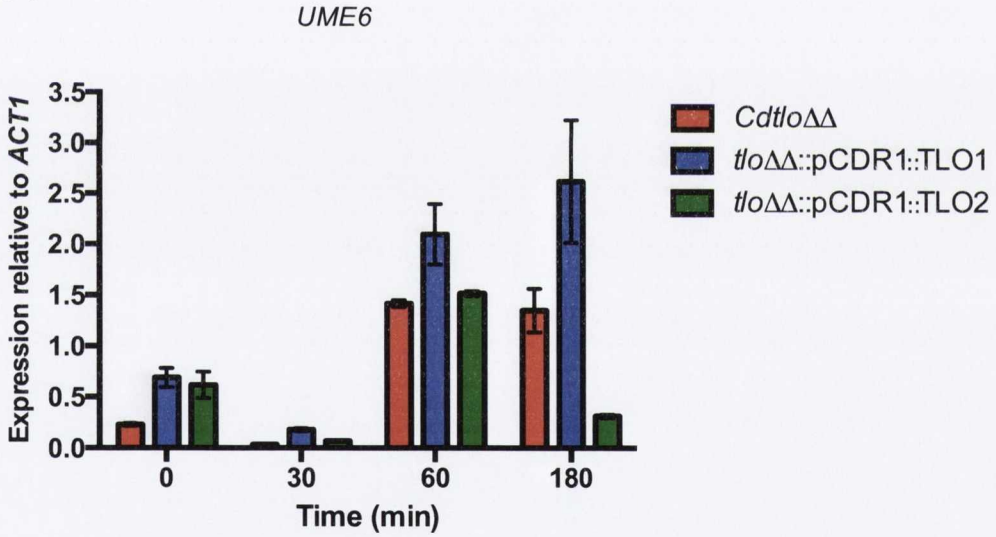

Figure 3.13. continued.

(E)

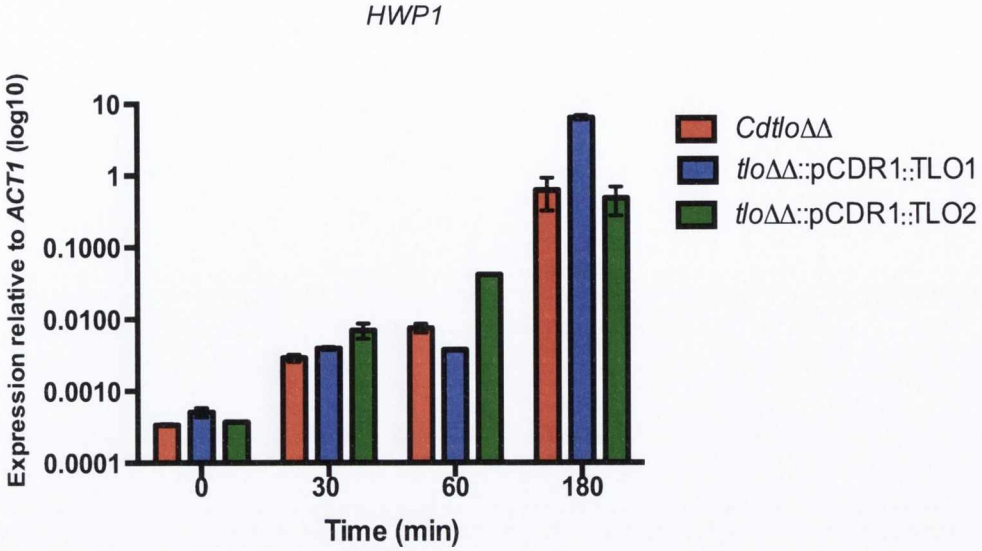

(F)

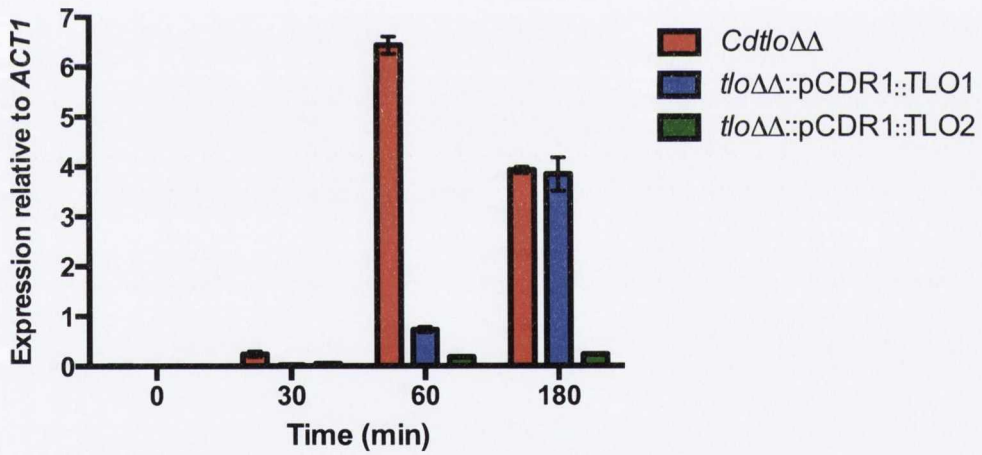

Figure 3.13. continued.

expression of *RBT5* is increased slightly at 30 min, dropped slightly at 60 min, then increased again at 180 min. In the reintegrated *CdTLO2* strain the expression of *RBT5* did not vary significantly over the first three time points but showed an increase at 180 min. According to the qRT-PCR data the expression of *RBT5* is higher in *Cdtlo*ΔΔ and in *CdTLO2* than in *CdTLO1* at 180 min.

3.3.9.4. UME6

The 60 min expression profiles for *UME6* agreed with the results of the microarray studies [Figure 3.13 (D)], as *UME6* expression was observed to be higher in the *CdTLO1* reintegrant than in the *Cdtlo*ΔΔ mutant and than in reintegrated *CdTLO2*. With regards to the time-course experiment the expression levels of *UME6* dropped in all three strains at 30 min but increased at 60 min and 180 min [Figure 3.13 (D)]. At 180 min expression of *UME6* in the *CdTLO2* reintegrant dropped while in the *Cdtlo*ΔΔ mutant and in the reintegrated *CdTLO1* strain expression of *UME6* remained higher.

3.3.9.5. HWP1

The expression patterns of *HWP1* in the *Cdtlo*ΔΔ mutant, the *CdTLO1* reintegrant and the *CdTLO2* reintegrant did not correlate with what was found in the microarray expression profiles of *HWP1* [Figure 3.13 (E)]. According to the qRT-PCR results at 60 min expression of *HWP1* is higher in the *Cdtlo*ΔΔ mutant than in reintegrated *CdTLO1*. However, the microarray results suggest that *HWP1* is down-regulated significantly in the absence of the *CdTLO*s, up-regulated notably in the presence of *CdTLO1* and up-regulated even further in the presence of *CdTLO2*. The expression levels of *HWP1* in each strain were noted to increase as cell density increased throughout the time course experiment [Figure 3.13 (E)].

3.3.9.6. ECE1

ECE1 was up-regulated in the absence of the *CdTLOs* in DNA microarray studies. The re-introduction of *CdTLO1* and *CdTLO2* resulted in a significant decrease in the expression of *ECE1*. These findings were confirmed by the expression analysis of *ECE1* by qRT-PCR, given that at 60 min, expression of *ECE1* was higher in the *Cdtlo*ΔΔ mutant than in reintegrated *CdTLO1* and *CdTLO2* [Figure 3.13 (F)]. In the qRT-PCR time-course the expression levels of *ECE1* in each strain increased as cell density increased [Figure 3.13 (F)].

The expression analysis time-course experiments carried out in this study suggest that the absence of the *CdTLO* genes may retard gene expression, rather than resulting in a complete impediment of gene expression.

3.4. Discussion

3.4.1. DOX-inducible *CdTLO1* and *CdTLO2* in the *Cdtlo*ΔΔ background

It has been proposed that the *TLO* gene family may contribute to the significant disparity in virulence between these two otherwise extremely closely related species (Jackson *et al.*, 2011). As previously mentioned, experiments carried out in our laboratory have shown that the homozygous deletion of both *TLO1* and *TLO2* in *C. dubliniensis* results in a range of effects including the inhibition of true hyphal formation, increased sensitivity to oxidative stress induced by H_2O_2 and poor growth in the presence of alternative carbon sources (i.e. galactose). The aim of this section of the study was to investigate the functions of the Tlo family of proteins by reintroducing the *Candida dubliniensis TLO* genes into the *C. dubliniensis TLO* double mutant (*Cdtlo*ΔΔ).

It was initially planned to attempt to overexpress *CdTLO1* and *CdTLO2* in a *Cdtlo*ΔΔ background using the pTet DOX-inducible promoter to observe if overexpression resulted in an alteration in phenotype. In addition, previous studies in our lab re-integrated *CdTLO1* and *CdTLO2* into the *Cdtlo*ΔΔ double mutant under the control of their native promoter in the pCDRI plasmid. Both sets of reintegrants were found to have identical phenotypes. The mRNA expression levels of the *CdTLO*s in both sets of reintegrants were measured and compared to wild type. As seen in Figure 3.3, *CdTLO1* was expressed 2-fold higher in wild type than in both the pTet and pCDRI *CdTLO1* reintegrant. This may be explained by the presence of two copies of *CdTLO1* in Wü284 as opposed to one copy of *CdTLO1* in the reintegrants. Interestingly, while wild type and pTet-*CdTLO2* expression levels were similarly low, the expression of *CdTLO2* in the pCDRI reintegrant was fifteen times higher, and significantly higher than *CdTLO1* expression in all strains. This difference in expression despite the use of the native promoter was surprising, and demonstrates the effect of reintegration location on gene expression (Storey *et al.*, 2005).

However, despite the low expression level of *CdTLO2* in the pTet-*CdTLO2* reintegrant, an identical phenotype was observed to that of the pCDRI-*CdTLO2*. This suggests that regardless of how highly *CdTLO2* is expressed, it will not alter the phenotype as significantly as *CdTLO1*. Many cellular functions are carried out by proteins, and therefore functionally important alterations in transcript levels are expected to be reflected in changes in the levels of corresponding proteins. However, various mechanisms of post-transcriptional regulation can either moderate changes in transcript abundance so that they do not lead to changes in protein abundance or alter protein abundance in the absence of a corresponding effect on transcripts (Gygi *et al.*, 1999; Foss *et al.*, 2007). This could also explain why the higher expression of *CdTLO2* does not result in a more significant transcript profile. Given that the DOX-inducible reintegrants behaved identically to the *CdTLO1* and *CdTLO2* reintegrants under the control of their native *CDRI* promoter, and the higher expression level observed for *CdTLO2* in the pCDRI reintegrant, the native promoter reintegrants were used for DNA microarray studies. Use of these mutants precluded the use of DOX in the microarray experiments, which may have had an effect on global gene expression.

3.4.2. Effect of *CdTLO1* and *CdTLO2* on true hypha formation and genes with hyphal and cell wall functions

It was observed that the presence of *CdTLO1* and *CdTLO2* restored the ability to form true hyphae. The reintroduction of *CdTLO1* had a more positive effect on the formation of true hyphae, with near wild type levels being formed. This is in agreement with the observation that the null mutant of *CdTLO1* resulted in a more significant reduction in the formation of hyphae compared to a *CdTLO2* mutant (Haran *et al.*, 2014). The reintroduction of *CdTLO2* resulted in 45%-50% true hyphae being formed after 4 h. This was reflected to a certain extent in the expression profiles of the *CdTLO* reintegrant DNA microarray experiment, which was carried out in order to examine if CdTlo1 and CdTlo2 differ in their functionality.

Transcriptomic analysis using *C. dubliniensis* microarrays revealed that following down-regulation in the absence of both *CdTLO*s, the majority of genes involved in filamentation and cell wall functions appear to be more highly expressed upon re-introduction of *CdTLO1* than *CdTLO2*, even though *CdTLO2* is more highly expressed than *CdTLO1* in the reintegrants. These genes include regulators of filamentation such as *RIM101, EFG1* and *UME6* (O'Connor *et al.,* 2010). This, along with phenotypic data would suggest that *CdTLO1* plays a more important role in hyphal formation, a major virulence factor associated with *Candida* species. However, it should be noted that a number of genes appear to be more highly expressed in the presence of *CdTLO2.* These include cell wall and hypha-specific genes *HWP1, DSE1* and *EAP1*, while *CdTLO2* also up regulates hyphal regulators *TEC1* and *RAS1* to a greater extent. The observation that some genes are more highly expressed in the presence of *CdTLO2* could be due to the fact that qRT-PCR studies revealed that *CdTLO2* expression was higher than *CdTLO1* expression. This is particularly interesting given that *CdTLO1* restores hyphal formation more efficiently than *CdTLO2* when reintroduced to the *Cdtlo*ΔΔ mutant.

In general terms of expression, comparisons of genes commonly up-regulated and down-regulated in the serum dataset between *CdTLO1* and *CdTLO2* yielded an overlap of just 58 genes out of 696 and 95 genes out of 718 respectively, which suggests that the *CdTLO* genes carry out different functions and our data suggest the two Tlo proteins may differ in their levels of expression and/or their efficiency. Some unexpected results were found with regards to a number of genes associated with hyphae. *EED1* and *ECE1* were both up-regulated in the *Cdtlo*ΔΔ mutant, even though this mutant cannot form true hyphae, and were down-regulated when *TLO1* and *TLO2* were reintroduced, when the ability to form hyphae was restored. *ECE1* codes for a protein involved in cell elongation and *EED1* encodes a protein with a role in hyphal extension (Martin *et al.,* 2011). Both genes are required for hyphal formation, therefore it seems unusual that they are down-regulated in the presence of *CdTLO1* and *CdTLO2*, given that the *CdTLO*s have the ability to restore hyphal formation.

However, hyphal induction is regulated by a number of complex pathways, and as we have not yet elucidated the role of the *TLO*s in morphogenesis, it is difficult to determine why hyphal specific genes such as *EED1* and *ECE1* are affected in this manner.

Hyphal induction is regulated by a series of complex pathways, and morphogenesis and filamentation are impacted by a range of environmental factors such as temperature, pH, serum and low nitrogen sources (Sudbery, 2001). In a recent review, Sudbery (2011) outlined the key genes involved in the formation of hyphae in *C. albicans*. Positive regulation is attributed to a number of transcription factors, such as Efg1, Tec1 and Rim101. Efg1 is thought to be the main positive regulator necessary for the formation of hyphae under most conditions (Braun and Johnson, 2000) and is activated by the cAMP pathway, which is stimulated by Ras1 (Feng *et al.*, 1999; Leberer *et al.*, 2001). *TEC1, RAS1, RIM101* and *EFG1*, which were all down-regulated in the absence of the *CdTLO*s, were up-regulated upon reintroduction of *CdTLO1* and *CdTLO2*. Temperature increase is a known hyphal inducer, and is mediated by heat shock protein 90 (Hsp90), which inhibits Ras1. *HSP90* was up-regulated in the absence of the *CdTLO*s, and down-regulated massively in the presence of *CdTLO1*, with only a slight decrease in expression in the presence of *TLO2*. *UME6* and *EED1* were among the genes stated to have a vital role in hypha formation in *C. albicans* (Banerjee *et al.*, 2008; Martin *et al.*, 2011). However, both are differentially regulated in *Cdtlo*ΔΔ compared to Wü284, and in *Cdtlo*ΔΔ compared to *CdTLO1* and *CdTLO2*. These data suggest that the Tlos play an important role in the global control of positive and negative regulators of morphogenesis. Another possible role of the *CdTLO* genes could be rapid induction of gene activation, given that the time-course qRT-PCR shows that the expression of a number of genes in the *Cdtlo*ΔΔ mutant increases over time and eventually match wild type levels. This suggests that the *Cdtlo*ΔΔ mutant reduces the efficiency of gene expression, rather than preventing it completely.

3.4.3. Effect of *CdTLO1* and *CdTLO2* on growth in the presence of H_2O_2 and genes involved in oxidative stress response

Reactive oxygen species (ROS) are a key component in the phagolysosome, and play an important role in the destruction of invading microorganisms. The production of ROS is initiated in phagocytes through the assembly and activation of nicotinamide adenine dinucleotide phosphate (NADPH) oxidase, resulting in oxidative burst being triggered (Frohner *et al.*, 2009). To combat the effects of superoxide radicals, *Candida* spp. express superoxide dismutases (Sods) that convert superoxide radicals to H_2O_2, which is in turn converted to H_2O by catalase (Martchenko *et al.*, 2004). *Candida* species express six *SOD* genes encoding Cu-dependent Sod1, Sod4, Sod5 and Sod6, and the Mn-dependent Sod2 and Sod3. *SOD1* and *SOD5* play a role in the pathogenesis of *C. albicans*, with *SOD5* known to have a role in osmotic and oxidative stress response, as well as a role in the transition of yeast to hyphae (Martchenko *et al.*, 2004). Interestingly, microarray analysis revealed that the *SOD* genes were differentially expressed in the *Cdtlo*ΔΔ mutant compared to wild type, with *SOD* genes 1-4 down-regulated in the absence of the *CdTLO*s and *SOD5* and *SOD6* up-regulated in their absence. It is possible that *SOD1*, *SOD3* and *SOD4* may be up-regulated in order to compensate for the down-regulation of *SOD5* and *SOD6*, however this compensation is not enough to reverse the poor growth of the *Cdtlo*ΔΔ mutant in the presence of oxidative stress induced by H_2O_2. According to microarray analysis, *SOD5* and *SOD6* are differentially expressed between *CdTLO1* and *CdTLO2*, with significant up-regulation of both observed in *CdTLO1* only. This could explain why *CdTLO1* restores growth under oxidative stress better than *CdTLO2*.

3.4.4. Effect of *CdTLO1* and *CdTLO2* on growth in an alternative carbon source and genes involved in carbohydrate metabolism

Previous growth rate experiments carried out in our laboratory observed that the *Cdtlo*ΔΔ mutant appeared to grow slowly in the presence of galactose as the main carbon source,

which suggested a difficulty in the utilisation of galactose. The reintroduction of *CdTLO1* resulted in an increase in the growth rate to nearer wild type levels; while growth remained slow upon the reintroduction of *CdTLO2,* even though it is expressed more highly than *CdTLO1.* The *Cdtlo*ΔΔ mutant growth impairment in the presence of galactose was supported by DNA microarray studies. It was found that in the absence of the *CdTLO* genes, key genes involved in galactose utilisation such as *GAL1, GAL7* and *GAL10* were down-regulated. These genes were up-regulated upon reintroduction of *TLO1* (to a greater extent) and *TLO2.*

Previous studies in our laboratory found that as well as growing poorly on media containing alternative carbon sources, the *Cdtlo*ΔΔ mutant doubling time was increased by almost 50% in Lee's medium (Lee *et al.,* 1975). Lee's medium is a synthetic, minimal medium comprised of amino acids, inorganic salts and glucose, but lacks the nutrient-rich yeast extract of YEPD and YEP-Gal, which further suggests a role for the Tlos in general metabolism. A vital characteristic of pathogens is metabolic flexibility. In order for virulent microorganisms to grow in a wide range of hosts, they must be able to assimilate a variety of carbon sources (Askew *et al.,* 2009).

The ability of organisms to utilise galactose as a sugar source is enabled through the Leloir pathway (Martchenko *et al.,* 2007). The inability of the *Cdtlo*ΔΔ mutant to grow successfully in the presence of galactose may be attributed to the down-regulation of the *GAL* genes in the absence of the *CdTLO*s. Interestingly, *GAL10,* the epimerase that catalyses the third step of the Leloir pathway (Figure 3.14) has been associated with a range of important traits in *C. albicans* such as filamentation, cell wall properties and oxidative stress (Singh *et al.,* 2007; Sen *et al.,* 2011). Gal4 regulates galactose-metabolising genes in *Saccharomyces cerevisiae,* and serves as a transcriptional activator. It was previously thought that transcriptional regulation by Gal4 was conserved between *S. cerevisiae* and *Candida* spp. However, Martchenko *et al.* (2007) identified rewiring of the regulation mechanisms between *S.*

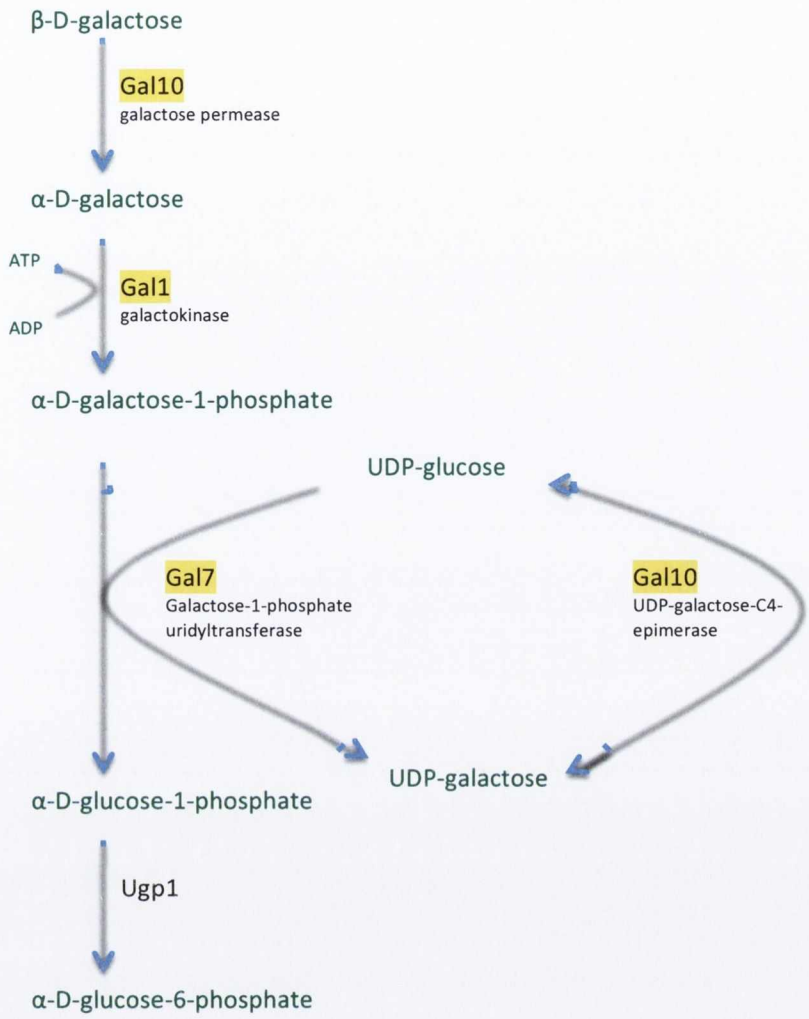

Figure 3.14. Schematic diagram of the Leloir (galactose degradation) pathway in *Candida albicans,* and, by homology, *Candida dubliniensis.* Products are shown in green. Genes are highlighted in yellow and their encoded enzymes are underneath. Diagram adapted from publications by Singh *et al.* (2007) and Holden *et al.* (2003).

cerevisiae and *C. albicans*. They found that Cph1 (a filamentous regulator) regulates *GAL10* in *C. albicans*, as opposed to being regulated by Gal4 as in *S. cerevisiae*. The same study showed that the *C. albicans TLO* promoter regions contain a Gal4 protein-binding site and suggests that *GAL4* is involved in *TLO* gene regulation. The *C. albicans TLO* genes were expressed at lower levels when *GAL4* and its *TLO* binding site were deleted (Martchenko *et al.* 2007). These findings, in conjunction with our data in which the *GAL* genes are down-regulated in the absence of the *CdTLO* genes could lead to the possibility that the Tlos may be involved in a Gal4-mediated alternative regulatory circuit that may indirectly activate *GAL10* expression, via the *TLO* genes. Furthermore, data in this study has revealed that although the reintroduction of *CdTLO1* and *CdTLO2* results in an increase in expression of the *GAL* genes, expression is higher in the presence of *CdTLO1* and the slow-growing phenotype is more successfully reversed by *CdTLO1*, which suggests that *CdTLO1* may be more important in this hypothetical alternative regulatory circuit than *CdTLO2*.

3.4.5. Closing remarks

From the phenotypic and microarray data generated in this section of the study it is apparent that the absence of the *TLO*s has a significant effect on the phenotype and transcriptome of *C. dubliniensis*. Our data suggest that with regards to the expression of genes down-regulated in the absence of the *CdTLO*s, it seems that CdTlo1 has a greater capacity to affect global gene expression, which is reflected in its greater capacity to restore hypha formation. This transcriptional analysis of the *CdTLO1* and *CdTLO2* reintegrated strains demonstrates functional diversification of the Tlo proteins and suggests that different Tlos can regulate distinct subsets of genes. qRT-PCR was used to confirm a selection of genes from the microarray analysis that were significantly up- or down-regulated in the presence of *CdTLO1* and *CdTLO2*. Of the six genes selected four confirmed the microarray findings. The lower correlation between the microarray and qRT-PCR for *GAL10* and *HWP1* may be due to the effects of greater variability associated with decreased reaction efficiencies found in qRT-PCR

measurements at later cycles, where genes with low expression levels respond (Morey *et al.*, 2006). In terms of what the Tlo proteins are actually doing it seems that they play an important role in maximising the speed and scale of transcriptional changes in response to environmental cues, with CdTlo1 having a greater effect than CdTlo2. This characteristic is likely to be of great importance in the host where rapid responses could be important for survival, e.g. following phagocytosis or translocation (Haran *et al.*, 2014).

Chapter 4

Deletion of *MED3* in *C. dubliniensis* Wild Type and in *Cdtlo*ΔΔ and Comparative Analysis of the *CdMED3* and *CdTLO* mutant strains

4.1. Introduction

4.1.1. Analysis of Mediator subunits in yeast species

The conserved Mediator complex interacts directly with RNA polymerase II (Pol II) to control the recruitment of Pol II to target genes and its role in transcription initiation and elongation (Conaway & Conaway, 2011). van de Peppel *et al.* (2005) investigated the role of individual subunits of Mediator in *Saccharomyces cerevisiae* by generating null mutants for the 15 subunits that have been previously described in the literature as non-essential and comparing them using DNA microarrays, with the expression profiles used as a molecular phenotype. Hierarchical clustering of their data revealed three distinct groups which are summarised in Table 4.1: (i) Subunits whose deletion decreased transcript levels, e.g. tail subunits Med15, Med3 and Med2, head subunits Med20 and Med18, and middle subunit Med31; (ii) subunits whose deletion resulted in increased transcript levels, e.g. Cdk subunits Cdk8, CycC, Med12 and Med13 and (iii) head subunit Med19 and subunits whose deletion appears to have no effect, e.g. middle subunits Med5, Med1, Med9 and tail subunit Med16 (van de Peppel *et al.*, 2005). It was previously observed by Myers *et al.* (1998) that in *S. cerevisiae* the incorporation of Med3 and Med15 requires the presence of Med2, which explains the findings that van de Peppel *et al.* (2005) observed where *med2*Δ, *med3*Δ and *med15*Δ mutants had very similar expression profiles.

In 2008, Linder *et al.* conducted a comparative analysis of Mediator in the model yeasts *S. cerevisiae* and *Schizosaccharomyces pombe* that revealed high levels of conservation of the roles of Mediator despite the phylogenetic divergence of the two species. Conserved functions include a broad role in stress responses and distinct, specific roles in the regulation of cell wall dynamics and cell morphology; a role also conserved among plant and animal pathogens such as *Cryptococcus neoformans, Candida albicans* and *Fusarium* spp. (Linder *et al.*, 2008). The head and middle domains are required for the expression of cytokinesis genes

under the control of Ace2, (Linder *et al.,* 2008; Lenstra *et al.,* 2011). In *C. glabrata,* the tail subunit Med15 has a conserved role with *S. cerevisiae* in drug resistance mediated by the transcription factor Pdr1 (Thakur *et al.,* 2008; Paul *et al.,* 2011).

A number of other studies have focused on dissecting the Mediator complex. Deletion of the gene encoding Med17 in the head module in *S. cerevisiae* results in rapid loss of transcription of most transcribed genes, while loss of individual tail subunits results in variable effects on transcription (Thompson & Young, 1995; Holstege *et al.,* 1998; van de Peppel *et al.,* 2005). A study carried out by Ansari *et al.* (2012) where the genes encoding the tail subunits Med2, Med3 and Med15 were disrupted in *S. cerevisiae,* observed a range of effects of the deletions on the transcriptome. Genes involved in transport and metabolism of diverse nutrients and metabolites such as drug molecules, carbohydrates, amino acids, metal ions as well as stress response genes showed decreased expression. Ansari *et al.* hypothesised that the subunits of the tail module may regulate the expression of genes with roles in diverse metabolic pathways by direct or indirect interaction with their transcriptional activators.

Zhang *et al.,* (2012) also examined the deleterious effect of *MED3* in *C. albicans* in relation to its effect on the stability of the tail and the effect on the Ca*TLO*s, which will be discussed further in the discussion section of this chapter. In 2012, Uwamahoro *et al.* investigated Mediator functions in *C. albicans* by making homozygous deletions of the gene encoding the middle domain subunit Med31 and the gene encoding the head domain subunit Med20. Both subunits were found to be required for the yeast to hyphal transition and for biofilm formation, two important virulence traits of *C. albicans* (Uwamahoro *et al.,* 2012; Zhang *et al.,* 2012). It was also observed that Med31 is required for *ALS1* and *ALS3* expression, genes encoding cell-surface proteins involved in biofilm formation. Med31 is also required for the expression of genes regulated by the transcription factor Ace2, which regulates genes involved in cell wall remodelling during cell separation (Haran *et al.,* 2014).

	Tail	Middle	Head	Cdk
Deletion=↓ transcript levels	Med15 Med2 Med3	Med31	Med20 Med18	-
Deletion=↑ transcript levels	-	-	Med19	Cdk8 CycC Med12 Med13
Deletion= no effect on transcript levels	Med16	Med5 Med1 Med9	-	-

Table 4.1. Summary of the effect of the deletion of Mediator subunits on the transcriptome of *Saccharomyces cerevisiae.* Adapted from van de Peppel *et al.,* (2005).

4.1.2. Gene deletion in *Candida* spp.

A commonly used approach in assessing gene function is to use targeted mutagenesis to inactivate the gene of interest. Molecular gene disruption in *Candida* spp. is difficult for a number of reasons. The diploid nature of *Candida* spp. means that in most cases two alleles of a gene must be manipulated (Samaranayake & Hanes, 2011). In comparison to *S. cerevisiae*, *C. albicans* lacks natural plasmids such as the 2-micron plasmid for use in transformation, and lower transformation and recombination frequencies make homozygous manipulation even more challenging (De Backer *et al.*, 2000; Magee *et al.*, 2003). *C. albicans* also utilises non-conventional codon usage where the CUG codon is decoded as serine, rather than leucine (Santos and Tuite, 1995). Therefore, when marker gene sequences from other organisms are used for gene manipulation in *C. albicans*, the codons need to be optimised. Furthermore, the use of selectable markers remains a challenge given that some markers affect the virulence of *Candida* spp. Additionally, *C. albicans* shows natural resistance to drugs such as hygromycin B, G418 and cycloheximide, which are used for selection in *S. cerevisiae* (De Backer *et al.*, 2000).

4.1.3. Gene deletion strategies

4.1.3.1. The URA3 selective marker

Fonzi & Irwin (1993) targeted the *URA3* gene encoding an orotidine-5-phosphate decarboxylase in *C. albicans* to develop a method now referred to as the *URA3* blaster approach. This method was used to construct a homozygous *ura3Δ/ura3Δ* mutant strain that requires supplementation with uridine for normal growth (Negredo *et al.*, 1997; Wilson *et al.*, 2000). Therefore, complementation of *ura3Δ/ura3Δ* strain with DNA containing a *URA3* gene in addition to a gene or construct of interest enables selection of transformants on minimal media without uridine. It subsequently became evident that there are problems associated with the use of the *URA3* marker for genetic engineering. The expression level of the inserted *URA3* marker depends on the integration locus, and since uridine auxotrophy results in

reduced virulence in *C. albicans*, the *URA3* marker is not suitable for the analysis of virulence and virulence-associated traits (Cole *et al.*, 1995; Lay *et al.*, 1998; Bain *et al.*, 2001; Sundstrom *et al.*, 2002; Cheng *et al.*, 2003). Given the challenges involved in utilising the *URA3* method, there have been many studies undertaken to find alternative selectable markers that do not affect fungal growth or virulence.

4.1.3.2. The MPA marker

The first dominant selection marker used for targeted integration in *C. albicans* was the MPA^R marker that confers resistance to mycophenolic acid (MPA) (Wirsching *et al.*, 2000). Recycling of the selective marker was achieved by the construction of a gene deletion cassette, the MPA^R flipper, which also contains a *C. albicans*-adapted *FLP* gene (*CaFLP*) encoding the site-specific recombinase FLP, under control of the *SAP2* inducible promoter (Reuss *et al.*, 2004). Following the selection of transformants in which the MPA^R flipper has been inserted into one allele of the target gene, *FLP* expression is induced by growing the transformants in *SAP2*-inducing medium, which results in FLP-mediated excision of the cassette from the genome (Wirsching *et al.*, 2000). The MPA^R flipping method has been used successfully in a number of studies. However a drawback of the MPA^R flipping method is that selection of MPA-resistant transformants takes 5-7 days. Furthermore, given that the MPA^R marker is derived from the *IMH3* gene encoding the target enzyme of MPA, transformants can be generated by substitution of the *IMH3* locus by the MPA^R marker, though a high number of MPA-resistant transformants have the propensity to substitute the MPA^R marker for the genomic *IMH3* gene and do not contain the mutagenesis cassette. This results in a gene deletion strategy with a tedious screening process (Reuss *et al.*, 2004).

4.1.3.3. The SAT1 marker

Based on the previous generations of selectable markers with significant drawbacks, Reuss *et al.* (2004) generated the *SAT1* flipper method. This consisted of the combination of recycling

the FLP-mediated marker and the use of a new dominant selection marker, *SAT1* (streptothricin acetyltransferase), which confers resistance to nourseothricin, placed under the control of the *ACT1* promoter (Reuss *et al.*, 2004). The *SAT1* flipping method relies on the use of a cassette that contains a nourseothricin resistance marker for the selection of transformants and a *MAL2* promoter-*FLP* fusion that allows maltose induced expression of the FLP1 recombinase which allows for the excision of the cassette when grown in maltose. Due to the problems associated with other commonly used methods it was decided that the *SAT1* flipper method would be employed in this study to disrupt the *MED3* gene in *Candida dubliniensis*, which codes for a subunit of the tail region of the yeast Mediator complex.

4.1.4. Aims of this section of the study

At the outset of this study the discovery that the Tlos were components of Mediator had yet to be confirmed. We carried out a homozygous deletion of *MED3* to compare the phenotype of this mutant with the Cd*tlo*ΔΔ mutant and to investigate Med3 function in *C. dubliniensis.* We then studied the effects of the re-integration of a single wild-type *MED3* allele.

4.2. Specific materials and methods

4.2.1. Primer tail method of gene deletion using the *SAT1* cassette

In order to replace a gene of interest, the *SAT1* cassette was amplified from the plasmid pSFS2A as described by Wilson *et al.* (1999). In order to target the flanking regions of the gene, 80 base pairs of the 5' and 3' up- and downstream gene sequence were incorporated at the 5' end of the M13 primers (Table 2.2). The Expand High Fidelity Enzyme System (Roche Diagnostics) was used to amplify the *SAT1* cassette from pSFS2A by PCR. Upon amplification of the cassette, the 4.2 kb product was purified using the Genelute™ PCR Clean-Up Kit (Sigma Aldrich). The purified product was transformed into wild type strain *Candida dubliniensis* Wü284 by electroporation as described in Section 2.2.4. Correct integration of the cassette in nourseothricin resistant transformants was verified using the primer pair MED3_F/FLPR (Table 2.2).

4.2.2. Recovery of nourseothricin sensitive revertants with the *SAT1* flipper

In order to excise the cassette, the *SAT1*-flipper, which contains the *MAL2* promoter-*FLP* fusion that allows maltose-induced expression of the FLP1 recombinase was used. To recover nourseothricin sensitive revertants, transformants were grown in 2 ml Yeast Extract Peptone Maltose (YEPM) broth. Cultures were grown overnight at 30 °C in an orbital shaking incubator. Cells were then counted using a Neubauer haemocytometer (Merienfield glassware, Germany) and ~200 cells were spread on NAT_2 plates. Following overnight incubation at 37 °C plates exhibited resistant colonies (large colonies) and sensitive revertants (small colonies). The small colonies were subjected to genomic DNA extraction as described in Section 2.3.1. and the removal of the cassette confirmed by PCR using the primer pair MED3_DKO_F/MED3_DKO_R (Table 2.2). Upon confirmation, the *SAT1* flipper was recycled, and the transformation was repeated to disrupt the second gene copy, yielding 7

colonies. Deletion of both gene copies was confirmed by PCR using the primer pairs MED3_DKO_F/ MED3_DKO_R and MED3_INT_F/ MED3_INT_R (Table 2.2).

4.2.3. Complementation studies

In order to confirm the phenotype associated with deleting *MED3*, a single copy of the gene was reintroduced into the *med3Δ* strain to form a reintegrant. The primer pair MED3_notI_F/ MED3_sacII_R (Table 2.2) containing *Not*I and *Sac*II restriction sites were used to amplify a 1,169 bp fragment encompassing the *MED3* gene which was purified and ligated using the pGEM-T Easy Vector. Transformants were PCR screened using the MED3_notI_F/ MED3_sacII_R primer pair, plasmids were purified and five positive transformants were sequenced. Plasmid DNA from transformants was digested with *Not*I and *Sac*II, gel purified and then ligated to the digested pCDR1 plasmid and transformed in *E. coli* XL10 Gold electrocompetent cells. Positive transformants were identified by digestion with *Not*I and *Sac*II. A single positive transformant was selected and the plasmid linearised using *Nco*I. The linearised plasmid was transformed by electroporation into *CDR1* locus of *Cdmed3Δ* as described in Section 2.2.4. Positive transformants were subjected to genomic DNA extraction as described in Section 2.3.1. Positive transformants were identified by PCR using the primer pair MED3_notI_F/ MED3_sacII_R and correct integration of the plasmid into the *CDR1* locus was confirmed by PCR using the primer pair M13R/TAGR (Table 2.2).

4.3. Results

The results of this study have been published in part in the Haran *et al.* (2014) publication.

4.3.1. Utilisation of the primer-tail method for *CdMED3* knockout using the SAT1 cassette

One of the most effective methods for the identification of a gene function is to investigate the effect of the deletion on the phenotype of the organism. In order to investigate the association between the Tlos and the yeast Mediator complex we generated a homozygous deletion of the gene encoding the Mediator tail components Med3 in *Candida dubliniensis* using the *SAT1*-flipper cassette [Figure 4.1 (A), (B)]. To achieve the disruption of the *MED3* gene, 80 base pairs of the 5' and 3' up- and downstream gene sequence were incorporated at the 5' end of the M13 primers (Table 2.2), which were used to amplify the *SAT1* cassette (4.2 KB) from the pSFS2A plasmid using the Expand High Fidelity PCR system. The purified DNA fragment was transformed into *C. dubliniensis* wild type strain Wü284 by electroporation, with the *SAT1* cassette replacing the first copy of the *MED3* gene. Transformation yields were low, with 3 colonies formed. Correct integration of the cassette in nourseothricin resistant transformants was verified using the primer pair MED3_F/FLPR. In order to excise the cassette two positive transformants were grown in YPM overnight. Putative revertants were spread onto NAT_2 plates, which allowed drug-sensitive revertants to be identified as tiny colonies, 36 of which were sub-cultured onto YEPD plates, genomic DNA extracted and PCR screened for the absence of one copy of *MED3* using the primer pair MED3_DKO_F/MED3_DKO_R. The second gene copy was disrupted and transformants were screened using the primer pairs MED3_DKO_F/ MED3_DKO_R and MED3_INT_F/ MED3_INT_R (Table 2.2).

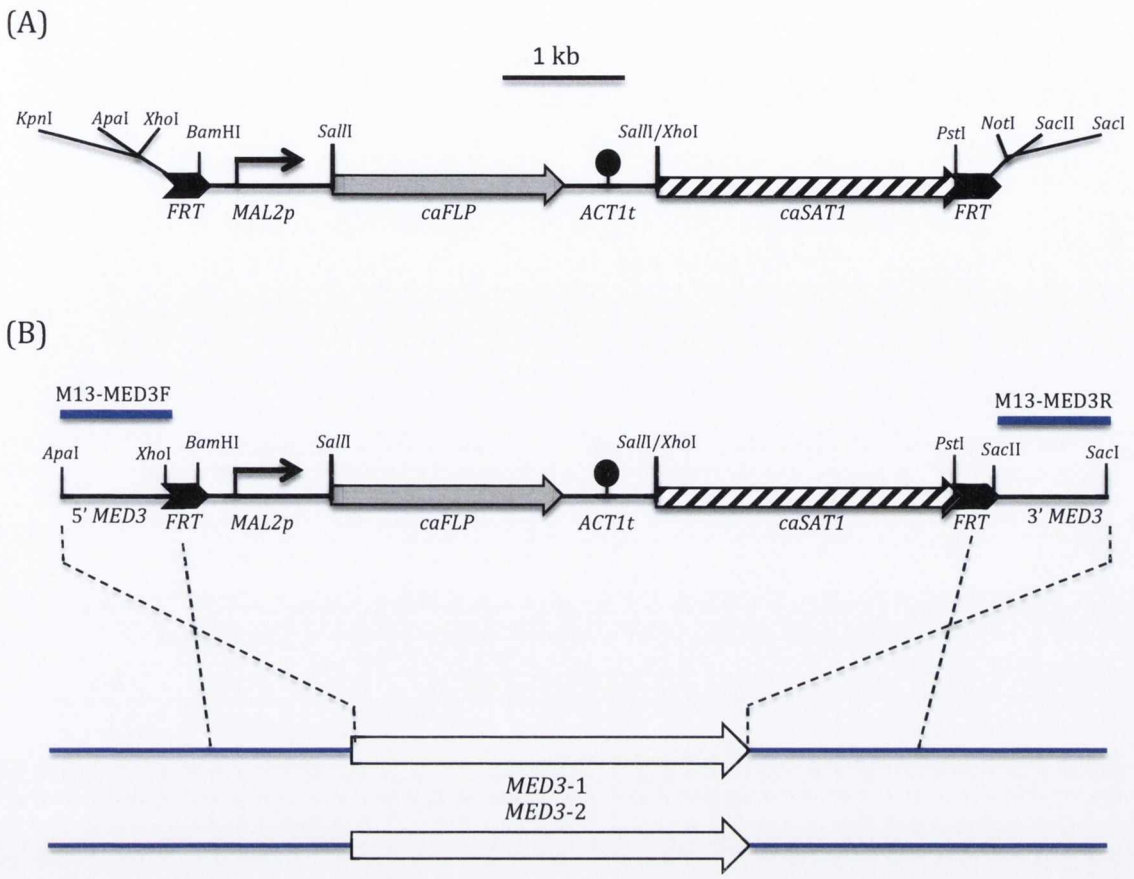

Figure 4.1. (A) Structure of the *SAT1* flipper contained in plasmid pSFS2. The *FLP* gene is represented by the grey arrow, the nourseothricin resistance marker by the hatched arrow, the *MAL2* promoter by the bent arrow, and the transcription termination sequence of *ACT1* by the filled circle. Relevant restriction sites and oligonucleotides are present. **(B)** Structure of deletion cassette as applied to *MED3* in this study. Adapted from Reuss *et al.,* (2004).

4.3.2. Complementation of a *MED3* allele

In order to confirm the phenotype associated with deleting *MED3* a single copy of the gene was reintroduced into the *Cdmed3*Δ strain to form a reintegrant. The primer pair MED3_notI_F/ MED3_sacII_R containing *Not*I and *Sac*II restriction sites (Table 2.2) was used to amplify a 1,169 bp fragment encompassing the *MED3* gene which was purified and ligated using the pGEM-T Easy Vector. Transformants were screened by PCR using the MED3_notI_F/ MED3_sacII_R primer pair, plasmids were purified and five positive transformants were sequenced. Positive transformants' plasmid DNA was digested with *Not*I and *Sac*II and ligated to the digested pCDRI plasmid and transformed in *E. coli* XL10 Gold electrocompetent cells. Transformants with the correct insert were identified by digestion with *Not*I and *Sac*II. A single positive transformant was selected and the plasmid linearised using *Nco*I. The linearised plasmid was transformed by electroporation into *CDRI* locus of *Cdmed3*Δ.

4.3.3. Effect of homozygous *MED3* disruption on hypha formation

The main aim of this part of the study was to compare the phenotypes of the *Cdmed3*Δ mutant and the *Cdtlo*ΔΔ mutant to provide further evidence that the Tlos are components of Mediator. As expected, the wild type strain Wü284 was 80%- 90% truly hyphal by 3-4 hours of growth at 37 °C in water supplemented with 10% FBS [Figure 4.2 (A)]. The *Cdtlo*ΔΔ mutant, as previously observed, was unable to form true hyphae at any time point, with only pseudohyphae present [Figure 4.2 (B)]. The phenotype of the *Cdmed3*Δ mutant was almost identical to that of the *Cdtlo*ΔΔ strain, i.e. no true hyphae were formed [Figure 4.2 (A) and (B)]. The re-introduction of a single allele of *MED3* to the *Cdmed3*Δ mutant resulted in the formation of true hyphae, with the strain forming wild type levels of hyphae by 3-4 hours [Figure 4.2 (A) and (B)].

4.3.4. Effect of homozygous *MED3* disruption on growth on chlamydospore-inducing medium

When *C. dubliniensis* was originally described, it was observed that it produces higher levels of chlamydospores than *C. albicans* when grown on rice agar Tween agar (RAT) (Sullivan *et al.*, 1995). Wild type Wü284, *Cdtlo*ΔΔ, *Cdmed3*Δ and *Cdmed3*Δ::*MED3* were cultured on RAT agar in order to observe whether the homozygous deletion of *MED3* affected chlamydospore production. The inoculum was applied in several shallow parallel grooves in the agar, covered with a sterile coverslip and incubated for 3 days at 25 °C in the dark. Wü284 formed chlamydospores readily on RAT medium, while as previously observed the *Cdtlo*ΔΔ could not form chlamydospores, instead forming long chains of yeast-like cells. Interestingly, the *Cdmed3*Δ mutant could form chlamydospores on RAT medium, though to a lesser degree than wild type, with clumps of pseudomycelium also present. The *Cdmed3*Δ with an allele of *MED3* reintroduced produced chlamydospores on RAT medium similar to wild type (Figure 4.3).

4.3.5. Effect of homozygous *MED3* disruption on oxidative stress response

The susceptibility of the *Cdmed3*Δ mutant to H_2O_2 was assessed by incubation on agar plates supplemented with 6 mM H_2O_2. It was observed that the wild type strain Wü284 grew efficiently in the presence of 6 mM H_2O_2 (Figure 4.4). The ability of the *Cdmed3*Δ mutant to grow in the presence of 6 mM H_2O_2 was poor, resulting in an identical phenotype to that of the *Cdtlo*ΔΔ mutant. Furthermore, the *Cdmed3*Δ mutant with an allele of *MED3* re-introduced restored the phenotype to near wild type levels.

4.3.6 Effect of homozygous *MED3* disruption on growth in an alternative carbon source

As previously described in Chapter 3.2.5., the glucose/dextrose element of YEPD was replaced with galactose in order to compare the growth rate of the *Cdmed3*Δ mutant in the presence of alternative carbon sources with the *Cdtlo*ΔΔ mutant. The wild type strain Wü284 was not affected by the substitution of glucose with galactose, with a doubling time of 115.5

(A)

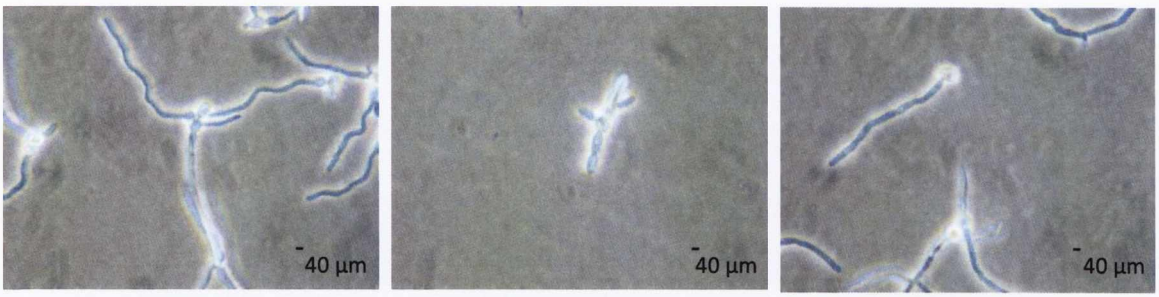

Wü284 *Cdmed3Δ* *Cdmed3Δ::MED3*

(B)

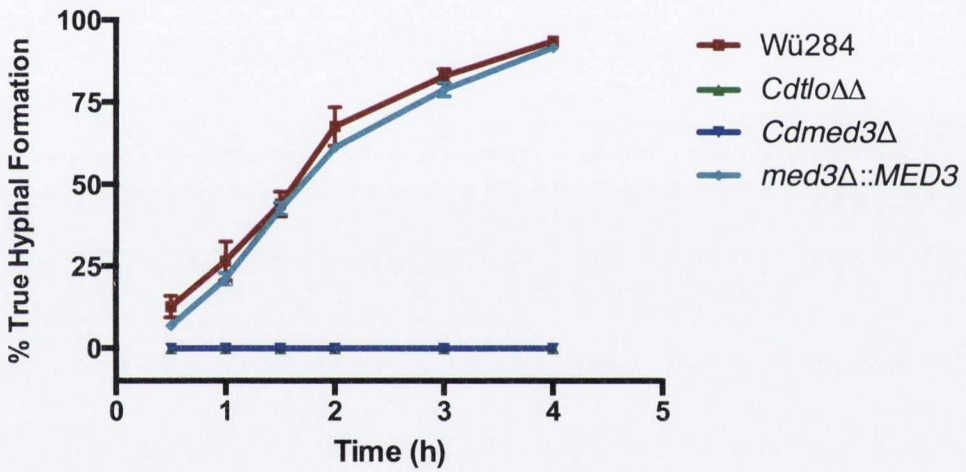

Figure 4.2. (A) Photomicrographs of each wild type Wü284, *Cdmed3Δ* and *Cdmed3Δ* with a single allele re-introduced grown overnight in YEPD followed by inoculation into water and 10% FBS, taken after 3 h. **(B)** Rate of true hyphae in wild type and mutant *MED3* strains under hyphal-inducing conditions (water with 10% v/v FBS). Percentage of true hyphae is represented as a proportion of 100 cells counted at random. Experiments carried out on three separate occasions. Scale bar is equal to 40 µm. Error bars represent the standard error of the mean (SEM) of three replicates.

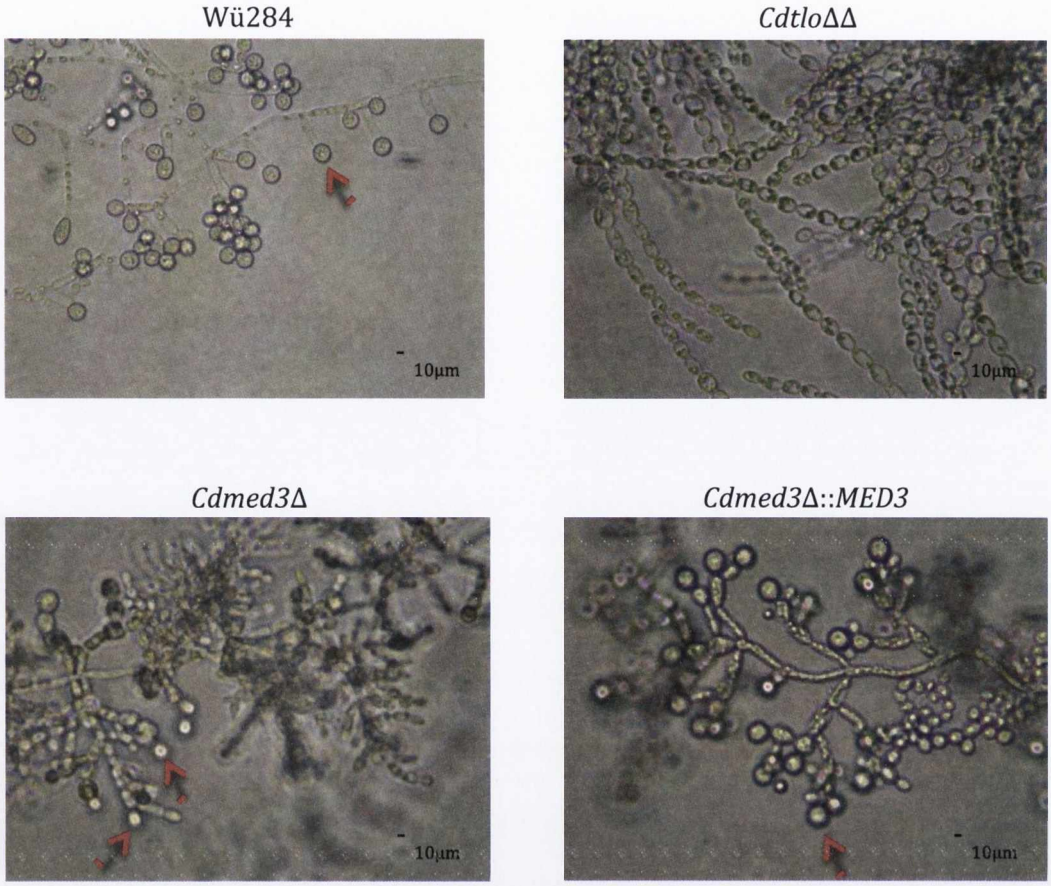

Figure 4.3. Photomicrographs of each wild type Wü284, Cd*tlo*ΔΔ, *Cdmed3*Δ and *Cdmed3*Δ with a single allele re-introduced grown overnight in YEPD followed by sub culturing onto Rice agar Tween (RAT) chlamydospore-inducing medium for 5 days at 30 °C. Experiments carried out on three separate occasions. Scale bars, approximately 10 μm. Red arrows indicate chlamydospores.

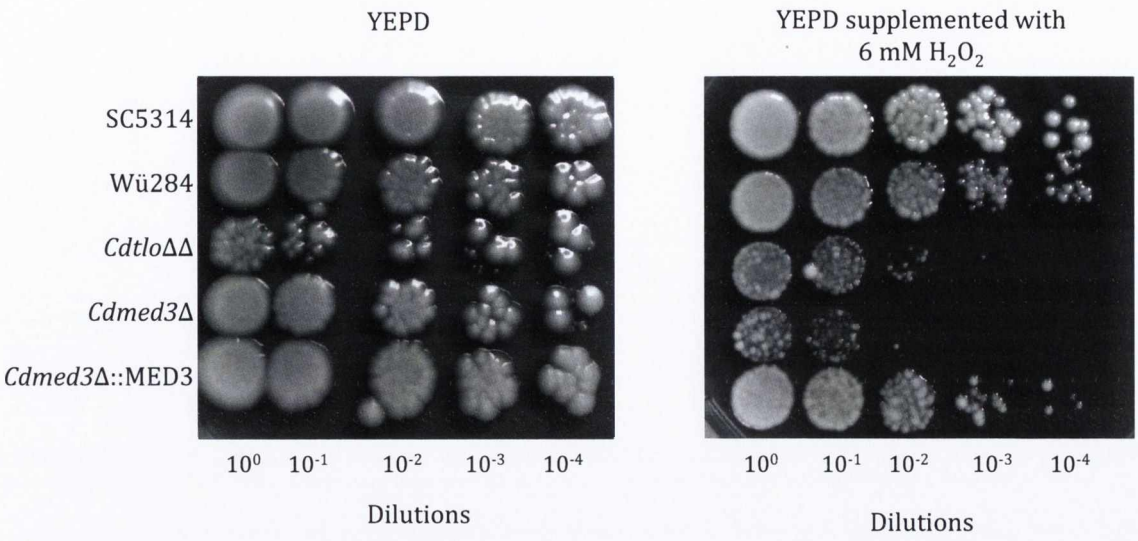

Figure 4.4. Growth of SC5314, Wü284, *Cdtlo*ΔΔ, *Cdmed3*Δ and *Cdmed3*Δ complemented with one allele in the presence of oxidative stress induced by the presence of 6 mM H_2O_2 on nutrient rich YEPD medium following serial dilutions. Plates were incubated for 48 h at 37 °C. Experiments carried out on three separate occasions.

min, however, the growth rate of the *Cdmed3*Δ mutant was significantly slower, with a doubling time of 169.56 min, very similar to the slower doubling time of the *Cdtlo*ΔΔ mutant (163.14 min), which suggests that the *Cdmed3*Δ mutant also has difficulty utilising galactose as an alternative carbon source. The re-introduction of a single allele of *MED3* to the *Cdmed3*Δ mutant resulted decrease in the doubling time to nearer that of wild type [Figure 4.5 (A) and (B)].

4.3.7. Two-colour DNA microarray analysis of the *Cdmed3*Δ mutant

Given that the homozygous deletion of *CdMED3* resulted in very similar phenotypes such as the inability to form true hyphae, poor growth in the presence of alternative carbon source (i.e. galactose) and increased sensitivity to oxidative stress induced by H_2O_2, DNA microarray studies were carried out to determine whether the similarities between the *Cdtlo*ΔΔ mutant and *Cdmed3*Δ mutant extended to the transcriptome. The expression profile of *Cdmed3*Δ was compared to wild type Wü284 when cultured in nutrient rich medium and for 1 h during the early stages of hyphal-induced growth (i.e. 1 h growth in water supplemented with 10% w/v FBS). The data sets were then compared to the expression profiles of the *Cdtlo*ΔΔ compared to Wü284 in order to observe whether the changes in gene expression in the absence of *MED3* matched those of the *Cdtlo*ΔΔ double mutant (Figure 4.6). Results were filtered by 1.5-fold change in expression in an attempt to isolate the most significant effects. Hierarchical clustering of expression data was generated between the *Cdtlo*ΔΔ mutant array and the *Cdmed3*Δ mutant array in YEPD and 1 h serum. Analysis of the hierarchical clusters in both conditions yielded distinctly different results. In the YEPD experiment [Figure 4.6 (A)] the expression profiles of *Cdtlo*ΔΔ and *Cdmed3*Δ were quite similar. However in the hyphal-inducing 1 h serum experiment it was observed that there was a greater disparity in expression between the two mutants [Figure 4.6 (B)].

Venn diagrams were created in order to quantify the number of genes similarly regulated between the datasets and the number of genes specifically up- or down-regulated in either the *Cdtlo*ΔΔ mutant or the *Cdmed3*Δ mutant. In the YEPD dataset, of the 927 genes that were down-regulated, 214 overlapped between the two mutants, while 421 were specific to the *Cdtlo*ΔΔ mutant and 292 were specific to the *Cdmed3*Δ mutant [Figure 4.7 (A)]. Of the 1,031 genes that were up-regulated in the YEPD dataset, 349 were commonly up-regulated between the two mutants, while 397 were specific to the *Cdtlo*ΔΔ mutant and 285 were specific to the *Cdmed3*Δ mutant [Figure 4.7 (B)]. With regards to the serum datasets, of the 1,647 down-regulated genes, 202 genes were commonly down-regulated between mutants, while 616 were specific to the *Cdtlo*ΔΔ mutant and 829 were specific to the *Cdmed3*Δ mutant [Figure 4.7 (C)]. Of the 1,631 genes that were up-regulated in the serum dataset, 219 were up-regulated in both mutants, while 649 were specific to the *Cdtlo*ΔΔ mutant and 763 were specific to the *Cdmed3*Δ mutant [Figure 4.7 (D)].

GO Term analysis of the genes similarly up-regulated in the YEPD dataset of the *Cdtlo*ΔΔ and the *Cdmed3*Δ mutant showed genes involved in a wide range of processes were affected, 26.9% of which were attributed to the regulation of biological processes, with 19.5% of genes involved in transport and 18.5% involved in stress response. Of the down-regulated genes, 21.2% had roles in the regulation of biological processes, 17.6% were involved in transport and 16.1% had roles in organelle organisation. GO Term analysis of genes similarly up-regulated in the serum data sets of the two mutants revealed that genes involved in a vast array of processes were up-regulated in the absence of the *TLO*s and *MED3.* The highest percentage of the 495 genes (18%) were attributed to the regulation of biological process, while 13.5% of genes were involved in stress response functions and 12.9% of genes were involved in organelle organisation. A summary of the frequencies of up-regulated genes attributed to various processes is shown in Tables 4.2, 4.3, 4.4 and 4.5.

(A)

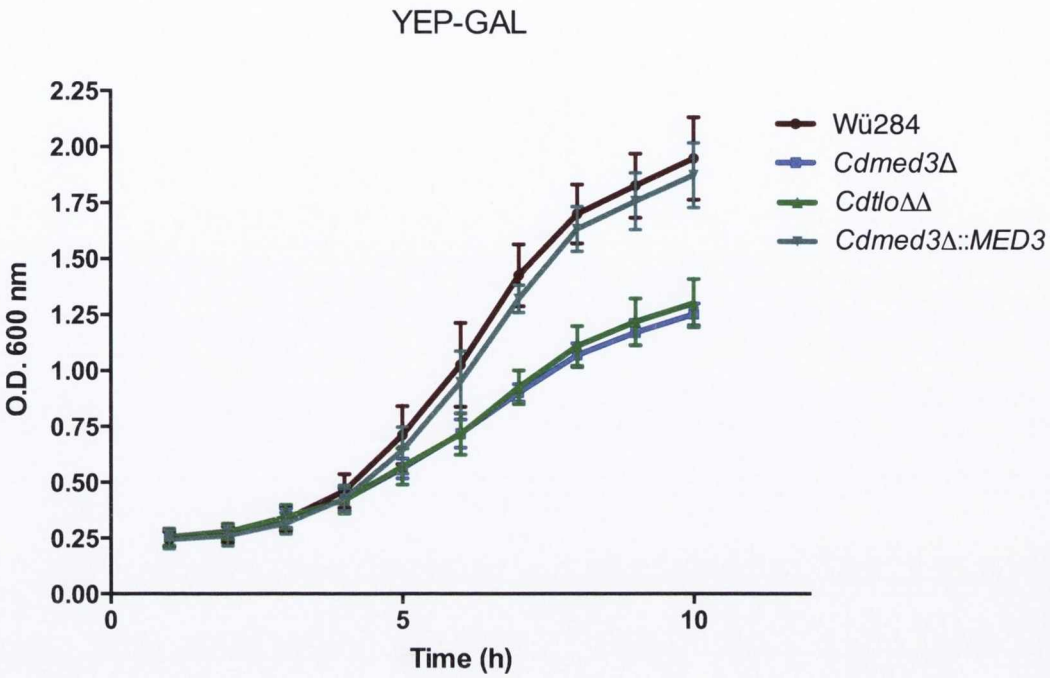

(B)

Strains	Wü284	*Cdmed3Δ*	*CdtloΔΔ*	*ΔCdmed3::MED3*
Doubling time (min)	115.5 *+/- 12.72*	169.56 *+/- 8.49*	163.14 *+/- 4.58*	114.0 *+/- 10.65*

Figure 4.5. (A) Graph depicting growth rates of Wü284, *CdtloΔΔ*, *Cdmed3Δ* and *Cdmed3Δ* complemented with one allele*3* grown in nutrient rich YEPD where the dextrose/glucose is substituted with galactose. **(B)** Doubling times, in minutes. Standard deviations are italicised below each value and represent an average of 3 replicates. Error bars represent the standard error of the mean (SEM) of three replicates.

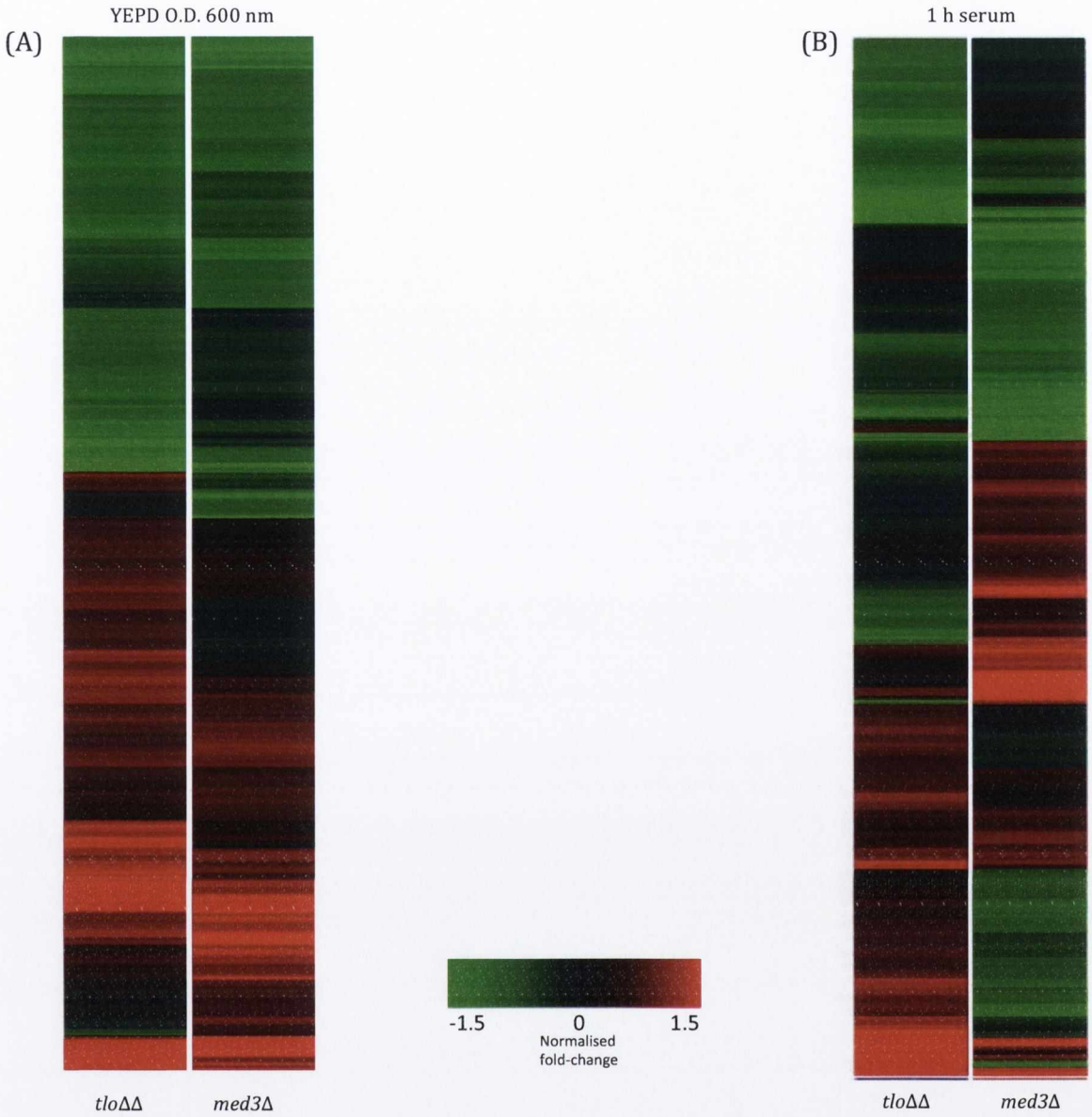

Figure 4.6. Whole genome heatmap of a comparison of gene expression in a *Cdtlo*ΔΔ mutant and a *Cdmed3*Δ mutant in *C. dubliniensis* in **(A)** YEPD and **(B)** water supplemented with 10% (v/v) FBS. Data represents all genes and is filtered by a 1.5-fold change in expression. Expression levels displayed represent the expression of *Cdmed3*Δ compared to Wü284 and *Cdtlo*ΔΔ compared to Wü284. The legend conveys the relative colouring for normalised expression level of each gene in *Cdmed3*Δ compared to Wü284 and *Cdtlo*ΔΔ compared to Wü284. The hierarchical clusters were created using Agilent GeneSpring GX v11.5 (Agilent Technologies Inc).

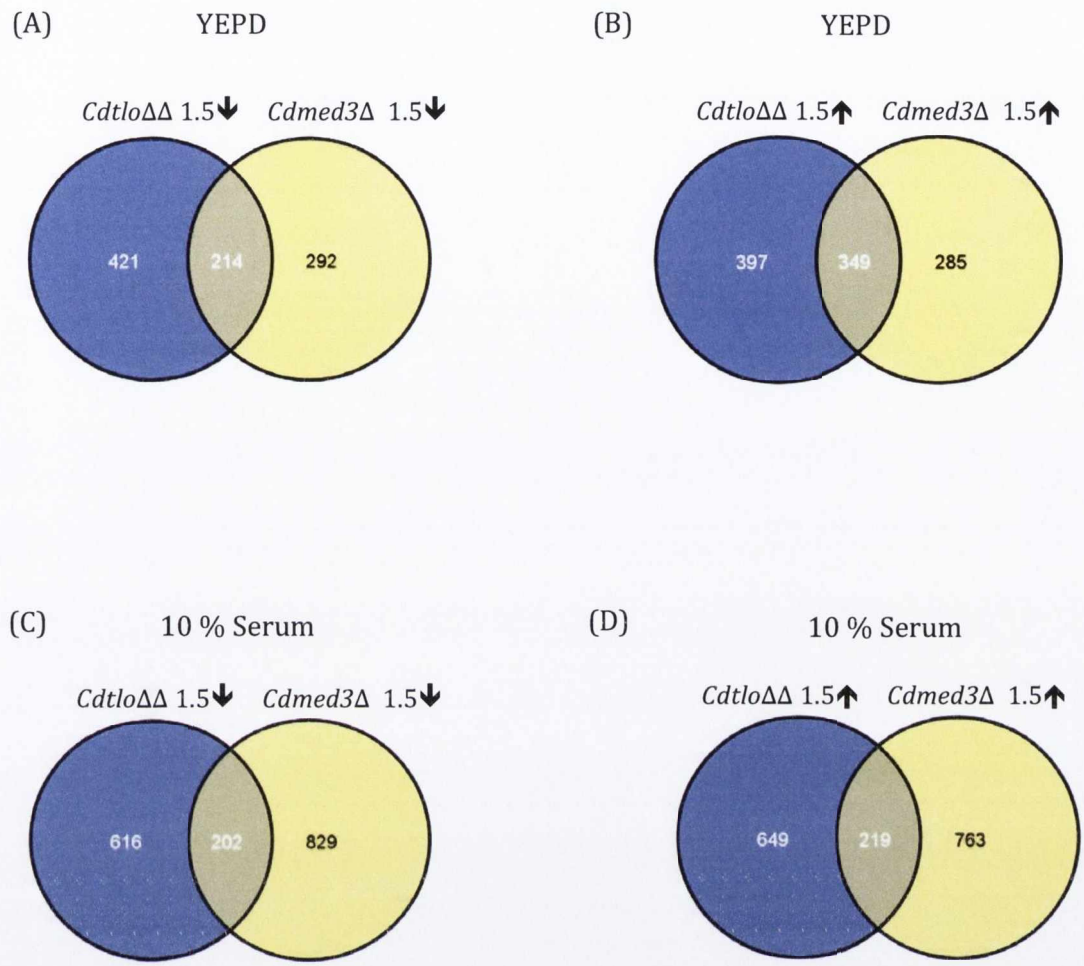

Figure 4.7. Venn Diagrams of *Cdtlo*∆∆ versus *Cdmed3*∆ representing overlapping and distinct gene numbers from the two mutant microarray datasets. Data is filtered based a 1.5-fold change in expression. **(A)** and **(B)** represent genes down-regulated and up-regulated in the YEPD microarray dataset. **(C)** and **(D)** represent genes down-regulated and up-regulated in the 1 h serum microarray dataset. Graphs were created using Agilent GeneSpring GX v11.5 (Agilent Technologies Inc).

Process	%
Regulation of biological process	26.9
Transport	19.6
Response to stress	18.5
Organelle organisation	17.2
Filamentous growth	14.4
Response to chemical	11.4
RNA metabolic process	10.3
Cellular protein modification process	9
Cell cycle	6.7
DNA metabolic process	6
Response to drug, Pathogenesis	5.8
Signal transduction	5.4
Vesicle-mediated transport	5.2
Carbohydrate metabolic process	4.9
Lipid metabolic process	4.7
Cellular homeostasis	4.5
Cytoskeleton organisation	4.3
Cell wall organisation	4.1
Biofilm formation, Cell development	3.4
Hyphal growth, protein catabolism	3.2

Table 4.2. Go-Term process mapping of 349 genes up-regulated in *Cdtlo*ΔΔ and *Cdmed3*Δ mutants in the YEPD DNA microarray. Frequency of 3% or lower not shown. Processes classified using GO Term finder at CGD.

Process	%
Regulation of biological process	21.2
Transport	17.6
Organelle organisation	16.1
Response to stress	15.2
RNA metabolic process	14
Response to chemical	13.4
Filamentous growth	9
Cellular protein modification process, Ribosome biogenesis	7.8
Cell cycle, Translation	7.5
Response to drug	6
Carbohydrate metabolic process, DNA metabolic process	5.1
Lipid metabolic process	4.8
Generation of precursor metabolites and energy, Pathogenesis	3.3

Table 4.3. Go-Term process mapping of 214 genes down-regulated in *Cdtlo*ΔΔ and *Cdmed3*Δ mutants in the YEPD DNA microarray. Frequency of 3% or lower not shown. Processes classified using GO Term finder at CGD.

Process	%
Regulation of biological process	18
Response to stress	13.5
Organelle organisation	12.9
Transport	12.5
Response to chemical	11.7
Filamentous growth	10.1
RNA metabolic process	8.9
Cellular protein modification process	8.3
Protein catabolic process	6.5
Lipid metabolic process	5.7
Cell cycle	4.8
Response to drug	4.6
Cellular homeostasis	4
DNA metabolic process	3.8
Pathogenesis	3.4

Table 4.4. Go-Term process mapping of 219 genes up-regulated in *Cdtlo*ΔΔ and *Cdmed3*Δ mutants in 10% (v/v) serum DNA microarray. Frequency of 3% or lower not shown. Processes classified using GO Term finder at CGD.

Process	%
Regulation of biological process	26.5
Transport	21
Filamentous growth	15.2
Organelle organisation	14.6
Response to chemical	14.3
RNA metabolic process	13.9
Ribosome biogenesis	8.6
Cellular protein modification process	8.2
Response to drug	7.9
Cell cycle	7.7
Carbohydrate metabolic process, Biofilm formation, Pathogenesis	5.7
Translation, Interspecies interaction between organisms, Vesicle-mediated transport	4.2
Signal transduction	4
Hyphal growth	3.8
Cytoskeleton organisation	3.5
Cell wall organisation, cellular homeostasis, DNA metabolic process	3.3

Table 4.5. Go-Term process mapping of 202 genes down-regulated in *Cdtlo*ΔΔ and *Cdmed3*Δ mutants in 10% (v/v) serum DNA microarray. Frequency of 3% or lower not shown. Processes classified using GO Term finder at CGD.

GO Term analysis of genes down-regulated in the serum data sets of the two mutant strains highlighted processes for 453 genes. The highest number of genes (26.5%) was found to be involved in regulation of biological processes, 21% of genes were involved in transport and 15.2% of genes were involved in filamentous growth. A summary of the frequencies of down-regulated genes attributed to various processes is shown in Table 4.3. Interestingly, the *Cdmed3*Δ mutant showed an increase in the expression of glycolytic genes (n=11) and genes encoding histones and proteins involved in chromatin assembly (n=18); increases in expression that were not observed in the *Cdtlo*ΔΔ. The *Cdmed3*Δ mutant also exhibited a down-regulation of genes associated with the GO Terms "DNA replication" (n=43) and "telomere maintenance" (n=18) (Figure 4.8) (Haran *et al.*, 2014). The differences in gene expression observed between the mutants and wild type, based on previously studied phenotypes are described below.

4.3.7.1. Hyphal and cell wall-associated genes

As with the *Cdtlo*ΔΔ mutant, assays to observe the formation of true hyphae carried out in this study have shown that the homozygous deletion of *MED3* in *C. dubliniensis* inhibits its ability to form true hyphae. The re-introduction of a single *MED3* allele restored the ability to form hyphae to near wild type levels. As with the *Cdtlo*ΔΔ double mutant, differential expression was observed between the *Cdmed3*Δ mutant and Wü284 (Figure 4.9). Genes encoding regulatory proteins implicated in hypha formation such as *EFG1, RIM101, RAS1, TEC1* and *UME6* were all down-regulated in the *Cdmed3*Δ mutant with fold changes ranging from -1.7-fold to -6-fold, an expression profile that was also observed in the *Cdtlo*ΔΔ double mutant. Similarly, *SOD5, HWP1, DCK1, DSE1* and *EAP1* all showed decreased expression in both mutants when compared to wild type.

The expression patterns of the majority of genes involved in filamentation and cell wall functions correlate between the two data sets. It was observed in the *Cdtlo*ΔΔ versus wild

type microarray that certain anomalies occurred regarding gene expression. Genes that are also involved in filamentation, morphogenesis and cell wall functions such as *ECE1, SOD4, SAP7, SAP10, DEF1* (*EED1*) and *YWP1* showed increased expression levels in the *Cdtlo*ΔΔ mutant, despite the lack of hyphae. The same genes were also found to have increased expression in the *Cdmed3*Δ mutant. *ECE1* was up-regulated 6-fold in the *Cdmed3*Δ mutant and up-regulated 16- fold in the *Cdtlo*ΔΔ mutant. *EED1* was up-regulated 3-fold in the *Cdmed3*Δ mutant and up-regulated 4-fold in the *Cdtlo*ΔΔ mutant.

Differences in expression patterns were also observed between the two mutant microarrays. Genes that code for cell wall proteins such as *RBT5, PGA31, CRH11, SMI1* and *ECM21* were all down-regulated in the absence of the *TLOs*, however in the absence of *MED3* these genes show increased expression levels in comparison to Wü284. The opposite expression pattern was also observed, with the expression of *SFL1* and *HSP90* up-regulated in the absence of the *TLOs* and down-regulated in the absence of *MED3.* Microarray data suggest that while there are many important overlapping functions for Med3 and Tlos, they may regulate different sets of genes.

4.3.7.2. Response to oxidative stress

As previously outlined, phenotypic analysis of the *Cdtlo*ΔΔ mutant in the presence of oxidative stress results in poor growth. This was also true for the *Cdmed3*Δ mutant. As previously stated, the *SOD* genes, associated with the conversion of superoxide radicals into hydrogen peroxide, showed differential expression in the *Cdtlo*ΔΔ mutant relative to Wü284. *SOD5* and *SOD6* displayed a significant decrease in expression under hyphal-inducing conditions. This was also observed in the *Cdmed3*Δ mutant in comparison to Wü284, although the decrease in expression was less than that of the *Cdtlo*ΔΔ mutant [Figure 4.10 (A)]. *SOD4* expression was also found to be different in the *Cdmed3*Δ microarray; with expression levels significantly increased 23-fold in comparison to wild type. The expression

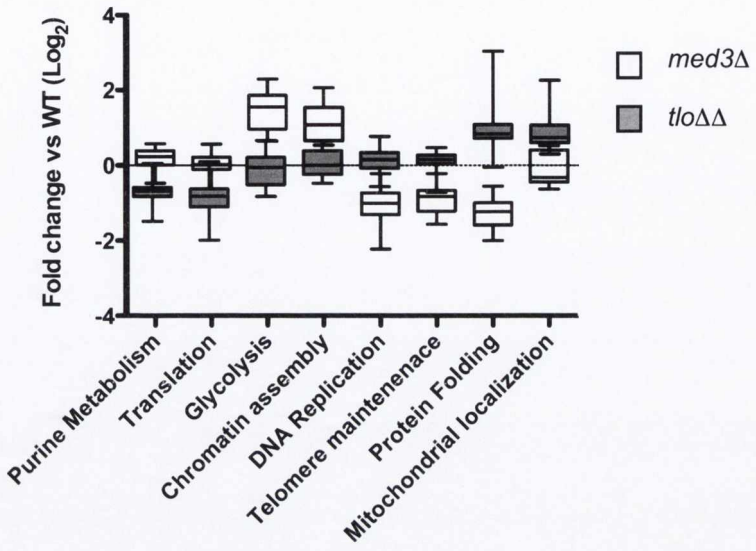

Figure 4.8. Graph plotting the expression levels (Log_2 fold change versus wild type) of genes associated with selected GO Terms in the *Cdtlo*ΔΔ mutant and the *Cdmed3*Δ mutant during growth in 10% (v/v) FBS. Adapted from Haran *et al.,* 2014.

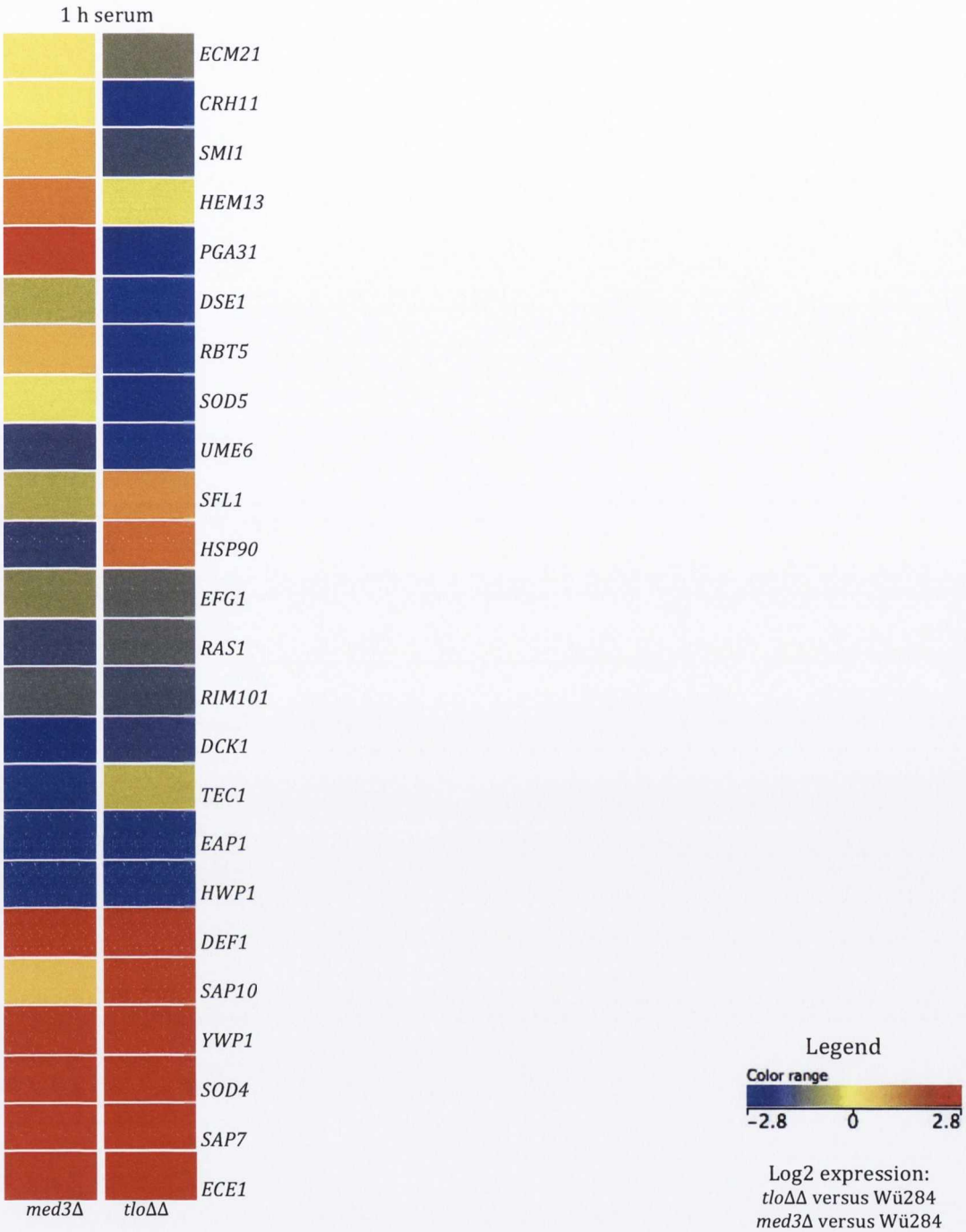

Figure 4.9. Genes shown have hyphal and cell wall functions. Visual heatmap of a comparison of gene expression in the *Cdtlo*ΔΔ double mutant and the *Cdmed3*Δ mutant relative to wild type Wü284 in water supplemented with 10% (v/v) FBS. Each gene is labelled on the right side of the heatmap, using the common gene alias in *C. dubliniensis*, usually named in *C. albicans*. The legend conveys the relative colouring for normalised expression level of each gene in *Cdtlo*ΔΔ compared to Wü284 and *Cdmed3*Δ compared to Wü284. The image (hierarchical clustering) was created using Agilent GeneSpring GX v11.5 (Agilent Technologies Inc).

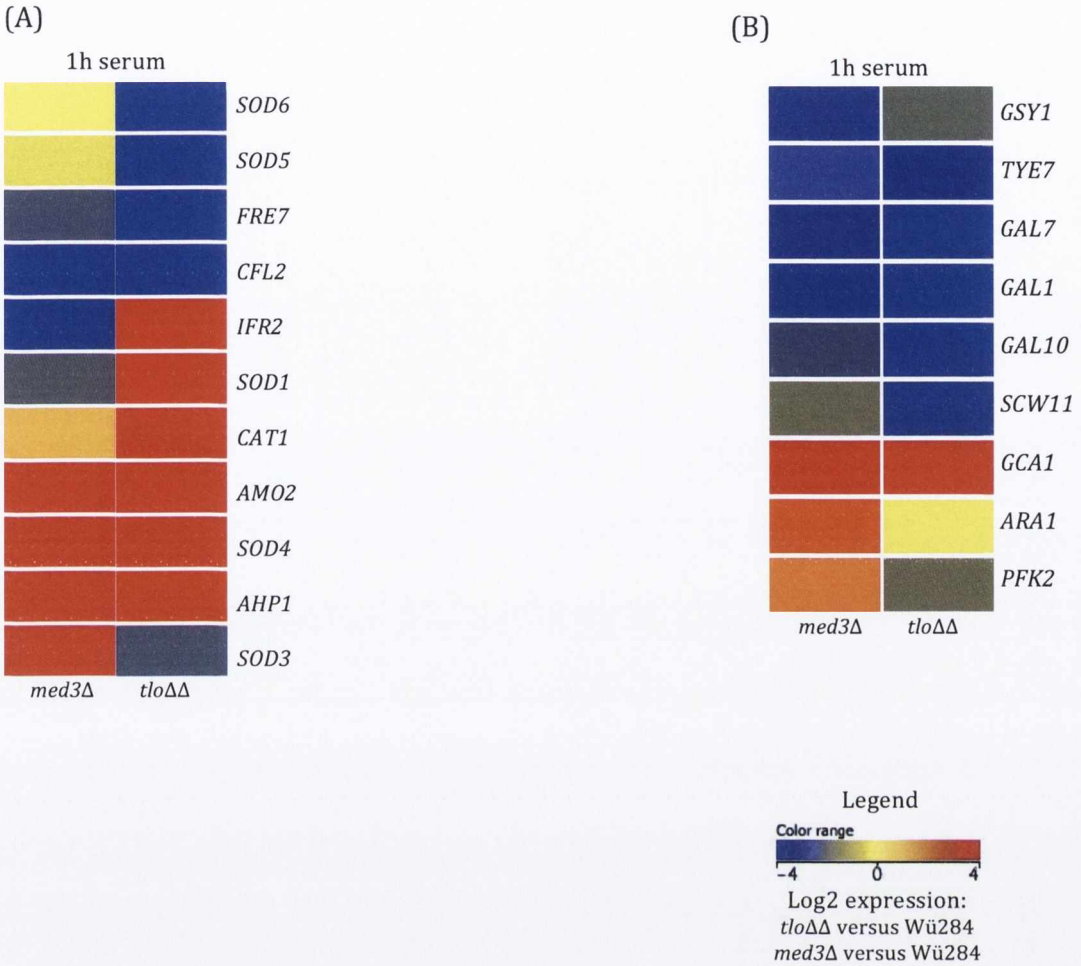

Figure 4.10. Visual heatmap of a comparison of gene expression in the *Cdtlo*ΔΔ double mutant and the *Cdmed3*Δ mutant relative to wild type Wü284 in water supplemented with 10% (v/v) FBS. Each gene is labelled on the right side of the heatmap, using the common gene alias in *C. dubliniensis*, usually named in *C. albicans*. Genes are grouped by associated process: **(A)** genes involved in oxidative stress response, **(B)** genes involved in carbohydrate utilisation. The legend conveys the relative colouring for normalised expression level of each gene in *Cdtlo*ΔΔ compared to Wü284 and *Cdmed3*Δ compared to Wü284. The image was created using Agilent GeneSpring GX v11.5 (Agilent Technologies Inc).

patterns of *FRE7* and *CFL2*, oxidoreductases involved in iron utilisation, correlated between the two mutants as both were down-regulated. *AMO2*, a copper amino oxidase was up-regulated in both *Cdmed3Δ* and *CdtloΔΔ*, as was *CAT1* and *AHP1*, which codes for a catalase and an alkyl hydroperoxidase respectively. Among the *SOD* gene family there were also results showing differences between the *Cdmed3Δ* and *CdtloΔΔ* mutants; *SOD1*, which was up-regulated 3-fold in the absence of the *TLO*s, was down-regulated 1.8-fold in the absence of *MED3*, and *SOD3*, which was down regulated 2-fold in the absence of the *TLO*s, was up regulated 6-fold in the absence of *MED3*. Similarly the expression pattern of *IFR2*, a zinc-binding dehydrogenase was different between the two mutants. Expression was decreased in *Cdmed3Δ* but increased in *CdtloΔΔ*.

4.3.7.3. Galactose utilisation

As was observed in *CdtloΔΔ*, the *GAL* 1, 7 and 10 genes were also down regulated in *Cdmed3Δ* compared to Wü284 [Figure 4.10 (B)], exhibiting decreases of 4-fold, 3-fold and 2.5-fold respectively. Expression levels of other genes were also decreased in the absence of *Cdmed3Δ*, matching the expression patterns of *CdtloΔΔ*. *TYE7*, *GSY1* and *SCW11*, all genes encoding proteins involved in carbohydrate metabolism showed decreased expression in the absence of the *MED3*, as was found with the absence of the *TLO*s. Furthermore, *GCA1*, which is regulated by galactose concentration and was found to be strongly up-regulated (9.5-fold) in the absence of the *TLO* genes, was also up-regulated (3.5-fold) in the absence of *MED3*. A disparity was found in the hierarchical clustering of carbohydrate genes in the form of *PFK2*, a phosphofructokinase with a role in glycolysis, which showed, increased expression (2-fold) in the absence of *MED3* but decreased expression (2- fold) in the absence of the *TLO*s. With regards to the genes showing similar expression profiles in the comparison between *Cdmed3Δ* and *CdtloΔΔ*, a noteworthy observation is that the changes in expression levels in *CdtloΔΔ* are generally higher in magnitude than in *Cdmed3Δ*, with the exception of *GSY1* expression.

4.3.8. Quantitative Real Time-PCR of selected genes

In order to confirm the comparative findings of the *CdMED3* mutant and the *CdTLO* mutant DNA microarray studies, quantitative real time PCR (qRT-PCR) was carried out on a selection of genes that represent similarities and differences between the two datasets.

4.3.8.1. ECE1

Real-time PCR data generated in this study confirmed DNA microarray findings that *ECE1* expression is increased significantly (i.e. 10-fold and 5-fold respectively) in the absence of the *TLO*s and *MED3* in comparison to wild type. Expression was higher in the *TLO* mutant than in the *MED3* mutant and this was confirmed by qRT-PCR relative to *ACT1* [Figure 4.11 (A)].

4.3.8.2 GAL10

DNA microarray expression analysis revealed that in the absence of the *TLO* and *MED3* genes *GAL10* was down-regulated 2-fold in comparison to wild type. This was confirmed by qRT-PCR [Figure 4.11 (B)].

4.3.8.3 RBT5

RBT5 expression was decreased in *Cdtlo*ΔΔ compared to wild type microarray studies and conversely, increased in *Cdmed3*Δ versus wild type microarray studies. This contrast was confirmed by qRT-PCR, where *RBT5* expression was 4-fold lower in the *Cdtlo*ΔΔ mutant compared to wild type, and 1.5-fold higher in the *Cdmed3*Δ mutant compared to wild type [Figure 4.11 (C)].

4.3.8.4 PCK1

According to microarray results, *PCK1* expression is decreased in the absence of the *TLO* genes, and decreased further in the absence of *MED3* when compared to wild type. This result

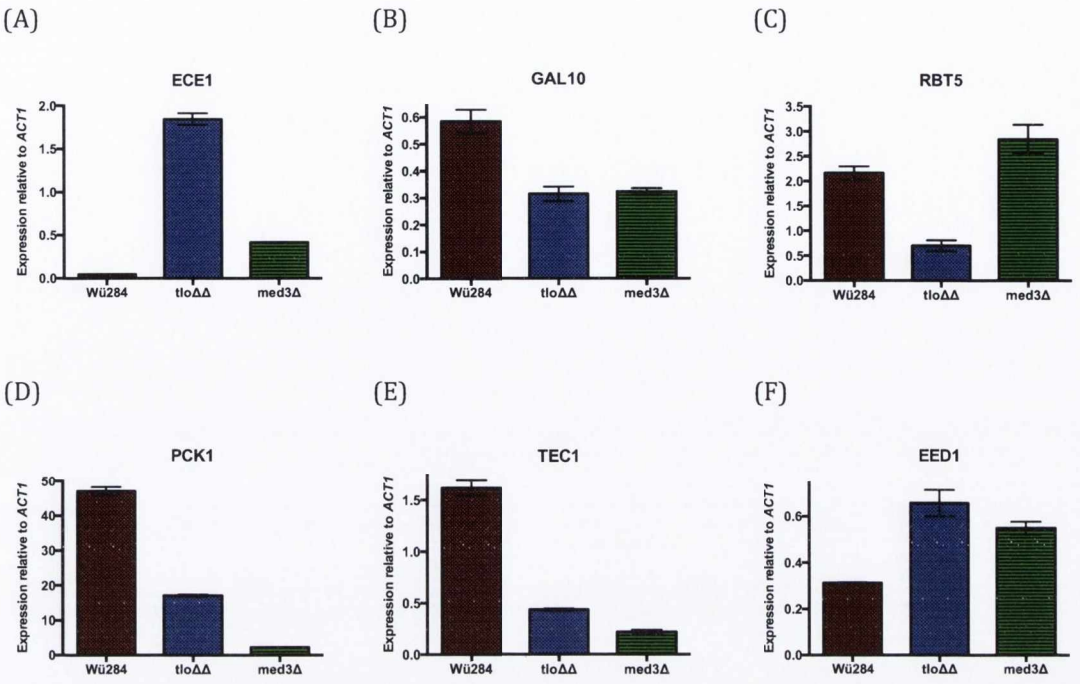

Figure 4.11. qRT-PCR experiments of gene expression in *Cdtlo*ΔΔ, *Cdmed3*Δ and wild type Wü284. Results are interpreted and displayed relative to *ACT1* expression. Values displayed represent $2^{-\Delta CT}$ values. Graphs show expression of (A) *ECE1,* (B) *GAL10,* (C) *RBT5,* (D) *PCK1,* (E) *TEC1* and (F) *EED1* in the absence of the *TLO*s and *MED3* in comparison to wild type in hyphal inducing conditions (10% v/v FBS). Error bars represent the standard error of the mean (SEM) of three replicates.

was confirmed by qRT-PCR, with *PCK1* expression 3-fold and 10-fold lower in the *Cdtlo*ΔΔ and *Cdmed3*Δ mutants respectively [Figure 4.11 (D)].

4.3.8.5 TEC1

TEC1 expression was decreased in both mutant strains in comparison to wild type, a result that was confirmed by qRT-PCR as *TEC1* expression was 3-fold and 6-fold lower in the *Cdtlo*ΔΔ and *Cdmed3*Δ mutants respectively [Figure 4.11 (E)].

4.3.8.6 EED1 (DEF1)

The expression of *EED1* was significantly increased upon deletion of the *TLO*s and *MED3* in Wü284, and this pattern was confirmed by qRT-PCR, with a 2-fold increase of *EED1* expression in the *Cdtlo*ΔΔ and *Cdmed3*Δ mutants compared to wild type [Figure 4.11 (F)]. The comparative findings of a selection of genes between the two mutant arrays have been confirmed by qRT-PCR.

4.3.9. The deletion of *CdMED3* in the *Cdtlo*ΔΔ mutant

In order to investigate the effect of a complete lack of Mediator association on *C. dubliniensis* we attempted to generate a homozygous *MED3* mutant in a *Cdtlo*ΔΔ mutant background. Although it was possible to generate a heterozygous mutant through the use of the *SAT1* cassette as previously described in this section, it proved impossible to delete the second allele, suggesting that a *tlo*ΔΔ/*med3*Δ mutant is non-viable.

4.4. Discussion

4.4.1. The Tlos and the yeast Mediator complex

The recent findings of Zhang *et al.* (2012) that the *C. albicans* Tlo proteins are stoichiometric components of the Mediator complex prompted us to further investigate this hypothesis. The head and middle regions are thought to interact with Pol II, while the tail region is responsible for recognition and binding of activators. The Med3 protein subunit of the Mediator is proposed to interact with Med2 within the tail module (Bhoite *et al.*, 2001). The absence of an annotated *MED2* gene in *C. albicans* and *C. dubliniensis* and the presence of a Med2 domain in the Tlos would suggest that the Tlos are orthologues of the tail region of the Mediator. Based on protein expression analysis of individual *C. albicans* Tlos and the purification of tagged Tlo proteins, Zhang *et al.* (2012) confirmed that the Tlo proteins are subunits of the Mediator complex and are *Candida* orthologues of the *S. cerevisiae* Med2 protein.

Given that the Tlos and Med3 are proposed to stabilise each other's presence in the Mediator tail, we hypothesised that deleting either the *CdTLO*s or *CdMED3* would have a similar effect on phenotype. In order to observe whether the Tlos carry out a similar function to that of Med3, a homozygous *Cdmed3*Δ mutant strain was constructed, and the phenotype was compared to that of the *Cdtlo*ΔΔ mutant. It was observed that the phenotypes of the two mutants were remarkably similar: the *Cdmed3*Δ mutant was also unable to form true hyphae in 10% v/v FBS and water, it grew slowly in galactose as an alternative carbon source to glucose and was susceptible to oxidative stress induced by hydrogen peroxide. The only phenotypic difference observed in this study between the two mutants was the ability of the *Cdmed3*Δ mutant to form chlamydospores on RAT medium, where the *Cdtlo*ΔΔ mutant could not. Despite chlamydospore formation being important for the identification of *Candida* spp., given that only *C. albicans* and *C. dubliniensis* can form chlamydospores, their function

remains unclear (Staib & Morschhäuser, 2007; Citiulo *et al.,* 2009). Previous studies have shown that chlamydospore production is controlled by the same morphogenetic pathways that control the formation of hyphae, such as the Efg1 and Hog1 pathways (Sonneborn *et al.,* 1999; Eisman *et al.,* 2006).

Interestingly, Zhang *et al.* (2012) deleted the gene encoding Med3 in *C. albicans* and also observed a defect in true hyphal formation under hyphal inducing conditions (i.e. FBS and temperature shift). Furthermore, biochemical analysis of the Mediator complex in the *Cdtlo*ΔΔ and the *Cdmed3*Δ mutants resulted in the absence of Med5 and Med16 in Mediator purified from both mutants, which suggests that the entire tail region becomes de-stabilised upon the loss of either the Tlos or Med3 proteins (Haran *et al.,* 2014). The formation of hyphae in *Candida* spp. is a complex transcriptional program that responds to a variety of signals and involves an array of sequence-specific DNA-bound transcription factors (Sudbery, 2011). However, little is known about the downstream targets of these transcription factors. Chromatin remodelling and modification has also been revealed to be important in facilitating the roles of these DNA-bound transcription factors (Lu *et al.,* 2008; Lu *et al.,* 2011). It is well established that Mediator plays a role in facilitating the regulation of specific gene expression pathways. Given that CaMed3 and the Tlo proteins have a clear role in cell morphology, it is possible that these subunits work with DNA-bound transcription factors to regulate genes involved in the yeast-to-hypha switch (Zhang *et al.,* 2012).

4.4.2. Comparative DNA microarray expression profiles of Cd*med3*Δ and Cd*tlo*ΔΔ

With regards to the phenotypes studied in this section of the study, the only notable difference observed between the *Cdtlo*ΔΔ mutant and the *Cdmed3*Δ mutant was chlamydospore formation. However, significant differences were observed between the YEPD and serum microarray datasets as shown in Figure 4.6 (A) and (B). In the YEPD dataset, just 22% of down-regulated genes overlapped between the two mutants, while 34 % of up-

regulated genes overlapped. In the serum datasets an overlap of just 12 % in the down-regulated genes was observed and an overlap of 13% of the up-regulated genes between the *Cdmed3*Δ and *Cdtlo*ΔΔ mutants, which suggests that other than the phenotypes studied in our laboratory, there may be other differences between the *Cdtlo*ΔΔ mutant and the *Cdmed3*Δ mutant. Therefore there may be additional as yet unidentified phenotypic differences between the two mutants. In terms of the GO Term analysis carried out it is interesting that the second highest number of genes up-regulated in the *Cdtlo*ΔΔ mutant and the *Cdmed3*Δ mutant in 10% serum were involved in stress response, given that both mutants were susceptible to oxidative stress induced by H_2O_2. Furthermore, the third highest number of down-regulated genes in the two mutants are involved in filamentous growth, which is unsurprising, given that neither mutants can form true hyphae. In the YEPD dataset it is interesting that genes involved in filamentous growth and stress response are among the highest gene processes up-regulated, given that the condition is nutrient-rich and neither the *Cdtlo*ΔΔ mutant nor the *Cdmed3*Δ mutant can form true hyphae.

If the Tlos are in fact orthologues of Med2, it is reasonable to assume that the Tlos and Med3 would carry out some related functions, given that Med2 and Med3 reside in the same module of the Mediator. The exact role of Med2 and Med3 in *S. cerevisiae* is unknown, however Ansari *et al.* (2012) hypothesised that the tail module of the Mediator complex may regulate the expression of genes involved in diverse metabolic pathways by interacting directly or indirectly with their transcriptional activators. Furthermore, the differences found in the transcriptome patterns of the *Cdtlo*ΔΔ mutant and the *Cdmed3*Δ mutant in response to hyphal inducing conditions suggests that if Mediator complexes with different tail substituents exist *in vivo* they the could respond differently to specific environmental conditions (Haran *et al.*, 2014). Alternatively, deleting Med2 or Med3 may have different effects on the 3-D architecture of Mediator and this may affect its function.

4.4.3. The disruption of CaMed7 and CdMed3 yield similar mutant profiles

A study carried out by Tebbji *et al.* (2014) provided an in-depth analysis of the effect of deleting the gene encoding CaMed7, a Middle subunit of the Mediator. When a homozygous deletion of *MED7* was carried out, they observed that although *MED7* is not essential for viability in *C. albicans,* the deletion resulted in a filamentation defect and a carbohydrate defect, similar to the effects of the deletion of *MED3* in *C. dubliniensis* observed in this study (Tebbji *et al.,* 2014). Similar to the deletion of the gene coding Med3, the loss of Med7 had significant consequences on a number of cellular functions. In addition to examining the effect of the deletion of *MED7* on filamentation and carbohydrate utilisation, Tebbji *et al.* also observed the effect of the deletion on biofilm formation and colonisation in a mouse model, and found that biofilm formation was decreased 3-fold in comparison to wild type, while cells lacking *MED7* failed to colonise the GI tract in a mouse model, which was probably due to the lack of filamentation. Furthermore, DNA microarray analysis of the *med7*Δ mutant revealed some similarities between the *Cdmed3*Δ and the *Camed7*Δ. It was observed that in nutrient rich YEPD conditions, genes involved in rRNA and ribosome biogenesis were up regulated in both mutants (Haran *et al.,* 2014; Tebjii *et al.,* 2014). Under hyphal-inducing conditions there were similarities in the expression profiles of the epimerase, *GAL10,* involved in galactose utilisation, *SFL1*, a transcription factor involved in the negative regulation of morphogenesis and the hyphal regulator *TEC1*; they were all down-regulated in the absence of *CaMED7* and *CdMED3.*

Tebbji *et al.* observed through ChIP-Chip and transcription profiling that Med7 appears to be involved in the activation of the glycolytic pathway, given that Med7 was detected at the promoters of glycolytic cells during growth in glucose, and the *med7* mutant strain revealed a down-regulation of several glycolytic genes under nutrient rich conditions. These results are similar to those observed by Haran *et al.,* (2014), where ChIP-Chip analysis of CdTlo1 showed enrichment at genes involved in glycolysis and deletion of the CdTlos and CdMed3

resulted in the down-regulation of genes involved in glycolytic roles. If Mediator subunits have both general and specific functions, then perhaps control of carbohydrate metabolism is a general function of Mediator, given that Tail (Med3, Med2) and Middle (Med7) subunits appear to have similar roles in carbohydrate metabolism.

4.4.4. Mediator subunit functions conserved between *Saccharomyces cerevisiae*, *Schizosaccharomyces pombe* and *Candida albicans*

In spite of the fact that the two model yeasts are highly divergent, a comparative analysis of *Saccharomyces cerevisiae* and *Schizosaccharomyces pombe* revealed significant conservation of the roles of Mediator (Linder *et al.*, 2008). A study carried out by Uwamahoro *et al.*, (2012) illustrated that the *C. albicans* Mediator has some conserved functions with *S. cerevisiae* and *S. pombe.* Generating a homozygous *MED31* gene deletion in *C. albicans* revealed that 7.8% of the genome was differentially expressed, which is consistent with data from *S. cerevisiae* and *S. pombe,* and in agreement with a general role for Med31 in gene expression. Furthermore, of the genes that were differentially expressed in *C. albicans* in the absence of *MED31* 61.7% of genes were down-regulated, which is consistent with the data obtained for *S. cerevisiae* and *S. pombe,* and consistent with a mostly positive role of Med31 in transcription (van de Peppel *et al.*, 2005; Linder *et al.*, 2008; Miklos *et al.*, 2008; Koschubs *et al.*, 2009). In *S. cerevisiae* and *S. pombe,* mutants in the Head and Middle domain have been shown to agree in regards to gene expression and cellular phenotypes (van de Peppel *et al.*, 2005; Linder *et al.*, 2008; Koschubs *et al.*, 2009). Uwamahoro also observed this for the *C. albicans med31*Δ and *med20*Δ mutants, where the expression of the cell wall adhesins *ALS1, ALS3, EAP1* were found to be down-regulated in the absence of either *MED31* or *MED20* and both mutants displayed biofilm and filamentation defects, as well as both being sensitive to compounds such as formamide, DMSO, SDS, ethanol and congo red.

In order to support the hypothesis put forward by Zhang *et al.* (2013) that the Tlo proteins are the candidal orthologues of *S. cerevisiae* Med2, Haran *et al.* (2014) compared the transcript profile of the *Cdtlo*ΔΔ mutant and the *S. cerevisiae med2*Δ mutant in an attempt to identify conserved roles between the proteins. An overlap was observed in genes down-regulated with roles in carbohydrate metabolism (*TYE7*) and carbohydrate catabolism and glycerol biosynthesis (*PFK1, FBA1, GPH1, GDB1*). Genes involved in sulphur amino acid metabolism, such as *MET6* and *MET13* were also down-regulated in both mutants, as well as other conserved genes involved in amino acid catabolism; *GCV1, GCV2* and *SHM2.* Furthermore, both mutants showed an increase in the expression of genes encoding enzymes involved in oxidation-reduction processes (Haran *et al.,* 2014).

4.4.5. Closing remarks

We attempted to generate a homozygous *MED3* mutant in a *Cdtlo*ΔΔ mutant background in order to investigate the effect of a complete lack of Mediator association on *C. dubliniensis.* We were able to generate a heterozygous mutant but it proved very difficult to delete the second allele, therefore we propose that the absence of both Med2 and Med3 results in a non-viable mutant in *C. dubliniensis.* In the future, it may be worth considering performing a heterozygous deletion of *MED3* in a *Cdtlo*ΔΔ mutant background and using a Tet-off system whereby the expression of the second allele of *MED3* is turned down. Furthermore, it may be useful to investigate the phenotypic effects of a heterozygous *MED3* mutant in a *Cdtlo*ΔΔ mutant background, as the loss of a single allele may have an effect.

Chapter 5

Truncation of CdTlo1 Protein

5.1. Introduction

5.1.1. Analysis of functional domains in *Candida* proteins

Polypeptides are frequently composed of multiple functional domains, which can have a distinct 3-D structure from the remainder of the protein. These functional domains can carry out separate functions, e.g. the N-terminus of Hsp90 in *Candida albicans* shows homology to other members of the heat shock protein family but also to members of the ATPase/kinase superfamily, while the C-terminus contains an alternative ATP-binding site which becomes accessible when the N-terminus is occupied (Marcu *et al.*, 2000; Söti *et al.*, 2002; Prodromou & Pearl, 2003). Interruption of functional domains can alter protein folding and result in changes in the conformation of a protein. A commonly used strategy to dissect the roles of specific domains is to truncate the protein and investigate the effect of truncation of one domain on the other. Chin *et al.* (2013) carried out an N-terminal deletion study on the *C. albicans* Cdc4 protein, which acts as a repressor of filamentous development (Atir-Lande *et al.*, 2004; Shieh, *et al.*, 2005). Chin *et al.* (2013) found that the N-terminus of Cdc4 was vital for filamentation and flocculation inhibition and, in the absence of the N-terminus, the truncated protein could suppress filamentation but not revert fully back to yeast form, as was observed for the full length protein. Chin *et al.* (2013) also observed that the N-terminal truncate was slower to reach exponential growth in a range of media and converted to filamentous growth earlier in repressed conditions and concluded that loss of the N-terminus impairs the ability to flocculate and the ability to reverse filamentous growth in *C. albicans*.

In another study of the functional domains of a *C. albicans* protein, Schubert *et al.* (2011) investigated Mrr1, a zinc cluster transcription factor that controls *MDR1* expression in response to chemical inducers. In this study, Schubert *et al.* undertook a systematic analysis of Mrr1 in *C. albicans* in order to identify the functional domains required to target it to the promoter of the *MDR1* efflux pump, to activate transcription in response to the inducer

benomyl, and to retain it in an active state when inducing conditions are absent. The results of this study revealed that the C-terminus of Mrr1 is dispensable for targeting Mrr1 to the *MDR1* promoter when fused to a heterologous transactivator domain. Schuber *et al.* also observed that in the absence of the N-terminal domain the C-terminus is not sufficient to stimulate *MDR1* expression, and noted that the absence of any region prevents Mrr1 from achieving inducible conformation and results in the protein becoming unstable.

5.1.2. Functional domains of the *TLO*s

A study carried out by Anderson *et al.* (2012) that characterised the expression and structures of the *C. albicans TLO*s organised them into clades based on sequence similarity. Briefly, the *TLO* genes were organised into three regions: the 5′ region (i.e. the N-terminus), which includes the proposed Med2 domain, a middle region of varying length and the 3′ region (i.e. the C-terminus) which is clade-specific and contributes to the majority of the variation between the TLOs. This study will be discussed further in Chapter 7. The *Candida dubliniensis TLO1* gene encodes a protein of 320 amino acids while the *TLO2* gene encodes a protein of 355 amino acids. The Cd*TLO*s share 58% identity, with 81% homology to each other concentrated in the Med2 domain-containing N-terminal region (Figure 5.1) (Haran *et al.*, 2014).

5.1.3. The use of epitope tagging

Epitope tagging is a technique used where a known epitope is fused to a recombinant protein using genetic engineering (Brizzard, 2008). Epitope tags are important tools for biochemical analyses such as affinity purification and protein level quantification (Gerami-Nejad *et al.*, 2009). Commonly used epitope tags include FLAG, 6 X His, HA and c-myc tags, while a further advancement in the technology is the use of multiple tags in order to increase the signal strength when used in detection applications (Brizzard, 2008). In this study a 3 X human influenza haemagluttinin (HA) tag was used. This tag may be used to detect proteins and

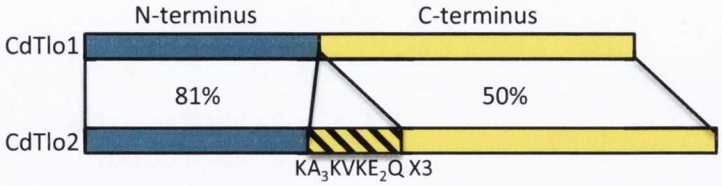

Figure 5.1. Structure of *C. dubliniensis TLO1* and *TLO2* genes. *TLO1* and *TLO2* encode proteins of 320 and 355 amino acids respectively that exhibit 81% identity in the N-terminal Med2-like domain, and 50% identity in the C-terminal of the protein. In addition, Tlo2 has an internal triplet repeat, indicated. Adapted from Haran *et al.* (2014).

peptides, and to facilitate functional analysis of proteins of interest (Field *et al.*, 1988). Generally, the tag is placed at either the N or C terminus of the target protein. These locations are usually preferred as they reduce the chances of interference in protein architecture as proteins tolerate additions at the termini more readily than at other sites. Furthermore, the termini are favorable because they are likely to be on the outside of the folded protein, rather than within the hydrophobic core (Jarvik and Telmer, 1998). There are a number of advantages associated with epitope tagging; a tag can be easily and rapidly added to a known location in a gene, multiple tags can be added to increase sensitivity, well-characterised antibodies are used against tags and specific antibodies can be used, which avoids cross-reaction with related proteins. One limitation of the use of epitope tagging is that the tagged proteins are often expressed using heterologous promoters, which can lead to abnormal gene expression (Jarvik and Telmer, 1998). Another limitation is that despite tagging the termini of proteins, tags can sometimes inhibit protein function.

5.1.4. Rationale for the truncation of CdTlo1

The presence of a Med2 domain at the N-terminal of the *TLO* ORFs originally suggested homology to Med2, which has been confirmed by Zhang *et al.* (2012). The C-terminus of the Tlo proteins is also proposed to contain a potent transactivator domain (Larry Myers, Dartmouth University, personal communication). Transactivator domains are regions of a transcription factor which, in conjunction with a DNA binding domain, can activate transcription by contacting transcriptional machinery (general transcription factors + RNA Polymerase). In order to investigate this hypothesis, we attempted to delete the N-terminal and the C-terminal domains of CdTlo1 respectively, in conjuction with the application of a 3X HA epitope tag in order to observe whether the presence of either the N-terminus or the C-terminus were sufficient to illicit a phenotype in the *Cdtlo*ΔΔ mutant background. It has also been observed by Zhang *et al.* (2012) that in *C. albicans* there is a large population of "Free" Tlo present after what is required for the yeast Mediator complex. If this substantial amount

of "Free" Tlo is present separate to Mediator, then it may be possible that the C-terminus could be carrying out functions independent to those associated with Mediator. A 3X HA epitope tag was added to the truncated Tlo1 protein to enable possible downstream protein purification and interaction experiments.

5.1.5. Aims of this section

Based on the findings of Zhang *et al.* (2012) we truncated the CdTlo1 protein into its functional domains in an attempt to elucidate whether each functional domain had the ability to restore the phenotypes we have previously observed independently of one another.

5.2. Results

5.2.1. Truncation of *CdTLO1*

The *TLO1* gene was truncated and tagged by amplifying the 5′ two-thirds of the gene using the primer pair P_tlo1_F/ N_tlo1_3XHA_R containing the restriction sites *Xho*I and *Hind*III, with the 3 X HA tag attached to the reverse primer (Table 2.2). This truncation deletes the C-terminus region (i.e. the remaining 366 bp). The truncated gene was amplified using the Expand High Fidelity PCR system (Roche Diagnostics Ltd.) according to manufacturers' instructions. The PCR product was cleaned up as previously described in Section 2.3.2. An untagged version of the N-*TLO1* strain was also constructed to ensure that any variation in expression levels or phenotype observed were as a result of the truncation, rather than the presence of an epitope tag. The purified DNA fragments for both the tagged and untagged strains were ligated to the pCDRI plasmid (which had also been digested with *Xho*I and *Hind*III) as described in Section 2.4.2. The ligation mixes were then transformed into *E. coli* XL10 Gold electrocompetent cells, which were plated onto L_{amp} agar as described in Section 2.4.3. Digesting plasmid DNA with the restriction enzymes *Xho*I and *Hind*III and identifying inserts of the correct size identified positive transformants. Following confirmation of correct inserts by DNA sequencing, the pCDRI plasmid containing the correct insert was linearised with the restriction enzyme *Nco*I and the digested product cleaned up as described in Section 2.3.2. pCDRI::N-*TLO1* linear plasmid DNA constructs were transformed into the *C. dubliniensis tlo*ΔΔ mutant by electroporation. Transformations were carried out multiple times, using a range of DNA concentrations from 0.5 μg-2 μg that yielded ~ 5 colonies when grown on NAT_{100} agar plates. Transformants containing the correctly tagged and untagged truncated genes were identified by PCR screening of isolated genomic DNA for the N-terminus of the *TLO1* gene and using the primer pair TAGR/M13R to confirm correct integration into the *CDRI* locus.

5.2.2. qRT-PCR expression analysis of truncated Tlo1

In order to measure the mRNA expression levels of the tagged and untagged N-*TLO1* constructs qRT-PCR was carried out under exponential growth (0.8 $O.D._{600}$ in YEPD) and hyphal inducing conditions (water supplemented with 10% w/v FBS). Expression levels were compared to wild type Wü284 and to a strain in which the intact *CdTLO1* gene was inserted into the *CDRI* locus of the *Cdtlo*ΔΔ mutant. The analysis was carried out using the comparative C_T method as previously described in Section 3.2.3. In YEPD, mRNA expression levels for all four strains were consistently low. The untagged N-*TLO1* strain exhibited the same expression levels as wild type, while the 3X HA-tagged N-*TLO1* is expressed at the same level of the full-length reintegrated *TLO1* as shown in Figure 5.2 (A). Expression was generally higher in water supplemented with 10% w/v FBS. Wild type was expressed the highest, while the tagged N-*TLO1* was the second highest, with expression at half that of wild type. The full *TLO1* and untagged N-Tlo1 strains were expressed at similarly lower levels, as shown in Figure 5.2 (B).

5.2.3. Effect of truncation of Tlo1 on hyphal induction in liquid medium

The ability of the truncated version of *CdTLO1* to restore the formation of true hyphae in the *Cdtlo*ΔΔ double mutant was tested. As previously observed, the wild type strain Wü284 and reintegrated full *TLO1* gene both produced 80%- 90% true hyphae by 4 hours of growth at 37 °C in water with 10% FBS [Figure 5.3 and 5.4 (A)]. The *Cdtlo*ΔΔ mutant, as previously observed, was unable to form true hyphae at any time point, with only pseudohyphae present [Figure 5.3 and 5.4 (B)]. The mutant expressing the tagged *CdTLO1* truncate behaved similarly to the *Cdtlo*ΔΔ double mutant, with only pseudohyphae being formed [Figure 5.3 and 5.4 (C)]. However, the untagged truncated *CdTLO1* was able to restore true hyphal formation to a certain extent, with 60% of cells truly hyphal at 4 h (Figure 5.3). Photomicrographs of cells expressing the untagged truncate at 4 h showed a mix of yeast cells and hyphal cells [Figure 5.4 (D)].

(A)

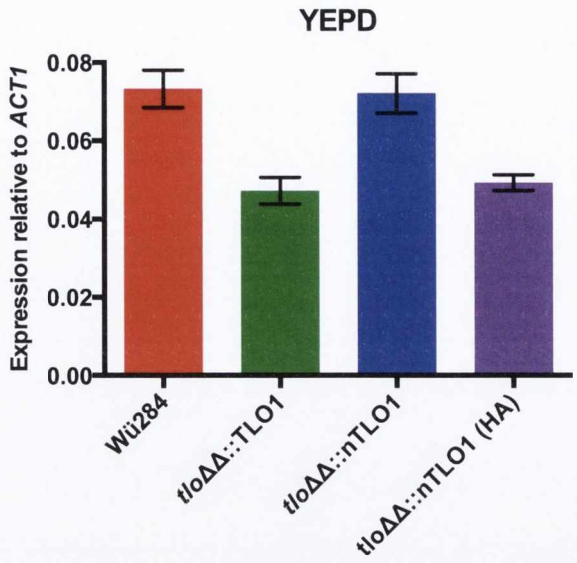

(B)

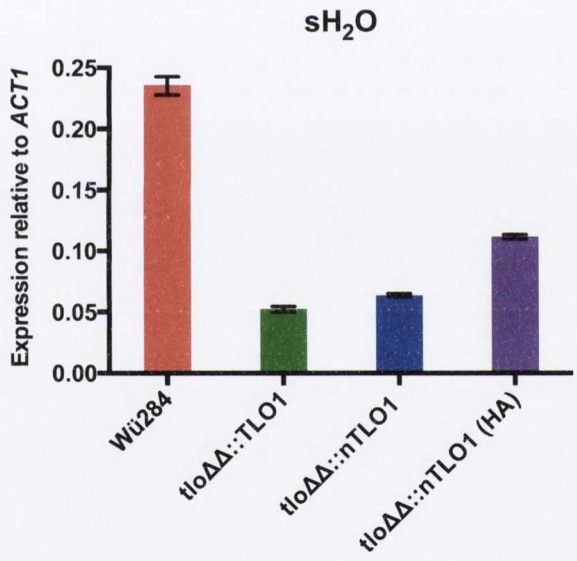

Figure 5.2. RNA expression levels of wild type Wü284, *Cdtlo*ΔΔ double mutant, n*TLO1* in the double mutant background without a HA tag and n*TLO1* in the double mutant background with a HA tag using primers for *TLO1.* **(A)** Represents RNA expression at exponential growth phase in YEPD (i.e. 0.8 $O.D._{600}$) and **(B)** represents RNA expression in hyphal-inducing conditions 10% (v/v) FBS in H_2O. Error bars represent the standard error of the mean (SEM) of three replicates.

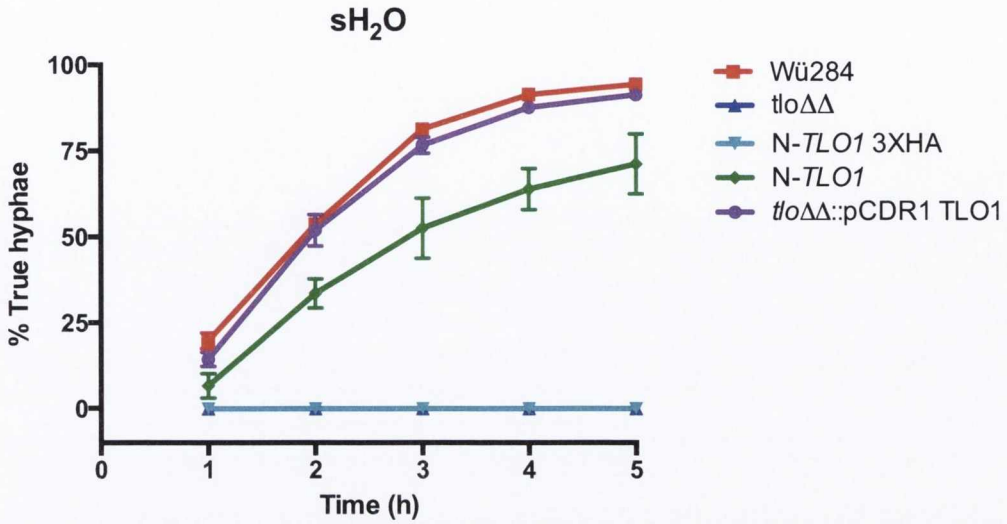

Figure 5.3. Rate of true hypha formation in wild type Wü284, *Cdtlo*ΔΔ, reintegrated *TLO1*, tagged and untagged N-*TLO1* under hyphal-inducing conditions (water with 10% v/v FBS). Percentage of true hyphae is represented as a proportion of 100 randomly selected cells. The experiment was carried out on three separate occasions. Error bars represent the standard error of the mean (SEM) of three replicates.

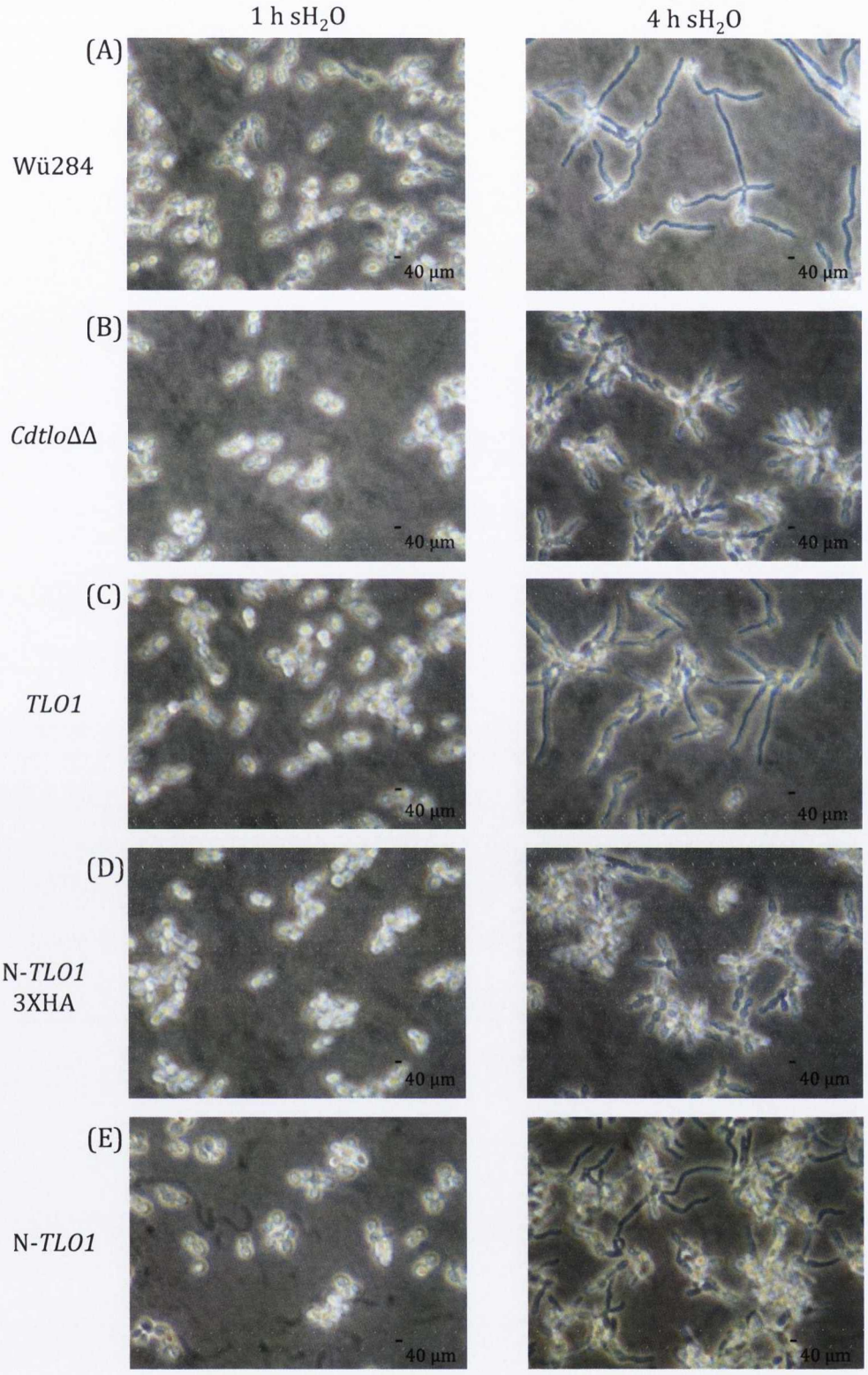

Figure 5.4. Images of **(A)** wild type Wü284, **(B)** *Cdtlo*ΔΔ, **(C)** reintegrated *TLO1,* **(D)** tagged and **(E)** untagged N-*TLO1* under hyphal-inducing conditions (water with 10 % v/v FBS). Photomicrographs of growth at 1 h and 4 h. Scale bar is equal to 40 µm.

5.2.4. Effect of truncation of Tlo1 on hyphal induction on solid medium

A single colony from a fresh YEPD plate of Wü284, *Cdtlo*ΔΔ mutant, pCDRI::*CdTLO1* in the *Cdtlo*ΔΔ background, 3X HA-tagged and untagged N-*TLO1* in the *Cdtlo*ΔΔ background were sub-cultured on fresh Spider medium agar plates. The plates were incubated at 37 °C in a static incubator for 5 days. Wild type Wü284 colonies were smooth on Spider medium, with no wrinkling observed [Figure 5.5 (A)]. The colonies formed by the *Cdtlo*ΔΔ mutant were very wrinkled [Figure 5.5 (B)]. Both the tagged and untagged truncated strains formed smooth colonies similar to those of Wü284 [Figure 5.5 (C) and (D)].

5.2.5. Effect of truncation of Tlo1 on growth rate in YEP-Gal

It has previously been shown that the deletion of the *TLO*s affected the ability of *C. dubliniensis* to grow in the presence of alternative carbon sources, such as galactose. In order to observe the effect of truncating Tlo1 on growth in an alternative carbon source, growth rates of Wü284, *Cdtlo*ΔΔ mutant, pCDRI::*CdTLO1* in the *Cdtlo*ΔΔ background, 3X HA-tagged and untagged N-*TLO1* in the *Cdtlo*ΔΔ background were measured. To examine the effect of the truncation of *CdTLO1* on the growth rate in galactose, the strains were grown first in YEPD overnight. The dextrose/glucose in YEPD was replaced by galactose and growth patterns at 37 °C were analysed for 10 h, as shown in Figure 5.6 (A). Data were fitted to a regression curve, as described in Section 2.2.4. and the doubling times were calculated [Figure 5.6 (B)]. In YEP-Gal, the wild type Wü284 had a doubling time of 94.9 min. As previously observed in *Cdtlo*ΔΔ disruption studies, the growth rate of the *Cdtlo*ΔΔ mutant was significantly increased at 142.1 min. The full *CdTLO1* reintegrant had a doubling time of 87.7 min. The 3X HA-tagged N-*TLO1* strain had a doubling time of 120.8 min, higher than that of wild type but not as slow as the double mutant. Interestingly, the untagged N-*CdTLO1* strain had a doubling time of 107.8 min, closer to that of wild type, and lower than the tagged truncate, indicating that the presence of the 3X HA tag could be affecting the metabolism of alternative carbon sources to glucose.

5.2.6. Effect of truncation of Tlo1 on oxidative stress tolerance

Spot plate experiments were performed to investigate if the truncation of *CdTLO1* affected growth in the presence of oxidative stress conditions induced by 5mM and 6mM H_2O_2 in combination with a nutrient-rich medium (YEPD). Strains were pre-incubated in 2 ml YEPD overnight. It was observed that the wild type strain Wü284 grew efficiently in the presence of H_2O_2, while, as expected, the ability of the *Cdtlo*ΔΔ mutant was greatly diminished. As previously observed, the presence of the full *CdTLO1* gene restored the ability to tolerate oxidative stress. The 3X HA-tagged N-*CdTLO1* grew poorly in the presence of 5 mM and 6 mM H_2O_2, however the untagged *CdTLO1* resulted in growth in the presence of H_2O_2 similar to that of the full *CdTLO1* gene, as observed in Figure 5.7.

5.2.7. Deletion of N-*CdTLO1*

It was also attempted to express a truncate of *CdTLO1* missing the 5′ two-thirds of the gene in the *Cdtlo*ΔΔ mutant background to observe if Tlo1 has activating activity and if the absence of the N-terminus that contains the Med2-domain had an effect on the phenotype. A strategy was designed to amplify the promoter and the 3X HA-tagged C-terminus and to fuse these amplicons together using PCR. Unfortunately, this strategy was unsuccessful; although we were able to amplify the promoter region we were unable to amplify the C-terminus alone.

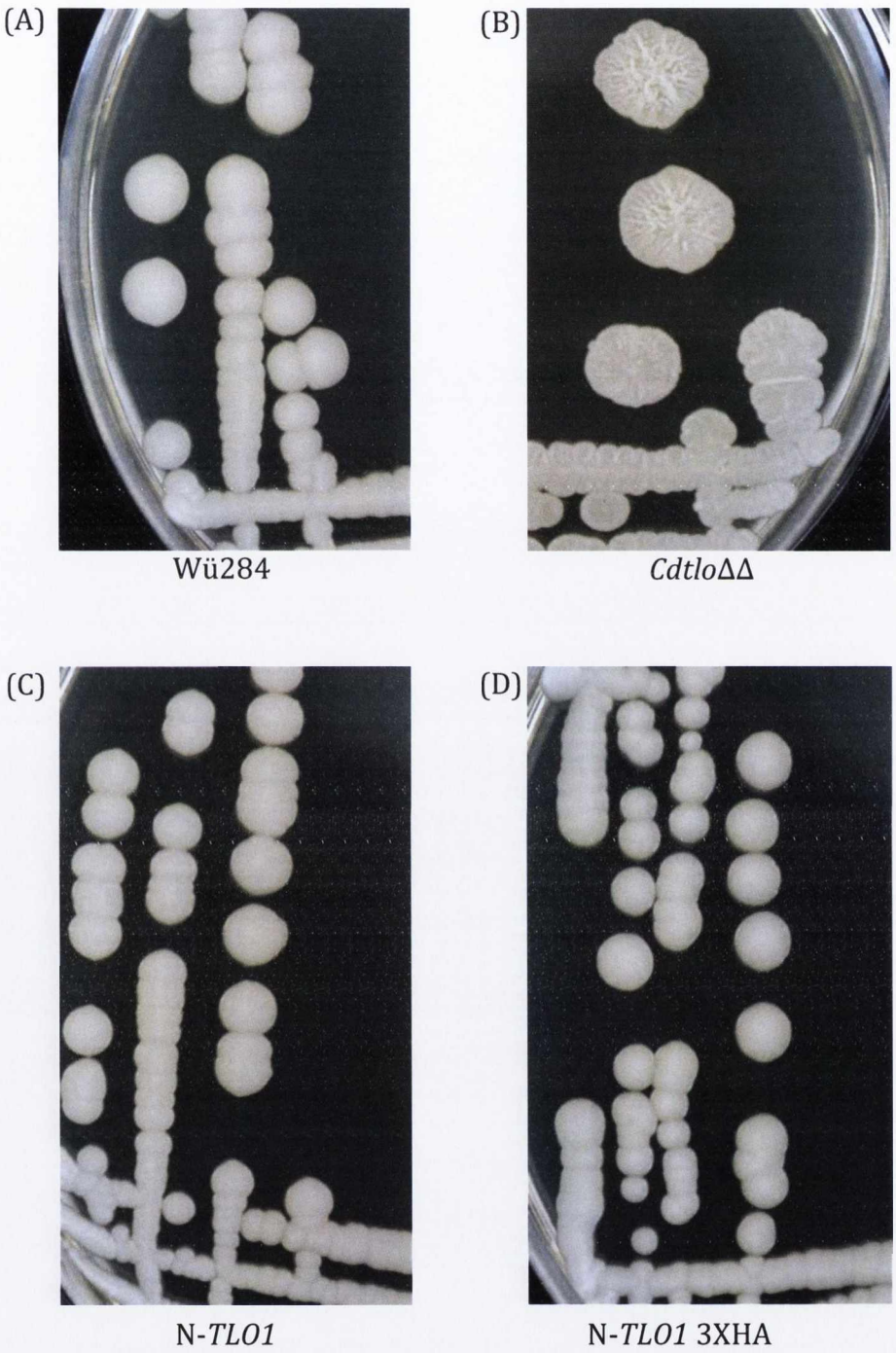

Figure 5.5. Growth of **(A)** wild type Wü284, **(B)** *Cdtlo*ΔΔ, **(C)** tagged and **(D)** untagged N-*TLO1* on solid Spider medium.

(A)

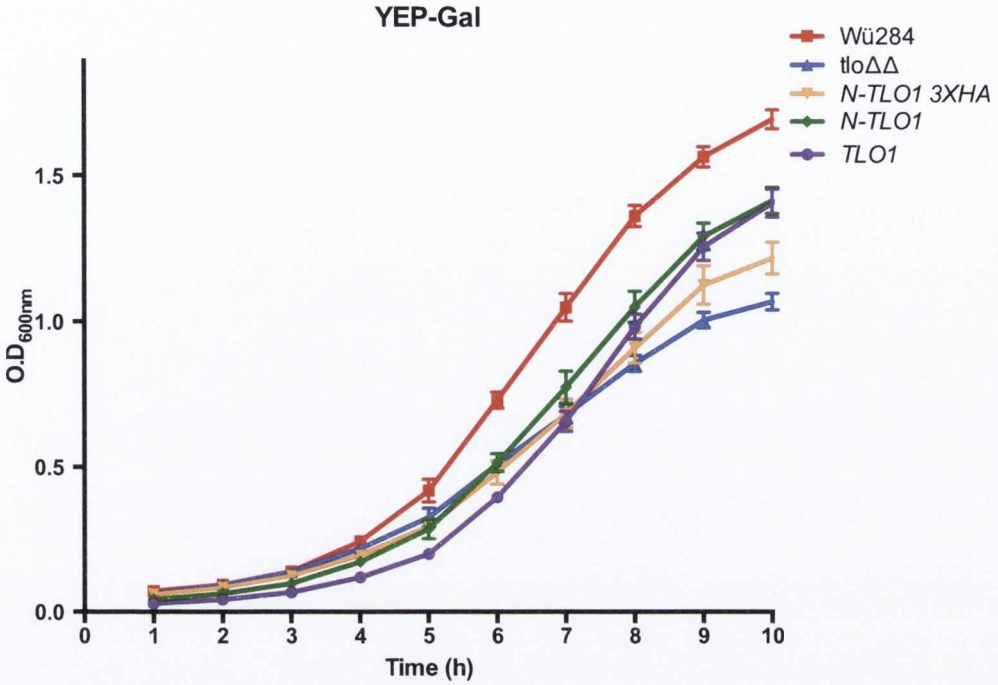

(B)

Strain	Wü284	tloΔΔ	N-*TLO1* 3XHA	N-*TLO1*	*TLO1*
Doubling time (min)	94.9 *+/- 7.9*	142.1 *+/- 11.0*	120.8 *+/- 3.4*	107.8 *+/- 6.2*	87.7 *+/- 1.2*

Figure 5.6. (A) Graph depicting growth rates of wild type Wü284, *Cdtlo*ΔΔ, reintegrated *TLO1*, tagged and untagged N-*TLO1* in nutrient-rich YEPD media with the dextrose/glucose substituted with galactose. **(B)** Doubling times, in minutes. Standard deviations are italicised below each value and represent an average of 3 replicates. Error bars represent the standard error of the mean (SEM) of three replicates.

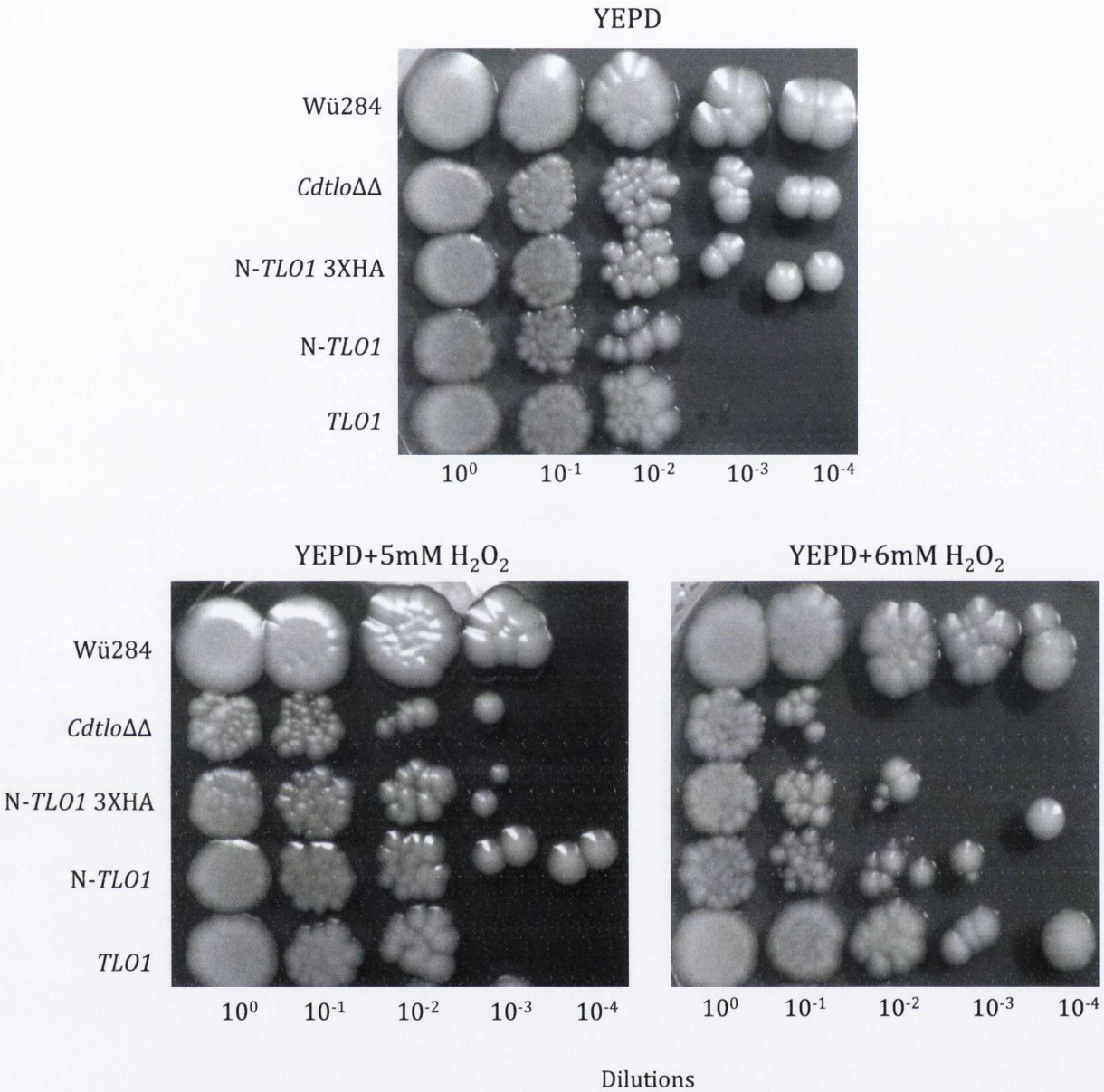

Figure 5.7. Growth of wild type Wü284, *CdtloΔΔ*, reintegrated *TLO1,* tagged and untagged N-*TLO1* in nutrient-rich YEPD media, YEPD supplemented with 5mM H_2O_2 and YEPD supplemented with 6 mM H_2O_2. Serial dilutions were carried out and 7 µl of each dilution plated.

5.3. Discussion

5.3.1. The effect of the deletion of the C-terminus on CdTlo1

The RNA expression level of the *CdTLO1* truncate in YEPD is similar to that of wild type gene expression in Wü284, suggesting that in nutrient rich conditions, the absence of the C-terminus of *CdTLO1* does not affect expression. In nutrient-poor, hypha-inducing conditions (i.e. H_2O supplemented with 10% v/v FBS) the expression of *CdTLO1* in the N-*TLO1* strain, both HA tagged and untagged, is significantly lower than wild type, however the level of expression is similar to that of the full-length *TLO1* gene. It is clear that the native promoter is more sensitive to hyphal-inducing conditions than nutrient-rich conditions given that the scale of mRNA expression is higher in the former than the latter, as can be seen in Figure 5.2. From the phenotypes studied, it is apparent that the low mRNA expression level of the truncated *CdTLO1* does not affect the phenotype, given that the expression level is similar to that of the full length *CdTLO1* gene, which can restore all phenotypes to levels similar to wild type. In hypha-inducing conditions the N-terminus of *CdTLO1* is sufficient to restore hyphal formation to 60% after 4 h incubation. As the full length *CdTLO1* reintegrant is 90% truly hyphal after 4 h, it would appear that the absence of the C-terminus of Tlo1 does have some impact on hypha formation but does not result in the loss of ability to form true hyphae.

Interestingly, the presence of a 3X HA epitope tag results in the inability of the truncate to form true hyphae. The presence of the tag also slows growth when YEP-Gal is used as an alternative carbon source. The 3X HA-tagged N-*CdTLO1* has a doubling time of 120.8 min, 20 mins less than the *CdtloΔ*Δ mutant, which has a doubling time of 142.1 min. However, in the absence of the tag, the truncate has a doubling time of 107.8 min, similar to that of wild type. The untagged N-*TLO1* truncated gene restores growth in oxidative stress conditions induced by H_2O_2, however the presence of the 3X HA tag results in the inability of the truncate to grow in the presence of H_2O_2.

5.3.2. Epitope tagging affects phenotypic expression

The truncated *TLO1* gene was tagged with a 3X HA epitope tag to allow for downstream protein interaction and purification applications. In order to ensure that a phenotype associated with the truncation of *CdTLO1* was due to the absence of the C-terminal and not the effect of the presence of a 3X HA tag, a truncate was also made without an epitope tag. Interestingly, it was observed that the presence of a 3X HA tag did in fact have an effect on all of the phenotypes previously associated with the *CdTLO*s. In the absence of the tag, N-*TLO1* had the ability to form true hyphae, grew at a similar rate to that of wild type in YEP-Gal and could grow in the presence of oxidative stress. These observations would suggest that the presence of an epitope tag affects the phenotype of N-*CdTLO1.*

An early review of epitope tagging carried out by Jarvik & Telmer (1998) surmised that most proteins could accept a tag at one terminus or the other without a severe loss of function. The surveying of the literature by Jarvik & Telmer (1998) also revealed that it is difficult to provide a quantitative estimate of the success of terminal epitope tagging as successful tagging experiments, where a functional and correctly localised protein are yielded, are more likely to be published than unsuccessful ones. However, it is clear from the data provided in this study that the presence of a 3X HA tag affected the function of the truncated CdTlo1 protein. It is difficult to hypothesise why the addition of the tag affected the functionality of CdTlo1, although according to the literature there is no simple correlation between the size of a tag and how well the tag is tolerated. In this experiment however, it is clear that the tag is somehow interfering with the structure and function of the Tlo1 protein.

5.3.3. Closing remarks

This section of the study describes the deletion of the C-terminal domain of the *Cd*Tlo1 protein. The C-terminus was deleted in an attempt to elucidate whether the N-terminal domain of CdTlo1 had the ability to restore the phenotypes we have previously observed. The

truncated protein is able to complement the *Cdtlo*ΔΔ mutant, which suggests that the C-terminus is not essential for the phenotypes observed. However, the phenotype is not restored as completely as it is in the full *TLO1* reintegrant, which suggests that the absence of the C-terminus affects the conformation of the protein. We also attempted to express the N-terminally deleted form of *CdTLO1* in the *Cdtlo*ΔΔ mutant background to observe if it had activating activity. A strategy was designed to amplify the promoter and the HA tagged C-terminus and to fuse these together. Unfortunately, we were unable to amplify the C-terminus by itself. The C-termini of Med2 proteins are highly variable and species-specific, and are thought to confer specificity for different transcription factors in different species (Novatchkova & Eisenhaber, 2004). It is possible that the the C-terminus may be unstable in the absence of the N-terminus, and thus could not be isolated without the N-terminus being present.

Chapter 6

Tandem affinity purification of CdTlo1 and analysis by mass spectrophotometry

6.1. Introduction

6.1.1. The abundance of Tlo proteins

As previously described a study carried out by Zhang *et al.* in 2012 revealed that 5 members of the 14 *Candida albicans* Tlo proteins are confirmed members of the yeast Mediator complex. Through silver staining, Western blotting and mass spectrometry they observed that Tloβ2, Tloα3, Tloα9, Tloα12, and Tloα34 could associate with Mediator. Given the homology between *C. albicans* Tlos it is probable that other expressed members of the Tlo family, such as Tloα1 and Tloα10, can also be incorporated into the yeast Mediator complex. Furthermore, *Candida dubliniensis* Tlo1 was also found to associate with Mediator. As previously suggested, the Tlo proteins are proposed to be orthologues of *Saccharomyces cerevisiae* Med2, a hypothesis that was strengthened as the level of CdTlo protein present is in a one-to-one ratio with other Mediator subunits, which is consistent with previous findings by Myers *et al.* that scMed2 is present in a 1:1 stoichiometric ratio with other members of the *S. cerevisiae* Mediator complex (Myers *et al.*, 1998, Zhang *et al.*, 2012). Further experimentation carried out by Zhang *et al.* (2012) led to the observation that after what is required for Mediator function, a substantial excess of Tlo protein is available in *C. albicans*, which lead to the hypothesis that the non-Mediator associated free Tlo protein may be carrying out non-Mediator associated functions.

6.1.2. Tandem affinity purification strategy

A limited number of proteins carry out their functions alone; most interact transiently with other proteins or are part of multi-subunit complexes. Many protein-protein interactions are dependent on subcellular location, transportation or post-translational modifications such as ubiquitination or phosphorylation. Purification of these complexes and identification of protein-protein interactions is crucial in helping to identify protein functions (Blackwell *et al.* 2003). Tandem affinity purification (TAP) tagging, in conjunction with mass spectrometry

was developed to allow for fast purification with high yield of protein complexes under standard conditions (Puig *et al.* 2001). The TAP-tagging method of protein purification involves the fusion of the TAP tag (see below) to the protein of interest to generate a TAP tag construct that is introduced into host cells. The TAP tag acts as a bait to purify protein complexes that aggregate to the tagged protein (Kaiser *et al.*, 2008). A natural level of protein expression is desirable as over-expression can result in interactions of the desired protein with non-natural partners (Swaffield *et al.*, 1996).

The TAP tag can be fused either C- or N- terminally. TAP-tagging is a two-step method made up of two IgG binding domains of staphylococcal protein A (ProtA) and a calmodulin binding peptide (CBP) separated by a tobacco etch virus (TEV) protease site to allow for cleavage. The Protein A component binds to an IgG-Sepharose matrix, and the TEV protease elutes the protein complex from the IgG-Sepharose. Binding to calmodulin-coated beads further purifies the eluate from the first affinity purification step. Contaminants and the remaining TEV protease are removed by washing and the purified protein is eluted by EGTA or TCA (Puig *et al.* 2001, Kaiser *et al.* 2008) (Figure 6.1).

6.1.3. SDS-PAGE separation of protein precipitates and protein detection using mass spectrometry

Sodium-dodecyl-sulphate polyacrylamide gel electrophoresis (SDS-PAGE) is a highly useful method to use in conjunction with TAP-tagging to identify protein interactions. SDS-PAGE enables the precipitated proteins to be separated into their subunits and provides information about the approximate stoichiometry of the proteins present. Furthermore, SDS-PAGE removes low molecular weight impurities such as detergents and buffer components, which can negatively impact results of mass spectrometry (Shevchenko *et al.*, 2007).

(A)

(B)

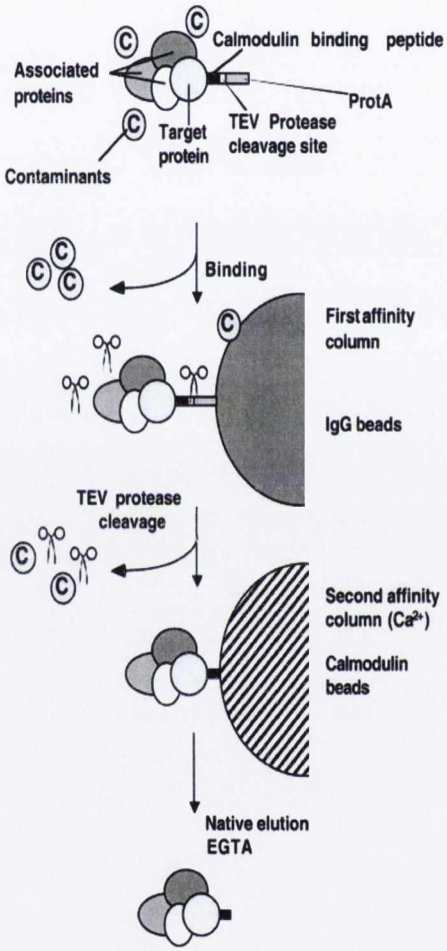

Figure 6.1. (A) Schematic representation of C-terminal TAP tag. **(B)** Overview of tandem affinity purification strategy. Adapted from Puig *et al.,* (2001).

A mass spectrometer typically consists of three main components; an ionization device, a mass separator and a detector (Figeys *et al.,* 2001). The most common forms of mass spectrometry performed to identify protein and peptide interactions are matrix-assisted laser desorption ionization time-of-flight (MALDI-TOF) and liquid chromatography (LC) mass spectrometry.

MALDI-TOF analysis involves co-crystallization of proteins and peptides in an acidified matrix (Nelson *et al.* 1994). The matrix consists of a small molecule that absorbs in the ultraviolet (UV) range and dissipates the absorbed energy thermally. A pulse laser beam rapidly transfers energy to the matrix, which causes the matrix to rapidly dissociate from the surface, generating a plume of matrix and the co-crystalized analytes into the gas phase, resulting in a small quantity of charged analytes present in the gas phase. The time of flight aspect of mass spectrometry measures the time it takes the analytes to travel across the chamber. After a time delay, the analytes are moved into the TOF tube (chamber) by a high voltage being applied to the MALDI plate, which generates a strong electric field between the MALDI plate and the TOF chamber entrance. Smaller analytes reach the chamber entrance quicker than large analytes, and thus reach the detector before larger analytes. The detector is synced with the laser shots and time delay, and measures the peptide and protein ions as they arrive over time. The mass range is calibrated using standards of known mass and charge, therefore the time-of-flight for an ion can be converted to masses, resulting in a spectrum that compares the intensity observed with ion (protein or peptide) mass (Figeys *et al.,* 2001).

Liquid chromatography (LC) mass spectrometry is typically used if the proteins of interest are present in very small concentrations. This form of LC mass spectrometry is a high performance liquid chromatography (HPLC) system with a mass spec detector. The HPLC separates particles on a column using reverse phase chromatography, where the metabolite

binds to the column by hydrophobic interactions in the presence of a hydrophilic solvent (e.g. water) and is eluted off by a more hydrophobic solvent (e.g. methanol). As the analytes appear from the end of the column they enter the mass detector, where the solvent is removed and the analytes are ionized. The mass detector then scans the molecules it sees by mass and produces a full high-resolution spectrum, separating all ions (proteins and peptides) with different masses.

Following peptide fractionation, typically the top three most intense precursor ions are selected for MS/MS fragmentation for every MS scan. Raw spectra are then processed and the sequences are submitted for database searching using databases such as MASCOT and SEQUEST (Eng *et al.*, 1994; Perkins *et al.*, 2009). Spectra matching with sequences in the database are scored by parameters such as mass accuracy and fragment ion matches and filtered to obtain high-confidence peptide identifications. Peptides are then clustered to protein sequences and scores are assigned to protein identifications, which are usually clustered to remove redundancy and common contaminant protein identifications (Keratin, trypsin, TEV, etc.). Proteins identified in the control purifications are subtracted from the list of proteins identified in the tagged-protein purification (Collins and Choudhary, 2008).

6.1.4. Aims of this section of the project

The aims of this section of the project were to confirm that the CdTlos are part of Mediator and to identify other proteins that they may interact with, either directly or indirectly. Evidence provided by Zhang *et al.* (2012) suggests that one of the two *C. dubliniensis* Tlos (Tlo1) can be detected within the Mediator complex. Tandem affinity purification and mass spectrometry were used in an attempt to identify protein interactions in order to discover other functions of the Tlo proteins in addition to the role they play within the yeast Mediator complex. Identification of interacting proteins, whether as part of a sub-complex or a

transient interaction could potentially aid us in the identification of additional functions of the Tlos.

6.2. Specific materials and methods

6.2.1. Buffers and solutions

HB wash buffer containing 25 mM Tris-HCl, 15 mM EGTA, 15 mM $MgCl_2$, 0.1% NP40, 1 mM DTT, 1 mM NaF and 1 mM PMSF was used to wash cells for immunoprecipitation experiments. IPP150 buffer containing 10 mM Tris-HCl, 150 mM NaCl and 0.1% NP40 was used to wash protein-binding beads. TEV cleavage buffer containing 50 mM Tris-HCl, 0.5 mM EDTA, 0.1% NP40 and 1 mM DTT diluted in ultrapure water was used to remove contaminants and TEV protease during protein purification.

6.2.2. PCR amplification and construction of TAP-tagged Tlo1 and Tlo2 cassettes

The tandem affinity purification (TAP)-tagged Tlo1 and Tlo2 fusion proteins were generated using the pFA-TAP-CaURA3 plasmid template and the Tlo1_TAP_F/ Tlo1_TAP_R and TAP_TLO2F/TAP_TLO2R primer pairs (Table 2.1)[Figure 6.2 (A)]. The primers consisted of ~100 bp specific to *TLO1* and *TLO2* and 20 bp homologous to pFA-TAP-CaURA3 plasmid in order to amplify the TAP tag and the $URA3^-$ marker for selectivity. The tag was to be fused to the *TLO1* and *TLO2* genes C-terminally [Figure 6.2 (B)]. PCR reactions were carried out in 50 µl volumes containing 100 ng of plasmid template with Expand High Fidelity PCR system (Roche Diagnostics Ltd.) following manufacturer's instructions. PCR parameters were 1 cycle at 94 °C, 5 min followed by 35 cycles at 95 °C, 30 sec; 58 °C, 1 min; 68 °C, 3 min.

6.2.3. Transformation by electroporation of Tlo1-TAP construct into Wü284 URA^-

A single colony of Wü284 Ura^- grown on a YEPD plate supplemented with 50 µg/ml uridine was inoculated into 50 ml of YEPD broth supplemented with 50 µg/ml uridine and grown overnight at 30 °C with shaking at 200 r.p.m in an orbital incubator to an $O.D._{600}$ of 1.6 to 2.0 (approximately 0.5 to 1.0 x 10^7 cells/ml). The protocol was followed as previously described

in Section 2.4.4. and the recovered cells were plated onto yeast nitrogen base (YNB) agar plates supplemented with amino acids (Sigma Aldrich).

6.2.4. Tandem affinity purification

6.2.4.1. Cultivation of cells

In order to grow the tagged (Tlo1-TAP) and untagged control (CD36) strains 10 L of YEPD broth were formulated and 1 L was decanted into 10 separate 2 L conical flasks. A loop of tagged and untagged cells were inoculated consecutively into 100 ml of YEPD and grown for 8 h at 30 °C with shaking at 200 r.p.m in an orbital incubator to generate the pre-inoculum. Each 1 L of YEPD was inoculated with 4 ml of the overnight pre-inoculum, with five of the 1 L flasks inoculated with the tagged strain and the other five 1 L flasks inoculated with the untagged strain. The ten cultures were grown overnight at 30 °C.

6.2.4.2. Harvesting of cells

Cells were harvested using a JA10 rotor (Beckman-Coulter, Indianapolis, USA), spun at 3000 r.p.m for 5 min. Each of the five individual flasks for both strains were pooled into two separate centrifuge pots by re-suspending in chilled dH_2O using a glass rod. Cells were washed once with chilled dH_2O. Each pellet was re-suspended in 20 ml chilled HB buffer with 1 protease inhibitor tablet added (Roche Diagnostics Ltd.). Cells were added drop-wise to liquid nitrogen through a 50 ml syringe to form frozen cell beads. Beaded cells were scooped into 50 ml Falcon tubes (Greiner Bio-One) with 2 holes pierced in the lid and stored at -80 °C overnight.

6.2.4.3. Grinding frozen cells

Prior to use, the grinding vessel was cooled by adding a small volume of LN_2. Untagged cells from five Falcon tubes (Greiner Bio-One) were added to the cooled vessel. A small amount of LN_2 was added, allowed to evaporate and the cells were ground for 15 s on a low setting. This

grinding procedure was repeated five times. The powder was scooped into pre-cooled Falcon tubes (Greiner Bio-One) with a pre-cooled spatula. The Falcon tubes were stored at -80 °C and the procedure was repeated for the tagged cells.

6.2.4.4. Immunoprecipitation

Powdered cell tubes were thawed in cold water at 4 °C for 1 h. Once thawed, phenylmethylsulfonyl fluoride (PMSF) (Sigma Aldrich) was added to the cells at a concentration of 1:100 (v/v). Tagged and untagged cells were poured into separate lidded centrifuge tubes and centrifuged at 3,000 r.p.m in a JA10 rotor (Beckman-Coulter) for 20 min. The supernatants were transferred to smaller centrifuge pots and centrifuged in a JA20 rotor (Beckman-Coulter) at 15,000 r.p.m for 1 h. The lipid layer was removed from each sample using a p1000 pipette (Star Labs, Germany) and discarded. The supernatants for both untagged and tagged cells were pooled separately. In a 15 ml Falcon tube (Greiner Bio-One) 4 ml of Sepharose IgG beads (GE Healthcare, Buckinghamshire, United Kingdom) were equilibrated with HB buffer and washed x 3 with 2 min spins at 400 r.p.m. Each sample was divided into 50 ml Falcon tubes (Greiner Bio-One) and 1.2 ml of IgG slurry was added to each tube. Tubes were sealed with Parafilm (Bemis, USA) and incubated for 2 h at 4 °C on a shaking platform. Tubes were centrifuged for 2 min at 400 r.p.m to pellet the IgG Sepharose beads (GE Healthcare). The majority of the supernatant was removed and discarded. The IgG Sepharose beads (GE Healthcare) were re-suspended in 5 ml HB buffer and like samples were pooled. Falcon tubes (Greiner Bio-One) were washed with HB buffer to transfer all beads. Beads were washed once with 2 ml of IPP_{150} (10 mM Tris-HCl (pH 8.0); 150 mM NaCl; 0.1% Nonidet P-40; 0.1% sodium azide) and pre-washed in 2 ml of TEV cleavage buffer and transferred to separate 1.5 ml microcentrifuge tubes (Eppendorf) for the tagged and untagged samples.

To each tube 500 µl TEV cleavage buffer and 30 µl TEV protease were added and the tubes were incubated for 1h at room temperature on a shaking platform. The tubes were washed twice with 750 µl TEV buffer and centrifuged at 400 r.p.m with 500 µl of TEV buffer added to the beads to elute the protein.

Calmodulin beads (Stratagene, Agilent) were equilibrated in 1 ml of binding buffer. The supernatant of each tube was transferred to a 15 ml Falcon tube and 1 ml of the calmodulin bead slurry was added. One milliliter of 2 mM $CaCl_2$ (Sigma Aldrich) was added to each supernatant and the tubes incubated with the calmodulin resin for 1 h at 4 °C. The resin from each tube was transferred to a separate poly-prep column (Bio-Rad, Hercules, California, USA). The columns for each sample were washed x 3 with 750 µl of binding buffer with the eluate collected in three 1.5 ml microcentrifuge tubes (Eppendorf) for each sample. The resin was eluted with 750 µl of calmodulin elution buffer (CEB), with the eluate collected in three separate microcentrifuge tubes per sample. Each 750 µl aliquot was TCA precipitated by adding 750 µl of 20% v/v TCA (Sigma-Aldrich) and incubated on ice for 30 min. Tubes were centrifuged at 13,000 r.p.m for 15 min at 4 °C. Each pellet was washed in 500 µl of acetone (Sigma Aldrich) and centrifuged at 13,000 r.p.m for 5 min at 4 °C. Each pellet was re-suspended in 10 µl SDS loading buffer (1 ml 100% glycerol, 500 µl β-mercaptoethanol, 3 ml 10% sodium dodecyl sulfate, 5 ml 4 X upper buffer, 0.5 g bromophenol blue, 250 µl dH_2O). The three like-samples for each strain were pooled and loaded onto an SDS-PAGE gel.

6.2.5. Separation of purified proteins by SDS-PAGE

A Criterion™ Precast Gel (Bio-Rad, USA) was placed in an electrophoresis gel tank (Thermo Fisher Scientific, Waltham, MA, USA) and immersed in 1X Tris-glycine-SDS Buffer (25 mM Tris, 192 mM glycine, 0.1% SDS). The gel was loaded with 6 µl of PageRuler™ protein ladder (Thermo Fisher Scientific, USA) and 30 µl of the untagged control sample and 30 µl of the tagged sample. The gel was run at 200 V for 1.5 h and rinsed x 3 with 100 ml dH_2O to remove

SDS and buffer salts. The gel was stained using enough Simply Blue™ safe stain (Invitrogen) to cover the gel in a plastic container with gentle shaking for 1 h. The gel was washed in 100 ml dH_2O for 1.5 h. Following washing, the gel was scanned and a photomicrograph was taken of the gel. Peptide bands were excised from the gel and sent to the mass spectrophotometry laboratory of the Aberdeen Proteomics Facility to be analyzed by mass spectrophotometry by Dr. David Stead.

6.3. Results

6.3.1. PCR amplification and construction of TAP-tagged Tlo1 and Tlo2 cassettes

In order to generate heterozygous TAP-tagged Tlo1 and Tlo2 strains, pairs of long oligonucleotides named Tlo1F/Tlo1R and Tlo2F/Tlo2R were generated that contained 100 bp homologous to the 3′ end of the gene of interest, i.e. *TLO1/TLO2* and 20 bp homologous to the pFA-TAP-CaURA3 plasmid, kindly provided by Professor Janet Quinn (The University of Newcastle) that contained the TAP tag and a *URA3* marker for selectivity [Figure 6.2 (A) and (B)]. The TAP-tag was amplified by PCR as described in Section 6.2.2. Upon amplification of a correct product of 2.4 kb, the PCR products were cleaned up as previously described in Section 2.3.2.

6.3.2. Transformation by electroporation of TAP construct into Wü284 Ura$^-$

The TAP tag construct was transformed into the *C. dubliniensis* Wü284 Ura$^-$ strain by electroporation. Transformations were carried out multiple times, using a range of DNA concentrations from 0.5 μg-5 μg that yielded an average of five colonies per transformation when plated onto yeast nitrogen base (YNB) agar plates with amino acids and incubated at 30 °C for five days. The presence of the *URA3* marker generates uridine, which allows colonies to appear on the agar. Transformants containing the correctly inserted *TLO1* and *TLO2* constructs were identified by PCR screening of isolated genomic DNA using oligonucleotides to confirm the presence and correct integration of the TAP tag, namely: Tlo1_TAPscrF/Tlo1_amp_R, Tlo2_TAPscrF/Tlo2_amp_R and Tlo1_ampF/Tlo1_integr_R, Tlo2_ampF/Tlo2_integr_R. Transformants with the correctly inserted constructs were also confirmed by DNA sequencing.

6.3.3. Expression confirmation of TAP-tagged strains

The TAP-tagged strains were sent to Professor J. Quinn's laboratory to confirm that the tagged *TLO1* and *TLO2* genes were being expressed. Seventy-five micrograms of protein extract from the tagged strains were subjected to SDS-PAGE on 12% (w/v) gels, and analysed by Western blotting probed with peroxidase anti-peroxidase which recognises the protein A of the Tap-tag. It was observed that the approximate molecular weight of Tlo1 was ~ 80 kDa (Figure 6.3). It was not possible to detect Tlo2, suggesting that the protein was not expressed at a high enough level to be detected by Western blot. As a result of this, immunoprecipitation of Tlo1 only was carried out.

6.3.4. Tandem affinity purification of CdTlo1

The mutant expressing the tagged *TLO1* gene and wild type CD36 control cells were grown, harvested, flash frozen and ground as described in Section 6.2.4. The immunoprecipitation procedure described in Section 6.2.4. resulted in a final volume of 30 µl of protein product for each Tlo1-TAP and CD36.

6.3.5. Separation of purified proteins by SDS-PAGE and analysis by mass spectrophotometry

The protein products for each strain were electrophoresed on a SDS-PAGE gel to separate the purified proteins. Protein bands present in the Tlo1-TAP lane only were excised from the gel, as were the equivalent blank gel spaces of CD36 and sent to Dr. David Stead (University of Aberdeen) for mass spectrophotometry analysis using MASCOT (Matrix Science, London, UK) which compares the acquired MS/MS spectrum to theoretical spectra generated from protein sequences in an appropriate database (Gingras *et al.*, 2005). Results were subjected to a p-value of greater than 0.05 with standard probability scoring, where the higher the score, the more peptides of a protein are present, which increases the possibility that the protein interacts with the protein of interest. A score greater than 22 indicates homology, while a

(A)

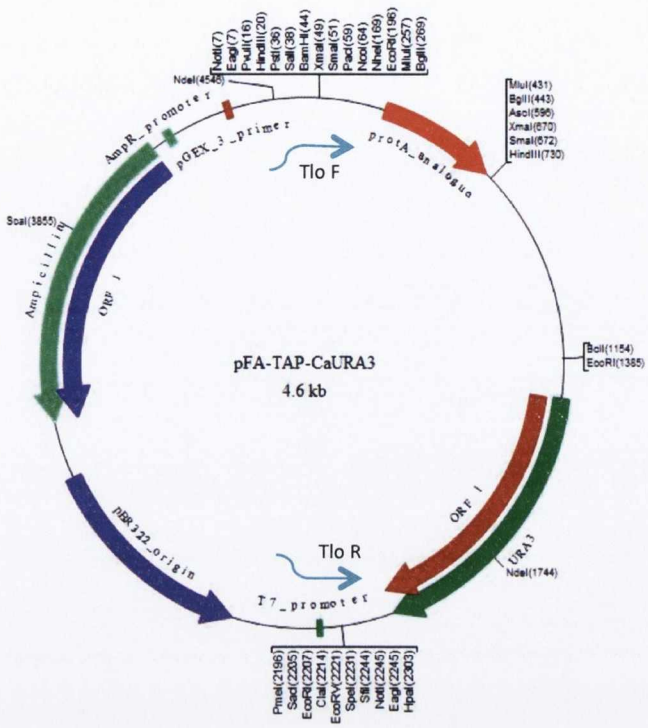

(B)

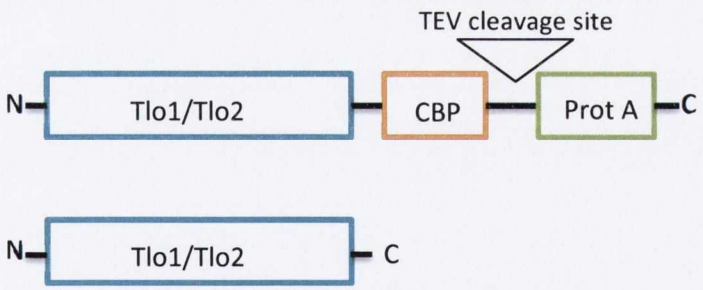

Figure 6.2. (A) Protein A-tagging plasmid used in this study, provided by J. Quinn (University of Newcastle) with blue arrows indicating primers with 100 base pairs of homology to the gene of interest used to amplify the Protein A analogue and URA3 marker. **(B)** Schematic representation of the heterozygous C-terminus tandem affinity tag fused to Tlo1/Tlo2. Adapted from Lavoie *et al.,* (2008).

Figure 6.3. Western blot visualising expression of TAP-tagged CdTlo1, which is indicated by the red arrow. Sourced from Dr. A. Day (Quinn Laboratory, University of Newcastle).

score greater than 29 indicates identity. Based on their CD36 numbers, twenty hypothetical interacting proteins were identified using the Candida Genome Database, as shown in Figure 6.4 and in Table 6.1. The scores for each identified protein that potentially interacts with Tlo1 are all above 29, indicating correct identity.

6.3.6. Putative interacting proteins of CdTlo1

The twenty proteins that were identified as possibly interacting with CdTlo1 carry out a diverse range of functions. Five Mediator subunits, Med17, Med5, Med16, Med15 and Med14 were co-purified with CdTlo1. Med14, Med15 and Med16 reside in the tail domain of the Mediator, while Med5 is part of the Cdk submodule and Med17 is part of the head submodule (Guglielmi *et al.*, 2004). All of the tail subunits, with the exception of Med3 were co-purified with CdTlo1. Two translation elongation factors were also pulled down with CdTlo1. Their proteins, Cef3 and Tef2 are involved in ribosome-dependent ATPase activity (Myers *et al.*, 1992). Rbl8B is a predicted ribosomal protein regulated upon the yeast-to-hypha switch (Nantel *et al.*, 2002). Three of the proteins co-purified with CdTlo1 have been identified in *Saccharomyces cerevisiae,* Nug1, Eis1 and Smy2. Nug1 is involved in GTPase and RNA binding and has roles in cell division and positive regulation of growth rate, as well as RNA processing (Bassler *et al.*, 2006).

The additional proteins pulled down with CdTlo1 are involved in a range of functions. Eis1 is a component of the eisosome with a possible regulatory role. It is required for correct eisosome assembly, and marks location for endocytosis (Anguilar *et al.*, 2010). Smy2 is a GYF domain protein involved in COPII vesicle formation and cytoplasmic mRNA processing (Higasho *et al.*, 2008). Srv2 is an adenylate cyclase-associated protein that regulates adenylate cyclase activity and is required for wild-type germ tube formation and for virulence in mice (Nobile *et al.*, 2012). Djp1 plays a role in peroxisome biosynthesis, while Nip1 is a putative translation initiation factor (Lan *et al.*, 2004; Lorenz *et al.*, 2004). Sro77 is a

fungal-specific protein induced during filamentous growth with a predicted role in docking and fusion of post-Golgi vesicles with the plasma membrane (Kadosh & Johnson, 2005). Slk19 is integral to the plasma membrane and has roles in cell wall organisation, pathogenesis and cytoplasm (Nobile *et al.*, 2003).

Examples of transcriptional regulators that appear to interact with Tlo1 are Cna1 and Try4. Cna1 is a catalytic subunit of calcineurin with roles in drug resistance, hyphal growth and virulence (Chen *et al.*, 2011). Try4 is a C2H2 transcription factor, involved in the positive regulation of cell surface targets of adherence regulator (CSTAR) genes, which are a group of 37 genes that code for cell wall or secreted proteins (Finkel *et al.*, 2011).

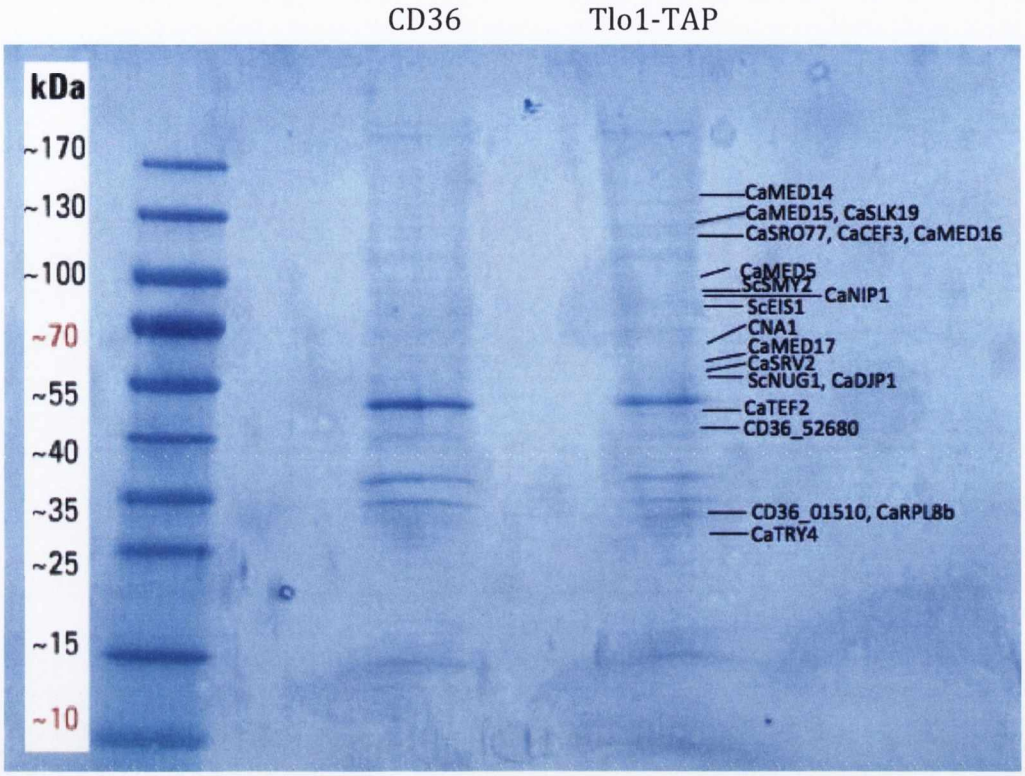

Figure 6.4. Photomicrograph of purified CdTlo1-TAP and CD36 and separated by SDS-PAGE. Predicted Tlo1-interacting proteins labeled on the gel.

Score	Protein (kDa)	Gene Name	Protein	Function
57.6	29	CD36_85230	CaRpl8B	Predicted ribosomal protein
67.4	29	CD36_01510	C1_0160W_A	Ortholog(s) have structural constituent of ribosome activity and 90S preribosome
31.9	44.4	CD36_52680	C5_02920W_A	Ortholog(s) have trimethyllysine dioxygenase activity and role in carnitine biosynthetic process
35.9	55.5	CD36_45730	ScNug1	Ortholog(s) have GTPase & RNA binding activity, role in cell division, positive reg of growth rate, rRNA processing
95.1	59.2	CD36_29500	CaSrv2	Adenylate cyclase-associated protein
77.3	55.5	CD36_09870	CaDjp1	Role in peroxisome biosynthesis
35.1	66.6	CD36_00650	Cna1	Catalytic subunit of calcineurin, involved in control of drug resistance, hyphal growth and virulence
29.2	62.9	CD36_03320	CaMed17	Putative RNA polymerase II mediator complex subunit; possibly an essential gene
49.5	95.7	CD36_41490	CaNip1	Putative translation initiation factor
36	110.5	CD36_30350	CaMed5	RNA polymerase II mediator complex subunit
48.9	118.4	CD36_72970	CaMed16	Putative RNA polymerase II mediator complex subunit
75.7	88.8	CD36_80780	ScEis1	Ortholog(s) have role in eisosome assembly
47.3	118.4	CD36_60360	CaSro77	Protein with a predicted role in docking and fusion of post-Golgi vesicles with the plasma membrane
40.9	118	CD36_50780	CaCef3	Translation elongation factor 3, possibly essential
35.4	99.9	CD36_46150	ScSmy2	Ortholog(s) have role in ER to Golgi vesicle-mediated transport and cytoplasmic mRNA processing
50.3	129.5	CD36_07790	CaMed15	RNA polymerase II mediator complex subunit; possibly an essential gene
62.1	140.6	CD36_52950	CaMed14	RNA polymerase II mediator complex subunit
66.6	51.8	CD36_07890	CaTef2	Translation elongation factor 1-alpha
60.4	129.5	CD36_87220	CaSlk19	Ortholog(s) have role in fungal-type cell wall organization, pathogenesis and cytoplasm, eisosome, integral to plasma membrane
31.3	32.6	CD36_85020	CaTry4	C2H2 transcription factor; required for yeast cell adherence to silicone substrate

Table 6.1. Proteins that putatively interact with CdTlo1 identified by mass spectrophotometry. CD36 number represents the *C. dubliniensis* gene annotation ID, protein names are representative of the protein homologue in *C. albicans* or *S. cerevisiae* as found in the CGD. The function is putatively based on predictions found in the CGD.

6.4. Discussion

6.4.1. Interacting proteins of CdTlo1

The purpose of these TAP-tagging experiments was to confirm that CdTlo1 is a component of the yeast Mediator complex and to identify what other proteins it may interact with, either directly or indirectly. The findings that yeast Mediator subunits were co-purified with CdTlo1 in the TAP-tagging experiment further supports the role of the Tlos in the Mediator complex. All of the tail subunits, i.e. Med5 Med16 and Med15 were found to be co-purified with CdTlo1, with the exception of Med3. The finding that Med3 was not co-purified with CdTlo1 could possibly mean that CdTlo1 does not interact with Med3 directly within the Mediator. It is thought that the tail module of the Mediator plays a direct role in transcriptional regulation, while the middle and head submodules are involved in regulation and interaction with Pol II respectively (Ansari *et al.*, 2011). Med14 from the middle submodule and Med17 from the head submodule were also co-purified with CdTlo1. In *Saccharomyces cerevisiae* Med17 was observed to be an essential component of Mediator (van de Peppel, 2005). Med14 bridges the tail and middle submodules (Dotson *et al.*, 2000; Guglielmi *et al.*, 2004). Therefore, if Med14 is anchored to Med16 to form this bridge, it is not surprising that Med14 was co-purified with CdTlo1.

Proteins involved in a wide range of functions were co-purified with CdTlo1, including proteins with ribosomal functions (such as Rpl8B and CD36_01510), translation proteins Cef3 and Tef2 and RNA processing functions, such as Nug1 and Smy2. Interestingly, proteins with virulence-associated functions such as Slk19 and Cna1, were also co-purified. The interaction of CdTlo1 with proteins involved in a range of functions is unsurprising given that the yeast Mediator complex is involved in a number of diverse processes. It is noteworthy that CdTlo1 pulled down the transcription factor Try4, given that it is common for transcriptional regulators to interact with other transcriptional regulators.

In *S. cerevisiae* the Mediator tail, including Med2, interacts with activators of transcription to facilitate inducible gene transcription and is thought to play an important role in the regulation of stress responses and nutrient acquisition (Ansari *et al.,* 2011). These roles could translate to *Candida* species, given that roles in stress response, nutrient acquisition and gene induction had been previously associated with the Tlos.

6.4.2. Confirmation of CdTlo1 protein interactions

The co-purification of the regulators Cna1 and Try4 could potentially indicate examples of direct interaction with CdTlo1. In order to confirm that these interactions with CdTlo1 are not an artefact, co-immunoprecipitation experiments will be carried out in the future to observe whether CdTlo1 is co-purified with Cna1 and Try4. Although it should be noted that it has been proposed that interactions of Mediator with promoters could be transient. (Fan & Struhl, 2009).

6.4.3. A TAP-tagging study in *Candida albicans* Mediator

In 2014, Tebbji *et al.* carried out TAP-tagging studies on CaMed7, following the observation that the deletion of the *MED7* gene in *C. albicans* resulted in the loss of a number of functions. Although it was observed that Med7 was not essential for viability in *C. albicans* as it is in *S. cerevisiae,* the deletion of *MED7* resulted in the inability of cells to colonise the GI tract of a mouse model, the mutant grew poorly in alternative carbon sources to glucose such as galactose, fructose and mannose and, interestingly, could not form true hyphae (Tebbji *et al.,* 2014). TAP-tagging was carried out on Med7 and 179 *C. albicans* proteins were identified, including 15 of the 25 Mediator subunits. This number of proteins is significantly higher than the number of proteins that co-purified with CdTlo1, although the number of proteins pulled down generally depends on the method of detection. Given that the samples used in our study were subjected to SDS-PAGE and staining, as were those used in the Tebbji *et al.* study, it is probable that they carried out the experiment on more than one occasion. Furthermore,

protein detection can be limited by the sensitivity of the stain, which could also explain the significant difference in the number of proteins co-purified in this study and the Tebbji *et al.* study.

6.4.4. The "free" Tlo protein of *C. albicans*

Zhang *et al.* (2012) have observed through biochemical characterisation studies that *C. albicans* cells contain an excess of non-Mediator-associated Tlo protein. Purification of the *C. albicans* Mediator and the use of mass spectrometry identified the presence of several Tlo proteins but did not reveal the existence of a non-Mediator associated form. In order to quantify the amount of Tlo protein in the cell in comparison to other Mediator subunits, five Tlo and two Mediator subunits were HA-tagged. Western blotting revealed that the five Tlos were expressed and the combined expression levels of the five Tlos vastly exceeded the expression levels of the other Mediator subunits. Zhang *et al.* (2012) hypothesised that seeing as *S. cerevisiae* Mediator subunits are present in a stoichiometric ratio (Myers *et al.*, 1998), there must be a large population of non-Mediator associated Tlo. This "free Tlo" is thought to be at least 10-fold more abundant than the Mediator-associated form (Sullivan *et al.*, 2015). In order to determine if the excess CaTlo population discovered by Zhang *et al.* (2012) is carrying out other functions separate to those governed by Mediator, it may be interesting to carry out protein purification experiments on the CaTlos, although the presence of 14 CaTlos represents a daunting challenge.

6.4.5. Closing remarks

The results of the TAP-tagging experiment confirmed that the Tlos are subunits of the Mediator tail module and suggest that the Tlos are carrying out additional roles that Mediator may not be involved in. Zhang *et al.* (2012) observed that Mediator purified from a *med3*Δ mutant in *C. albicans* did not contain the Tlo subunit, which suggests that the Tlos are anchored to Mediator via Med3. This finding is interesting considering Med3 was not co-

purified with CdTlo1, which could mean that they do not interact directly. In the future it may be worthwhile to TAP-tag CdTlo1 in a *Cdmed3Δ* mutant background and observed whether Mediator subunits co-purify with CdTlo1.

Chapter 7

Construction of *C. dubliniensis tlo*ΔΔ mutant expressing *C. albicans TLO* genes

7.1. Introduction

7.1.1. The role of telomeres

Telomeres are the sequences at the end of linear eukaryotic chromosomes that maintain genomic stability and protect the chromosome from degradation. The sequences adjacent to the telomere, known as subtelomeres are often characterised by repetitive, gene-poor sequences of heterochromatin with varying lengths (Pryde *et al.*, 1997; Mefford & Trask, 2002; Kupiec. 2014). Subtelomeric sequences and their organisation are generally poorly characterised as a result of their repetitiveness and highly similar sequences (Gardner *et al.*, 2002). Subtelomeres are made up of two sections that differ in their repetitiveness and divergence (Anderson *et al.*, 2015). The sequences closest to the telomeres are made up of 1-4 short tandem repeats, while the sequences furthest from the telomeres encode unique genes, gene families and repetitive elements that vary in their frequency (Pryde *et al.*, 1997). These loci are potential sources of genomic instability, as they can recombine with telomeric sequences (Aksenova *et al.*, 2013; Gazy & Kupiec, 2013). In eukaryotes, subtelomeres are often the most variable region of the genome, which can be partially attributed to the presence of single nucleotide polymorphisms (SNPs) and insertions/deletions (indels) (Carreto *et al.*, 2008; Brown *et al.*, 2010). This variability means the subtelomeres are the ideal environment for rapid gene evolution, which is a genetic response to growth in new and stressful environments (Dujon, *et al.*, 2004; Carreto *et al.*, 2008). The telomere-associated (*TLO*) gene family in *Candida albicans* is an example of telomeric gene family expansion. The *TLO*s are the gene family that has undergone the greatest gene expansion in *C. albicans* in comparison to the other less pathogenic *Candida* species (Butler *et al.*, 2009).

7.1.2. The *TLO* genes of *Candida albicans*

The *TLO* genes are the only widespread subtelomeric family in *C. albicans* (van het Hoog *et al.*, 2007). *Candida albicans* SC5314 strain has 14 functional *TLO* genes, and 13 of these genes

are located within 12 kb of a telomere and are often the terminal predicted open reading frame (ORF) of each chromosome arm. The *TLO*s can be found at all but three chromosome arms; Chr2R, Chr6R and Chr7L, with a single *TLO* located at an internal locus on chromosome 1 (Anderson *et al.*, 2012). In 2012, Anderson *et al.* characterised the structure and expression patterns of the *C. albicans TLO* genes, and through phylogenetic analysis found that the *TLO* genes can be distinguished by three clades, α, β and γ (Figure 7.1). The clades differ by the presence of indels in the C-terminus of the gene that alter the coding sequences. Within a clade, the *TLO*s are approximately 97% identical, however when indels are excluded, there is 82% homology between clades. The five *TLO*α clade genes are between 675-750 base pairs (bp) in length, the single *TLO*β is 822 bp long, while the seven *TLO*γ clade genes are the shortest at approximately 525 bp in length. Tlo proteins encoded by the three clades can be detected in the nucleus and the Tloγ proteins have also been detected in the mitochondria. The gene expression levels vary between clades, with *TLO*α genes expressed the highest and *TLO*γ clade genes expressed at much lower levels (Anderson *et al.*, 2012).

The N-terminus of the Tlo proteins contains a conserved Med2 domain, followed by a repetitive region of variable length that is gene-specific (Anderson *et al.*, 2012; Zhang *et al.*, 2012). The presence of the Med2 domain suggests that the multiple *TLO* genes may encode interchangeable components of the yeast Mediator complex (Zhang *et al.*, 2012). The broad range of expression levels and alternative localisation patterns have been proposed to contribute to a range of Mediator complex subunit compositions, which could facilitate *C. albicans* adaptation to the wide range of host niches it can occupy (Anderson *et al.*, 2012). While characterising the *CaTLO*s, Anderson *et al.* (2012) identified two tandem ORFs on the right arm of Chr1. The centromere proximal *TLO*, previously identified as *TLO4*, lacks the Med2 domain and the conserved *TLO* promoter sequence, with no transcript detected by qRT-PCR. This gene was named *TLO*ψ*4* and characterised as a pseudogene. The telomere proximal *TLO* has been characterised as *TLO*γ4 and is expressed and encodes a protein

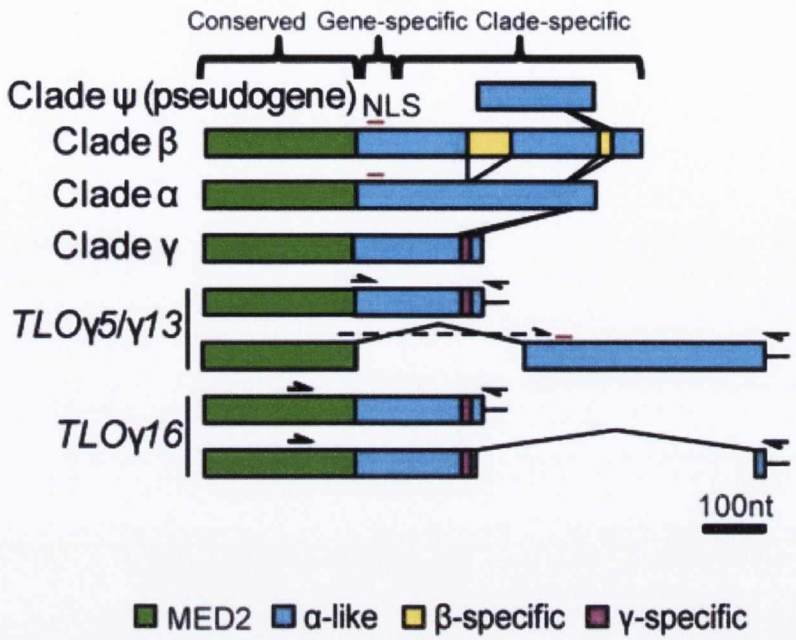

Figure 7.1. The clades of the *Candida albicans TLO* gene family. The conserved Med2 domain is highlighted in green, while the insertion of clade specific sequences are colour coded as indicated. Adapted from Anderson *et al.* (2012).

containing the Med2 domain, similar to the other *TLO* genes. Therefore, *C. albicans* contains 14 transcribed *TLO* genes and one pseudogene (Anderson *et al.*, 2012).

7.1.3. The cross-functionality of the Tlos of *C. albicans* and *C. dubliniensis*

Previous studies carried out in our laboratory have demonstrated that there is a degree of cross-functionality between the *C. albicans TLO*s and the *C. dubliniensis TLO*s. A *tlo1*Δ mutant strain was constructed and was observed to have decreased ability to form true hyphae under hyphal-inducing conditions (i.e. water supplemented with 10% w/v FBS) in comparison to *C. dubliniensis* wild type Wü284. However, upon complementation of the *tlo1*Δ mutant strain with *CaTLO11* and *CaTLO12* independently, hyphal formation was restored to higher levels than that of wild type (Figure 7.2) (Jackson *et al.*, 2008).

7.1.4. Aims of this section of the project

The aims of this section of the project were to systematically complement the *Cdtlo*ΔΔ mutant strain with representative *CaTLO*s in order to observe whether the *CaTLO*s could reverse the phenotype associated with the absence of the *TLO*s in *C. dubliniensis*, i.e. inability to form true hyphae, sensitivity to oxidative stress induced by H_2O_2 and slow growth in an alternative carbon source (YEP-Gal). Furthermore, we also aimed to determine whether the *CaTLO*s carried out different functions to each other, and to observe whether certain *CaTLO*s could restore the phenotype more successfully than others. Of the 14 *CaTLO* genes, we were able to complement the *Cdtlo*ΔΔ mutant with *CaTLO1*α, *CaTLO3*α and *CaTLO4*γ (using the Anderson *et al.*, 2012 nomenclature) to investigate whether clade variation results in a variation of gene function.

7.2. Specific materials & Methods

7.2.1. RNA extraction of cells pre-cultured in YEPD supplemented with H_2O_2

The *Cdtlo*ΔΔ mutant expressing *Candida albicans TLO1* and *TLO4* cells to be used in DNA microarray experiments were grown in 2 ml overnight cultures of YEPD at 30 °C. The cells were then standardised to an $O.D._{600}$ of 0.1 in 100 ml of YEPD and grown to an $O.D._{600}$ of 0.8 at 37 °C. Each culture was divided into two 50 ml cultures, with one treated with 5 mM H_2O_2 and both cultures were incubated for a further 30 min at 37 °C. Before centrifugation, 10 µl of each H_2O_2-treated culture was examined under a confocal microscope to ensure the cells remained viable after exposure to 5 mM H_2O_2. The cells were then flash frozen in LN_2 and RNA extraction was carried out as described in Section 2.3.3. The DNA Microarray protocol was followed as described in Section 2.5., with the microarray tile layout described in Figure 7.3.

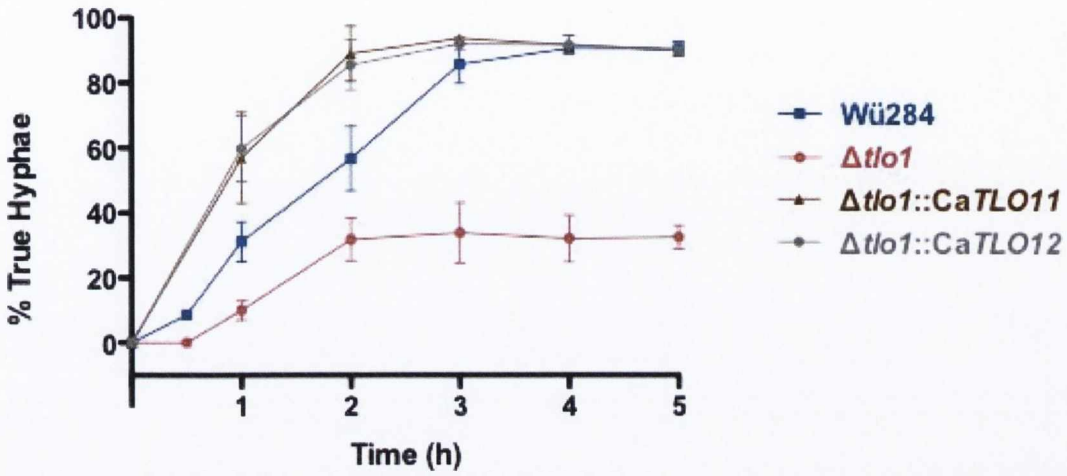

Figure 7.2. Previous studies demonstrated a degree of cross-functionality between the *Candida albicans TLO* genes and the *Candida dubliniensis TLO* genes. Graph depicting true hypha formation in *C. dubliniensis* wild type Wü284, *tlo1*Δ where one allele of *CdTLO1* has been deleted and *tlo1*Δ complemented with *CaTLO11* and *CaTLO12*. Adapted from Jackson *et al.* (2008).

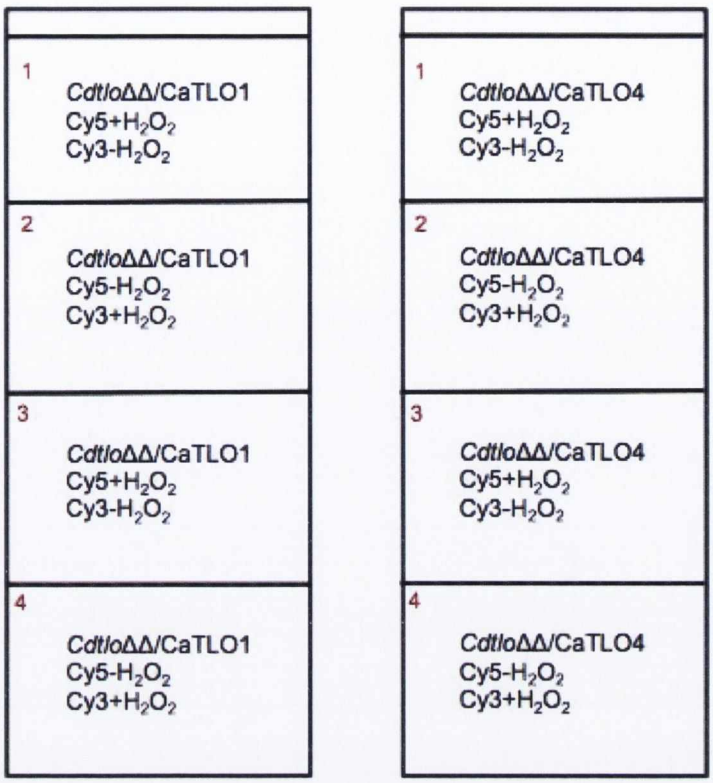

Figure 7.3. Representation of layout microarray tile for *CaTLO1* and *CaTLO4* DNA microarrays outlining method for pre-treating cells with H_2O_2 where + indicates treated with H_2O_2 and – indicates untreated with H_2O_2.

7.3. Results

7.3.1. Generation of *CaTLO* plasmid constructs

In order to introduce a single allele of *Candida albicans TLO1, TLO3* and *TLO4* into the *CDRI* locus in the *Candida dubliniensis tlo*ΔΔ mutant background primer pairs were designed for each gene containing the restriction sites *Xho*I and *Hind*III, namely CaTLO1F/CaTLO1R, CaTLO3F/CaTLO3R and CaTLO4F/CaTLO4R (Table 2.2.). These primer pairs were used to amplify *CaTLO1, CaTLO3* and *CaTLO4* from *C. albicans* wild type SC5314 using the Expand High Fidelity PCR system (Roche Diagnostics Ltd.) according to manufacturers' instructions. The 1.6 kb, 1.4 kb and 1.3 kb PCR products respectively were cleaned up as previously described in Section 2.3.2. The purified DNA fragments were ligated to the pCDRI plasmid (which had also been digested with *Xho*I and *Hind*III and cleaned up) as described in Section 2.4.2. The ligation mixes were then transformed into *E. coli* XL10 Gold electrocompetent cells, which were plated onto L_{amp} agar as described in Section 2.4.3. Digesting plasmid DNA with the restriction enzymes *Xho*I and *Hind*III and identifying inserts of the correct size identified positive transformants. Following confirmation of correct inserts by DNA sequencing, the pCDRI plasmid containing a correct insert for each *C. albicans TLO* gene was linearised with the restriction enzyme *Eco47*III and the digested product cleaned up as described in Section 2.3.2.

7.3.2. Transformation of Ca*TLO* plasmid constructs by electroporation into *Cdtlo*ΔΔ and selection with nourseothricin

pCDRI::*CaTLO1,* pCDRI::*CaTLO3* and pCDRI::*CaTLO4* linear plasmid DNA constructs were transformed into the *Cdtlo*ΔΔ mutant by electroporation. Transformations were carried out multiple times, using a range of DNA concentrations from 1 μg-2 μg that yielded ~ 30 colonies for pCDRI::*CaTLO1* and pCDRI::*CaTLO4*, ~ 5 colonies for pCDRI::*CaTLO3* when grown on NAT_{100} agar plates. Transformants were identified by PCR screening of isolated genomic

DNA for the *CaTLO1, CaTLO3* and *CaTLO4* genes and using the primer pair TAGR/M13R to confirm correct integration into the *CDRI* locus.

7.3.3. qRT-PCR expression analysis of *C. albicans TLOs* in *Cdtlo*ΔΔ

In order to measure the mRNA expression levels of *CaTLO1, CaTLO3* and *CaTLO4* in the *Cdtlo*ΔΔ mutant background, qRT-PCR was carried out under exponential growth conditions (0.8 $O.D._{600}$ in YEPD) and compared to *C. albicans* wild type SC5314. The analysis was carried out using the comparative C_T method as previously described in Section 3.2.3. The expression of the three *TLOs* was far lower in the *Cdtlo*ΔΔ mutant background than in wild type. *CaTLO1* expression in SC5314 was 10-fold higher than when introduced to the *Cdtlo*ΔΔ mutant background, as was *CaTLO3* expression. The expression of *CaTLO4* was 100-fold lower in the *Cdtlo*ΔΔ mutant than in SC5314, and had the lowest expression of the three *CaTLOs* (Figure 7.4).

7.3.4. Induction of hyphae in liquid media

The ability of the *CaTLOs* to restore the formation of true hyphae in the *Cdtlo*ΔΔ double mutant was tested. The *C. albicans* wild type strain SC5314 was 100% hyphal and *C. dubliniensis* wild type strain Wü284 was 90% hyphal by 4 hours of growth at 37 °C in water supplemented with 10% FBS. The *Cdtlo*ΔΔ mutant, as previously observed, was unable to form true hyphae at any time point, with only pseudohyphae present. The *Cdtlo*ΔΔ mutant expressing the *C. albicans TLOs* were all able to form true hyphae and were 90% - 100% truly hyphal by 5 hours of growth (Figure 7.5 and Figure 7.6). One notable difference between the *CaTLO* constructs was that the *Cdtlo*ΔΔ::*CaTLO3* hyphae appeared to be more clumped than the hyphae formed by *Cdtlo*ΔΔ::*CaTLO1* and *Cdtlo*ΔΔ::*CaTLO4.*

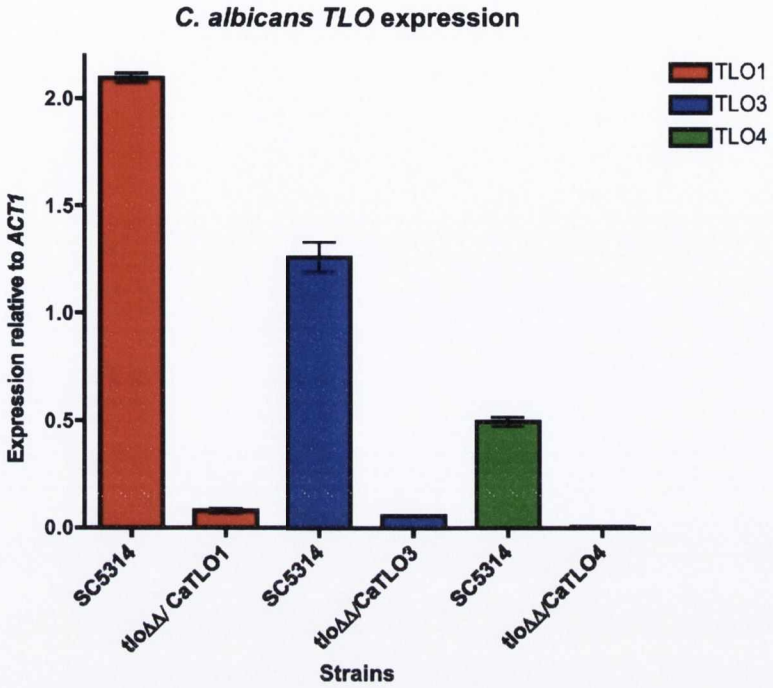

Figure 7.4. RNA expression levels of *Candida albicans* wild type SC5314, *CaTLO1, CaTLO3* and *CaTLO4* in the *Candida dubliniensis tloΔΔ* double mutant background during exponential growth phase in YEPD (0.8 $O.D._{600}$). Error bars represent the standard error of the mean (SEM) of three replicates.

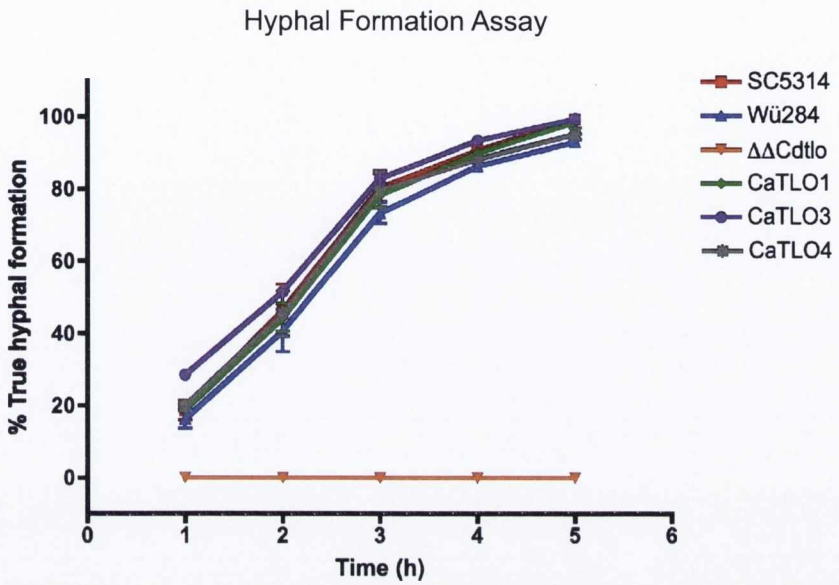

Figure 7.5. True hypha formation in *Candida albicans* wild type SC5314, *Candida dubliniensis tlo*ΔΔ mutant, and *CaTLO1, CaTLO3* and *CaTLO4* in the *Cdtlo*ΔΔ mutant background under hyphal-inducing conditions (water with 10% v/v FBS). Percentage of true hyphae is represented as a proportion of 100 randomly selected cells. The experiment was carried out on three separate occasions. Error bars represent the standard error of the mean (SEM) of three replicates.

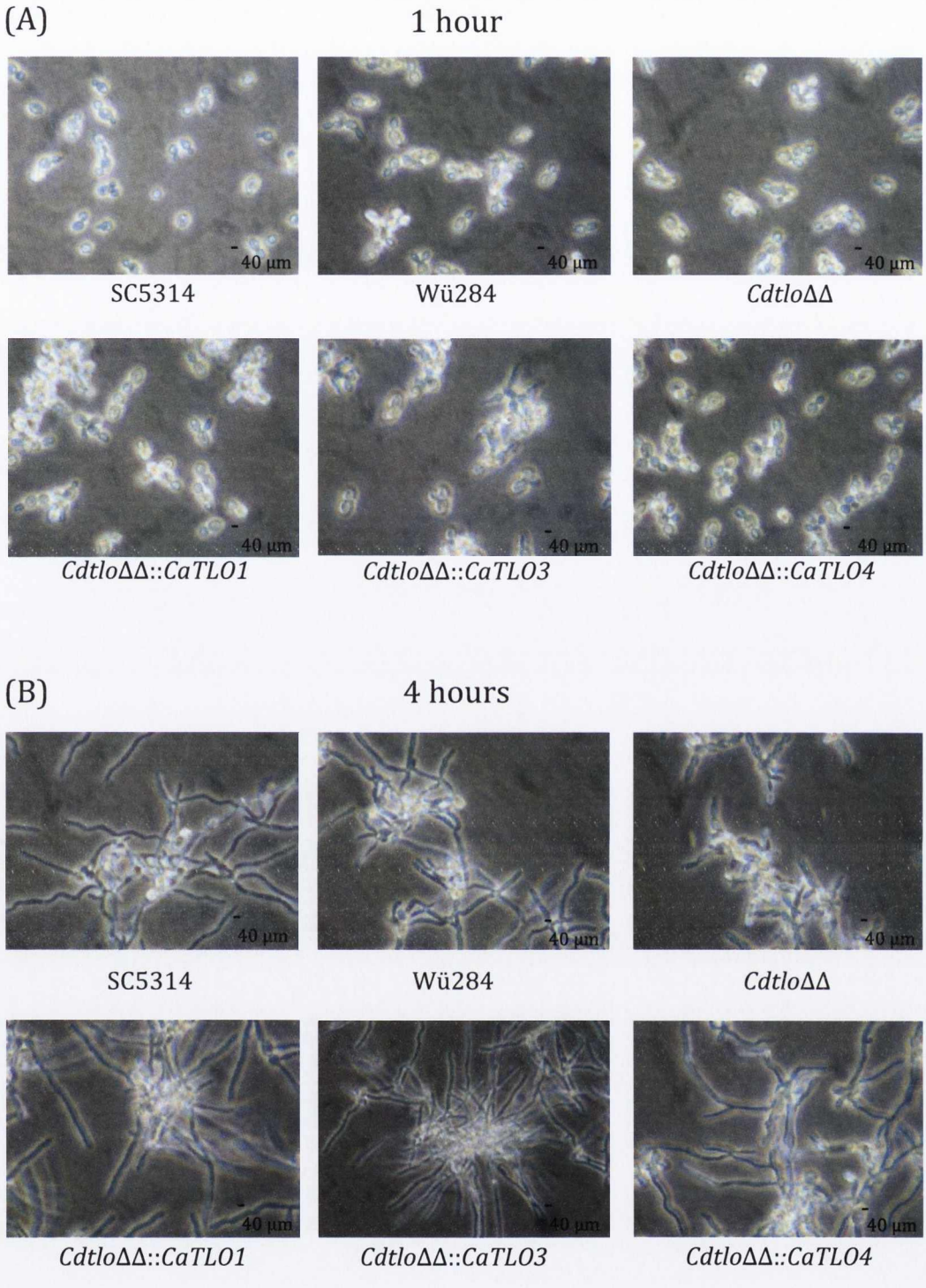

Figure 7.6. Photomicrographs of hyphal and pseudohyphal induction in *Candida albicans* wild type SC5314, *Candida dubliniensis tlo*ΔΔ mutant, and *CaTLO1, CaTLO3* and *CaTLO4* in the *Cdtlo*ΔΔ mutant background in water supplemented with 10% (v/v) FBS at **(A)** 1 h and **(B)** 4 h. Scale bar is equal to 40 µm.

7.3.5. Induction of hyphae on solid media

A single colony from a fresh YEPD plate of SC5314, *Cdtlo*ΔΔ::*CaTLO1*, , *Cdtlo*ΔΔ::*CaTLO3* and , *Cdtlo*ΔΔ::*CaTLO4* were sub-cultured on fresh Spider medium agar plates. The plates were incubated at 37 °C in a static incubator for 5 days. Wild type SC5314 colonies were extremely wrinkled on Spider medium, as were the colonies of the *Cdtlo*ΔΔ, while the colonies of *Cdtlo*ΔΔ::*CaTLO3* and *Cdtlo*ΔΔ::*CaTLO4* were smooth with no wrinkling observed. However, the *Cdtlo*ΔΔ::*CaTLO1* strain had a slight mix of both phenotypes; the colonies were mostly smooth with small areas of wrinkling (Figure 7.7).

7.3.6. Growth rate analysis

Growth rates of wild type strains SC5314, Wü284 and the *CaTLO* genes in the *Cdtlo*ΔΔ mutant background were measured and differences in the doubling times were observed. Growth in YEPD at 37 °C was analysed over a 10 h incubation period. To examine the effect of growth in an alternative carbon source, experiments were also performed in which the dextrose/glucose in YEPD was replaced by galactose and growth at 37 °C was analysed over a 10 h incubation period. Data were fitted to a regression curve, as described in Section 2.2.4 and the doubling times were calculated. In YEPD the growth rate of SC5314 was the highest, with a doubling time of 84.3 min. Wü284, the *Cdtlo*ΔΔ mutant, and the *Cdtlo*ΔΔ mutant expressing *CaTLO1* and *CaTLO4* all had similar growth rates, with doubling times between 96.6 min and 102.1 min. *CaTLO3* in the *Cdtlo*ΔΔ mutant background was the slowest, with a doubling time of 114.3 min [Figure 7.8 (A)]. In YEP-Gal, SC5314 had the quickest doubling time of 81.9 min, with *Cdtlo*ΔΔ::*CaTLO1* at a similar rate of 88 min. Wü284, *Cdtlo*ΔΔ::*CaTLO3* and *Cdtlo*ΔΔ::*CaTLO4* had similar doubling times between 94.1 min and 105.8 min, while the *Cdtlo*ΔΔ mutant was the slowest growing strain, with a doubling time of 124.8 min [Figure 7.8 (B)].

7.3.7. Spot plate assays

7.3.7.1. Oxidative stress

Spot plate experiments were performed to investigate if the integration of *CaTLO1, CaTLO3* and *CaTLO4* into the *Cdtlo*ΔΔ mutant background affected growth in the presence of oxidative stress conditions induced by 5mM and 6mM H_2O_2 in combination with a nutrient-rich medium (YEPD). It was observed that the wild type strains SC5314 and Wü284 grew efficiently in the presence of H_2O_2, while, as expected, the growth of the *Cdtlo*ΔΔ mutant was very poor. All three *CaTLOs* in the *Cdtlo*ΔΔ mutant background were able to somewhat restore growth in the presence of H_2O_2, although only *Cdtlo*ΔΔ::*CaTLO4* could restore growth to levels similar to those observed in wild type SC5314 (Figure 7.9).

7.3.7.2. Temperature stress

Spot plate experiments were carried out in order to observe whether an increase or decrease in temperature affected the *CaTLOs* integrated into the *Cdtlo*ΔΔ mutant background. Spot plates were incubated at room temperature (i.e. ~ 20 °C), 30 °C, 37 °C and 40 °C for 48 h. It was observed that all strains grew at similar rates at 30 °C and 37 °C, however at 20 °C and 40 °C there were some apparent differences in growth rates between strains. At 20 °C wild type SC5314 and *Cdtlo*ΔΔ::*CaTLO3* grew normally, while Wü284, the *Cdtlo*ΔΔ mutant, *Cdtlo*ΔΔ::*CaTLO1* and *Cdtlo*ΔΔ::*CaTLO4* growth was impaired. Similarly, at 40 °C SC5314 and *Cdtlo*ΔΔ::*CaTLO3* had the highest growth rates, while Wü284, *Cdtlo*ΔΔ::*CaTLO1* and *Cdtlo*ΔΔ::*CaTLO4* grew more slowly and the *Cdtlo*ΔΔ mutant struggled to grow (Figure 7.10).

7.3.8. Two Colour DNA Microarray-based gene expression and analysis

The phenotypic data above suggest that the *CaTLO1, CaTLO3* and *CaTLO4* genes have the capacity to complement the *Cdtlo*ΔΔ double mutation, confirming that there is cross-functionality between the *C. dubliniensis TLOs* and the *C. albicans TLOs*. Interestingly, although all three *C. albicans TLOs* can restore the phenotypes previously altered by the

(A)

SC5314

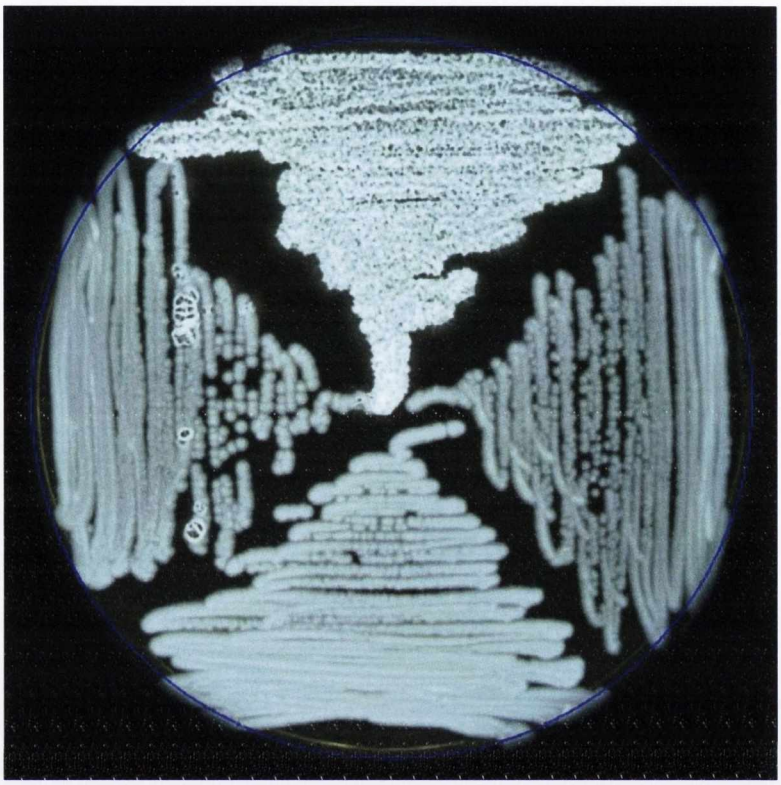

*Cdtlo*ΔΔ::
CaTLO1

*Cdtlo*ΔΔ::
CaTLO4

*Cdtlo*ΔΔ::
CaTLO3

(B)

*Cdtlo*ΔΔ

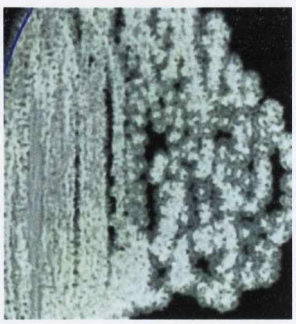

Figure 7.7. Photomicrograph of (A) *Candida albicans* wild type SC5314, the *Cdtlo*ΔΔ mutant expressing *CaTLO1, CaTLO3, CaTLO4* and (B) the *Cdtlo*ΔΔ mutant growth on hyphal-inducing solid Spider medium. Plate incubated for 5 days at 37 °C.

(A)

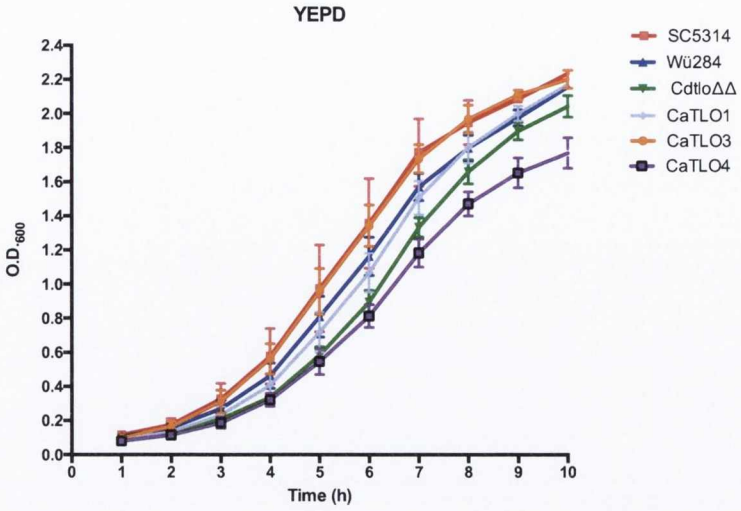

Strain	*SC5314*	*Wü284*	*CdtloΔΔ*	*CaTLO1*	*CaTLO3*	*CaTLO4*
Doubling time (min)	84.3 *+/- 40.2*	98.5 *+/- 21*	96.6 *+/- 6.1*	101.8 *+/- 17.1*	114.3 *+/- 17.3*	102.1 *+/- 9*

(B)

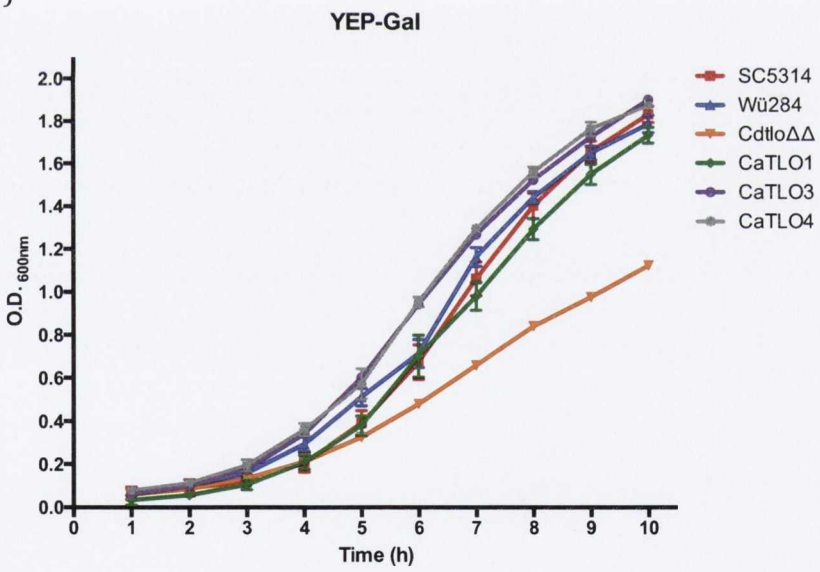

Strain	*SC5314*	*Wü284*	*CdtloΔΔ*	*CaTLO1*	*CaTLO3*	*CaTLO4*
Doubling time (min)	81.9 *+/- 10.5*	94.1 *+/- 18.4*	124.8 *+/- 7.1*	88 *+/- 10.2*	105.8 *+/- 4.2*	103.8 *+/- 13.8*

Figure 7.8. (A) Graph depicting growth rates of SC5314, Wü284, *Cdtlo*ΔΔ mutant and re-integrated *CaTLO1, CaTLO3* and *CaTLO4* in nutrient-rich YEPD media and **(B)** in YEP-Gal.. Doubling times in minutes. Standard deviations are italicised below each value and represent an average of 3 replicates. Error bars represent the standard error of the mean (SEM) of three replicates.

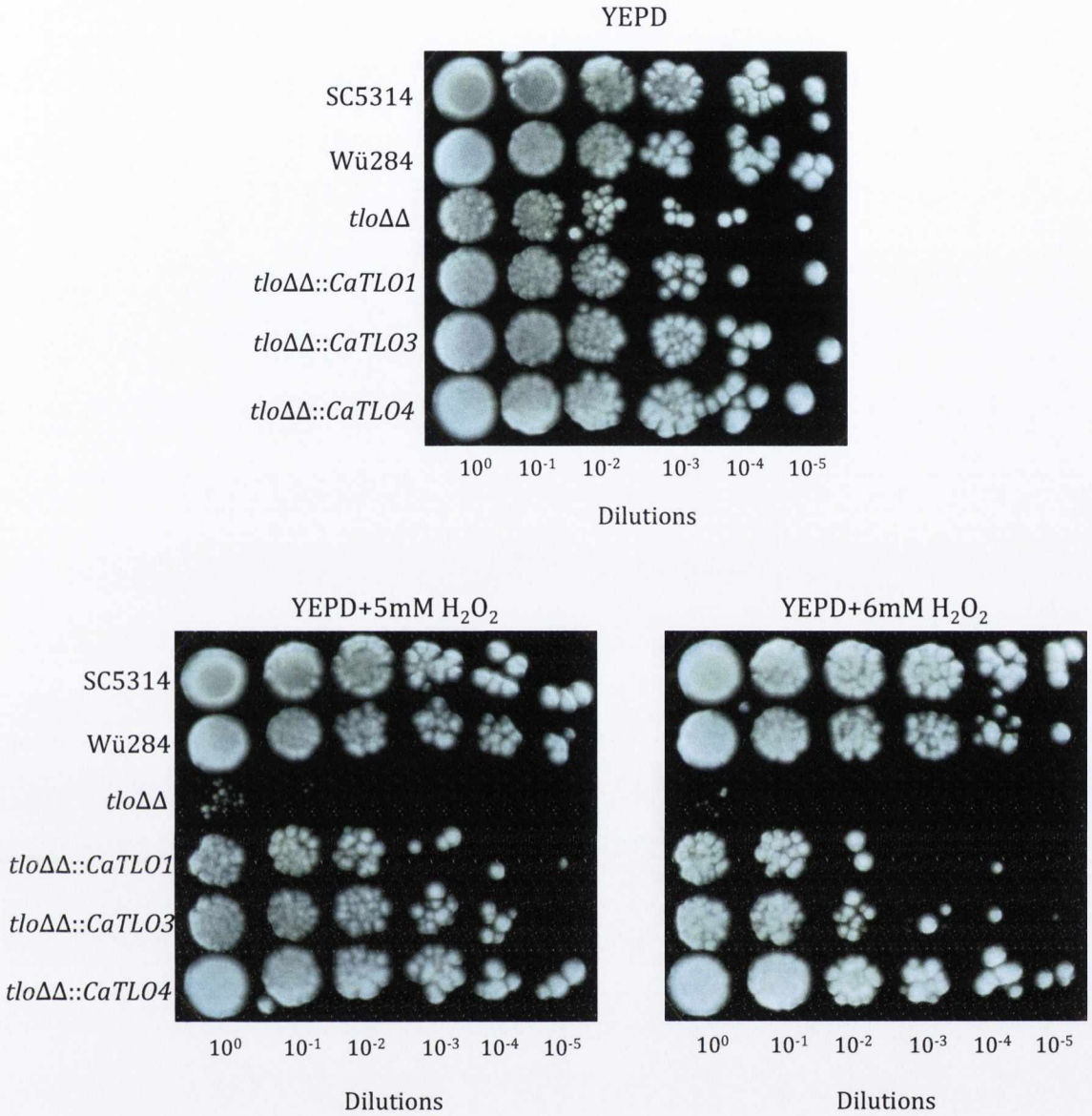

Figure 7.9. Growth of *Candida albicans* and *Candida dubliniensis* wild types SC5314, Wü284, the *Cdtlo*ΔΔ mutant and the *Cdtlo*ΔΔ mutant with *CaTLO1, CaTLO3* and *CaTLO4* individually introduced in the presence of oxidative stress induced by the presence of 5 mM and 6 mM H_2O_2 on nutrient rich YEPD medium following serial dilutions. Plates were incubated for 48 h at 37 °C. Experiments carried out on three separate occasions.

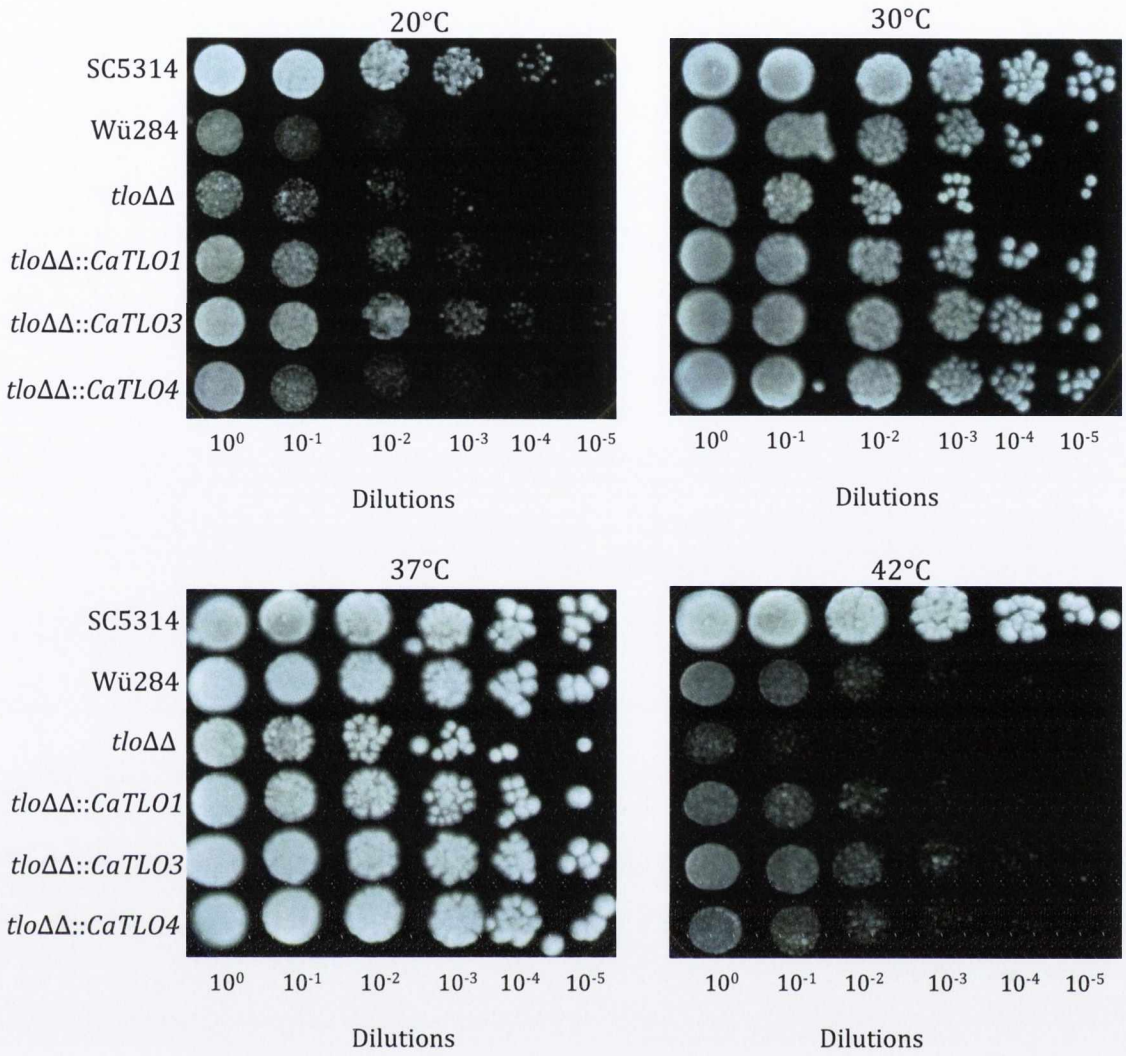

Figure 7.10. Growth of *Candida albicans* and *Candida dubliniensis* wild types SC5314, Wü284, the *CdtloΔΔ* mutant and the *CdtloΔΔ* mutant with *CaTLO1, CaTLO3* and *CaTLO4* individually expressed on nutrient rich YEPD medium following serial dilutions. Plates were incubated for 48 h at 20 °C, 30 °C, 37 °C and 42 °C. Experiments carried out on three separate occasions.

deletion of the *CdTLO*s, it is apparent that with regards to oxidative stress response, *CaTLO4* restores growth better than either *CaTLO1* or *CaTLO3.* Given this observation we investigated the effect of expressing *CaTLO1* in the *Cdtlo*ΔΔ mutant background and *CaTLO4* in the *Cdtlo*ΔΔ mutant background in comparison to the *Cdtlo*ΔΔ double mutant by using DNA microarrays under oxidative stress conditions (i.e. YEPD supplemented with 5 mM H_2O_2). This condition was chosen as a result of it being the only condition in which a detectable phenotype variation was observed between the *C. albicans TLO*s. The microarray data underwent the same data normalisation and data filtering as described in Section 3.2.7. Entity lists were created from Scatter Plot analysis of the normalised and filtered data. The Scatter Plot shows a 2-D scatter of the normalised and averaged entities, with the axes of the scatter plot representative of the samples in each dataset.

Venn diagrams were created in order to quantify the number of genes similarly regulated between the datasets and the number of genes specifically up- or down-regulated in either the *Cdtlo*ΔΔ::*CaTLO1* construct or the *Cdtlo*ΔΔ::*CaTLO4* construct (Figure 7.11). Of the 2429 genes up-regulated overall in the *Cdtlo*ΔΔ::*CaTLO1* construct and the *Cdtlo*ΔΔ::*CaTLO4* construct, 65% (n=1568) of genes were up-regulated in both constructs, while 19% (n=458) of genes were only up-regulated in *Cdtlo*ΔΔ::*CaTLO1* and 17% (n=403) of genes were only up-regulated in *Cdtlo*ΔΔ::*CaTLO4.* With regards to genes that were down-regulated, 2748 genes showed reduced expression in the presence of oxidative stress induced by 5 mM H_2O_2. A total of 59% (n=1617) of genes were observed to be down-regulated in both datasets, with 22% (n=614) of genes down-regulated in the *Cdtlo*ΔΔ::*CaTLO1* dataset only and 19% (n=517) of genes down-regulated in the *Cdtlo*ΔΔ::*CaTLO4* dataset only. GO Term analysis of genes with significantly altered expression in the presence of 5 mM H_2O_2 in the *Cdtlo*ΔΔ::*CaTLO1* construct and the *Cdtlo*ΔΔ::*CaTLO4* construct revealed that genes involved in a vast array of processes were affected. Similar numbers of genes involved in the same processes were

observed to be altered in both datasets. A summary of the frequencies of up-regulated genes attributed to various processes is shown in Tables 7.1 and 7.2.

Hierarchical clustering of the *CaTLO1* and the *CaTLO4* datasets was carried out in an attempt to identify differences in the expression profiles of genes involved in oxidative stress response, filamentation, pathogenesis, biofilm formation, cell wall functions and carbohydrate metabolism in the presence of H_2O_2. Genes involved in these processes were identified using the GO-Term slim mapper process identifier on the CGD website. Whole genome clustering revealed many similar changes in gene expression between *Cdtlo*ΔΔ::*CaTLO1* and *Cdtlo*ΔΔ::*CaTLO4* however it can be observed that there are a number of genes with diametrically opposing expression between the two datasets (Figure 7.12).

7.3.8.1. Genes involved in oxidative stress response

Eleven genes involved in oxidative stress response were identified as having altered gene expression in *Cdtlo*ΔΔ::*CaTLO1* and *Cdtlo*ΔΔ::*CaTLO4* in the presence of oxidative stress induced by 5 mM H_2O_2 (Figure 7.13). Of these 11 genes, three were diametrically opposite between *Cdtlo*ΔΔ::*CaTLO1* and *Cdtlo*ΔΔ::*CaTLO4*, namely *CFL4, HEM13* and *TPS1. CFL4* and *HEM13,* two genes involved in oxidation-reduction processes were up-regulated 0.2-fold and 0.7-fold in *Cdtlo*ΔΔ::*CaTLO1* respectively and down-regulated 1.1-fold and 0.5-fold in *Cdtlo*ΔΔ::*CaTLO4* respectively. *TPS1,* a gene involved in cellular response to oxidative stress was up-regulated 2-fold in *Cdtlo*ΔΔ::*CaTLO1* and down-regulated 0.3-fold in *Cdtlo*ΔΔ::*CaTLO4.*

7.3.8.2. Genes involved in filamentation and pathogenesis

Of the 73 genes attributed to filamentation (Figure 7.14), the expression of 25 genes was diametrically opposite in the datasets of the *CaTLO1* and *CaTLO4* constructs; 14 genes were found to be up-regulated in *Cdtlo*ΔΔ::*CaTLO1* and down-regulated in *Cdtlo*ΔΔ::*CaTLO4. BUB2,* a negative regulator of septation initiation was expressed 2-fold higher in *Cdtlo*ΔΔ::*CaTLO1*

(A)

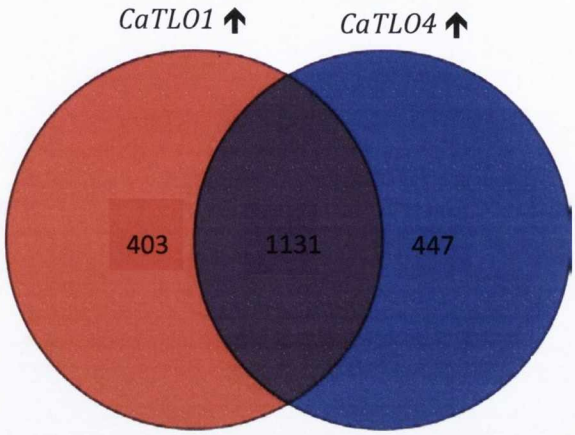

(B)

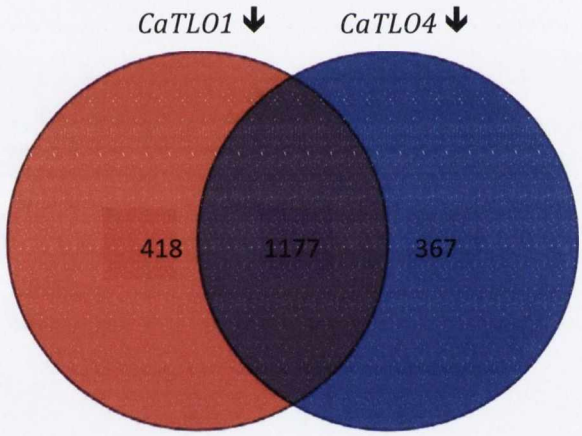

Figure 7.11. Venn Diagrams of *CaTLO1* versus *CaTLO4* representing overlapping and distinct gene numbers from the two mutant microarray datasets. **(A)** represents genes up-regulated in the presence of 5 mM H_2O_2 and **(B)** represents genes down-regulated in the presence of 5 mM H_2O_2. Graphs were created using Agilent GeneSpring GX v11.5 (Agilent Technologies Inc).

Process	%
Regulation of biological process	16.1
Transport	14.3
RNA metabolic process	13.2
Response to chemical	13.0
Response to stress	11.1
Ribosome biogenesis	9.2
Organelle organisation	9
Filamentous growth	8.3
Response to drug	7.7
Cellular protein modification process	6.2
Cell cycle	4.9
Pathogenesis	4.7
DNA metabolic process	4.1
Carbohydrate metabolic process	3.8
Lipid metabolic process	3.4

Table 7.1. Go-Term process mapping of genes with significantly altered expression in the presence of 5 mM H_2O_2 in *CaTLO1* in the *Cdtlo*ΔΔ mutant background. Frequency of 3% or lower not shown. Processes classified using GO Term finder in the CGD.

Process	%
Regulation of biological process	17.9
Transport	16.9
Organelle organisation	10.8
Response to stress	10.5
Filamentous growth	8.6
Response to chemical	8.4
Cell cycle	7
RNA metabolic process	7
Cellular protein modification process	6.1
Carbohydrate metabolic process	5.7
Lipid metabolic process	4.6
Response to drug	4.6
DNA metabolic process	4.6
Pathogenesis	4.0

Table 7.2. Go-Term process mapping of genes with significantly altered expression in the presence of 5 mM H_2O_2 in *CaTLO4* in the *Cdtlo*ΔΔ mutant background. Frequency of 3% or lower not shown. Processes classified using GO Term finder in the CGD.

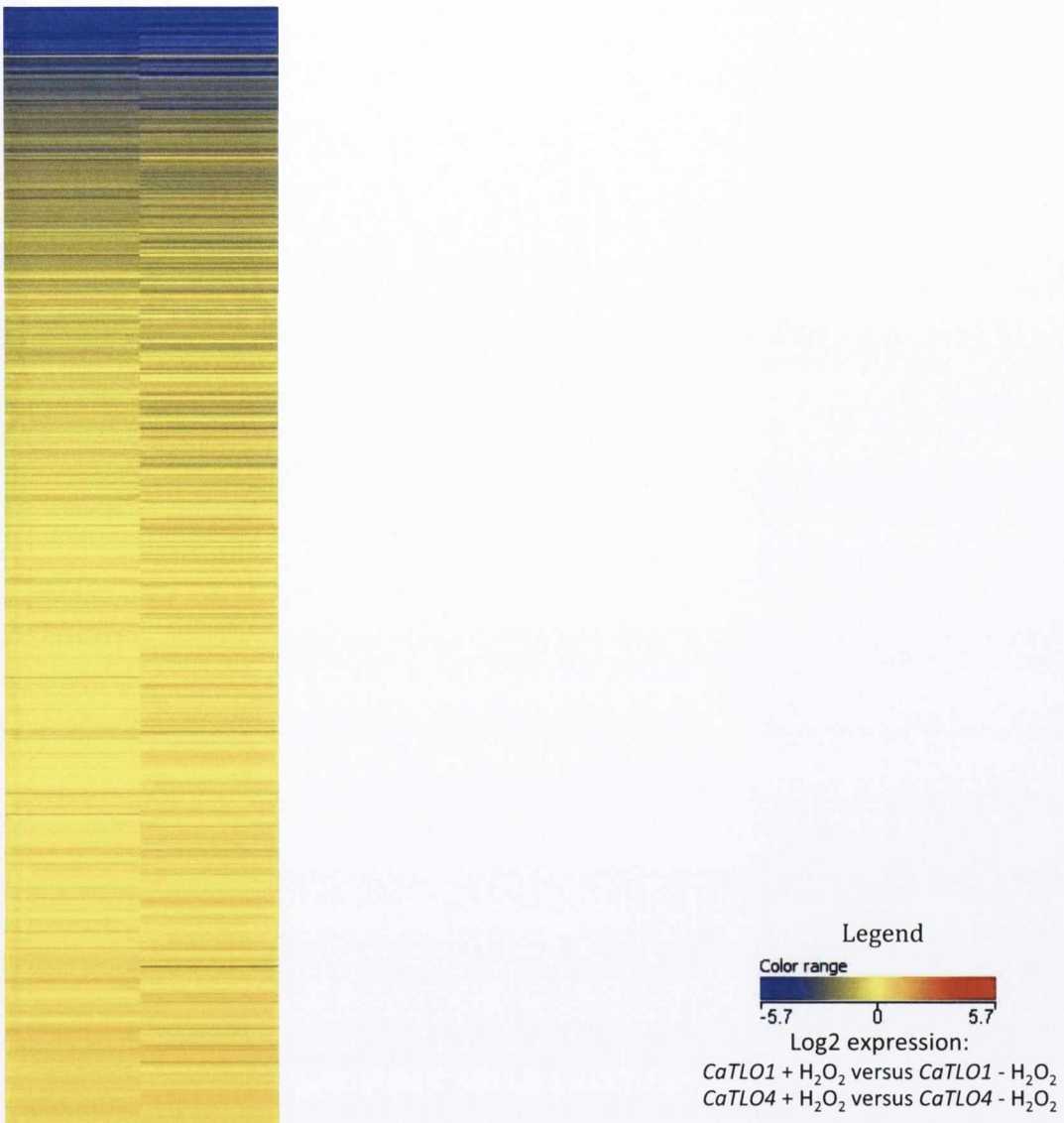

Figure 7.12. Visual heatmap showing whole genome expression of genes in *CaTLO1* and *CaTLO4* in the *Cdtlo*ΔΔ background in the presence of oxidative stress induced by 5 mM H_2O_2. The legend conveys the relative colouring for normalised expression level of each gene in *CaTLO1* and *CaTLO4* treated with 5 mM H_2O_2 compared untreated cells. The image (hierarchical clustering) was created using Agilent GeneSpring GX v11.5 (Agilent Technologies Inc).

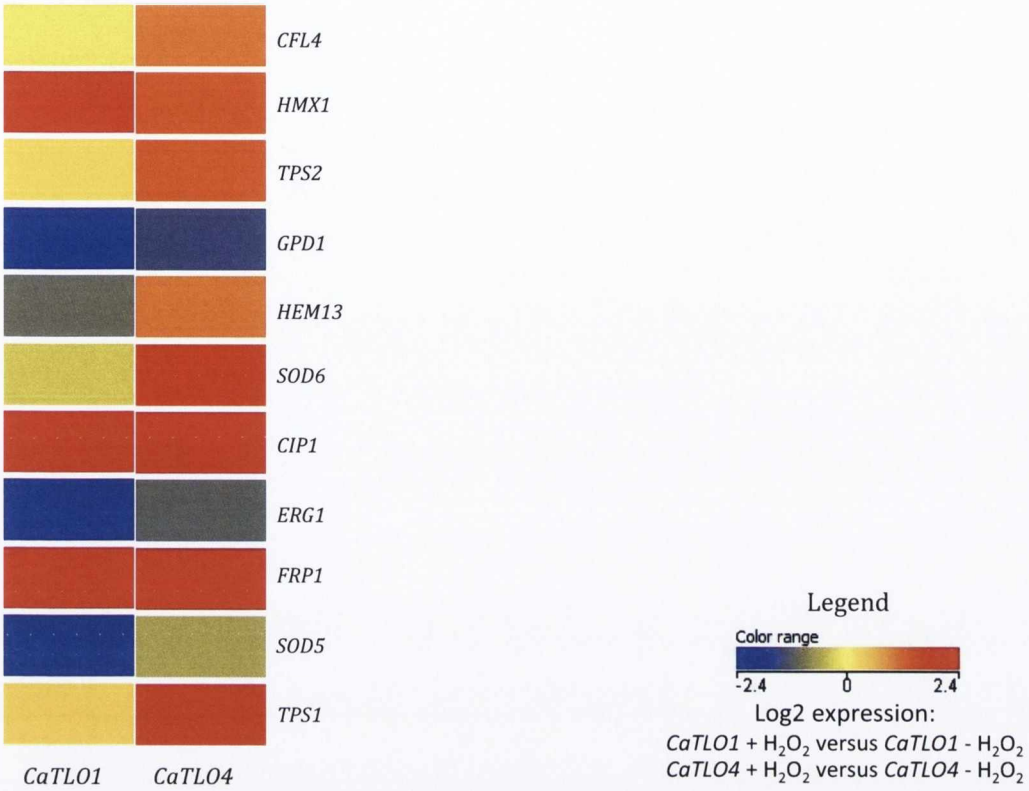

Figure 7.13. Visual heatmap showing expression of genes associated with the GO Term "Oxidative stress response" in *CaTLO1* and *CaTLO4* in the *Cdtlo*ΔΔ background in the presence of oxidative stress induced by 5 mM H_2O_2. Each gene is labelled on the right side of the heatmap, using the common gene alias in *C. dubliniensis*, usually named in *C. albicans*. The legend conveys the relative colouring for normalised expression level of each gene in *CaTLO1* and *CaTLO4* treated with 5 mM H_2O_2 compared untreated cells. The image (hierarchical clustering) was created using Agilent GeneSpring GX v11.5 (Agilent Technologies Inc).

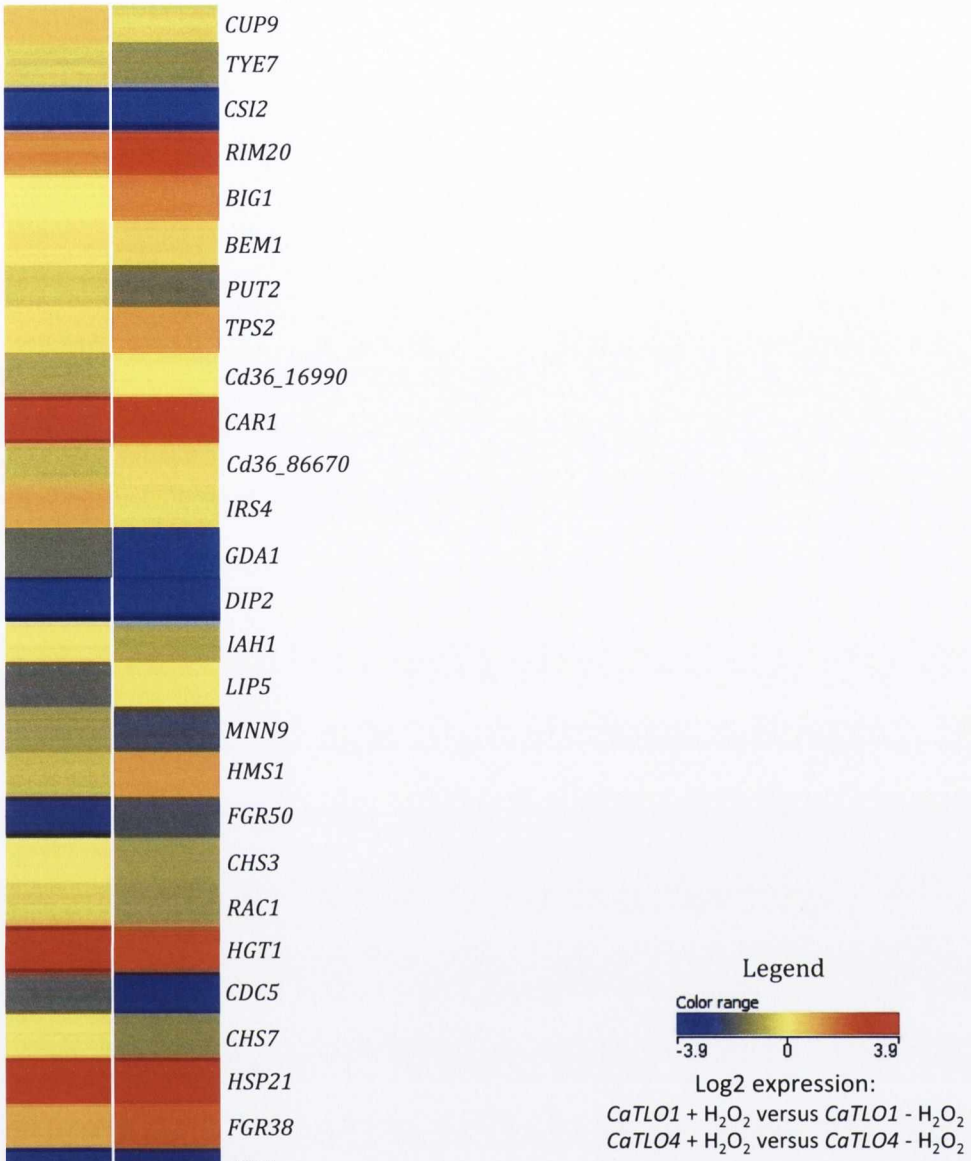

Figure 7.14. Visual heatmap showing expression of genes associated with the GO Term "Filamentation" in *CaTLO1* and *CaTLO4* in the *Cdtlo*ΔΔ background in the presence of oxidative stress induced by 5 mM H_2O_2. Each gene is labelled on the right side of the heatmap, using the common gene alias in *C. dubliniensis*, usually named in *C. albicans*. The legend conveys the relative colouring for normalised expression level of each gene in *CaTLO1* and *CaTLO4* treated with 5 mM H_2O_2 compared untreated cells. The image (hierarchical clustering) was created using Agilent GeneSpring GX v11.5 (Agilent Technologies Inc).

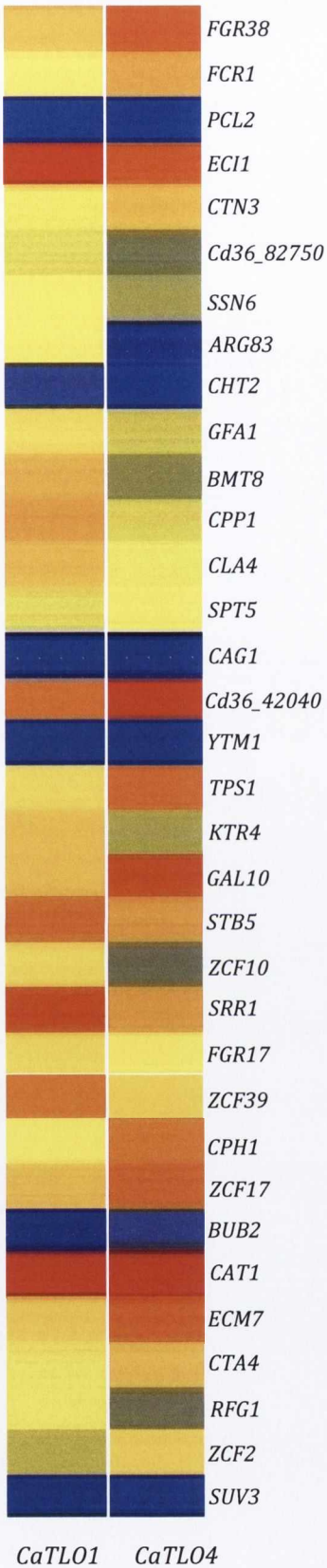

Figure 7.14. continued

than *Cdtlo*ΔΔ::*CaTLO4* in the presence of H_2O_2. *BIG1*, the endoplasmic reticulum (ER) protein required for beta-1,6-glucan synthesis, filamentation, adhesion, and virulence was up-regulated 1.4-fold in *Cdtlo*ΔΔ::*CaTLO1* and slightly down-regulated 0.2-fold in *Cdtlo*ΔΔ::*CaTLO4*. A 4-fold disparity in the expression of *HWP2* was observed between the two reintegrants, with an increase in *HWP2* expression in *Cdtlo*ΔΔ::*CaTLO1* and a decrease in expression in *Cdtlo*ΔΔ::*CaTLO4*. *HWP2* is a GPI-anchored, glycosylated cell wall protein required for biofilm formation, adhesion, filamentous growth on some media. *ECM7*, a gene with a role in hyphal growth and oxidative stress response was slightly up-regulated 0.5-fold in *Cdtlo*ΔΔ::*CaTLO1* and was down-regulated 1-fold in *Cdtlo*ΔΔ::*CaTLO4*. *GAL10*, the UDP-glucose 4-epimerase with a role in filamentation was up-regulated in *Cdtlo*ΔΔ::*CaTLO1* and down-regulated in *Cdtlo*ΔΔ::*CaTLO4*. *SFL2*, which encodes a transcription factor involved in regulation of morphogenesis and *CAG1*, a gene involved in morphogenesis both had a 1.2-fold disparity between the two reintegrants, with increased expression observed in *Cdtlo*ΔΔ::*CaTLO1* and decreased expression observed in *Cdtlo*ΔΔ::*CaTLO4*. *TPS1*, a gene involved in hyphal growth showed a 2-fold increase in expression in *Cdtlo*ΔΔ::*CaTLO1* with a slight decrease of 0.2-fold in expression in *Cdtlo*ΔΔ::*CaTLO4*. The expression of *FGR38*, a filamentous growth regulator with a proposed role in filamentous growth and *RIM20*, also involved in filamentous growth was slightly increased in *Cdtlo*ΔΔ::*CaTLO1*, however *FGR38* expression was decreased 1.6-fold and *RIM20* expression was decreased 0.7-fold in *Cdtlo*ΔΔ::*CaTLO4*. The transcription factor *ZCF2* was up-regulated 1-fold in *Cdtlo*ΔΔ::*CaTLO1*, with a down-regulation 0.5 observed in *Cdtlo*ΔΔ::*CaTLO4*. *SUV3*, a RNA helicase required for chlamydospore formation and embedded hyphal growth was up-regulated 0.5-fold in *Cdtlo*ΔΔ::*CaTLO1* and down-regulated 1-fold in *Cdtlo*ΔΔ::*CaTLO4*.

Eleven genes with roles in filamentation were observed to be down-regulated in *Cdtlo*ΔΔ::*CaTLO1* and up-regulated in *Cdtlo*ΔΔ::*CaTLO4* when exposed to oxidative stress induced by H_2O_2. The transcription factor *CUP9*, which is involved in filamentous growth was

0.5-fold up-regulated in *Cdtlo*ΔΔ::*CaTLO4* and 0.8-fold down-regulated in *Cdtlo*ΔΔ::*CaTLO1. IRS4,* a gene encoding a protein with roles in cell wall integrity, systemic murine infection, adherence, hyphal growth, and agar-embedded filamentous growth was slightly up-regulated in *Cdtlo*ΔΔ::*CaTLO4* but was observed to be 1.1-fold down-regulated in *Cdtlo*ΔΔ::*CaTLO1. HMS1,* a heat-inducible transcription factor involved in morphogenesis was shown to down-regulated 0.7-fold in *Cdtlo*ΔΔ::*CaTLO1* and up-regulated 1.3-fold in *Cdtlo*ΔΔ::*CaTLO4.* Two other transcription factors, *UME6* with roles in hyphal extension and virulence and *ADR1* involved in filamentous growth were down-regulated 0.4-fold in *Cdtlo*ΔΔ::*CaTLO1* and up-regulated 0.9-fold in *Cdtlo*ΔΔ::*CaTLO4. BMT8,* a putative beta-mannosyltransferase with a role in filamentation was found to be 0.7-fold down-regulated in *Cdtlo*ΔΔ::*CaTLO1* and 1.2-fold up-regulated in *Cdtlo*ΔΔ::*CaTLO4. CPP1,* a MAPK phosphatase that regulates the Cph1 filamentation pathway was found to be 1.3-fold down-regulated in *Cdtlo*ΔΔ::*CaTLO1* and 0.5-fold up-regulated in *Cdtlo*ΔΔ::*CaTLO4. CLA4* a gene involved in filamentous growth was 1-fold down-regulated in *Cdtlo*ΔΔ::*CaTLO1,* with a slight increase in expression in *Cdtlo*ΔΔ::*CaTLO4. KTR4,* a mannosyltransferase induced during cell wall regeneration and involved in hyphal growth was down-regulated 0.7-fold in *Cdtlo*ΔΔ::*CaTLO1* and up-regulated 1-fold in *Cdtlo*ΔΔ::*CaTLO4.* The zinc transcription factor *ARG83,* with a role in filamentous growth was observed to be 0.5-fold down-regulated in *Cdtlo*ΔΔ::*CaTLO1* and 1.8-fold up-regulated in *Cdtlo*ΔΔ::*CaTLO4.* The glucosamine-6-phosphate synthase *GFA1,* with roles in chitin biosynthesis and hyphal growth was observed to be down-regulated 1-fold in *Cdtlo*ΔΔ::*CaTLO1* and up-regulated 0.5-fold in *Cdtlo*ΔΔ:: *CaTLO4.*

Of the eighteen genes attributed to roles in pathogenesis, nine were up-regulated in *Cdtlo*ΔΔ::*CaTLO4* and down-regulated in *Cdtlo*ΔΔ::*CaTLO1,* with no genes up-regulated in *Cdtlo*ΔΔ::*CaTLO1* that were down-regulated in *Cdtlo*ΔΔ::*CaTLO4* (Figure 7.15). These up-regulated genes include the previously mentioned *IRS4, CPP1, CLA4* and *UME6,* as well as the

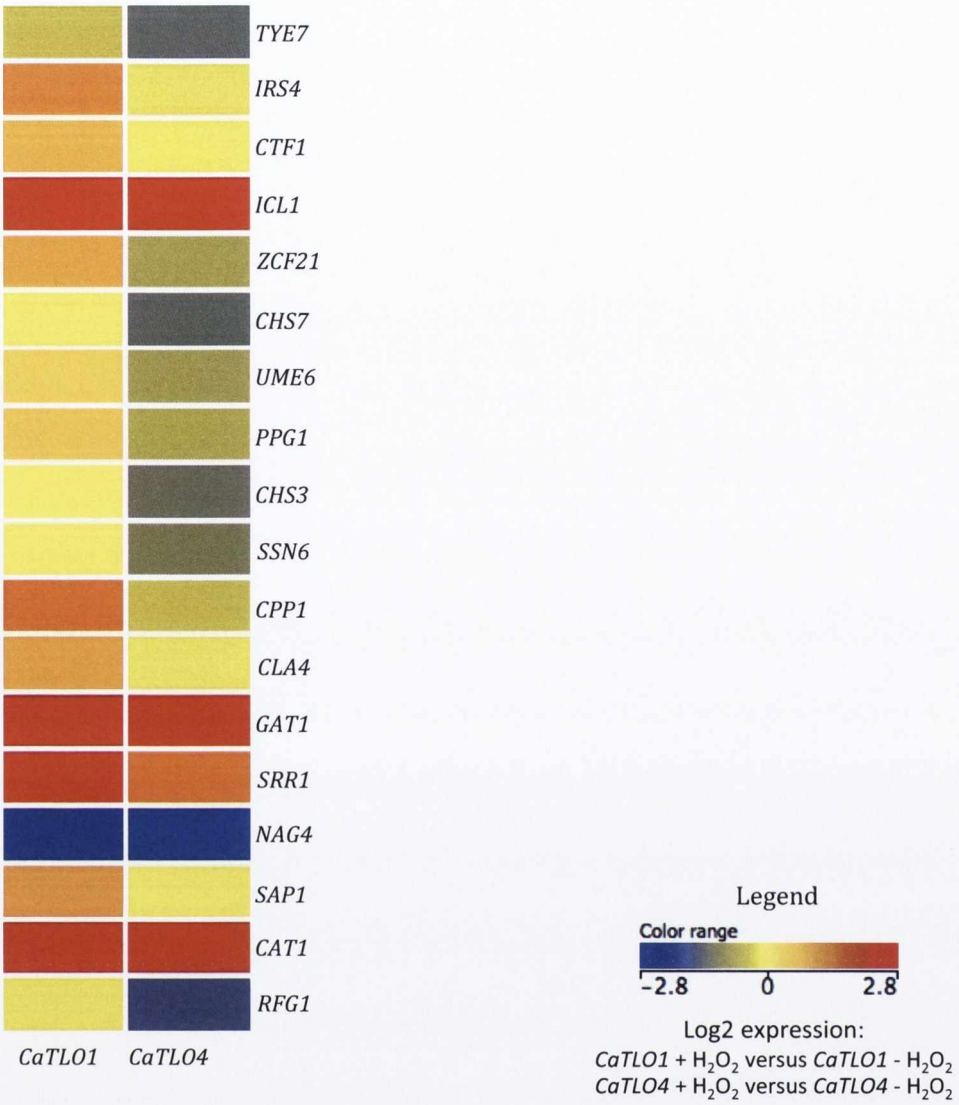

Figure 7.15. Visual heatmap showing expression of genes associated with the GO Term "Pathogenesis" in *CaTLO1* and *CaTLO4* in the *Cdtlo*ΔΔ background in the presence of oxidative stress induced by 5 mM H_2O_2. Each gene is labelled on the right side of the heatmap, using the common gene alias in *C. dubliniensis*, usually named in *C. albicans*. The legend conveys the relative colouring for normalised expression level of each gene in *CaTLO1* and *CaTLO4* treated with 5 mM H_2O_2 compared untreated cells. The image (hierarchical clustering) was created using Agilent GeneSpring GX v11.5 (Agilent Technologies Inc).

transcription factors *ZCF21* and *CTF1*, the hyphal regulator *SSN6*, the secreted aspartyl protease *SAP1* and the protein phosphatase *PPG1*.

7.3.8.3. Biofilm and cell wall genes

Twenty-two genes were identified as having roles in biofilm formation and cell wall function, in *CdtloΔΔ::CaTLO1* and *CdtloΔΔ::CaTLO4*, many of which have overlapping roles in filamentation and pathogenesis such as *IRS4*, *CHS3*, *TYE7* and *ZCF39* (Figure 7.16). Of these 22 genes, six were shown to be expressed diametrically opposite in *CdtloΔΔ::CaTLO1* and *CdtloΔΔ::CaTLO4*. *IRS4* and *WSC2*, genes with roles in cell wall integrity were differentially expressed between the two reintegrants. *IRS4* was down-regulated 1.2-fold in the presence of *CdtloΔΔ::CaTLO1* and up-regulated 0.3-fold in the presence of *CdtloΔΔ::CaTLO4*. *WSC2* was down-regulated 0.5-fold in the presence of *CdtloΔΔ::CaTLO1* and up-regulated *CdtloΔΔ*::0.6-fold in the presence of *CaTLO4*, as was the unknown ORF Cd36_40260, with a role in ascospore assembly in *Saccharomyces cerevisiae*. *RBT5*, which encodes a GPI-anchored cell wall protein was shown to be down regulated 1-fold in the presence of *CdtloΔΔ::CaTLO1* and up-regulated 0.8-fold in the presence of *CdtloΔΔ::CaTLO4*. *IFD6* a gene with a role in biofilm formation was down-regulated 0.5-fold in *CdtloΔΔ::CaTLO1* and up-regulated 0.7-fold in *CdtloΔΔ::CaTLO4*. The transcription factor *ARG81*, which is required for yeast cell adherence was observed to be down-regulated 0.4-fold in the presence of *CdtloΔΔ::CaTLO1* and up-regulated 1.7-fold in the presence of *CdtloΔΔ::CaTLO4*. It is worth noting that of the six genes differentially expressed between *CdtloΔΔ::CaTLO1* and *CdtloΔΔ::CaTLO4*, all six appear to be down-regulated in *CdtloΔΔ::CaTLO1* and up-regulated in *CdtloΔΔ::CaTLO4*.

7.3.8.4. Genes involved in carbohydrate metabolism

It was observed in the presence of *CaTLO1* and *CaTLO4* in the *CdtloΔΔ* mutant background altered the expression of 29 genes with roles in carbohydrate metabolism (Figure 7.17). Ten genes with roles in carbohydrate metabolic process were observed to have diametrically

opposing expression between *Cdtlo*ΔΔ::*CaTLO1* and *Cdtlo*ΔΔ::*CaTLO4* in the presence of oxidative stress induced by 5 mM H_2O_2. The mannosyltransferases *MNN1* and *KTR4* were both down-regulated in *Cdtlo*ΔΔ::*CaTLO1* and up-regulated in *Cdtlo*ΔΔ::*CaTLO4*, as were unknown ORFs Cd36_41210 and Cd36_31460 and the previously mentioned *GFA1*; all with roles in carbohydrate metabolism. *PET9*, a gene involved in glucose catabolism and *MDH1*, a gene involved in gluconeogenesis were also down-regulated in the presence of *Cdtlo*ΔΔ::*CaTLO1* and up-regulated in the presence of *Cdtlo*ΔΔ::*CaTLO4*. *GAL10*, a gene involved in galactose utilisation appeared to be the only gene with increased expression in the presence of *Cdtlo*ΔΔ::*CaTLO1* and decreased expression in *Cdtlo*ΔΔ::*CaTLO4*, with a 0.6-fold up-regulation in *Cdtlo*ΔΔ::*CaTLO1* and a 1-fold down-regulation in *Cdtlo*ΔΔ::*CaTLO4*.

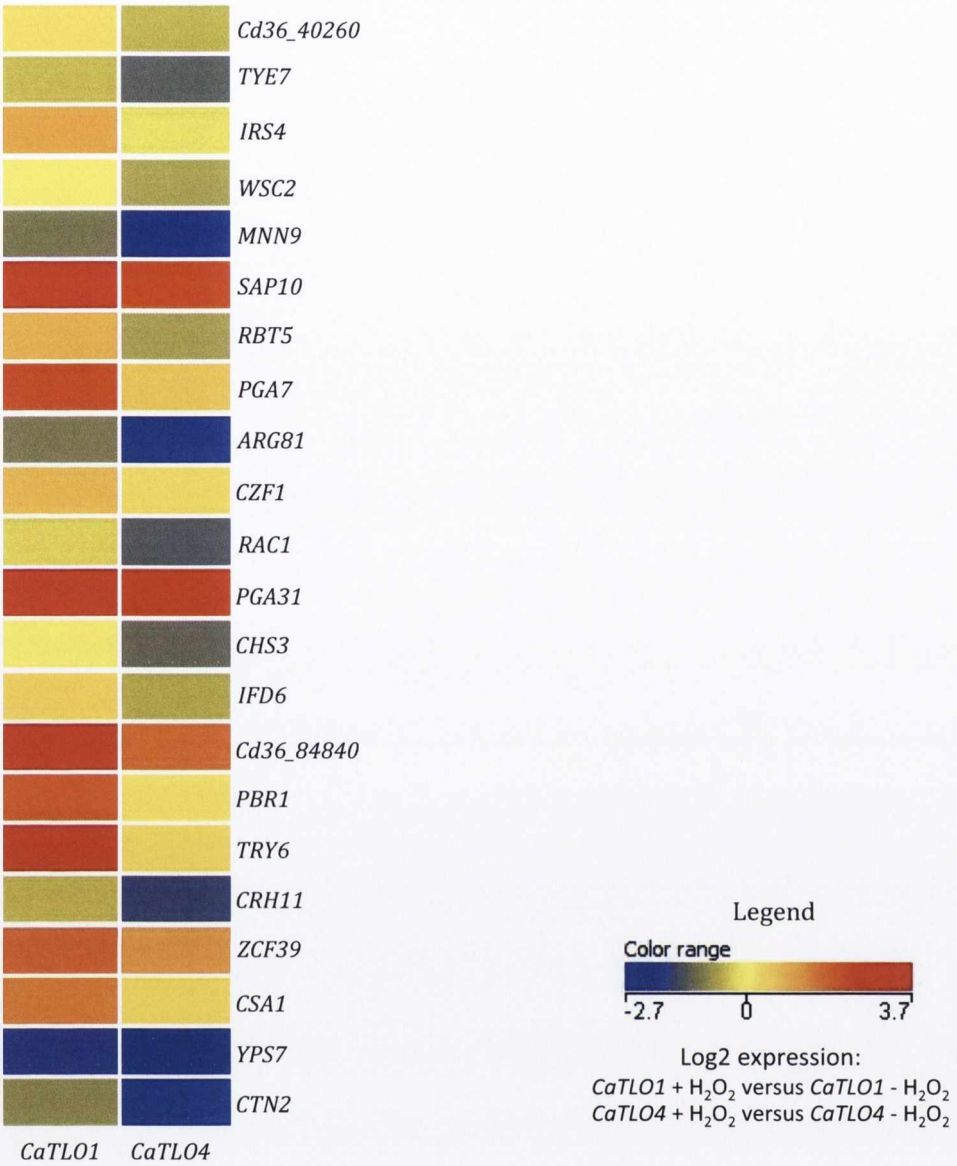

Figure 7.16. Visual heatmap showing expression of genes associated with the GO Terms "Cell wall function" and "Biofilm" in *CaTLO1* and *CaTLO4* in the *Cdtlo*ΔΔ background in the presence of oxidative stress induced by 5 mM H_2O_2. Each gene is labelled on the right side of the heatmap, using the common gene alias in *C. dubliniensis*, usually named in *C. albicans*.. The legend conveys the relative colouring for normalised expression level of each gene in *CaTLO1* and *CaTLO4* treated with 5 mM H_2O_2 compared untreated cells. The image (hierarchical clustering) was created using Agilent GeneSpring GX v11.5 (Agilent Technologies Inc).

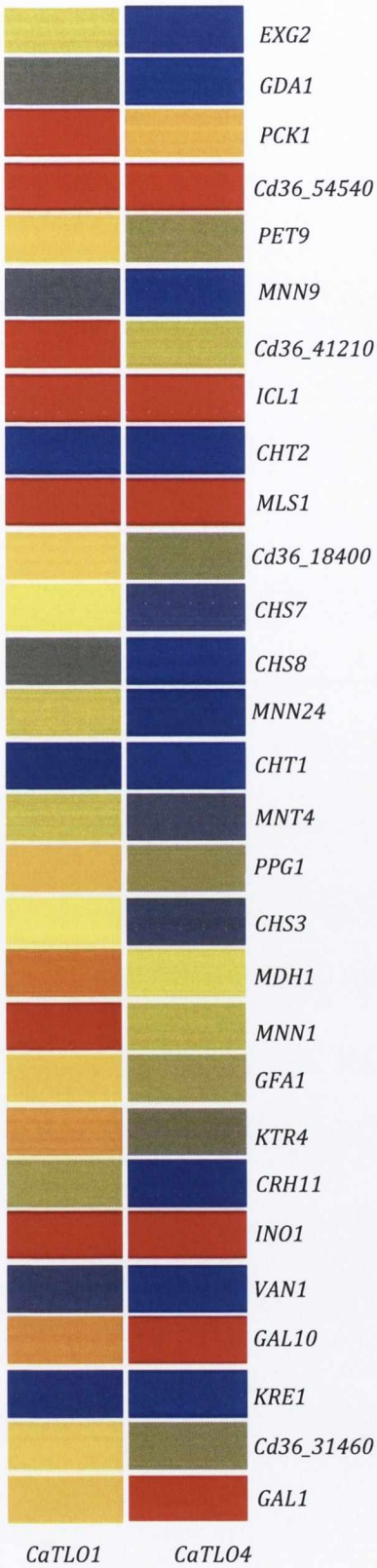

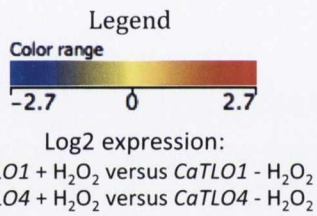

Figure 7.17. Visual heatmap showing expression of genes associated with the GO Term "Carbohydrate metabolism" in *CaTLO1* and *CaTLO4* in the *Cdtlo*ΔΔ background in the presence of oxidative stress induced by 5 mM H_2O_2. Each gene is labelled on the right side of the heatmap, using the common gene alias in *C. dubliniensis*, usually named in *C. albicans*. The legend conveys the relative colouring for normalised expression level of each gene in *CaTLO1* and *CaTLO4* treated with 5 mM H_2O_2 compared untreated cells. The image (hierarchical clustering) was created using Agilent GeneSpring GX v11.5 (Agilent Technologies Inc).

7.4. Discussion

7.4.1. Expression of *CaTLO1, CaTLO3* and *CaTLO4* in the *Cdtlo*ΔΔ mutant background

Characterisation of the *Candida albicans TLO* gene family carried out by Anderson *et al.* (2012) revealed a variation in gene expression levels between clades. The α clade, of which both *CaTLO1* and *CaTLO3* are members, is the most highly expressed. This was reflected in the qRT-PCR experiment carried out in this study, given that the expression of *CaTLO1* and *CaTLO3* was higher than *CaTLO4* of the γ clade, which has the lowest expression of the three clades. There is only one member of the β clade; *CaTLO2,* however as this *TLO* gene does not have its own promoter, we felt that it would not reflect a direct comparison of the functionality of the *CaTLO*s in the *Cdtlo*ΔΔ mutant background, given that promoter usage can affect gene function. Comparing the expression levels between the *CdTLO* reintegrants and the *CaTLO* constructs in the *Cdtlo*ΔΔ mutant background in the *CDRI* locus yields interesting results. Although the expression levels of *CdTLO2, CaTLO1* and *CaTLO3* were similar, *CdTLO1* expression was ten-fold higher. Even though the *CaTLO*s and *CdTLO*s were inserted into the same locus it would appear that use of the native promoter has a bigger impact than the locus. Furthermore, it is possible that the integration of *C. albicans* genes into a *C. dubliniensis* background resulted in lower expression of the *CaTLO*s.

It would appear that low expression of specific *TLO* genes does not affect the phenotypes tested as the presence of all three *C. albicans TLO*s in the *Cdtlo*ΔΔ mutant background resulted in restoration of the growth of true hyphae, increased doubling times in YEP-Gal as an alternative carbohydrate source to glucose and reduced sensitivity to oxidative stress induced by H_2O_2. There was little variation between the *CaTLO*s in their ability to restore phenotypes, with the exception of their growth in the presence oxidative stress. It was observed that in the presence of 5 mM and 6 mM H_2O_2, *Cdtlo*ΔΔ::*CaTLO4* was able to restore growth better than *Cdtlo*ΔΔ::*CaTLO1* and *Cdtlo*ΔΔ::*CaTLO3.* Based on this finding we decided

to carry out DNA microarray studies to compare the α clade *CdtloΔΔ::CaTLO1* and the γ clade *CdtloΔΔ::CaTLO4* under oxidative stress conditions in an attempt to observe if the presence of oxidative stress induced by 5 mM H_2O_2 resulted in an altered transcriptome between *CdtloΔΔ::CaTLO1* and *CdtloΔΔ::CaTLO4,* which could in turn highlight different functions between the two genes.

7.4.2. *CaTLO4* restores growth in the presence of oxidative stress induced by H_2O_2 better than *CaTLO1* in the *CdtloΔΔ* mutant background

The main reason for comparing the transcriptomic responses of expressing *CdtloΔΔ::CaTLO1* and *CdtloΔΔ::CaTLO4* in YEPD supplemented with 5 mM H_2O_2 was due to the observation that *CdtloΔΔ::CaTLO4* was less sensitive than *CdtloΔΔ::CaTLO1* and *CdtloΔΔ::CaTLO3* to oxidative stress induced by 5 mM and 6 mM H_2O_2. The transcription of 11 genes directly involved in stress response were significantly altered in *CdtloΔΔ::CaTLO1* or *CdtloΔΔ::CaTLO4* the presence of 5 mM H_2O_2. Four genes were up-regulated and four were down-regulated in both *CdtloΔΔ::CaTLO1* and *CdtloΔΔ::CaTLO4.* The up-regulated genes were *TPS2, CIP1, ERG1* and *GPD1.* The phosphatase *TPS2* was up-regulated 2.8-fold and 1.5-fold in *CdtloΔΔ::CaTLO1* and *CdtloΔΔ::CaTLO4* respectively. The oxidoreductase *CIP2* was up-regulated 3.5-fold and 2.5-fold in *CdtloΔΔ::CaTLO1* and *CdtloΔΔ::CaTLO4* respectively. *ERG1,* a gene encoding a protein involved in oxidation reduction processes was up-regulated 1.1-fold in *CdtloΔΔ::CaTLO1* while *ERG1* expression was not altered in *CdtloΔΔ::CaTLO4.* The dehydrogenase *GPD1* was up-regulated 2.2-fold and 0.8-fold in *CdtloΔΔ::CaTLO1* and *CdtloΔΔ::CaTLO4* respectively. The heme oxygenase *HMX1,* which is involved in oxidative stress response was down-regulated 4.5-fold in *CdtloΔΔ::CaTLO1* and 1.3-fold in *CdtloΔΔ::CaTLO4.* The ferric reductase *FRP1* was down-regulated 4-fold and 3-fold in *CdtloΔΔ::CaTLO1* and *CdtloΔΔ::CaTLO4* respectively. The catalase *CAT1* was down-regulated 5-fold and 4-fold in *CdtloΔΔ::CaTLO1* and *CdtloΔΔ::CaTLO4* respectively Interestingly, a number of these genes were more highly expressed in *CdtloΔΔ::CaTLO1* than *CdtloΔΔ::CaTLO4,* which is surprising given that

*Cdtlo*ΔΔ::*CaTLO1* cells are more sensitive to oxidative stress induced by H_2O_2. For instance the trehalose phosphate genes *TPS1* and *TPS2* were both more highly up-regulated in *Cdtlo*ΔΔ::*CaTLO1* than in *Cdtlo*ΔΔ::*CaTLO4.* Trehalose is a stress protectant that is induced upon severe oxidative stress induced by H_2O_2 (Martína-Esparza *et al.,* 2009). Perhaps this is an indicator of a greater response in *Cdtlo*ΔΔ::*CaTLO1* due to increased sensitivity to oxidative stress.

SOD5 and *SOD6* are members of the superoxide dismutase family with roles in superoxide metabolism and protection against oxidative stress. Expression of *SOD5* was found to be unaffected in *Cdtlo*ΔΔ::*CaTLO1* and was down-regulated 1.7-fold in *Cdtlo*ΔΔ::*CaTLO4,* while *SOD6* expression was down-regulated 5-fold and 6-fold in *Cdtlo*ΔΔ::*CaTLO1* and *Cdtlo*ΔΔ::*CaTLO4* respectively. The *SOD* genes play a major role in the detoxification of reactive oxygen species and mediate cellular stress adaptation (Brown *et al.,* 2014). Sod5 is a CuZn-containing superoxide dismutase GPI-anchored cell surface protein required for virulence of *C. albicans* and for catalysing destruction of host-derived ROS (Fradin *et al.,* 2005; Frohner *et al.,* 2009). Sod6 is also a CuZn-containing superoxide dismutase GPI-anchored cell surface protein involved in the protection of *C. albicans* against oxidative stress, although its specific function remains unclear (Bink *et al.,* 2011). Previous DNA microarray studies observed that upon reintegration of *CdTLO1* and *CdTLO2* to the *Cdtlo*ΔΔ mutant under hyphal-inducing conditions (i.e. water supplemented with 10% w/v FBS), differential expression of *SOD5* was also observed between *Cdtlo*ΔΔ::*CdTLO1* and *Cdtlo*ΔΔ::*CdTLO2.* However in that experiment the expression of *SOD5* was consistent with the oxidative stress phenotype, given that *Cdtlo*ΔΔ::*CdTLO1* grew better than *Cdtlo*ΔΔ::*CdTLO2* on YEPD supplemented with 5 mM H_2O_2 and expression of *SOD5* was observed to be higher in *Cdtlo*ΔΔ::*CdTLO1.* It is noteworthy that in the case of the *C. albicans TLO*s, *SOD5* is expressed more highly in *Cdtlo*ΔΔ::*CaTLO1,* which is more sensitive to oxidative stress conditions than *Cdtlo*ΔΔ::*CaTLO4.*

7.4.3. The *CaTLOs* restore hyphal formation in the *CdtloΔΔ* mutant background and alter the expression of genes involved in filamentation and pathogenesis

It was observed that the introduction of *CaTLO1, CaTLO3* and *CaTLO4* restored the ability to form true hyphae in the *CdtloΔΔ* mutant, with all three genes forming wild type levels of hyphae. In the DNA microarray study, 73 genes attributed to roles in filamentation were found to have altered expression in *CaTLO1* and *CaTLO4* in the presence of 5 mM H_2O_2, 25 of which were diametrically expressed between the two *TLOs*. Many of the differentially expressed genes were shown to have increased expression in the presence of *CaTLO1* and decreased expression in the presence of *CaTLO4,* such as *BIG1, HWP2, ECM7, GAL10, TPS1, ZCF1* and *SUV3.* Interestingly, a number of transcription factors involved in morphogenesis and filamentation were down-regulated in the presence of *CaTLO1* and up-regulated in the presence of *CaTLO4,* including *HMS1, UME6* and *ADR1.* The transcriptional analysis of genes involved in filamentation does not reveal any obvious differences between the two *TLOs*. This could be due to the fact that the microarray was not carried out under hyphal-inducing conditions.

Filamentation is governed by a number of complex pathways, which results in a wide range of genes being affected. However, it has been demonstrated that a number of cell surface antigens related to acute candidaemia are involved in oxidative stress in *C. albicans* (Mochon *et al.,* 2010). Furthermore, Lorenz *et al.* (2004) observed that in *C. albicans,* hyphal cells are more resistant to oxidative stress, which could explain why a large proportion of genes involved in filamentation have altered gene expression in the presence of H_2O_2. A noteworthy observation is that *HWP2,* the cell wall protein involved in adhesion, biofilm formation and oxidative stress resistance is up-regulated in *CdtloΔΔ::CaTLO1* and down-regulated in *CdtloΔΔ::CaTLO4,* which seems slightly anomalous given that *CdtloΔΔ::CaTLO4* is less sensitive to oxidative stress induced by H_2O_2. Interestingly, of the eighteen genes attributed to roles in pathogenesis that were identified as having altered gene expression patterns in the

presence of oxidative stress, 13 genes were up-regulated or more highly expressed in *CdtloΔΔ::CaTLO4* and down-regulated in *CdtloΔΔ::CaTLO1.* This higher expression of virulence genes in *CdtloΔΔ::CaTLO4* could explain the ability of *CdtloΔΔ::CaTLO4* to grow in the presence of oxidative stress induced by H_2O_2 more succesfully than *CdtloΔΔ::CaTLO1.*

Eighteen genes with altered gene expression in *CdtloΔΔ::CaTLO1* and *CdtloΔΔ::CaTLO4* were identified as having roles in pathogenesis. Six genes were observed to be up-regulated and 4 genes were down-regulated in both *CdtloΔΔ::CaTLO1* and *CdtloΔΔ::CaTLO4* in the presence of 5 mM H_2O_2. In particular, the expression of the transporter *NAG4* was signficantly increased in both datasets. The genes significantly down-regulated in both datasets included *ICL1, CAT1* and *GAT1.* Interestingly, there were nine genes up-regulated in *CdtloΔΔ::CaTLO4* and down-regulated in *CdtloΔΔ::CaTLO1,* with no genes up-regulated in *CdtloΔΔ::CaTLO1* that were down-regulated in *CdtloΔΔ::CaTLO4.* It would appear that in oxidative stress conditions induced by the presence of 5 mM H_2O_2, *CdtloΔΔ::CaTLO4* may be more important for pathogenesis than *CdtloΔΔ::CaTLO1.*

7.4.4. Genes involved in cell wall function and biofilm formation are altered in the presence of 5 mM H_2O_2

The reactive nature of reactive oxygen species (ROS) results in the ability to cause oxidative damage to cellular components, including the cell wall, which can lead to extensive cell damage and ultimately cell death (Cáp *et al.,* 2012). With regards to the genes involved in cell wall and biofilm functions with altered transcription in the presence of H_2O_2, a number of genes were down-regulated in both *CdtloΔΔ::CaTLO4* and *CdtloΔΔ::CaTLO1,* with many down-regulated in *CdtloΔΔ::CaTLO1* only. The observation that more genes involved in cell wall and biofilm functions were down-regulated in *CdtloΔΔ::CaTLO1* than *CdtloΔΔ::CaTLO4* could be an indication that cells expressing *CaTLO1* are more susceptible to cell damage by oxidative stress and therefore cannot grow as well as cells expressing *CaTLO4* in oxidative stress

conditions induced by H_2O_2. Genes with cell wall functions that were down-regulated more significantly in *Cdtlo*ΔΔ::*CaTLO1* include *IRS4, WSC2, RBT5* and *CSA1.* Genes with roles in biofilm formation that were down-regulated more significantly in *Cdtlo*ΔΔ::*CaTLO1* include *PGA7, IFD6, PBR1, TRY6* and the transcription factors *ZCF39* and *CZF1.* Interestingly, the secreted aspartyl protease *SAP10* was down-regulated more than 2.5-fold in both *Cdtlo*ΔΔ::*CaTLO1* and *Cdtlo*ΔΔ::*CaTLO4,* as was the gene encoding the cell wall protein *PGA31.* However, it is clear that the significant down-regulation of these two genes was not sufficient to affect the ability of *Cdtlo*ΔΔ::*CaTLO4* to grow in the presence of oxidative stress induced by H_2O_2. The majority of genes were up-regulated more highly in *Cdtlo*ΔΔ::*CaTLO4.* A number of genes were very highly expressed in *Cdtlo*ΔΔ::*CaTLO4* compared to *Cdtlo*ΔΔ::*CaTLO1,* such as the biofilm genes *RAC1, TYE7, ARG81* and *CTN2,* and the genes with cell wall functions; *MNN9* and *CRH11.* The cell wall gene *YPS7* was up-regulated in both *Cdtlo*ΔΔ::*CaTLO1* and *Cdtlo*ΔΔ::*CaTLO4,* however the significant disparity in the number of genes involved in cell wall and biofilm functions that are more highly expressed in *Cdtlo*ΔΔ::*CaTLO4* could contribute to the decreased sensitivity of *Cdtlo*ΔΔ::*CaTLO4* in comparison to *Cdtlo*ΔΔ::*CaTLO1.*

7.4.5. The *CaTLO*s restore growth in YEP-Gal in the *Cdtlo*ΔΔ mutant background and alter the expression of genes involved in carbohydrate metabolism

In YEPD, the growth rates of the *CaTLO*s in the *Cdtlo*ΔΔ mutant background were similar, however when grown in YEP-Gal it was observed that *Cdtlo*ΔΔ::*CaTLO1* had the highest doubling time after wild-type SC5314, which could mean that *Cdtlo*ΔΔ::*CaTLO1* is better than *Cdtlo*ΔΔ::*CaTLO3* and *Cdtlo*ΔΔ::*CaTLO4* at adapting to growth where galactose is the only carbohydrate source. The ability of fungal cells to combat environmental stresses and host defences is strongly influenced by its metabolic and physiological status, and by local nutrients that are available. A number of recently published studies have shown links between metabolism and the ability of fungi to adapt to stresses. Metabolism also promotes

the virulence of *C. albicans* indirectly by enhancing stress adaptation. Stress resistance is required for virulence in *C. albicans* (Brown *et al.*, 2014). Reducing the vulnerability of fungal cells to local environmental stresses and to phagocytic killing increases their survival in host niches (Arana *et al.*, 2007; Brown *et al.*, 2012; Patterson *et al.*, 2013).

These studies that have elucidated links between carbohydrate metabolism and stress response could help explain the DNA microarray findings in this study. Twenty-nine genes attributed to roles in carbohydrate metabolism were shown to have altered expression in *CdtloΔΔ::CaTLO1* and *CdtloΔΔ::CaTLO4* in the presence of 5 mM H_2O_2. The down-regulated genes were the galactokinase *GAL1*, which was 2-fold and 3-fold down-regulated in the presence of *CdtloΔΔ::CaTLO1* and *CdtloΔΔ::CaTLO4* respectively, the phosphofructokinase *PCK1* which was 2-fold down-regulated in *CaTLO1* and 0.5-fold down-regulated in *CdtloΔΔ::CaTLO4* and the uncharacterised ORF Cd36_54540 with orthologues involved in maltose alpha-glucosidase activity was down-regulated 3.7-fold and 2.5-fold in the presence of *CdtloΔΔ::CaTLO1* and *CdtloΔΔ::CaTLO4* respectively. Expression of the glyoxylate cycle enzymes *ICL1* and *MLS1* with roles in carbon utilisation were signficantly down-regulated in both *CdtloΔΔ::CaTLO1* and *CdtloΔΔ::CaTLO4*, with 8-fold and 6.7-fold decreases of *ICL1* and 4.5-fold and 3-fold decreases of *MLS1* expression observed respectively. *INO1*, the inositol-1-phosphate synthase involved in inositol biosynthesis was observed to be down-regulated 4-fold in the presence of *CdtloΔΔ::CaTLO1* and 2-fold in the presence of *CdtloΔΔ::CaTLO4.*

Of the 13 genes up-regulated in the presence of both *CdtloΔΔ::CaTLO1* and *CdtloΔΔ::CaTLO4*, many of these genes have similar functions. The GDPase *GDA1, MNN9, MNT4* and *MNN24* are all associated with mannan biosynthesis and mannosylation and were all observed to be up-regulated in both *CdtloΔΔ::CaTLO1* and *CdtloΔΔ::CaTLO4* in the presence of 5 mM H_2O_2. Interestingly, all four of the genes were more highly expressed in the presence of *CdtloΔΔ::CaTLO4. CHS3, CHS7, CHS8, CHT1* and *CHT2* are five genes involved in chitin

synthesis and carbohydrate metabolism and again were all observed to be more highly up-regulated in *CdtloΔΔ::CaTLO4* than in *CdtloΔΔ::CaTLO1. EXG2,* which codes for a cell wall protein with beta-glucosidase activity was up-regulated 0.4-fold and 1.5-fold in *CdtloΔΔ::CaTLO1* and *CdtloΔΔ::CaTLO4* respectively. The cell wall transglycosylase *CRH11* was observed to be up-regulated 0.6-fold and 1.6-fold in the presence of *CdtloΔΔ::CaTLO1* and *CdtloΔΔ::CaTLO4* respectively, while the mannosyltransferase *VAN1* was up-regulated 1.2-fold and 2.3 fold in the presence of *CdtloΔΔ::CaTLO1* and *CdtloΔΔ::CaTLO4* respectively.

Although the majority of these genes were similarly expressed between *CdtloΔΔ::CaTLO1* and *CdtloΔΔ::CaTLO4,* it is apparent from Figure 7.17 that the majority of genes attributed to carbohydrate metabolism are more highly expressed in *CdtloΔΔ::CaTLO4* than in *CdtloΔΔ::CaTLO1.* This could potentially explain the disparity in H_2O_2 sensitivity between *CdtloΔΔ::CaTLO1* and *CdtloΔΔ::CaTLO4.* Interestingly, there were 10 genes differentially regulated between the *CdtloΔΔ::CaTLOs*, all of which were up-regulated in *CdtloΔΔ::CaTLO4* and down-regulated in *CdtloΔΔ::CaTLO1.*

7.4.6. Closing remarks

The aim of this section of the study was to observe whether there is cross functionality between the *CaTLOs* and the *CdTLOs*, and whether different *CaTLOs* are carrying out different functions. In order to observe this *CaTLO1, CaTLO3* and *CaTLO4* were introduced into the *CdtloΔΔ* mutant background. Based on the phenotypes tested in this study, i.e. the ability to form true hyphae, the ability to grow in an alternative carbon source to glucose and the ability to grow under oxidative stress conditions, we have confirmed that there is cross-functionality between *C. albicans* and *C. dubliniensis TLOs*. It is also clear that there is a great overlap in the functionality of the CaTlos. The *CaTLO* genes tested were all able to complement the phenotypes of the *CdtloΔΔ* mutant and they yielded similar transcriptions. However, we have shown that there is a subtle difference in the ability of *CdtloΔΔ::CaTLO4* to

grow in 5 mM H_2O_2 and we have identified differences in the transcriptomes of the *CdtloΔΔ::CaTLO1* and *CdtloΔΔ::CaTLO4* constructs. This suggests that there are differences in the functionality of the CaTlo proteins. In order to confirm this it is essential that the microarray data be verified using qRT-PCR of selected genes. It will also be important to test the remaining *CaTLO* genes in a wider range of environmental conditions.

Chapter 8

General Discussion

Although *Candida* species are among the most pathogenic and medically important human fungal pathogens there is still a lot to learn about how these organisms colonise and cause disease. *Candida albicans* and *Candida dubliniensis* are very closely related and share many phenotypic traits, including the ability to form true hyphae. Despite this there is a significant disparity in the ability of the two species to cause infection. We believe that comparative analysis of these two species will allow us to identify specific attributes that have contributed to the relative success of *C. albicans* as a commensal and pathogen. The publication of the complete genome sequences of the two species several years ago revealed just how similar *C. albicans* and *C. dubliniensis* are (Jackson *et al.,* 2009). The most significant example of divergence between the two species lies in the disparity of the telomere associated (*TLO*) gene family. *Candida albicans* contains 14 functional *TLO*s and one pseudogene, whereas sequence analysis of multiple *C. dubliniensis* strains has revealed that this species only encodes two *TLO* genes (Jackson *et al.,* 2009; D. Sullivan, unpublished data). During this project the Tlos were confirmed as orthologues of Med2, and thus are of the tail region of the major transcriptional regulatory polypeptide complex, Mediator. Given the striking difference in the virulence of *C. albicans* and *C. dubliniensis* it has been shown that the difference in copy number of the *TLO* family between the two species could potentially contribute to the higher propensity of *C. albicans* to cause disease. The purpose of this study was to further characterise the function of the Tlo proteins in *C. dubliniensis* and to identify if different orthologues of the *TLO* genes in *C. albicans* and *C. dubliniensis* differ in their activity.

8.1. The Tlos are tail subunits of the yeast Mediator complex

Sequencing of the *C. albicans* genome by Braun *et al.* (2005) revealed that the *TLO* genes encode a domain that is homologous to the yeast Mediator tail subunit Med2 of *Saccharomyces cerevisiae* (Bourbon, 2008; Anderson *et al.,* 2012; Zhang *et al.,* 2012). The

yeast Mediator complex is a large complex containing 15 subunits that activates transcription by facilitating interactions between DNA-bound transcription factors and RNA polymerase II (Bourbon *et al.,* 2008; Ansari *et al.,* 2012). All *Candida TLO* genes contain the Med2-like domain and appear to be orthologues of *MED2* in these species (Haran *et al.,* 2014). Supporting evidence comes from biochemical studies which have shown that similar to the *S. cerevisiae* Med2 protein, Tlo proteins co-purify with the *C. albicans* Mediator tail subunits Med3 and Med15 (Zhang *et al.,* 2012). In order to address whether *C. dubliniensis* Tlo is a Mediator component, Haran *et al.* (2014) purified Mediator from whole cell extracts of *C. dubliniensis* wild-type and *CdtloΔΔ* mutant cells using a dual affinity tag on the *C. dubliniensis* orthologue of the Med8 subunit of Mediator. The resulting Mediator complex was purified by SDS-PAGE and analysed using mass spectroscopy, which revealed that the *C. dubliniensis* Mediator is made up of a complete set of orthologues of the *S. cerevisiae* complex. Purified Mediator from the *CdtloΔΔ* mutant cells lacked the tail subunits Tlo1, Med3, Med15, Med16 and Med5, while this study has shown that Mediator purified from a *Cdmed3Δ* mutant strain lacked the equivalent components (Haran *et al.,* 2014).

To further examine the function of the Tlo proteins, as part of this study tandem-affinity purification was used to immunoprecipitate and purify tagged CdTlo1 protein and mass spectrophotometry was used to identify interacting proteins of CdTlo1. Of the 20 proteins identified, 5 were Mediator subunits, which further confirms the role of CdTlo1 in the yeast Mediator complex. Of particular interest is the presence of Cna1 and Try4 regulators, which possibly interact with Tlo1.

Given that Tlo and Med3 are thought to be required to stabilise the Mediator tail in *C. dubliniensis,* we hypothesised that the deletion of *MED3* should phenocopy the deletion of *CdTLO1* and *CdTLO2.* The *Cdmed3Δ* mutant was unable to form true hyphae in 10% w/v FBS and water, grew slowly in galactose as an alternative carbon source to glucose and was

susceptible to oxidative stress induced by hydrogen peroxide. The only phenotypic difference observed between the two mutants was the ability of the *Cdmed3Δ* mutant to form chlamydospores on RAT medium, where the *CdtloΔΔ* mutant did not. Seeing as Mediator is vital for transcriptional regulation, the transcriptional profiles of the *CdtloΔΔ* mutant and the *Cdmed3Δ* mutant were compared. Under nutrient-rich conditions the transcript profiles were very similar, however, under hyphal-inducing conditions there were significant differences in key functions such as glycolysis, protein-folding and DNA replication observed between the two mutants. There are several possible explanations for how these differences might occur. One possibility is that *in vivo* different tail components may exist in the Mediator complex in response to specific environmental stimuli. Another possible explanation is that the absence of Tlo or Med3 may result in the detachment of the other tail subunits to form a sub-complex that can interact with cellular components independently of the remaining Mediator complex (Haran *et al.*, 2014). Another possibility is that the absence of Tlo or Med3 could result in changes in quaternary structure of Mediator, which affects its specificity. Ansari *et al.* (2012) hypothesised that the tail subunits of the yeast Mediator complex may function redundantly. However, given that we found it impossible to delete *CdMED3* in the *CdtloΔΔ* mutant to create a triple mutant strain, it is possible that the presence of either Tlo or Med3 in the tail is necessary to stabilise the tail and that the loss of both *MED3* and the *TLO*s may result in the loss of viability.

It is not known whether or not the Mediator tail subunits in *C. dubliniensis* bind directly to DNA, however they are proposed to be associated directly with DNA-bound transcription factors and histones, and have been isolated in association with DNA in other yeasts (Liu *et al.*, 2012; Ansari *et al.*, 2012). Haran *et al.* (2014) observed that Tlo1 bound to all chromosomes and over 1500 open reading frames, and was found to be concentrated specifically at both telomeric regions and the Major Repeat Sequence. Mediator has been best studied in *S. cerevisiae* where it has been shown to have a role in heterochromatin

maintenance and has been shown to bind to telomeres and sub-telomeric genes (Liu *et al.*, 2012; Peng *et al.*, 2012). The data described by Haran *et al.* (2014) suggest that Mediator could be carrying out a similar function in *Candida* spp.

Zhang *et al.* (2012) observed that, under growth conditions tested, despite *C. dubliniensis* having two Tlos, expression of CdTlo1 only was detectable at a level comparable to other Mediator subunits, and at least 5 of the 14 *C. albicans* Tlo proteins were found within the Mediator complex. Zhang *et al.* (2012) have proposed that all expressed Tlo proteins can associate with Mediator. It is interesting that multiple Tlos are expressed as it is thought that all other Mediator subunits are present as a single orthologue (Zhang *et al.*, 2012). In *C. albicans* the potential for 14 different Tlo-Mediator complex combinations with differing transcriptional activating activities could explain the unique expansion of the *TLO* family during the evolution of this species. These numerous combinations of Tlo and Mediator could be affecting Mediator interactions with other proteins due to the sequence variation, or the combinations could be functioning to produce more protein. Zhang *et al.* (2012) found that, in *C. albicans,* after what is required for Mediator there remains an excess of free Mediator-independent Tlo protein. This excess protein could be vital for some additional role in addition to Mediator association. These findings indicate a possible explanation for the phenotypic flexibility of *C. albicans* and its adaptability, which could contribute to the higher incidence of *C. albicans* infections in comparison to its close relative *C. tropicalis* and *C. dubliniensis,* which do not have as extensive an expansion of Med2 orthologues (Haran *et al.*, 2014).

8.2. The *TLO* genes of *Candida albicans* and *Candida dubliniensis*

A study carried out by Anderson *et al.* (2015) observed the real-time evolution of the *TLO* gene family in *C. albicans* during laboratory passaging for over four thousand generations. Anderson *et al.* (2015) observed that the complement of *TLO* genes changed rapidly, with

both recurrent and transient changes occurring. This is unsurprising given that subtelomeric regions (where the *TLO* genes are generally found) typically evolve more quickly, and are frequently the sites of gene duplication events (Dreszer *et al.*, 2007; Ames *et al.*, 2010). Anderson *et al.* (2015) observed that the expansion of some *TLO* paralogues through recombination, gene duplication and mutation could result in interaction with new partners without the molecular role of the original gene being disrupted. A bias was apparent in the selection of some family members over others; *TLOγ7* and *TLOα10* were lost from the genome during some strain passaging, while *TLOα12* was gained eight times during recombination, and the copy number of *TLOα9* was reduced in eight events and never lost. This bias in expansion and contraction of some *TLO* genes could reflect specialised roles for individual *TLO* genes in directing Mediator activity within the cell (Anderson *et al.*, 2015).

The *TLO* gene family expansion is unique to *C. albicans,* which is far more pathogenic than its closest relative *C. dubliniensis.* This gene expansion could be the result of selective pressure in the host in order to facilitate adaptation of the commensal to new host niches (Moran *et al.*, 2011). If this is the case, it has been proposed that the *TLO* family contributes to the success of the commensalism and opportunism of *C. albicans.* The homozygous deletion of the two *TLO* genes in *C. dubliniensis* resulted in the alteration of a number of virulence-associated traits. The *Cdtlo*ΔΔ mutant was observed to be unable to form true hyphae under potent hyphal inducing conditions (i.e. water supplemented with 10% w/v FBS), the mutant demonstrated increased doubling times in alternative carbon sources and struggled to grow under oxidative stress conditions induced by H_2O_2 (Haran *et al.*, 2014). Phenotypically, the reintroduction of *CdTLO1* to the *Cdtlo*ΔΔ mutant had a more positive effect on the formation of true hyphae, with near wild type levels being formed. The presence of *CdTLO2* resulted in ~ 50% true hyphae being formed. This was reflected somewhat in the expression profiles of the *CdTLO* reintegrant DNA microarray experiment, which was carried out in order to examine whether *CdTLO1* and *CdTLO2* carry out similar functions. The majority of genes

involved in filamentation and cell wall functions appear to be more highly expressed upon re-introduction of *CdTLO1* than *CdTLO2*, following down-regulation in the absence of both *CdTLO*s. These include positive regulators of filamentation such as *RIM101, EFG1* and *UME6* (O' Connor *et al.*, 2010). This, along with phenotypic data, suggests that *CdTLO1* plays a more important role in hyphal formation, a major virulence factor associated with *Candida* species.

However, it should be noted that a number of genes are more highly expressed in the presence of *CdTLO2.* These include cell wall genes *HWP1, DSE1* and *EAP1*, while hyphal regulators *TEC1* and *RAS1* are also up-regulated to a greater extent by *CdTLO2.* This could be due to the fact that in the qRT-PCR studies *CdTLO2* expression was higher than *CdTLO1* expression in the constructs tested. Overall, it would appear that the *CdTLO* genes carry out similar functions, however the two CdTlo proteins may differ in their levels of expression, their efficiency and/or their target genes. The gene expression time-course experiments suggest that the CdTlos play an important role in mediating the speed and scale of transcriptional changes in response to environmental cues, with CdTlo1 having a greater effect than CdTlo2. This characteristic is likely to be of great importance in the host where rapid responses could be important for survival, e.g. following phagocytosis or translocation (Haran *et al.*, 2014).

Deletion of the *CaTLO*s has not yet been attempted due to the large number of genes and the likelihood of redundancy. However, cross-functionality between *C. albicans* and *C. dubliniensis* has previously shown the ability of *CaTLO11* and *CaTLO12* to restore full hyphal formation in a *Cdtlo1*Δ mutant strain. Complementation of *CaTLO1, CaTLO3* and *CaTLO4* to the *Cdtlo*ΔΔ mutant background has proved to be sufficient to restore the hyphal morphogenesis phenotype, and also restores normal growth in the presence of an alternative carbon source (i.e. galactose). The ability of *TLO*s from one species to compensate for the absence of *TLO*s in another provides further evidence of common functions across species. Interestingly, the

growth of *Cdtlo*ΔΔ::*CaTLO1*, *Cdtlo*ΔΔ::*CaTLO3* and *Cdtlo*ΔΔ::*CaTLO4* on YEPD supplemented with 5 mM H_2O_2 revealed that *Cdtlo*ΔΔ::*CaTLO4* could grow better in the presence of oxidative stress. Furthermore, comparative DNA microarray analysis of *Cdtlo*ΔΔ::*CaTLO1* and *Cdtlo*ΔΔ::*CaTLO4* under oxidative stress conditions revealed that the *CaTLO*s may vary slightly in their function. Twenty-two genes with important roles in virulence-associated functions such as oxidative stress response (*TPS1, HEM13*), filamentation (*HWP2, BIG1, HMS1, KTR4, SFL2, ARG83, ZCF10, ZCF2*), pathogenesis (*ZCF21, UME6, PPG1, CPP1*), cell wall and biofilm formation (*IRS4, WSC2, RBT5, IFD6, ARG81*) and carbohydrate metabolism (*PET9, MNN1, GFA1*) were observed to have diametrically opposing expression patterns between *Cdtlo*ΔΔ::*CaTLO1* and *Cdtlo*ΔΔ::*CaTLO4* under oxidative stress conditions induced by 5 mM H_2O_2. This suggests that the individual *CaTLO*s might be carrying out separate functions with regards to virulence traits.

8.3. Concluding remarks and future directions

While there are many similarities in the expression patterns of *C. dubliniensis tlo* and *med3* null mutants, significant differences exist suggesting distinct regulatory behaviour. It may be interesting to further explore the absence of chlamydospore formation in the *Cdmed3*Δ mutant, given that this is the only divergent phenotype detected between the two mutants, possibly by carrying out a DNA microarray study of the *Cdtlo*ΔΔ mutant and the *Cdmed3*Δ mutant in chlamydospore-inducing media. There is a significant cross-functionality between *TLO*s in both *C. albicans* and *C. dubliniensis.* Although there are still 11 *CaTLO*s remaining that are yet to be introduced into the *Cdtlo*ΔΔ mutant background, thus far it would appear that they are carrying out similar, but not identical functions. The DNA microarray study revealed that under oxidative stress conditions 65% and 59% of genes are commonly up- and down-regulated respectively between *Cdtlo*ΔΔ::*CaTLO1* and *Cdtlo*ΔΔ::*CaTLO4.* qRT-PCR studies need to be carried out on a selection of genes affected in the DNA microarray experiment in order to confirm these findings. In the future, it may be of value to carry out DNA microarray

studies of *Cdtlo*ΔΔ::*CaTLO1, Cdtlo*ΔΔ::*CaTLO4* and the other *CaTLO* constructs in the *Cdtlo*ΔΔ mutant background under hyphal-inducing conditions, as it would allow us to directly compare the transciptomes of the *CdTLO*s and the *CaTLO*s. Furthermore it would be of interest to grow the *CaTLO*s in the *Cdtlo*ΔΔ mutant background on chlamydospore-inducing media to observe whether they can also form chlamydospores.

TAP-tagging has confirmed that the Tlos are components of the yeast Mediator complex. Ideally, this experiment should be repeated, as this could identify more potentially interacting proteins and confirm the previously co-purified proteins. Co-immunoprecipitation experiments on Cna1 and Try4 are necessary to verify that CdTlo1 interacts with these regulators. It would also be useful to correlate our microarray data with their interactomes. In addition, it would be interesting to TAP-tag Tlo1 in a *Cdmed3*Δ strain to investigate the purification of Tlo1 in the absence of other Mediator tail subunits, given that the Tlos are proposed to be anchored to Mediator via Med3.

Data described in this thesis and elsewhere clearly support the hypothesis that the Tlo proteins play a role in regulating the expression of various virulence traits in *Candida* species such as *C. albicans* and *C. dubliniensis.* It has also been widely suggested that the expansion of the *TLO* family in *C. albicans* has contributed to its relative success as a human commensal and pathogen. To date we haven't had the technology to investigate this effectively, however, the application of the CRISPR-Cas system would greatly facilitate the analysis of the *TLO* genes in *C. albicans* and could ultimately be instrumental of confirming the importance of these genes in the pathogenesis of this species.

Bibliography

Bibliography

Achterman, R. R. & White, T. C. (2012). A foot in the door for dermatophyte research. *Plos Pathogens,* 8, doi:10.1371/journal.ppat.1002564.

Agwu, E., Ihongbe, J. C., McManus, B. A., Moran, G. P., Coleman, D. C., Sullivan, D. J. (2008). Distribution of yeast species associated with oral lesions in HIV-infected patients in Southwest Uganda. *Medical Mycology,* 50, 276-280.

Aksenova, A. Y., Greenwell, P. W., Dominska, M., Shishkin, A. A., Kim, J. C., Petes, T. D., Mirkim, S. M. (2013). Genome rearrangements caused by interstitial telomeric sequences in yeast. *Proceedings of the National Academy of Science USA,* 110, 19866-19871.

Alexander, B. D. & Perfect, J. R. (1997). Antifungal resistance trends towards the year 2000. Implications for therapy and new approaches. *Drugs,* 54, 657-678.

Almeida, R. S., Brunke, S., Albrecht, A., Thewes, S., Laue, M., Edwards, J. E. Jr, Filler, S. G., Hube, B. (2008). The hyphal-associated adhesin and invasin Als3 of *Candida albicans* mediates iron acquisition from host ferritin. *PLoS Pathogens,* 4, 1-17.

Almeida, R. S., Wilson, D., Hube, B. (2009). *Candida albicans* iron acquisition within the host. FEMS *Yeast Research.* 9, 1000-1012.

Ames, R. M., Rash, B. M.,Hentges, K. E., Robertson, D. L., Delneri, D., Lovell, S. C. (2010). Gene duplication and environmental adaptation within yeast populations. *Genome Biology Evolution,* 2, 591-601.

Anderson, J. M. & Soll, D. R. (1987). Unique phenotype of opaque cells in the white-opaque transition of *Candida albicans. Journal of Bacteriology,* 169, 5579-5588.

Anderson, M. Z., Baller, J. A., Dulmage, K., Wigen, L. & Berman, J. (2012). The three clades of the telomere-associated *TLO* gene family of *Candida albicans* have different splicing, localization, and expression features. *Eukaryotic Cell,* 11, 1268-1275.

Anderson, M. Z., Wigen, L. J., Burrack, L. S., Berman, J. (2015). Real-time evolution of a subtelomeric gene family in *Candida albicans. Genetics,* 115.

Anguilar, P. S., Fröhlich, F., Rehman, M., Shales, M., Ulitsky, I., Olivera-Couto, A., Braberg, H., Shamir, R., Walter, P., Mann, M., Ejsing, C. S., Krogan, N. J., Walther, T. C. (2010). A plasma-membrane E-MAP reveals links of the eisosome with sphingolipid metabolism and endosomal trafficking. *Nature Structural & Molecular Biology,* 17, 901-908.

Ansari, S., Ganapathi, M., Benschop, J.J., Holstege, F.C.P., Wade, J.T., Morse, R.H. (2012). Distinct role of Mediator tail module in regulation of SAGA-dependent, TATA-containing genes in yeast. *EMBO Journal,* 31, 44–57.

Arana, D.M., Alonso-Monge, R., Du, C., Calderone, R., Pla, J. (2007). Differential susceptibility of mitogenactivated protein kinase pathway mutants to oxidative-mediated killing by phagocytes in the fungal pathogen *Candida albicans. Cell Microbiology,* 9, 1647–1659.

Askew, C., Sellam, A., Epp, E., Hogues, H., Mullick, A., Nantel, A. & Whiteway, M. (2009). Transcriptional regulation of carbohydrate metabolism in the human pathogen *Candida albicans. PLoS Pathogens,* 5, 1-19.

Atir-Lande, A., Gildor, T., Kornitzer, D. (2005). Role for the SCFCDC4 ubiquitin ligase in *Candida albicans* morphogenesis. *Molecular Biology of the Cell,* 16, 2772-2785.

Backen, A. C., Broadbent, I. D., Fetherston, R. W., Rosamund, J. D., Schnell, N. F., Stark, M. J. (2000). Evaluation of the *caMAL2* promoter for regulated expression of genes in *C. albicans. Yeast,* 16, 1121-1129.

Bailey, D. A., Feldmann, P. J., Bovey, M., Gow, N. A., Brown, A. J. (1996). The *Candida albicans HYR1* gene, which is activated in response to hyphal development, belongs to a gene family encoding yeast cell wall proteins. *Journal of Bacteriology,* 178, 5353–5360.

Bain, J. M., Stubberfield, C., Gow, N. A. (2001). Ura-status-dependent adhesion of *Candida albicans* mutants. *FEMS Microbiology Letters,* 204, 323-328.

Banerjee, M., Thompson, D. S., Lazzell, A., Carlisle, P. L., Pierce, C., Monteagudo, C., López-Ribot, J. L., Kadosh, D. (2008). *UME6,* a novel filament-specific regulator of *Candida albicans* hyphal extension and virulence. *Molecular Biology of the Cell,* 19, 1354–1365.

Baron, U. & Bujard, H. (2000). Tet repressor-based system for regulated gene expression in eukaryotic cells: principles and advances. *Methods in Enzymology,* 327, 401-421.

Bassler, J., Kallas, M. & Hurt, E. (2006). The NUG1 GTPase reveals an N-terminal RNA-binding domain that is essential for association with 60 S Pre-ribosomal particles. *Journal of Biological Chemistry,* 281, 24737-24744.

Bennett, R. J., Uhl, M. A., Miller, M. G., Johnson, A. D. (2003). Identification and characterization of a *Candida albicans* mating pheromone. *Molecular Cell Biology,* 23, 8189-8201.

Berman J. & Sudbery, P. (2002). *Candida albicans*: a molecular revolution built on lessons from budding yeast. *Nature,* 3, 918-930.

Bhoite, L. T., Yu, Y. & Stillman, D. J. (2001). The Swi5 activator recruits the Mediator complex to the HO promoter without RNA polymerase II. *Genes & Development,* 15, 2457-2469.

Bink, A., Vandenbosch, D., Coenye, T., Nelis, H., Cammue, B. P. A., Thevissen, K. (2011). Superoxide dismutases are involved in *Candida albicans* biofilm persistence against miconazole. *Antimicrobial Agents and Chemotherapy,* 55, 4033-4037.

Biswas, S., Van Dijck, P. & Datta, A. (2007). Environmental sensing and signal transduction pathways regulating morphopathogenic determinants of *Candida albicans. Microbiology and Molecular Biology Reviews,* 71, 348-376.

Björklund, S. & Gustafsson, C. M. (2005). The yeast mediator complex and its regulation. *Trends in Biochemical Science,* 30(5), 240-4.

Blackwell, C., Russell, C. L., Argimon, S., Brown, A., J., P., Brown, J., D. (2003). Protein A-tagging for purification of native macromolar complexes from *Candida albicans. Yeast,* 20, 1235-1241.

Blanco, M. T., Sacristan, B., Lucio, L., Blanco, J., Perez-Giraldo, C., and Gomez-Garcia, A. C. (2010). Cell surface hydrophobicity as an indicator of other virulence factors in *Candida albicans. Revista Iberoamericana Micología,* 27, 195–199.

Blignaut, E. (2007). Oral candidiasis and oral yeast carriage among institutionalised South African paediatric HIV/AIDS patients. *Mycopathologia*, 163, 67–73.

Bonhomme, J., Chauvel, M., Goyard, S., Roux, P., Rossignol, T., d'Enfert, C. (2011). Contribution of the glycolytic flux and hypoxia adaptation to efficient biofilm formation by *Candida albicans. Molecular Microbiology,* 80, 995-1013.

Borggrefe, T., Davis, R., Erdjument-Bromage, H., Tempst, P., Kornberg, R. D. (2002). A complex of the Srb8,-9,-10 and -11 transcriptional regulatory proteins from yeast. *Journal of Biological Chemistry,* 277, 44202-44207.

Bourbon, H. M. (2008). Comparative genomics supports a deep evolutionary origin for the large, four-module transcriptional mediator complex. *Nucleic Acids Research,* 36, 3993-4008.

Brand, A. (2012). Hyphal growth in human fungal pathogens and its role in virulence. *International Journal of Microbiology,* Article ID 517529, 1-11.

Braun, B. R. & Johnson, A. D. (1997). Control of filament formation in *Candida albicans* by the transcriptional repressor TUP1. *Science,* 277, 105–109.

Braun, B. R. & Johnson, A. D. (2000). *TUP1, CPH1* and *EFG1* make independent contributions to filamentation in *Candida albicans. Genetics,* 155, 57-67.

Brizzard, B. (2008). Epitope tagging. *BioTechniques,* 44, 693-695.

Brown, C. A., Murray, A. W. & Verstrepen, K. J. (2010). Rapid expansion and functional divergence of subtelomeric gene families in yeasts. *Current Biology*, 20, 895-903.

Brown, A. J. P., Haynes, K., Gow, N. A. R., Quinn, J (2012). Stress responses in *Candida*. In *Candida* and Candidiasis (2nd edn) (Clancy, C.J. and Calderone, R.A., eds), pp. 225–242, *ASM Press.*

Brown, G. D., Denning, D. W., Gow, N. A. R., Levitz, S. M., Netea, M. G., White, T. C. (2012). Hidden killers: human fungal infections. *Medical Mycology,* 165, 1-9.

Brown, A. J. P., Brown, G. D., Netea, M. G., Gow, N. A. R. (2014). Metabolism impacts upon *Candida* immunogenicity and pathogenicity at multiple levels. *Trends in Microbiology,* 22, 614-622.

Bruno, V. M., Wang, Z., Marjani, S. L., Euskirchen, G. M., Martin, J., Sherlock, G, Snyder, M. (2010). Comprehensive annotation of the transcriptome of the human fungal pathogen *Candida albicans* using RNA-seq. *Genetics and Molecular Research,* 20, 1451-1458.

Butler, G., Rasmussen, M. D., Lin, M. F., Santos, M. A., Sakthikumar, S., Munro, C. A., Rheinbay, E., Grabherr, M., Reedy, J. L., *et al.* (2009). Evolution of pathogenicity and reproduction in eight *Candida* genomes. *Nature,* 459, 657-622.

Cabral, V., Znaidi, S., Walker, L. A., Martin-Yken, H., Dague, E., Legrand, M., Lee, K., Chauvel, M., Firon, A., Rossignol, T., Richard, M. L., Munro, C. A., Bachellier-Bassi, S., d'Enfert, C. (2014). Targeted changes of the cell wall proteome influence *Candida albicans* ability to form single- and multi-strain biofilms. *PLoS Pathogens,* 10, 1-21.

Calderone, R. (2002). *Candida* and candidiasis. ASM Press.

Calderone, R & Fonzi, W. A. (2001). Virulence factors of *Candida albicans. Trends in Microbiology,* 9, 327-335.

Care, R. S., Trevethick, J., Binley, K. M., Sudbery, P. E. (1999). The *MET3* promoter: a new tool for *Candida albicans* molecular genetics. *Molecular Microbiology,* 34, 792-798.

Carreto, L., Eiriz, M. F., Gomes, A. C., Pereira, P. M., Schuller, D., Santos, M. S. (2008). Comparative genomics of wild type yeast strains unveils important genome diversity. *BMC Genomics,* 9, 524.

Čáp, M., Váchová, L. & Palková, Z. (2012). Reactive oxygen species in the signalling and adaptation of multicellular microbial communities. *Oxidative Medecine & Cell Longevity,* 976753, 1-13.

Chandra, J., Kuhn, D. M., Mukherjee, P. K., Hoyer, L. L., McCormick, T., Ghannoum, M. A. (2001). Biofilm formation by the fungal pathogen *Candida albicans*: development, architecture, and drug resistance. *Journal of Bacteriology*, 183, 5385-5394.

Chen, Y. L., Brand, A., Morrison, E. L., Silao, F. S., Bigol, U. S., Malbas, F. F., Nett, J. E., Anders, D. R., Solis, N. V., Filler, S. G., Averette, A., Heitman, J. (2011). Calcineurin controls drug tolerance, hyphal growth and virulence in *Candida dubliniensis*. *Eukaryotic Cell*, 10, 803-819.

Cheng, S., Nguyen, M. H., Zhang, Z., Jia, H., Handfield, M., Clancy, C. J. (2003). Evaluation of the roles of four *Candida albicans* genes in virulence by using gene disruption strains that express *URA3* from the native locus. *Infection and Immunity*, 71, 6101-6103.

Chin, C., Lai, W. C., Lee, T. L., Tseng, T. L., Shieh, J. C. (2013). Dissection of the *Candida albicans* Cdc4 protein reveals the involvement of domains in morphogenesis and cell flocculation. *Journal of Biomedical Science*, 20, 1-11.

Citiulo, F., Moran, G. P., Coleman, D. C., Sullivan, D. J. (2009). Purification and germination of *Candida albicans and Candida dubliniensis* chlamydospores cultured in liquid media. *FEMS Yeast Research*, 9, 1051–1060.

Citiulo, F., Jacobsen, I. D., Miramón, P., Schild, L., Brunke, S., Zipfel, P, Brock, M., Wilson, D., Hube, B. (2012). *Candida albicans* scavenges host zinc via Pra1 during endothelial invasion. *PLoS Pathogens*. 8, 1-14.

Cole, M. F., Bowen, W. H., Zhao, X. J., Cihlar, R. L. (1995). Avirulence of *Candida albicans* auxotrophic mutants in a rat model of oropharyngeal candidiasis. *FEMS Microbiology Letters*, 126, 177-180.

Coleman, D., Sullivan, D., Haynes, K., Henman, M., Shanley, D., Bennett, D., Moran, G., McCreary, C., O'Neill, L., Harrington, B. (1997). Molecular and phenotypic analysis of *Candida dubliniensis*: a recently identified species linked with oral candidosis in HIV-infected and AIDS patients. *Oral Disease*, 3, S96–S101.

Collins, M. O. & Choudhary J. S. (2008). Mapping protein interactions by affinity purification and mass spectrometry. *Current Opinion in Biotechnology*, 19, 324-330.

Conaway, R. C. & Conaway, J. W. (2011). Function and regulation of the mediator complex. *Current Opinion in Genetics & Development*, 21, 225- 230.

Cuéllar-Cruz, M., Vega-González, A., Mendoza-Novelo, B., Lópex-Romero, E., Ruiz-Baca, E., Quintanar-Escorza, M. A., Villagómez-Castro, J. C. (2012). The effect of biomaterials and antifungals on the biofilm formation by *Candida* species: a review. *European Journal of Clinical Microbiology & Infectious Diseases,* 31, 2513-2527.

Da Silva Dantas, A., Day, A., Ikeh, M., Kos, I., Achan, B., Quinn, J. (2015). Oxidative stress responses in the human fungal pathogen, *Candida albicans. Biomolecules,* 5, 142-165.

Davis, J. A., Takagi, Y., Kornberg, R. D., Asturias, F. A. (2002). Structure of the yeast RNA polymerase II holoenzyme: Mediator confirmation and polymerase interaction. *Molecular Cell,* 10, 409-415.

D'Enfert, C. (2009). Hidden killers: persistence of opportunistic fungal pathogens in the human host. *Current Opinion in Microbiology*, 4, 358-364.

De Backer, M. D., Magee, P. T., Pla, J. (2000). Recent developments in molecular genetics of *Candida albicans. Annual Review of Microbiology*, 54, 463–498.

De Bernardis, F., Arancia, S., Morelli, L., Hube, B., Sanglard, D., Schäfer, W., Cassone, A. (1999). Evidence that members of the secretory aspartyl proteinase gene family, in particular *SAP2,* are virulence factors for *Candida* vaginitis. *Journal of Infectious Disease,* 179, 201-208.

De Rosa, F. G., Garazzino, S., Pasero, D., Di Perri, G., Ranieri, V.M. (2009). Invasive candidiasis and candidemia: new guidelines. *Minerva anestesiologica,* 75(7-8), 453–458.

Donlan, R. M. & Costerton, J. W. (2002). Biofilms: survival mechanisms of clinically relevant microorganisms. *Clinical Microbiology Reviews,* 15, 167-193.

Donnelly, S. M., Sullivan, D. J., Shanley, D. B., Coleman, D. C. (1999). Phylogenetic analysis and rapid identification of *Candida dubliniensis* based on analysis of *ACT1* intron and exon sequences. *Microbiology,* 145, 1871-1882.

Dotson, M. R., Yuan, C. X., Roeder, R. G., Myers, L. C., Gustafsson, C. M., Jiang, Y. W., Li, Y., Kornberg, R. D., Asturias, F., J. (2000). Structural organization of yeast and mammalian mediator complexes. *Proceedings of the National Academy of Sciences,* 97, 14307-14310.

Douglas, J. L. (2003). *Candida* biofilms and their role in infection. TRENDS *in Microbiology,* 11, 30-36.

Dreszer, T. R., Wall, G. D., Haussler, D., Pollard, K. S. (2007). Biased clustered substitution in the human genome: The footprints of male-driven biased gene conversion. *Genome Research,* 17, 1420-1430.

Drgona, L., Khachatryan, A., Stephens, J., Charbonneau, C., Kantecki, M., Haider, S., Barnes, R. (2014). Clinical and economic burden of invasive fungal diseases in Europe: focus on pre-emptive and empirical treatment of *Aspergillus* and *Candida* species. *European Journal of Clinical Microbiology & Infectious Disease,* 33, 7-21.

Dujon, B., Sherman, D., Fischer, G., Durrens, P., Casaregola, S., *et al* (2004). Genome evolution in yeasts. *Nature,* 430, 35–44.

Eckert, S. E., Sheth, C. C., Mühlschlegel, F. A. (2007). Regulation of morphogenesis in *Candida* species. *Comparative and functional genomics.* D'Enfert, C., Hube, B. 263-291. Caister Academic Press, Norfolk.

Eggimann, P., Garbino, J., Pittet, D. (2003). Epidemiology of *Candida* species infections in critically ill non-immunosuppressed patients. *The Lancet Infectious Diseases,* 3, 685-702.

Eisman, B., Alonso-Monge, R., Roman, E., Arana, D., Nombela, C., Pla, J. (2006). The Cek1 and Hog1 mitogen-activated protein kinases play complementary roles in cell wall biogenesis and chlamydospore formation in the fungal pathogen *Candida albicans. Eukaryotic Cell,* 5, 347–358.

Elmlund, H., Baraznenok, V., Lindahl, M., Samuelsen, C. O., Koeck, P. J., Holmberg, S., Herbert, H., Gustafsson, C. M. (2006). The cyclin-dependent kinase 8 module sterically blocks Mediator interactions with RNA polymerase II. *Proceedings of the National Academy of Sciences USA,* 103, 15788-15793.

Eng, J. K., McCormack, A. L. & Yates, J. R. (1994). An approacj to correlate tandem mass spectral data of peptides with amino acid sequences in a protein database. *Journal of the American Society for Mass Spectrometry,* 11, 976-989.

Enjalbert, B., Nantel, A. & Whiteway, M. (2003). Stress-induced gene expression in *Candida albicans*: Absence of a general stress response. *Molecular Biology of the Cell,* 14, 1460–1467.

Enjalbert, B., Smith, D. A., Cornell, M. J., Alam, I., Nicholls, S., Brown, A. J., Quinn, J. (2006). Role of the Hog1 stress-activated protein kinase in the global transcriptional response to stress in the fungal pathogen *Candida albicans. Molecular Biology of the Cell,* 17, 1018–1032.

Estivill, D., Arias, A., Torres-Lana, A., Carrillo-Munoz, A. J., and Arevalo, M. P. (2011). Biofilm formation by five species of Candida on three clinical materials. *Journal of Microbiological Methods,* 86, 238–242.

Fan, X. & Struhl, K. (2009). Where does Mediator bind *in vivo*? *PLoS One,* 4, 1-6.

Felk, A., Kretschmar, M., Albrecht, A., Schaller, M., Beinhauer, S., Nichterlein, T., Sanglard, D., Korting, H. C., Schäfer, W., Hube, B. (2002). *Candida albicans* hyphal formation and the expression of the Efg1-regulated proteinases Sap4 to Sap6 are required for invasion of parenchymal organs. *Infection and Immunity,* 70, 3689-3700.

Feng, Q. H., Summers, E., Guo, B., Fink, G. (1999). Ras signaling is required for serum-induced hyphal differentiation in *Candida albicans. Journal of Bacteriology,* 181, 6339–6346.

Field, J., J. Nikawa, D. Broek, B. MacDonald, L. Rodgers,I.A. Wilson, R.A. Lerner, and M. Wigler. (1988). Purification of RAS-responsive adenylyl cyclase complex from *Saccharomyces ceverisiae* by use of an epitope addition method. *Molecular Cell Biology,* 8, 2159-2165.

Figeys, D., McBroom, L., D., Moran, M., F. (2001). Mass spectrometry for the study of protein-protein interactions. *Methods Proteomics.* 24, 230-239.

Filler, S. G. & Sheppard, D. C. (2006). Fungal invasion of normally non-phagocytic host cells. *PLoS Pathogens,* 2, e129, 13.

Finkel, J. S. & Mitchell, A. P. (2011). Genetic control of *Candida albicans* biofilm development. *Nature reviews. Microbiology,* 9, 109-118.

Fonzi, W. A. & Irwin, M. Y., (1993). Isogenic strain construction and gene mapping in *Candida albicans. Genetics,* 134, 717-728.

Foss, E. J., Radulovic, D., Shaffer, S. A., Ruderfer, D. M., Bedalov, A., Goodlett, D. R., Kruglyak, L. (2007). Genetic basis of proteome variation in yeast. *Nature Genetics,* 39, 1369-1375.

Fradin, C., De Groot, P., MacCallum, D., Schaller, M., Klis, F., Odds, F.C., Hube, B. (2005). Granulocytes govern the transcriptional response, morphology and proliferation of *Candida albicans* in human blood. *Molecular Microbiology,* 56, 397– 415.

Frohner, I. E., Bourgeois, C., Yatsyk, K., Majer, O. Kuchler, K. (2009). *Candida albicans* cell surface superoxide dismutases degrade host-derived reactive oxygen species to escape innate immune surveillance. *Molecular Microbiology,* 71, 240-252.

Fu, Y., Rieg, G., Fonzi, W. A., Belanger, P. H., Edwards, J. E. Jr, Filler, S. G. (1998). Expression of the *Candida albicans* gene *ALS1* in *Saccharomyces cerevisiae* induces adherence to endothelial and epithelial cells. *Infection and Immunity,* 66, 1783-1786.

Gale, C. A., Bendel, C. M., McCellan, M., Hauser, M., Becker, J. M., Berman, J., Hostetter, M. K. (1996). Linkage of adhesion, filamentous growth, and virulence in *Candida albicans* to a single gene, *INT1. Science,* 279, 1355-1358.

Gardner, M. J., Hall, N., Fung, E., White, O., Berriman, M. *et al.* (2002). Genome sequence of the human malaria parasite *Plasmodium falciparum. Nature,* 419, 498-511.

Gaur, N. K., Klotz, S. A., Henderson, R. L. (1999). Overexpression of the *Candida albicans* ALA1 gene in *Saccharomyces cerevisiae* results in aggregation following attachment of yeast cells to extracellular matrix proteins, adherence properties similar to those of *Candida albicans. Infection and Immunity,* 65, 6040-6074.

Gazy, I. & Kupiec, M. (2013). Genomic instability and repair mediated by common repeated sequences. *Proceedings of the National Academy of Sciences USA,* 110, 19664-19665.

Gerami-Nejad, M., Dulmage, K & Berman, J. (2009). Additional cassettes for epitope and fluorescent fusion proteins in *Candida albicans. Yeast,* 26, 399-406.

Gingras, A. C., Aerbersold, R. & Raught, B. (2005). Advances in protein complex analysis using mass spectrometry. *Journal of Physiology,* 563, 11-21.

Gola, S., Martin, R., Walther, A., Dünkler, Wendland, J. (2003). New modules for PCR-based gene targeting in *Candida albicans*: rapid and efficient targeting using 100 bp of flanking homology region. *Yeast,* 20, 1339-1347.

Grada, A. & Weinbrecht, K. (2013). Next-generation sequencing: methodology and application. *Journal of Investigative Dermatology,* 133, 1-4.

Granger, B. L., Flennikin, M. L., Davis, D. A., Mitchell, A. P., Cutler, J. E. (2005). Yeast wall protein 1 of *Candida albicans. Microbiology,* 151, 1631-1644.

Grover, N. (2010). Echinocandins: a ray of hope in antifungal drug therapy. *Indian Journal of Pharmacology*, 42, 9–11.

Guglielmi, B., van Berkum, N. L., Klapholz, B., Bijma, T., Boube, M., Boschiero, C., Bourbon, H. M., Frank, C., Holstege, P., Werner, M. (2004). A high resolution protein interaction map of the yeast Mediator complex. *Nucleic Acid Research,* 32, 5379-5391.

Gygi, S.P., Rochon, Y., Franza, B.R., Aebersold, R. (1999). Correlation between protein and mRNA abundance in yeast. *Molecular and Cell Biology,* 19, 1720–1730.

Hamal, P., Dostal, J., Raclavsky, V., Krylova, M., Pichova, I., Hruskova- Heidingsfeldova, O. (2004). Secreted aspartate proteinases, a virulence factor of *Candida* spp.: ocurrence among clinical isolates. *Folia Microbiologica,* 49, 491–496.

Hamza, O. J., Matee, M. I., Moshi, M. J., Simon, E. N., Mugusi, F., Mikx, F. H., Helderman W. H., Rijs, A. J., van der Ven, A. J., Verweij, P. E. (2008). Species distribution and *in vitro* antifungal susceptibility of oral yeast isolates from Tanzanian HIV-infected patients with primary and recurrent oropharyngeal candidiasis. *BMC Microbiology*, 8, 135.

Haran, J., Boyle, H., Hokamp, K., Yeomans, T., Liu, Z., Church, M., Fleming, A. B., Anderson, M. Z., Berman, J., Myers, L. C., Sullivan, D. J., Moran, G. P. (2014). Telomeric *ORFs* (*TLOs*) in *Candida* spp. encode Mediator subunits that regulate distinct virulence traits. *PLoS Genetics,* 10, 1-17.

Havlickova, B., Czaika, V. A., Friedrich, M. (2008). Epidemiological trends in skin mycoses worldwide. *Mycoses,* 51, 2-15.

Hay, R. J. (1999). The management of superficial candidiasis. *Journal of the American Academy of Dermatology,* 40, 35–42.

Heitman, J., Filler, S. G., Edwards, J. E. Jr, Mithcell, A. P. (2006). Molecular principles of fungal pathogenesis. *American Society for Microbiology Press,* Washington D.C. 197-212.

Higasho, H., Sato, K. & Nakano, A. (2008). Smy2p participates in COPII vesicle formation through the interaction with Sec23p/Sec24p subcomplex. *Traffic,* 9, 79-93.

Hillen, W. & Berens, C. (1994). Mechanisms underlying expression of Tn*10* encoded tetracycline resistance. *Annual Review of Microbiology,* 48, 345-369.

Hof, H. (2006). A new, broad-spectrum azole antifungal: posaconazole-mechanisms of action and resistance, spectrum of activity. *Mycoses,* 49, 2–6.

Hohl, T. M. & Feldmesser, M. (2007). *Aspergillus fumigatus*: principles of pathogenesis and host defense. *Eukaryotic Cell,* 6, 1953-1963.

Holden, H. M., Rayment, I. & Thoden, J. B. (2003). Structure and function of the enzymes of the Leloir pathway for galactose metabolism. *Journal of Biological Chemistry,* 278, 43885-43888.

Holmstrup, P. & Besserman, M. (1983). Clinical, therapeutic and pathogenic aspects of chronic oral multifocal candidiasis. *Oral Surgery Oral Medicine Oral Pathology,* 56, 388-395.

Holstege, F. C., Jennings, E. G., Wyrick, J. J., Lee, T. I., Hengartner, C. J., Green, M. R., Golub, T. R., Lander, E. S., Young, R. A. (1998). Dissecting the regulatory circuitry of a eukaryotic genome. *Cell,* 95, 717-728.

Hornbach A, Heyken A, Schild L, Hube B, Loffler J, Kursai O. (2009). The glycosylphosphatidylinositol-anchored protease Sap9 modulates the interaction of Candida albicans with human neutrophils. *Infection and Immunity,* 77, 5216–5224.

Hoyer, L. L., Payne, T. L., Bell, M., Myers, A. M., Scherer, S. (1998). *Candida albicans ALS3* and insights into the nature of the *ALS* gene family. *Current Genetics,* 33, 451–459.

Hoyer, L. L. (2001). *ALS* gene family of *Candida albicans*. *Trends in Microbiology,* 9, 176–180.

Inglis, D. O., Arnaud, M. B., Binkley, J., Prachi, S., Skrzypek, M. S., Wymore, F., Binkley, G., Miyasato, S. R., Simison, M., Sherlock, G. (2012). The *Candida* genome database incorporates multiple *Candida* species: multispecies search and analysis tools with curated gene and protein information for *Candida albicans* and *Candida glabrata*. *Nucleic Acids Research,* 40, 667-674.

Jackson, A. P., Gamble, J. A., Yeomans, T., Moran, G. P., Saunders, D., Harris, D., Aslett, M., Barrell, J. F., Butler, G., Citiulo, F., Coleman, D. C., Groot, P. W. J. De, Goodwin, T. J., Quail, M. A., Mcquillan, J., Munro, C. A., Pain, A., Renauld, H., Spiering, M. J., Poulter, R. T., Tivey, A., Gow, N. A. R., Barrell, B., Sullivan, D. J., Berriman, M. (2009). Comparative genomics of the fungal pathogens *Candida dubliniensis* and *Candida albicans*. *Genome Research,* 19, 2231–2244.

Jansen, J. P., Kern, W. V., Comely, O. A., Karthaus, M., Ruhnke, M., Ullmann, A. J., Resch, A. (2006). Economic evaluation of voriconazole versus conventional amphotericin B in the treatment of invasive apergillosis in Germany. *Val Health,* 9, 12-23.

Jarvik, J. W. & Telmer, C. A. (1998). Epitope tagging. *Annual Review of Genetics,* 32, 601-618.

Kadosh, D. & Johnson, A. D. (2001). Rfg1, a protein related to the *Saccharomyces cerevisiae* hypoxic regulator Rox1, controls filamentous growth and virulence in *Candida albicans*. *Molecular & Cell Biology,* 21, 2496-2505.

Kadosh, D. & Johnson, A. D. (2005). Induction of the *Candida albicans* filamentous growth program by relief of transcriptional repression: a genome-wide analysis. *Molecular Biology of the Cell,* 16, 2903–2912.

Kaiser, B., Munder, T., Saluz, H. P. & Ku, W. (1999). Identification of a Gene Encoding the Pyruvate Decarboxylase Gene Regulator CaPdc2p from *Candida albicans*. *Yeast,* 15, 585-591.

Kaiser, P., Meierhofer, D., Wang, X., Huang, L. (2008). Tandem affinity purification combined with mass spectrometry to identify components of protein complexes. *Methods in Molecular Biology,* 439, 309-326.

Karkowska-Kuleta, J., Rapala-Kozik, M., Kozik, A. (2009). Fungi pathogenic to humans: molecular bases of virulence of *Candida albicans, Cryptococcus neoformans* and *Aspergillus fumigatus. Acta Biochimica Polonica*, 56, 2, 211-224.

Kibbler, C., Seaton, S., Barnes, R., Gransden, W., Holliman, R., Johnson, E., Perry, J., Sullivan, D., Wilson, J. (2003). Management and outcome of bloodstream infections due to *Candida* species in England and Wales. *Journal of Hospital Infection*, 54, 18–24.

Kim, D. U., Hayles, J., Kim, D., Wood, V., Park, H. O., Won, M., Yoo, H. S., Duhig, T., Nam, P., Palmer, G., Hans, S., Jeffery, L., Baek, S. T., Lee, H., Shim, Y. S., Lee, M., Kim, L., Heo, K. S., Noh, E. J., Lee, A. R., Jang, Y. J., Chung, K. S., Choi, S. J., Park, J. Y., Park, Y., Kim, H. M., Park, S. K., Park, H. J., Kang, E. J., Kim, H. B., Kang, H. S., Park, H. M., Kim, K., Song, K., Song, K. B., Nurse, P., Hoe, K. L. (2010). Analysis of a genome-wide set of gene deletions in the fission yeast *Schizosaccharomyces pombe. Nature Biotechnology,* 28, 617-623.

Kim, H., Esser, L., Hossain, M. B., Xia, D., Yu, C. A., Rizo, J., Van Der Helm, D., Deisenhofer, J. (1999). Structure of antimycin A1, a specific electron transfer inhibitor of ubiquinol-cytochrome c oxidoreductase. *Journal of the American Chemical Society,* 121, 4902-4903.

Kim, J. & Sudbery, P. (2011). *Candida albicans*, a major human fungal pathogen. *Journal of Microbiology,* 49, 171–177.

Kim, J., Bjorklund, S., Li, Y., Sayre M. H., Kornberg, R. D. (1994). A multiprotein mediator of transcriptional activation and its interaction with the C- terminal repeat domain of RNA polymerase II. *Cell,* 77, 599-308.

Kirkpatrick, W. R., Revankar, S. G., Mcatee, R. K., Lopez-Ribot, J. L., Fothergill, W., McCarthy, D. I., Sanche, S. E., Cantu, R. A., Rinaldi, M.G., Patterson, T.F. (1998). Detection of *Candida dubliniensis* in oropharyngeal samples from human immunodeficiency virus-infected patients in North America by primary CHROMagar candida screening and susceptibility testing of isolates. *Journal of Clinical Microbiology,* 36, 3007–12.

Kontoyiannis, D.P. & Lewis, R.E. (2002). Antifungal resistance of pathogenic fungi. *The Lancet,* 359, 1135-1144.

Koschubs, T., Seizi, M., Larivière, L., Kurth, F., Baumli, S., Martin, D. E., Cramer, P. (2009). Identification, structure, and functional requirement of the Mediator submodule Med7N/31. *The EMBO Journal,* 28, 69-80.

Kuhn, D. M., Chandra, J., Mukherjee, P. K., Ghannoum, M. A. (2002). Comparison of biofilms formed by *Candida albicans* and *Candida parapsilosis* on bioprosthetic surfaces. *Infection and Immunity,* 70, 878–888.

Kumamoto, C. A. & Vinces, M. D. (2005). Contributions of hyphae and hypha-co-regulated genes to *Candida albicans* virulence. *Cell Microbiology,* 7, 1546-1554.

Kupiec, M. (2014). Biology of telomeres: lessons from budding yeast. *FEMS Microbiology Reviews,* 38, 144-171.

Kvaal C, Lachke SA, Srikantha T, Daniels K, McCoy J, Soll, D. R. (1999) Misexpression of the opaque-phase-specific gene *PEP1* (*SAP1*) in the white phase of *Candida albicans* confers increased virulence in a mouse model of cutaneous infection. *Infection and Immunity,* 67, 6652–6662.

Lachke, S. A., Lockhart, S. R., Daniels, K. J., Soll, D. R. (2003). Skin facilitates *Candida albicans* mating. *Infection and Immunity,* 71, 4970-4976.

Lan, C., Rodarte, G., Murilla, L. A., Jones, T., Davis, R. W., Dungan, J., Newport, G., Agabian, N. (2004). Regulatory networks affected by iron availability in *Candida albicans. Molecular Microbiology,* 53, 1451-1469.

Lay, J., Henry, L. K., Clifford, J., Koltin, Y., Bulawa, C. E., Becker, J. M. (1998). Altered expression of selectable marker *URA3* in gene-disrupted *Candida albicans* strains complicates interpretation of virulence studies. *Infection and Immunity,* 66, 5301-5306.

Leberer E, Harcus, D., Broadbent, I. D., Clark, K. L., Dignard, D., Ziegelbauer, K., Schmidt, A., Gow, N. A., Brown, A.J., Thomas, D.Y. (1996). Signal transduction through homologs of the Ste20p and Ste7p protein kinases can trigger hyphal formation in the pathogenic fungus *Candida albicans. Proceedings of the National Academy of Sciences USA,* 93, 13217–13222.

Leberer, E., Harcus, D., Dignard, D., Johnson, L., Ushinsky, S., Thomas, D. Y., Schröppel, K. (2001). Ras links cellular morphogenesis to virulence by regulation of the MAP

kinase and cAMP signalling pathways in the pathogenic fungus *Candida albicans*. *Molecular Microbiology*, 42, 673-687.

Lee, K. L., Buckley, H. R. & Cambell, C. C. (1975). An amino acid liquid synthetic medium for the development of mycelial and yeast forms of *Candida albicans*. *Sabouraudia*, 13, 148–153.

Lenstra, T. L., Benschop, J. J., Kim, T., Schulze, J. M., Brabers, N. A., Margaritis, T., van de Pasch, L. A., van Heesch, S. A., Brok, M. O., Groot Koerkamp, M. J., Ko, C. W., van Leenen, D., Sameith, K., van Hooff, S. R., Lijnzaad, P., Kemmeren, P., Hentrich, T., Kobor, M. S., Buratowski, S., Holstege, F. C. (2011). The specificity and topology of chromatin interaction pathways in yeast. *Molecular Cell*, 42, 536-549.

Leuker, C. E., Sonneborn, A., Delbrück, S., Ernst, J. F. (1997). Sequence and promoter regulation of the *PCK1* gene encoding phosphoenolpyruvate carboxykinase of the fungal pathogen *Candida albicans*. *Genetics*, 192, 235-240.

Li, F. & Palecek, S. P. (2008). Distinct domains of the *Candida albicans* adhesin Eap1p mediate cell-cell and cell-substrate interactions. *Microbiology*, 154, 1194-1203.

Linder, T., Rasmussen, N. N., Samuelsen, C. O., Chatzidaki, E., Baraznenok, V., Beve, J., Henriksen, P., Gustafsson, C. M., Holmberg, S. (2008). Two conserved modules of *Schizosaccharomyces pombe* Mediator regulate distinct cellular pathways. *Nucleic Acids Research*, 36, 2489-2504.

Lindsay, A. K., Morales, D. K., Liu, Z., Grahl, N., Zhang, A., Willger, S. D., Myers, L. C., Hogan, D. A. (2014). Analysis of *Candida albicans* mutants defective in the Cdk8 module of mediator reveal links between metabolism and biofilm formation. *PLoS Pathogens*, 10, 1-15.

Livak, K. J. (1997). ABI Prism 7700 Sequence Detection System, User Bulletin 2, *PE Applied Biosystems*.

Liu, H. P., Kohler, J. R. & Fink, G. R. (1994). Suppression of hyphal formation in *Candida albicans* by mutation of a *STE12* homolog. *Science*, 266, 1723–1726.

Liu, W. & Saint, D. A. (2002). A new quantitative method of real time reverse transcription polymerase chain reaction assay based on simulation of polymerase chain reaction kinetics. *Analytical Biochemistry*, 302, 52-59.

Liu, Z. & Myers, L. C. (2012). Med5 (Nut1) and Med17 (Srb4) are direct targets of mediator histone H4 tail interactions. *PLoS One,* 7, 1-11.

Lockhart, S. R., Daniels, K. J., Zhao, R., Wessels, D., Soll, D. R. (2003). Cell biology of mating in *Candida albicans. Eukaryotic Cell,* 2, 49-61.

Lockhart, S. R., Zhao, R., Daniels, K. J., Soll, D. R. (2003). Alpha-pheromone- induced "shmooing" and gene regulation require white-opaque switching during *Candida albicans mating. Eukaryotic Cell,* 2, 847-855.

Lopes da Rosa, J., Boyartchuk, V. L., Zhu, L. J., Kaufman, P. D. (2010). Histone acetyltransferase Rtt109 is required for *Candida albicans* pathogenesis. *Proceedings of the National Academy of Sciences USA,* 26, 1594-1599.

Lorenz, M.C., Bender, J. A., Fink. G. R. (2004). Transcriptional response of *Candida albicans* upon internalization by macrophages. *Eukaryotic Cell,* 3, 1076-1087

Lu, Y., Su, C., Mao, X., Raniga, P. P., Liu, H., Chen, J. (2008). Efg1-mediated recruitment of NuA4 to promoters is required for hypha-specific Swi/Snf binding and activation in *Candida albicans. Molecular Biology of the Cell,* 19, 4260-4272.

Lu, Y., Su, C., Wang, A., Liu, H. (2011). Hyphal development in *Candida albicans* requires two temporally linked changes in promoter chromatin for initiation and maintenance. *PLoS Biology,* 9, 1-17.

Ma, H. & May, R. C. (2009). Virulence in *Cryptococcus* species. *Advances in Applied Microbiology,* 67, 131-190.

Magee, P. T., Gale, C., Berman, J., Davis, D. (2003). Molecular genetic and genomic approaches to the study of medically important fungi. *Infection and Immunity,* 71, 2299–2309.

Marchetti, O., Bille, J., Fluckiger, U., Eggimann, P., Ruef, C., Garbino, J. (2004). Fungal Infection Network of Switzerland. Epidemiology of candidemia in Swiss tertiary care hospitals: secular trends, 1991-2000. *Clinical Infectious Diseases,* 38, 311-320.

Marcu, M. G., Chadli, A., Bouhouche, I., Catelli, M., Neckers, L. M. (2000). The heat shock protein 90 antagonist novobiocin interacts with a previously unrecognized ATP-

binding domain in the carboxyl terminus of the chaperone. *Journal of Biological Chemistry,* 275, 37181-37186.

Martchenko, M., Alarco, A. M., Harcus, D., Whiteway, M. (2004). Superoxide dismutases in *Candida albicans*: transcriptional regulation and functional characterization of the hyphal-induced SOD5 gene. *Molecular Biology of the Cell,* 15, 456-467.

Martchenko, M., Levitin, A., Hogues, H., Nantel, A., Whiteway, M. (2007). Transcriptional rewiring of fungal galactose-metabolism circuitry. *Current Opinion in Biology,* 17, 1-15.

Martin, R., Moran, G. P., Jacobsen, I. D., Heyken, A., Domey, J., Sullivan, D. J., Kurzai, O., Hube, B. (2011). The *Candida albicans*-specific gene *EED1* encodes a key regulator of hyphal extension. *PLoS One,* 6, 1-13.

Martínez-Esparza, M., Martínez-Vicente, E., González-Párraga, P., Ros, J. M., García-Peñarrubia, Argüelles, J. C. (2009). Role of trehalose-6P phosphatase (*TPS2*) in stress tolerance and resistance to macrophage killing in *Candida albicans. International Journal of Medical Microbiology,* 299, 453-464.

Mathew, B. P. & Nath, M. (2009). Recent approaches to antifungal therapy for invasive mycoses. *Chem Med Chem,* 3, 310-323.

Mavor, A. L., Thewes, S., Hube, B. (2005). Systemic fungal infections caused by *Candida* species: epidemiology, infection process and virulence attributes. *Current Drug Targets,* 6, 863-874.

Mayer, F. L., Wilson, D., Hube, B. (2013). *Candida albicans* pathogenicity mechanisms. *Virulence,* 4,2, 119-128.

Mefford, H. C. & Trask, B. J. (2002). The complex structure and dynamic evolution of human subtelomeres. *Nature Reviews Genetics,* 3, 91-102.

Menzin, J., Myers, J. L., Friedman, M., Perfect, J. R., Langston, A. A., Danna, R. P., Papadopoulos, G. (2009). Mortality, length of hospitalization and costs associated with invasive fungal infections in high-risk patients. *Am J Health Syst Pharm,* 66, 1711-1717.

Miceli, M., Díaz J. A., Lee S. A. (2011). Emerging opportunistic yeast infections. *The Lancet Infectious Diseases,* 11, 142-151.

Miklos, I., Szilagyi, Z., Watt. S., Zilahi, E., Batta, G., Antunovics, Z., Enczi, K., Bähler, J., Sipiczki, M. (2008). Genomic expression patterns in cell separation mutants of *Schizosaccharomyces pombe* defective in the genes sep10 (+) and sep15 (+) coding for the Mediator subunits Med31 and Med8. *Molecular Genetics and Genomics,* 279, 225-238.

Miller, M. G. & Johnson, A. D. (2002). White-opaque switching in *Candida albicans* is controlled by mating-type locus homeodomain proteins and allows efficient mating. *Cell,* 110, 293-302.

Miramon, P., Dunker, C., Windecker, H., Bohovych, I. M., Brown, A. J., Kurzai, O., Hube, B. (2012). Cellular responses of *Candida albicans* to phagocytosis and the extracellular activities of neutrophils are critical to counteract carbohydrate starvation, oxidative and nitrosative stress. *PLoS One,* 7, e52850.

Miyoshi, H., Tokutake, N., Imaeda, Y., Akagi, T., Iwamura, H. (1995). A model of Antimycin binding based on structure-activity studies of synthetic Antimycin A analogues. *Biochimica et Biophysica Acta,* 1229, 149-154.

Mochon, A. B., Ye, J., Kayala, M. A., Wingard, J. R., Clancy, C. J., Nguyen, M. H., Felgner, P., Baldi, P., Liu, H. (2010). Serological profiling of a *Candida albicans* protein Microarray reveals permanent host-pathogen interplay and stage-specific responsed during candidaemia. *Plos Pathogens,* 6, 1-14.

Monge, R. A., Román, E., Nombela, C., Pla, J. (2006). The MAP kinase signal transduction network in *Candida albicans. Microbiology,* 152, 905-912.

Moran, G. P., Coleman, D. C. & Sullivan D. J. (2012). *Candida albicans* versus *Candida dubliniensis*: Why is *C. albicans* more pathogenic? *International Journal of Micriobiology,* Article ID 20591.

Moran, G. P., MacCallum, D. M., Spiering, M. J., Coleman, D. C., Sullivan, D. J. (2007). Differential regulation of the transcriptional repressor NRG1 accounts for altered host-cell interactions in *Candida albicans* and *Candida dubliniensis. Molecular Microbiology,* 66, 915–29.

Moran, G. P., Stokes, C., Thewes, S., Hube, B., Coleman, D. C., Sullivan, D. (2004). Comparative genomics using *Candida albicans* DNA microarrays reveals absence and divergence of virulence-associated genes in *Candida dubliniensis. Microbiology,* 150, 3363-3382.

Morey, J. S., Ryan, J. C. & Van Dolah, F. M. (2006). Microarray validation: factors influencing correlation between oligonucleotide microarrays and real-time PCR. *Biological Procedures Online,* 8, 175-193.

Murad, A. M. Leng, P., Straffon, M., Wishart, J., Macaskill, S., MacCallum, D., Schnell, N., Talibi, D., Marechal, D., Tekaia, F., d'Enfert, C., Gaillardin, C., Odds F. C., Brown, A. J. (2001). Nrg1 represses yeast–hypha morphogenesis and hypha–specific gene expression in *Candida albicans. EMBO Journal,* 20, 4742–4752.

Mutch, D. M., Berger, A., Mansourian, R., Rytz, A., Roberts, M. A. (2001). Microarray data analysis: a practical approach for selecting differentially expressed genes. *Genome Biology,* 2.

Myers, K. K., Fonzi, W. A. & Sypherd, P. S. (1992). Isolation and sequence analysis of the gene for translation elongation factor 3 from *Candida albicans. Nuc Acids Res,* 20, 1705-1710.

Myers L. C., Gustafsson, C. M., Bushnell, D. A., Lui, M., Erdjument-Bromage, H., Tempst, P., Kornberg, R. D. (1998). The Med proteins of yeast and their function through the RNA I carboxy-terminal domain. *Genes & Development.* 12, 45–54.

Myers L. C. & Kornberg R. D. (2000). Mediator of transcriptional regulation. *Annual Review of Biochemistry,* 69, 729-749.

Naglik, J., Albrecht, A., Bader, O., Hube, B. *Candida albicans* proteinases and host/pathogen interactions. *Cellular Microbiology,* 6, 915-926.

Nantel, A., Dignard, D., Bachewich, C., Harcus, D., Marcil, A., Bouin, A. P., Sensen, C. W., Hogues, H., van het Hoog, M., Gordon, P., Rigby, T., Benoit, F., Tessier, D. C., Thomas, D. Y., Whiteway, M. (2002). Transcription profiling of *Candida albicans* cells undergoing the yeast-to-hyphal transition. *Molecular Biology of the Cell,* 13, 3452-3465.

Negredo, A., Monteoliva, L., Gil, C., Pla, J., Nombela, C. (1997). Cloning, analysis and one-step disruption of the *ARG5,6* gene of *Candida albicans. Microbiology,* 143, 297-302.

Nelson, R. W., Dogruel, D., Willams, P. (1994). Mass determination of human immunoglobulin IgM using matrix-assisted laser desorption/ionization time-of-flight mass spectrometry. *Rapid Communications in Mass Spectrometry.* 8, 627-631.

Nicholls, S., MacCallum, D. M., Kaffarnik, F. A., Selway, L., Peck, S. C., Brown, A. J. (2011). Activation of the heat shock transcription factor Hsf1 is essential for the full virulence of the fungal pathogen *Candida albicans. Fungal Genetics and Biology,* 48, 297-305.

Nikolaou, E., Agrafioti, I., Stumpf, M., Quinn, J., Stansfield, I., Brown, A. J. (2009). Phylogenetic diversity of stress signalling pathways in fungi. *BioMed Central Evolutionary Biology,* 9, 1-18.

Nobile, C. J., Bruno, V. M., Richard, M. L., Davis, D. A. Mitchell, A. P. (2003). Genetic control of chlamydospore formation in *Candida albicans. Microbiology,* 149, 3629-3637.

Nobile, C. J. & Mitchell, A. P. (2005). Regulation of cell surface genes and biofilm formation by the *C. albicans* transcription factor Bcr1p. *Current Opinion in Biology,* 15, 1150-1155.

Nobile, C. J. & Mitchell, A. P. (2006). Genetics and genomics of *Candida albicans* biofilm formation *in vitro* and *in vivo. Cell Microbiology,* 8, 1382-1391.

Nobile, C. J., Solis, N., Myers, C. L., Fay, A. J., Deneault, J. S., Nantel, A., Mitchell, A. P., Filler, S. G. (2008). *Candida albicans* transcription factor Rim101 mediates pathogenic interactions through cell wall functions. *Cell Microbiology,* 10, 2180-2196.

Nobile, C. J., Fox, E. P., Nett, J. E., Sorrells, T. R., Mitrovich, Q. M., Hernday, A. D., Tuch, B. B., Andes, D. R., Johnson, A. D. (2012). A recently evolved transcriptional network controls biofilm development in *Candida albicans. Cell,* 148, 126-138.

Novatchkova, M., and F. Eisenhaber. (2004). Linking transcriptional mediators via the GACKIX domain super family. *Current Opinion in Biology,* 14, 54-55.

O'Connor, L., Caplice, N., Coleman, D. C., Sullivan D. J., Moran, G. P. (2010). Differential filamentation of *Candida albicans* and *Candida dubliniensis* is governed by nutrient regulation of *UME6* expression. *Eukaryotic Cell,*. 9, 1383–1397.

Odds, F. C., Hanson, M. F., Davidson, A. D., Jacobsen, M. D., Wright, P., Whyte, J. A., Gow, N. A., Jones, B. L. (2007). One year prospective survey of Candida bloodstream infections in Scotland. *Journal of Medical Microbiology,* 56, 1066–1075.

Oh, S. H, Cheng, G., Nuessen J. A., Jajko, R., Yeater, K. M., Zhao, X., Pujol, C., Soll, D. R., Hoyer, L. L. (2005). Functional specificity of *Candida albicans* Als3p proteins and clade specificity of *ALS3* alleles discriminated by the number of copies of the tandem repeat sequence in the central domain. *Microbiology,* 151, 673–681.

Omrum, U. & Anaissie, E. J. (1996). Problems and controversies in the management of hematogenous-candidiasis. *Clinical & Infectious Disease,* 22, S95-S101.

Paraje, M. G., Correa, S. G., Albesa, I., Sotomayor, C. E. (2009). Lipase of *Candida albicans* induces activation of NADPH oxidase and L- arginine pathways on resting and activated macrophages. *Biochemical and Biophysical Research Communications,* 390, 263-268.

Park, K. K., Brodell, R. T., Helms, S. E., (2011). Angular cheilitis, part 1: local etiologies. *Cutis: Cutaneous Medicine for the Practioner,* 87, 289-295.

Park, Y. & Morschhäuser, J. (2005). Tetracyline-inducible gene expression and gene deletion in *Candida albicans. Eukaryotic Cell,* 4, 1328-1342.

Paul, S., Schmidt, J. A., Moye-Rowley, W. S. (2011). Regulation of the CgPdr1 transcription factor from the pathogen *Candida glabrata. Eukaryotic Cell,* 10, 187-197.

Patel, P. K., Erlandsen, J. E., Kirkpatrick, W. R., Berg, D. K., Westbrook, S. D., Louden, C., Cornell, J. E., Thompson, G. R., Vallor, A. C., Wickes, B. L., Wiederhold, N. P., Redding, S. W., Patterson, T. F. (2012). The Changing Epidemiology of Oropharyngeal Candidiasis in Patients with HIV/AIDS in the Era of Antiretroviral Therapy. *AIDS research and treatment.* Volume 2012, Article I.D. 262471.

Patterson, M. J., McKenzie, C. G., Smith, D. A., da Silva Dantas, A., Sherston, S., Veal, E. A., Morgan, B. A., MacCallum, D. M., Erwig, L., Quinn, J. (2013). Ybp1 and Gpx3 signaling in *Candida albicans* govern hydrogen peroxide-induced oxidation of the Cap1 transcription factor and macrophage escape. *Antioxidants & Redox Signalling,* 19, 2244-2260.

Peng, J. & Zhou, J. Q. (2012). The tail-module of the yeast Mediator complex is required for telomere heterochromatin maintenance. *Nucleic Acids Research,* 40, 581-593.

Peréz-Martín, J. & Di Pietro, A. (2012). *Morphogenesis and Pathogenicity in Fungi. Topics in Current Genetics,* 22.

Perkins, D. N., Pappin, D. J., Creasy, D. M., Cottrell, J. S. (1999). Probability-based protein identification by searching sequence databases using mass spectrometry data. *Electrophoresis,* 18, 3551-3567.

Perlin, D. S. (2015). Mechanisms of echinocandin antifungal drug resistance. *Annals of the New York Academy of Sciences,* 1354, 1-11.

Pfaller, M. A., Diekema, D. J., Jones, R. N., The SENTRY Participant Group, *et al.* (2001). International surveillance of bloodstream infections due to *Candida* species: frequency of occurrence and in vitro susceptibilities to fluconazole, ravuconazole, and voriconazole of isolates collected from 1997 through 1999 in the SENTRY antimicrobial surveillance program. *Journal of Clinical Microbiology,* 39, 3254-3259.

Phan, Q. T., Myers, C. L., Fu, Y., Sheppard, D. C., Yeaman, M. R., Welch, W. H., Ibrahim, A. S., Edwards, J. E. Jr, Filler, S. G. (2007). Als3 is a *Candida albicans* invasin that binds to cadherins and induces endocytosis by host cells. *PLoS Biology,* 5, 1-15.

Prodromou, C. & Pearl, L. K. (2003). Structure and functional relationships of Hsp90. *Current Cancer Drug Targets,* 3, 301-323.

Pryde, F. E., H. C. Gorham & Louis, E. J. (1997). Chromosome ends: all the same under their caps. *Current Opinion in Genetic Development,* 7, 822-828.

Puig, O., Caspary, F., Rigaut, G., Rutz, B., Bouveret, E., Bragado-Nilsson, E., Wilm, M., Séraphin, B. (2001). The tandem affinity purification (TAP) method: a general procedure of protein complex purification. *Methods* 24, 218-229.

Ramage, G., VandeWalle, K., Lopez-Ribot, J. L., Wickes, B. L. (2002). The filamentation pathway controlled by the Efg1 regulator protein is required for normal biofilm formation and development in *Candida albicans. FEMS Microbiology Letters,* 214, 95-100.

Ramírez-Zavala, B., Reuss, O., Park, Y. N., Ohlsen, K., Morschhäuser, J. (2008). Environmental induction of white-opaque switching in *Candida albicans. PLoS Pathogens,* 13, 1-14.

Ray, T. L. & Payne, C. D. (1990). Comparative production and rapid purification of Candida acid proteinase from protein-supplemented cultures. *Infection and Immunity,* 58, 508–514.

Rees, J. R., Pinner, R. W., Hajjeh, R. A., Brandt, M. E., Reingold, A. L. (1998). The epidemiological features of invasive mycotic infections in the San Francisco bay area, 1992-1993: results of population-based laboratory active surveillance. *Clinical & Infectious Disease,* 27, 1138-1147.

Reuss, O. Vik, A., Kolter, R., Morschhäuser, J. (2004). The *SAT1* flipper, an optimized tool for gene disruption in *Candida albicans. Gene,* 341, 119-127.

Samaranayake, D. P. & Hanes, S. D. (2011). Milestones in *Candida albicans* gene manipulation. *Fungal Genetics and Biology,* 48, 858-865.

Sanglard, D., Hube, B., Monod, M., Odds, F. C., Gow, N. A. R. (1997). A triple deletion of secreted aspartyl proteinase genes *SAP4, SAP5* and *SAP6* of *Candida albicans* causes attenuated virulence. *Journal of Microbiology, Immunology and Infection,* 65, 3539-3546.

Santos, M. A. & Tuite, M. F. (1995). The CUG codon is decoded in vivo as serine and not leucine in *Candida albicans. Nucleic Acids Research,* 23, 1481–1486.

Schmittgen, T. D. & Livak, K. J. (2008). Analyzing real-time PCR data by the comparative C_T method. *Nature protocols,* 3, 6, 1101-1108.

Schubert, S., Popp, C., Rogers, D. P., Morschhäuser, J. (2011). Functional dissection of a *Candida albicans* zinc cluster transcription factor, the multidrug resistance regulator Mrr1. *Eukaryot Cell,* 10, 1110-1121.

Sen, M., Shah, B., Rakshit, S., Singh, V., Padmanabhan, B., Ponnusamy, M., Pari, K., Vishwakarma, R., Nandi, D. & Sadhale, P. P. (2011). UDP-glucose-4, 6-dehydratase activity plays a role in maintaining cell wall integrity and virulence in *Candida albicans. PLoS Pathogens,* 7, 11, 1-17.

Shapiro, R. S., Uppuluri, P., Zaas, A. K., Collins, C., Senn, H., Perfect, J. R., Heitman, J., Cowen, L. E. (2009). Hsp90 orchestrates temperature-dependent *Candida albicans* morphogenesis via Ras1-PKA signaling. *Current Biology,* 19, 621-629.

Sheppard, D. C., Yeaman, M. R., Welch, W. H., Phan, Q. T., Fu, Y, Ibrahim, A. S., Filler, S. G., Zhang, M., Waring, A. J., Edwards, J. E. Jr. (2004). Functional and structural diversity in the Als protein family of *Candida albicans. Journal of Biological Chemistry,* 279, 30480–30489.

Shevchenko, A., Tomas, H., Havliš, J., Olsen, J. V., Mann, M., (2007). In-gel digestion for mass spectrometric characterization of proteins and proteasomes. *Nature protocols.* 1, 6, 2856-2860.

Shieh, J. C., White, A., Cheng, Y. C., Rosamond, J. (2005). Identification and functional characterization of *Candida albicans CDC4. Journal of Biomedical Science,* 16, 913-924.

Silva, S., Negri, M., Henriques, M., Oliveira, R., Williams, D. W., and Azeredo, J. (2012). *Candida glabrata, Candida parapsilosis* and *Candida tropicalis*: biology, epidemiology, pathogenicity and antifungal resistance. *FEMS Microbiology Review,* 36, 288–305.

Silva-Dias, A., Miranda, I. M., Branco, J., Monteiro-Soares, M., Pina-Vaz, C., Rodrigues, A. G. (2015). Adhesion, biofilm formation, cell surface hydrophobicity, and antifungal planktonic susceptibility: relationship amond *Candida* spp. *Frontiers in Microbiology,* 6, 1-8.

Singh, V., Satheesh, S. V., Raghavendra, M. L., Sadhale, P. P. (2007). The key enzyme in galactose metabolism, UDP-galactose-4-epimerase, affects cell-wall integrity and morphology in *Candida albicans* even in the absence of galactose. *Fungal Genet Biol,* 44, 563-574.

Slot, J. C. & Rokas, A. (2010). Multiple GAL pathway gene clusters evolved independently and by different mechanisms in fungi. *Proceedings of the National Academy of Science USA,* 107, 10136-10141.

Slutsky, B., Staebell, M., Anderson, J., Risen, L., Pfaller, M., Soll, D. R. (1987). "White-opaque transition": a second high-frequency switching system in *Candida albicans. Journal of Bacteriology,* 169, 189–197.

Sobel J. D. (1984). Vulvovaginal candidiasis: what we do and do not know. *Annals of Internal Medicine,* 101, 390-392.

Sobel, J. D. (1997). Vaginitis. *New England Journal of Medicine,* 337, 1896-903.

Soll, D. R. (2009). Why does *Candida albicans* switch? FEMS *Yeast Research,* 9, 978-989.

Sonneborn, A., Bockmuhl, D. P. & Ernst, J. F. (1999). Chlamydospore formation in *Candida albicans* requires the Efg1p morphogenetic regulator. *Infection and Immunity,* 67, 5514–5517.

Söti, C., Rácz, A. & Cseremly, P. (2002). A nucleotide-dependent molecular switch controls ATP binding at the C-terminal domain of Hsp90. N-terminal nucleotiide binding unmasks a C-terminal binding pocket. *Journal of Biological Chemistry,* 277, 7066-7075.

Spampinato, C. & Leonardi, D. (2013). *Candida* infections, causes, targets and resistance mechanisms: traditional and alternative antifungal agents. *Biomedical Research International,* 1-13.

Spiering, M. J., Moran, G. P., Chauvel, M., MacCallum, D. M., Higgins, J., Hokamp, K., Yeomans, T., d'Enfert, C., Coleman, D. C., Sullivan, D. J. (2010). Comparative transcript profiling of *Candida albicans* and *Candida dubliniensis* identifies *SFL2,* a *C. albicans* gene required for virulence in a reconstituted epithelial infection model. *Eukaryotic Cell,* 9, 251-265.

Staib, P. & Morschhäuser, J. (2005). Differential expression of the NRG1 repressor controls species-specific regulation of chlamydospore development in *Candida albicans* and *Candida dubliniensis. Molecular Microbiology,* 55, 637–52.

Staib, P. & Morschhäuser, J. (2007). Chlamydospore formation in *Candida albicans* and *Candida dubliniensis*- an enigmatic development programme. *Mycoses,* 50, 1-12.

Stokes, C., Moran, G. P., Spiering, M. J., Cole, G. T., Coleman, D. C., Sullivan, D. J. (2007). Lower filamentation rates of *Candida dubliniensis* contribute to its lower virulence in comparison with *Candida albicans*. *Fungal Genetic Biology*, 44, 920–31.

Stoldt, V. R., Sonneborn, A., Leuker, C. E., Ernst, J. F. (1997). Efg1p, an essential regulator of morphogenesis of the human pathogen *Candida albicans*, is a member of a conserved class of bHLH proteins regulating morphogenetic processes in fungi. *EMBO Journal*, 16, 1982–1991.

Storey, J. D., Akey, J. M., Kruglyak, L. (2005). Multiple locus linkage analysis of genomewide expression in yeast. *PLoS Biol*, 3, 1380-1391.

Sudbery, P. E. (2011). Growth of *Candida albicans* hyphae. *Nature Reviews Microbiology*, 9, 737-748.

Sullivan, D. J., Westerneng, T. J., Haynes, K. A., Bennett, D. E., Coleman, D. C. (1995). *Candida dubliniensis* sp. Nov.: phenotypic and molecular characterization of a novel species associated with oral candidosis in HIV-infected individuals. *Microbiology*, 141, 1507-1521.

Sullivan, D. J., Haynes, K. A., Bille, J., Boerlin, P., Rodero, L., Lloyd, S., Henman, M. & Coleman, D. C. (1997). Widespread geographic distribution of oral *Candida dubliniensis* strains in human immunodeficiency virus-infected individuals. *Journal of Clinical Microbiology*, 35, 960-964.

Sullivan, D. & Coleman, D. (1998). *Candida dubliniensis:* characteristics and identification. *Journal of Clinical Microbiology*, 36, 329-334.

Sullivan, D. J., Moran, G. P., Pinjon, E., Al-Mosaid, A., Stokes, C., Vaughan, C. & Coleman, D. C. (2004). Comparison of the epidemiology, drug resistance mechanisms, and virulence of *Candida dubliniensis* and *Candida albicans*. *FEMS Yeast Research*, 4, 369-76.

Sullivan, D. J., Moran, G. P. & Coleman, D. C. (2005). *Candida dubliniensis*: ten years on. *FEMS Microbiology Letters*, 253, 9-17.

Sullivan, D. J., Berman, J., Myers, L. C., Moran, G. P. (2015). Telomeric ORFs in *Candida albicans*: does Mediator tail wag the yeast? *PLoS Pathogens*, 11, 1-6.

Sundstrom, P. Cutler, J. E., Staab, J. F. (2002) Re-evaluation of the role of *HWP1* in systemic candidiasis by use of *Candida albicans* strains with selectable marker *URA3* targeted to the *ENO1* locus. *Infection and Immunity*, 70, 3281–3283.

Swaffield, J. C., Melcher, K., Johnston, S. A. (1996). A highly conserved ATPase protein as a mediator between acidic activation domains and the TATA-binding protein. *Nature,* 374, 88-91.

Taniguchi, M., Miura, K., Iwao, H., Yamanaka, S. (2001). Quantitative assessment of DNA microarrays-comparison with northern blot analyses. *Genomics,* 71, 34-39.

Tebbji, F., Chen, Y., Albert, J. R., Gunsalus, K. T. W., Kumamoto, C. A., Nantel, A., Sellam, A., Whiteway, M. (2014). A functional portrait of Med7 and the Mediator complex in *Candida albicans. PLoS Genetics,* 10, 1-17.

ten Cate, J. M., Klis, F.M., Pereira-Cenci, T., Crielaard, W., de Groot, P. W. (2009). Molecular and cellular mechanisms that lead to *Candida* biofilm formation. *Journal of Dental Research,* 88, 105-115.

Thakur, J. K., Arthanari, H., Yang, F., Pan, S. J., Fan, X., Breger, J., Frueh, D. P., Gulshan, K., Li, D. K., Mylonakis, E., Struhl, K., Moye-Rowley, W. S., Cormack, B. P., Wagner, G., Näär, A. M. (2008). A nuclear receptor-like pathway regulating multidrug resistance in fungi. *Nature,* 452, 604-609.

Thewes, S., Kretschmar, M., Park, H., Schaller, M., Filler, S. G., Hube, B. (2007). In vivo and ex vivo comparative transcriptional profiling of invasive and non-invasive *Candida albicans* isolates identifies genes associated with tissue invasion. *Molecular Microbiology,* 63, 1606-1628.

Thomas, J., Jacobson, G. A., Narkowicz, C. K., Peterson, G. M., Burnet, H., Sharpe, C. (2010). Toenail onchomycosis: an important global disease burden. *Journal of Clinical Pharmacology,* 35, 497-519.

Thompson, C. M & Young, R. A. (1995). General requirement for RNA polymerase II holoenzymes *in vivo. Proceedings of the National Academy of Science USA,* 92, 4587-4590.

Trevino, V., Falciani, F., Barrera-Saldaña, H. A. (2007). DNA microarrays: a powerful genomic tool for biomedical and clinical research. *Molecular Medicine,* 13, 527-541.

Tumbarello, M., Posteraro, B., Trecarichi, E. M., Fiori, B., Rossi, M., Porta, R., de Gaetano Donati, K., La Sorda, M., Spanu, T., Fadda, G., Cauda, R., Sanguinetti, M. (2007). Biofilm production by *Candida* species and inadequate antifungal therapy as predictors of mortality for patients with candidemia. *Journal of Clinical Microbiology*, 45, 1843–1850.

Uemura, H. & Fraenkel, D. G. (1990). Gcr2, a new mutation affecting glycolytic gene expression in *Saccharomyces cerevisiae*. *Molecular & Cell Biology* 10, 6389–6396.

Uppuluri, P., Chaturvedi, A. K., Srinivasan, A., Banerjee, M., Ramasubramaniam, A. K., Kohler, J. R., et al. (2010). Dispersion as an important step in the *Candida albicans* biofilm developmental cycle. *PLoS Pathogens,* 6, 1-13.

Uwamahoro, N., Qu, Y., Jelicic, B., Lo, T. L., Beaurepaire, C., Bantun, F., Quenalt, T., Boag, P. R., Ramm, G., Callaghan, J., Beilharz, T. H., Nantel, A., Peleg, A. Y., Traven, A. (2012). The functions of Mediator in *Candida albicans* support a role in shaping species-specific gene expression. *PLoS Genetics,* 8, 1-17.

van de Peppel, J., Kettelarij, N., van Bakel, H., Kockelkorn, T. T. J. P., van Leenen, D., Holstege, F. C. P. (2005). Mediator expression profiling epistasis reveals a signal transduction pathway with antagonistic submodules and highly specific downstream targets. *Molecular Cell,* 19, 511-522.

van het Hoog, M. V., Rast, T. J., Martchenko, M., Grindle, S., Dignard, D., Hogues, H., Cuomo, C., Berriman, M., Magee, B. B., Whiteway, M., Chibana, H., Nantel, A., Magee, P.T. (2007). Assembly of the *Candida albicans* genome into sixteen supercontigs. *Genome Biology,* 8, R52.

Walker, L. A., Maccallum, D. M., Bertram, G., Gow, N. A., Odds, F. C., Brown, A. J. (2009). Genome-wide analysis of *Candida albicans* gene expression patterns during infection of the mammalian kidney. *Fungal Genetic Biology,* 46, 210–219.

Walsh, T. J. & Groll, A. H. (1998). Emerging fungal pathogens: evolving challenges to immunocompromised patients for the twenty-first century. *Transplant Infectious Disease,* 1, 247-261.

Wang, Z., Gerstein, M. & Snyder, M. (2009). RNA-Seq: a revolutionary tool for transcriptomics. *Nature Review Genetics,* 10, 57-63.

White, T. C., Marr, K. A., Bowden, R. A. (1998). Clinical, cellular, and molecular factors that contribute to antifungal drug resistance. *Clinical Microbiology Review,* 11, 382-402.

Whiteway, M. & Bachewich, C. (2007). Morphogenesis in *Candida albicans. Annual Review Microbiology,* 61, 529-553.

Williams, D. & Lewis, M. (2011). Pathogenesis and treatment of oral candidosis. *Journal of Oral Microbiology,* 3, 5771-5782.

Wilson, R. B., Davis, D., Enloe, B .M., Mitchell, A. P. (2000). A recyclable *Candida albicans URA3* cassette for PCR product-directed gene disruptions. *Yeast,* 16, 65-70.

Wirsching, S., Michel, S., Köhler, G., Morschhäuser, J. (2000). Activation of the multiple drug resistance gene *MDR1* in fluconazole-resistant, clinical *Candida albicans* strains is caused by mutations in a transregulatory factor. *Journal of Bacteriology,* 183, 400-404.

Woods, J. P. (2003). Knocking on the right door and making a comfortable home; *Histoplasma capsulatum* intracellular pathogenesis. *Current Opinion in Microbiology,* 6, 327-331.

Wong S., Fares, M. A., Zimmermann, W., Butler, G., Wolfe, K. H. (2003). Evidence from comparative genomics for a complete sexual cycle in the 'asexual' pathogenic yeast *Candida glabrata. Genome Biology,* 4, R10.

Wu, W., Pujol, C., Lockhart, S. R., Soll, D. R. (2005). Chromosome loss followed by duplication is the major mechanism of spontaneous mating-type locus homozygosis in *Candida albicans. Genetics,* 169, 1311-1327.

Wu, W., Lockhart, S. R., Pujol, C., Srikantha, T., Soll, D. R. (2007). Heterozygosity of genes on the sex chromosome regulates *Candida albicans* virulence. *Molecular Microbiology,* 64, 1587-1604.

Wysong, D. R., Christin, L., Sugar, A. M., Robbins, P. W., Diamond, R. D. (1998). Cloning and sequencing of a *Candida albicans* catalase gene and effects of disruption of this

gene. *Infection and Immunity,* 66, 1953-1961.

Yang, Y. H., Dudoit, S., Luu, P., Lin, D. M., Peng, V., Ngai, J., Speed, T. P. (2001). Normalization for cDNA microarray data: a robust composite method addressing single and multiple slide systematic variation. *Nucleic Acids Research,* 30, 1-10.

Yang, Y. L. (2003). Virulence factors of *Candida* species. *Journla of Microbiology Immunology & Infection,* 36, 223-228.

Yue, H. P., Eastman, S., Wang, B. B., Minor, J., Doctolero, M. H., Nuttall, R. L., Stack, R., Becker, J. W., Montgomery, J. R., Vainer, M., Johnston, R. (2001). An evaluation of the performance of cDNA microarrays for detecting changes in global mRNA expression. *Nucleic Acids Research,* 29, 1-9.

Zakikhany, K., Naglik, J. R., Schmidt-Westhausen, A., Holland, G., Schnaller, M., Hube, B. (2007). In vivo transcript profiling of *Candida albicans* identifies a gene essential for interepithelial dissemination. *Cell Microbiology,* 9, 2938-2954.

Zhang, A., Petrov, K. O., Hyun, E. R., Zhongle, L., Gerber, S. A. & Myers, L. C. (2012). The Tlo proteins are stoichiometric components of *Candida albicans* mediator anchored via the Med3 subunit. *Eukaryotic Cell,* 11, 874- 884.

Zhao, X., Oh, S. H., Jajko, R., Diekema, D. J., Pfaller, M. A., Pujol, C., Soll, D. R., Hoyer, L. L. (2007). Analysis of ALS5 and ALS6 allelic variability in a geographically diverse collection of *Candida albicans* isolates. *Fungal Genetics Biology,* 44, 1298–1309.

Zheng, X., Wang, Y., Wang, Y. (2004). Hgc1, a novel hypha-specific G1 cyclin-related protein regulates *Candida albicans* hyphal morphogenesis. *EMBO Journal,* 23, 1845–1856.

Zhu, W. D. & Filler, S. G. (2010). Interactions of Candida albicans with epithelial cells. *Cell Microbiology,* 12, 273–282.